CHIBA
UNIVERSITY

On the perturbative and non-perturbative analysis of a gluon-ghost condensate of mass dimension two

Dissertation

In Partial Fulfillment of the Requirements
For the Degree of Doctor of Philosophy

Presented to the Department of Physics of the
Graduate School of Science
of
Chiba University
by

M. Sc. Matthias Warschinke
born on 28 May 1991 in Weimar, Germany

Chiba, 28 February 2019

Abstract

Recently, a reformulation of the $SU(N)$ Yang-Mills theory inspired by the Cho-Faddeev-Niemi decomposition has been developed in order to understand quark confinement from the viewpoint of the dual superconductivity. The concept of infrared Abelian dominance plays an important role in the realization of this idea and through numerical simulations on the lattice, evidence was found for example in the form of the dynamical mass generation for specific gluon degrees of freedom. A promising analytical attempt to explain the generation of such masses is through certain condensates of mass dimension two. In this thesis, we want to focus on the reformulated $SU(N)$ Yang-Mills theory in the previously overlooked minimal option with the non-Abelian $U(N-1)$ stability group, in contrast to the conventional maximal Abelian gauge (MAG), where the decomposition corresponds to the Abelian $U(1)^{N-1}$ stability group. Consequently, if the construction works in a similar way as in the MAG, the new option may allow us to establish a non-Abelian extension of the conventional infrared Abelian dominance and therefore represents progress towards a non-Abelian superconductivity picture for confinement. In fact, this new hypothesis is already supported by lattice simulations. We begin our investigations with a thorough one-loop analysis of the novel decomposition. We calculate all renormalization factors in light of the renormalizability of the theory and subsequently define an appropriate mixed gluon-ghost composite operator of mass dimension two as the candidate for the condensate. We then prove its (on-shell) invariance under Becchi-Rouet-Stora-Tyutin (BRST) symmetry transformations and the multiplicative renormalizability. Armed with these results, we argue the existence of the mixed gluon-ghost condensate by means of the so-called local composite operator formalism. In the last part of this work, we attempt to extend the perturbative results through a functional renormalization group (FRG) analysis. In a short digression related to the the derivation of lower Higgs mass bounds in Higgs-Yukawa toy models, we demonstrate how the FRG can improve perturbative calculations and acquire the necessary tools to finally discuss the existence of the gluon-ghost condensate in this framework. We find that the mechanism of condensate generation is present in our model, however, only under certain conditions.

Contents

Chapter 1

Introduction

As of now, quarks are considered to be the fundamental building blocks in particle physics. They are "glued" together by the strong force, whose carriers are called gluons. Theoretically, the interplay between quarks and gluons is described within quantum chromodynamics (QCD). However, interestingly, the quarks and gluons cannot be directly observed, but only color-neutral objects built from these fundamental pieces. The phenomenon that color-charged quarks and gluons are only existing in such bound states is called color confinement and still lacks a theoretical explanation.

Yet, Nambu, 't Hooft and Mandelstam proposed a promising mechanism that may explain at least quark confinement, the dual superconductivity picture [1–4]. In order for this mechanism to work, two problems need to be solved. First, the ordinary superconductor corresponds to an Abelian theory, whereas the underlying gauge symmetry of QCD is non-Abelian. Second, the mechanism requires the existence of magnetic monopoles, which are not included as fundamental degrees of freedom in QCD. This raises the question of how to extract them from the underlying theory. It was 't Hooft himself who suggested an interesting approach to the first problem, the "Abelian projection" [4]. The Abelian projection corresponds to a partial gauge fixing, with magnetic monopoles appearing at those points in spacetime where the gauge fixing fails to work due to degeneracies of the gauge fixing condition. In particular, the special case of the maximal Abelian gauge (MAG) [5, 6] turned out to be useful. The related gauge fixing condition loosely speaking minimizes the off-diagonal components of the gluons and hence yields in some sense the desired effective Abelian theory. Within this setting, a series of striking results related to the infrared Abelian dominance [7] was obtained through numerical simulations on the lattice for $SU(2)$, for example the exponential fall-off of the propagator corresponding to the off-diagonal gluon degrees of freedom, suggesting the dynamical generation of an off-diagonal gluon mass [8].

However, despite the success of this prescription, the fact that the identification of the monopoles is connected to adopting some kind of gauge fixing lead to the criticism that monopoles may be no physical objects but simply gauge artefacts. Moreover, the MAG explicitly breaks the color symmetry. The situation was recently improved by a reformulation of the Yang-Mills theory based on the Cho-Duan-Ge-Faddeev-Niemi-Shabanov decomposition of the gauge field with respect to the stability group H [9–22]. The reformulation was first obtained in the $SU(2)$ case [23, 24] and relies on the introduction of the so-called color field $\mathfrak{h}(x)$, which is used to define the decomposition. However, when extended to the general $G = SU(N)$ case [25], it turned out that the decomposition is not uniquely determined for $N > 2$, but enjoys several options. One of the options, the maximal option, is related to the MAG, which can be recovered in a certain limit. A new and interesting case is the minimal option, where the gauge field is decomposed with respect to the non-Abelian $U(N-1)$ stability group. Unlike in the maximal option, where the stability group is the Abelian $U(1)^{N-1}$ stability group, this allows for extracting non-Abelian monopoles. Within lattice simulations, the reformulation of the Yang-Mills theory also was able to reproduce key aspects of the equivalent to the infrared Abelian dominance, e.g. [26–28], just like in the case of the MAG, but it should again be stressed that no explicit color symmetry breaking as in the conventional approach is necessary to reveal these properties. This is a big advantage of the new prescription.

Now, certainly the numerical evidence for the "new type" of infrared Abelian dominance, where actually the dominant degrees of freedom corresponding to $H = U(N-1)$ are no longer Abelian for $N > 2$, is reassuring if one aims to explain confinement through the dual superconductivity picture. However, so far there is no analytical proof for it. The goal of this thesis is to complement the lattice simulations by an analytical study of the dynamical mass generation for the non-monopole degrees of freedom related to the coset G/H. In fact, the reformulation of the Yang-Mills theory allows the introduction of a gauge invariant mass term for exactly these degrees of freedom (irrespective of the particular choice of H) [23],

$$M^2 \operatorname{Tr}_{G/H} \left(\mathfrak{A}_\mu \mathfrak{A}^\mu \right), \tag{1.1}$$

where M is the bare mass and $\mathfrak{A}_\mu$ the gauge field. As explained, the trace is taken only over the coset part G/H. Clearly, we then would no longer discuss the original (pure) Yang-Mills theory and therefore, we must think of ways to generate such a mass term dynamically. This leads to the idea of a non-vanishing mass dimension-two coset gluon condensate. If existent, a mass term could result from the quartic self-interaction term of the Yang-Mills action. This idea is not new and has a long history. The conden-

sate $\langle \mathrm{Tr}_G \mathfrak{A}_\mu \mathfrak{A}^\mu \rangle$ was already shown to exist in the Landau gauge [29, 30]. Even ghost condensates were considered in the MAG [31, 32], although they were found to actually generate tachyonic gluon masses [33, 34]. In what follows, a combination of gluons and ghosts turns out to be very useful [35, 36],

$$\mathcal{O} = \mathrm{Tr}_{G/H} \left(\mathfrak{A}_\mu \mathfrak{A}^\mu - 2i\xi \mathfrak{C}\bar{\mathfrak{C}} \right), \tag{1.2}$$

where we denoted the ghost and anti-ghost by $\mathfrak{C}$ and $\bar{\mathfrak{C}}$, respectively. Furthermore, ξ is a certain "gauge fixing paramter", as will be explained later. The condensation of this operator (or its equivalent in other gauges) was already studied in the so-called Curci-Ferrari gauge [37, 38], as well as in the MAG, giving positive answer to the existence of the condensate, see [39, 40] and [41], respectively.

The condensate does not only play a key role in understanding the infrared Abelian dominance (or its equivalent in the minimal option), as shown in preceding works. For example, recall Savvidy's prediction that the $SU(2)$ vacuum with a non-zero homogeneous magnetic field strength is energetically favored [42], which has been immediately critisized by Nielsen and Olesen [43], as they showed that the effective potential in terms of the magnetic condensate actually develops an instability through a non-vanishing imaginary part. However, assumming the existence of the condensate as in Eq. (1.2), the potential can actually be stabilized [44, 45]. Furthermore, if the condensate exists, the Faddeev-Niemi model [46, 47] describing glueballs as knot-solitons can be derived as a low-energy effective theory of the reformulated Yang-Mills theory [48–50]. Even quark confinement at low temperatures can be a direct implication of the condensate [51].

In this thesis, we wish to clarify whether or not the described mechanism for generating the (coset) gluon mass can also work for the new option where the stability group is chosen to be $H = U(N-1)$. In the case of $N > 2$, the stability group is non-Abelian and therefore defines a novel scheme for the dual superconductivity picture, where the infrared dominant gluon degrees of freedom, and in particular the related monopoles, are of the non-Abelian type. The analysis will be first carried out within perturbation theory. Later, we will attempt to improve these results within the framework of the functional renormalization group, firstly for the $SU(2)$ case where minimal and maximal option of the reformulation coincide. In the end, this is extended to the general $SU(N)$ case. In more detail, this thesis is organized as follows. In chapter 2, we give a very brief introduction to Yang-Mills theory and shed a few more light onto the previously mentioned concepts and mechanisms. Chapter 3 is dedicated to the reformulated Yang-Mills theory in the minimal option. Within a certain approximation, we discuss the splitting of the Lagrangian with respect to the stability group $H = U(N-1)$ and perform

the one-loop renormalization, obtaining all renormalization group (RG) functions to this level which serve as the starting point for all further investigations. In this chapter, we also show the (on-shell) BRST invariance of the composite operator (1.2) and explicitly prove its one-loop multiplicative renormalizability in order to render this operator physically meaningful. In chapter 4, we introduce the so-called local composite operator (LCO) formalism [52, 53], which is also based on perturbation theory and explains how to deal with composite operators and the difficulties arising upon their introduction to a field theory. This formalism is then applied to our particular operator and the existence of the condensate is discussed. Chapter 5 corresponds to the attempt of improving these perturbative results by means of a non-perturbative tool called functional renormalization group (FRG). After explaining the key concept in the first part of this chapter, we apply the FRG to a slightly different problem related to the Higgs condensate in the standard model. It will illustrate how the FRG can improve perturbative calculations and will familiarize us with a certain recipe we subsequently apply to the composite operator in the third and last part of chapter 5. Finally, in chapter 6, we end with a summary and give an outlook towards possible future research.

Chapter 2

Theoretical foundations

In this chapter, we introduce a few theoretical basics, setting the stage for the actual goal of this thesis, the discussion of the existence of certain condensates in quantum field theory. The first section is devoted to a brief introduction to quantum field theory, in particular to non-Abelian Yang-Mills theory. The presented material can be found in about every quantum field theory textbook such as [54–56]. The second section deals with one of the key phenomena of Yang-Mills theory, confinement, which remains to be theoretically understood. A promising attempt at explaining confinement is the dual superconductivity picture, whose key aspects will also be discussed in the second section. Finally, the third section deals with a certain reformulation of Yang-Mills theory, which represents a remarkable progress towards the establishment of the dual superconductivity picture.

The content of this chapter is only presented in a reporting fashion and skips many technical details. For deeper discussions of the various topics we refer to the references cited in the related sections. In this chapter and throughout this thesis, we employ natural units $\hbar = c = k_B = 1$ and adopt the Einstein summation convention, if not stated otherwise. We will sometimes reintroduce $\hbar$ in order to clarify orders in loop expansions.

2.1 Elements of Yang-Mills theory

The field content of pure Yang-Mills theory is given by the so-called gauge field $\mathfrak{A}_\mu = A^A_\mu T^A \in \mathfrak{g}$, which takes value in the Lie algebra $\mathfrak{g}$ of the gauge group G. In this thesis, we focus on $G = SU(N)$. The matrices T^A denote the generators of $\mathfrak{g}$ and we normalize them according to $\mathrm{Tr}_G[T^A T^B] = \frac{1}{2}\delta^{AB}$. The classical Lagrangian of the

Yang-Mills theory in Minkowski space[1] is given by

$$\mathfrak{L}_{YM} = -\frac{1}{2}\,\mathrm{Tr}_G\left(\mathfrak{F}_{\mu\nu}\mathfrak{F}^{\mu\nu}\right), \tag{2.1}$$

where we defined the field strength tensor

$$\mathfrak{F}_{\mu\nu} = \frac{i}{g}[\mathfrak{D}_\mu, \mathfrak{D}_\nu], \tag{2.2}$$

and $\mathfrak{D}_\mu$ is the covariant derivative given by

$$\mathfrak{D}_\mu = \partial_\mu - ig\mathfrak{A}_\mu. \tag{2.3}$$

The field strength tensor is then alternatively rewritten as

$$\mathfrak{F}_{\mu\nu} = \partial_\mu\mathfrak{A}_\nu - \partial_\nu\mathfrak{A}_\mu - ig[\mathfrak{A}_\mu, \mathfrak{A}_\nu]. \tag{2.4}$$

Usually, we work in the adjoint representation, such that $F^A_{\mu\nu} = \partial_\mu A^A_\nu - \partial_\nu A^A_\mu + g f^{ABC} A^B_\mu A^C_\nu$ and $D^{AB}_\mu = \delta^{AB}\partial_\mu - g f^{ABC} A^C_\mu$ with f^{ABC} being the structure constants of $\mathfrak{g}$. The theory is invariant under the following gauge transformations,

$$\mathfrak{A}_\mu \to \mathfrak{A}^U_\mu = U\mathfrak{A}_\mu U^\dagger - \frac{i}{g}\left(\partial_\mu U\right)U^\dagger \qquad \forall U \in G, \tag{2.5}$$

where we will parametrize the group elements according to

$$U(x) = e^{igT^A\vartheta^A(x)}. \tag{2.6}$$

In the infinitesimal case, the gauge transformation of the gauge field takes the form

$$\delta A^A_\mu = \left(A^U_\mu\right)^A - A^A_\mu = D^{AB}_\mu\vartheta^B(x) + O(\vartheta^2). \tag{2.7}$$

Note that in particular, the existence of a gluon mass term $\frac{1}{2}M^2 A^A_\mu A^\mu_A$ in the bare action is forbidden according to gauge invariance.

As common for all quantum field theories, all physical information is stored in the correlators or n-point functions of the theory. Using one of the most popular ways of formulating field theories, the path integral formulation, one can obtain these correlators from the so-called generating functional $Z[J]$ through derivatives with respect to the

[1] We use for the metric $g_{\mu\nu} = (1, -1, -1, -1)$.

external source J,

$$Z[J] = \int \mathcal{D}A \; e^{iS_{YM}[A]+iJ\cdot A}, \tag{2.8}$$

with $J \cdot A \equiv \int_x J^A_\mu A^\mu_A$. In the case of gauge theories, however, one encounters an immediate problem. Due to the fact that all gauge fields on the same gauge orbit $\mathrm{Orb}(\mathfrak{A}) = \{\mathfrak{A}^U_\mu : U \in G\}$ yield equivalent physics, the naive path integral measure "overcounts" the contributions. To circumvent this problem, one tries to choose a representative of each gauge orbit by imposing a constraint called "gauge fixing condition", $\bar{f}[A] = f[A] - z(x) = 0$. More precisely, the functional $f[A]$ encodes the gauge fixing condition, while $z(x)$ is just an arbitrary auxiliary function to be eliminated later. This constraint is incorporated into the path integral via the Faddeev-Popov procedure [57]. First, we use the functional representation of the Delta function,

$$\begin{aligned} 1 = \int \mathcal{D}\bar{f} \; \delta(\bar{f}) &= \int \mathcal{D}U \; \delta\left(\bar{f}[\mathfrak{A}^U]\right) \; \det\left(\frac{\delta \bar{f}[\mathfrak{A}^U]}{\delta U}\right) \\ &= \int \mathcal{D}U \; \delta\left(\bar{f}[\mathfrak{A}^U]\right) \; \det\left(\frac{\delta f[\mathfrak{A}^U]}{\delta U}\right), \end{aligned} \tag{2.9}$$

where $\mathcal{D}U$ is the Haar measure. The determinant is then promoted to the action in the path integral by writing it as a functional integral over anticommuting fields $\mathfrak{C}$ and $\bar{\mathfrak{C}}$, the Fadeev-Popov ghosts and anti-ghosts. The determinant is conveniently parametrized by the representation of the gauge group element as in Eq. (2.6),

$$\det\left(\frac{\delta \bar{f}[\mathfrak{A}^U]}{\delta U}\right) = \det\left(\frac{\delta \bar{f}^A[\mathfrak{A}^U]}{\delta \vartheta^B}\right) = \det\left(\frac{\delta f^A[\mathfrak{A}^U]}{\delta \vartheta^B}\right) = \det \mathcal{M}^{AB}. \tag{2.10}$$

Moreover, it can be shown that $\mathcal{M}$ is actually independent of the representative, such that in the end we can replace $\mathfrak{A}^U_\mu \to \mathfrak{A}_\mu$. In a last step, the Delta function is eliminated by integrating over $\int \mathcal{D}z \; e^{-i\int_x [1/2\xi \; z^2]}$, where ξ is the so-called gauge fixing parameter. After this procedure, the generating functional reads

$$Z[K] = \int \mathcal{D}\Phi \; e^{iS_{YM}+iS_{GF+FP}+iK\cdot\Phi}, \tag{2.11}$$

with $\mathcal{D}\Phi = \mathcal{D}A\ \mathcal{D}C\ \mathcal{D}\bar{C}$ and

$$\begin{aligned} K \cdot \Phi &= \int_x \left(J^A_\mu A^\mu_A + \bar{\eta}^A C^A + \bar{C}^A \eta^A \right), \\ S_{GF+FP} &= \int_x \left(-\frac{(f^A)^2}{2\xi} + \bar{C}^A \mathcal{M}^{AB} C^B \right). \end{aligned} \tag{2.12}$$

Still, there remains an unsolved problem. Generally speaking, there is no guarantee that the gauge fixing condition picks a unique representative from each gauge orbit. This problem is known as the Gribov ambiguity [58, 59], but throughout this thesis, we do not further deal with this subtlety.

A consequence of the Faddeev-Popov procedure is the explicit breaking of the local gauge symmetry. Fortunately, as discovered by Becchi, Rouet, Stora, and Tyutin (BRST), the action still enjoys a residual global symmetry, the BRST symmetry [60, 61]. It is best revealed upon introducing the Nakanishi-Lautrup field $\mathfrak{N} = N^A T^A$ and rewriting the gauge fixing part,

$$-\frac{(f^A)^2}{2\xi} \to \frac{\xi}{2} N^A N^A + N^A f^A[A]. \tag{2.13}$$

The original version of the Lagrangian is then simply recovered by completing the square on the right hand side and integrating out the Nakanishi-Lautrup field. The BRST symmetry transformation acts onto the fields in the following way,

$$\begin{aligned} \delta_B A^A_\mu &= D^{AB}_\mu C^B, & \delta_B \bar{C}^A &= i N^A, \\ \delta_B C^A &= \frac{ig}{2} [C, C]^A, & \delta_B N^A &= 0, \end{aligned} \tag{2.14}$$

and maps bosons to fermions and vice versa. This transformation is nilpotent, $\delta_B^2 = 0$ and, as already mentioned, leaves the action invariant. The BRST symmetry can be used to define the physical Hilbert space. This is based on the observation that the Fadeev-Popov part of the action is BRST exact, i.e., it can be written as $S_{GF+FP} = \delta_B \Psi$, where Ψ is some functional of the fields. On the other hand, the Yang-Mills part of the action is also BRST invariant, but cannot be written in that way. The physical content of a

theory is thus defined by the cohomology

$$\text{Kernel } \delta_B \Big/ \text{Image } \delta_B. \tag{2.15}$$

It should be remarked that there exists another transformation with similar properties, the anti-BRST transformation $\bar{\delta}_B$ [62–65]. The anti-BRST transformation is also nilpotent and anticommutes with the standard BRST transformation. It is essentially obtained by interchanging the ghosts and anti-ghosts in the definition of the standard BRST transformation.

Having defined the path-integral properly, let us get back to the question of how to obtain the correlation functions of a theory. We already mentioned the generating functional $Z[K]$, but there are actually "more efficient" ways to store the physical information. In fact, all physics actually is contained in the "one-particle-irreducible" correlation functions. They are generated by an object called quantum effective action $\Gamma[\phi]$, which is defined as the Legendre transformation of the Schwinger functional $W[K] = -i \log Z[K]$, which itself is the generating functional of the connected correlation functions,

$$\Gamma[\phi] = \sup_K \left[W[K] - K \cdot \phi \right]. \tag{2.16}$$

The conjugated variables ϕ and K are related according to

$$\phi \equiv \langle \Phi \rangle_K = \frac{\delta W[K]}{\delta K}. \tag{2.17}$$

In other words, the field ϕ denotes the expectation value of the classical fields in the presence of the source K. From the definition of the effective action, we immediately obtain the quantum equations of motion,

$$\frac{\delta \Gamma[\phi]}{\delta \phi} = -K, \tag{2.18}$$

as well as an integro-differential equation for the effective action,

$$e^{i\Gamma[\phi]} = \int \mathcal{D}\Phi \, \text{Exp}\Big[iS[\Phi + \phi] - i \frac{\delta \Gamma[\phi]}{\delta \phi} \cdot \Phi \Big]. \tag{2.19}$$

If Γ could be obtained analytically, the theory is considered to be solved, as all physical quantities can be directly computed from Γ. Obviously, however, this is a hopeless task regarding the complexity of Eq. (2.19). There exist several approaches in trying to obtain approximative solutions. The most straightforward is of course perturbation

theory, where the integrand is expanded in powers of $\hbar$, which leads to the following one-loop expression,

$$\Gamma[\phi] = S[\phi] - \frac{i\hbar}{2} \operatorname{STr} S^{(2)} + O(\hbar^2), \tag{2.20}$$

Here, $S^{(2)}$ is the Hessian of the action and the supertrace operator STr corresponds to taking the trace over all internal indices, such as spacetime indices, color indices, spinor indices, and in particular also takes spin statistics into account, i.e., fermionic fields give rise to an additional minus sign. On the other hand, we have non-perturbative approaches such as the functional renormalization group which we will discuss in chapter 5.

The previously introduced BRST symmetry also implies an important identity satisfied by the effective action. Let us introduce another set of BRST invariant sources Ω related to the BRST transformations of the fields, i.e.,

$$e^{iW[K,\Omega]} = \int \mathcal{D}\Phi \; e^{iS[\Phi]+iK\cdot\Phi+i\Omega\cdot\delta_B\Phi}, \tag{2.21}$$

where Φ shall also contain the Nakanishi-Lautrup field and correspondingly the related source also appears in K and Ω. However, note that $\Omega_{\mathfrak{N}} = 0$ and $\Omega_{\bar{\mathfrak{C}}} = i\mathfrak{N}$ because $\delta_B\mathfrak{N} = 0$ and $\delta_B\bar{\mathfrak{C}} = i\mathfrak{N}$, respectively. From the BRST invariance of the action and the path integral measure [66] it then follows,

$$0 = \langle \delta_B S \rangle \Longrightarrow K \cdot \langle \delta_B \Phi \rangle = 0. \tag{2.22}$$

Next, we use a slightly modified definition of the effective action given by

$$\Gamma[\phi, \Omega] = \sup_K [W[K, \Omega] - K \cdot \phi] \tag{2.23}$$

to infer

$$\frac{\delta\Gamma}{\delta\phi} = -K; \quad \frac{\delta\Gamma}{\delta\Omega} = \frac{\delta W}{\delta\Omega}. \tag{2.24}$$

Combining this with the relation

$$\langle \delta_B \Phi \rangle = \frac{\delta W[K,\Omega]}{i\delta\Omega} \tag{2.25}$$

we can rewrite Eq. (2.22) according to

$$\frac{\delta\Gamma}{\delta\phi}\cdot\frac{\delta\Gamma}{\delta K}=0. \tag{2.26}$$

This equation is often referred to as the master equation. It allows to derive further identities for the correlation functions, the so-called generalized Ward-Takahashi or Slavnov-Taylor identities, by applying functional derivatives with respect to the fields to the master equation. These identities play an important role in the process of renormalization, especially since they have to hold at all orders in perturbation theory.

The derivation of the master equation has been presented here in a rather sketchy way. For a more serious treatment and further details, see, for example [67, 68].

2.2 Dual superconductivity picture and confinement

One of the most peculiar phenomena within the theory of strong interactions is the fact that color charged objects, i.e., gluons and quarks, can only be obersevd in color-neutral states. This effect is known as confinement and still lacks a profound analytical explanation. Among a variety of approaches such as the Kugo-Ojima scenario [69, 70] or the Gribov-Zwanziger scenario [58, 71], the toplogical approaches and in particular the so-called dual superconductivity picture first proposed by Nambu, 't Hooft, and Mandelstam [1–4] are considered as promising candidates for explaining confinement. In this section, we want to give a short introduction to the latter one.

Just like in the ordinary superconductivity, where electrically charged electrons condense in bound states known as Cooper pairs, the dual superconductivity picture advocates the idea of a superconducting Yang-Mills vacuum consisting of a color magnetic monopole condensate. If we put any color-electrically charged objects into such a vacuum, for example a static quark-antiquark pair, the equivalent of the dual Meissner effect would confine the color electric field into nearly one-dimensional objects, the flux tubes, leading to a linearly rising potential between the quarks. For a review on this field, see, for example, [72].

Obviously, the magnetic monopoles play a central role in this picture, even though there is no experimental evidence for magnetic monopoles so far. On the other hand, there exist several examples for them at the theoretical level. For instance, provided the gauge field is singular, the so-called Dirac magnetic monopole appears in the Abelian Maxwell theory [73]. In non-Abelian gauge theories, on the other hand, the so-called 't Hooft-Polyakov magnetic monopole is shown to exist in the presence of an adjoint

Higgs scalar field through the occurrence of dynamical symmetry breaking of a gauge group G down to some subgroup H.

Moreover, it has been shown in all cases where confinement could be proven analytically, the confinement is a consequence of monopole condensates. The theories where analytical proofs exist include $4d$ compact $U(1)$ electrodynamics [74], the $3d$ Georgi-Glashow model [75], and $\mathcal{N} = 2$ super Yang-Mills theory [76, 77].

Yet, these methods heavily rely on some kind of scalar field. In QCD or pure Yang-Mills theory, however, we do not have any scalar fields at hand. One therefore has to consider another way of extracting the monopole degrees of freedom. A first method has been developed by 't Hooft and is known as "Abelian projection" [4]. The idea behind the Abelian projection is to in some sense embed the Dirac monopole of the Abelian $U(1)$ Maxwell theory into the non-Abelian gauge theory. The way to achieve this is to partially gauge fix the "non-Abelian parts" of the theory in the following way. First, we choose some arbitrary operator $\chi(x) = \chi^A(x)T^A$ in the adjoint representation. The Abelian gauge is then defined as the gauge where this operator is diagonal. For simplicity, let us restrict ourselves to the $SU(2)$ case. In the Abelian gauge the operator thus becomes proportional to the last Cartan generator, which is diagonal,

$$\chi(x) \to \chi'(x) = \bar{U}\chi(x)\bar{U}^\dagger = \frac{1}{2}\begin{pmatrix} \chi'^3(x) & 0 \\ 0 & -\chi'^3(x) \end{pmatrix}. \tag{2.27}$$

Here, we denoted the gauge transformation that diagonalized χ by $\bar{U}$ and the eigenvalues χ'^3 in the $SU(2)$ case are explicitly obtained as $\chi'^3(x) = \frac{1}{2}\sqrt{\chi^A(x)\chi^A(x)}$. They are gauge invariant but depend on the choice of χ. Let us now assume that there exist points x_0 in spacetime, where this diagonalized matrix is degenerated. In the current simple case of $SU(2)$ this implies

$$\chi'^3(x_0) = -\chi'^3(x_0) \Longleftrightarrow \chi^A(x_0) = 0. \tag{2.28}$$

It is this point in spacetime, namely at which the Abelian gauge cannot be uniquely defined due to the degeneracy, where the monopole emerges. Let us therefore consider χ in the vicinity of x_0,

$$\chi(x) = 0 + T^A\partial_\mu\chi^A(x_0)(x - x_0)^\mu + O(x^2). \tag{2.29}$$

Assuming that the gradient exists and considering the static case only, we can identify the three remaining spacetime dimensions with the three color indices $A = 1, 2, 3$ and

may write χ as

$$\chi(x) = x^A T^A = r\sin\theta\cos\phi\ T_1 + r\sin\theta\sin\phi\ T_2 + r\cos\theta\ T_3, \tag{2.30}$$

where in the last step we introduced spherical coordinates. In this specific case, the diagonalizing gauge transformation matrix is explicitly given in terms of the Euler angles,

$$\bar{U} = \begin{pmatrix} e^{i\phi}\cos\frac{\theta}{2} & \sin\frac{\theta}{2} \\ -\sin\frac{\theta}{2} & e^{-i\phi}\cos\frac{\theta}{2} \end{pmatrix}. \tag{2.31}$$

If we now consider how the gauge field transforms under this gauge transformation, one finds that the diagonal component of the inhomogeneous part $\sim \mathrm{Tr}\, T^3 \bar{U}\nabla\bar{U}^\dagger$ develops a singularity of the Dirac type,

$$A_\phi^{3\,sing} \sim \frac{1}{g}\frac{1+\cos\theta}{r\sin\theta}, \tag{2.32}$$

leading to a quantized magnetic charge $q \sim \frac{4\pi}{g}$. This sketches how monopoles can be obtained in pure Yang-Mills theory without introducing additional matter fields.

So far, we have left the choice of χ open. There are in principle infinitely many choices, some of them more clever than others. A very successful special case is the maximal Abelian gauge (MAG) [4–6]. It is related to a partial gauge fixing $G = SU(N) \to H = U(1)^{N-1}$, corresponding to a minimization of the functional

$$\int_x \mathrm{Tr}_{G/H}\, \mathfrak{A}_\mu \mathfrak{A}^\mu. \tag{2.33}$$

The residual gauge group $H = U(1)^{N-1}$ is the Cartan subgoup of $SU(N)$ and loosely speaking contains all diagonal generators of $G = SU(N)$. Hence, the minimizing condition can be understood as minimizing the off-diagonal components of the gauge field. In terms of the operator χ, this gauge is obtained from the choice $\chi \sim [\mathfrak{D}_\mu, [\mathfrak{D}^\mu, T^3]]$ for the $SU(2)$ case. The MAG has been studied extensively and produced some important results with respect to the establishment of the dual superconductivity picture.

The first is related to a gauge invariant criterion for quark confinement, the area law, according to which confinement occurs if an object called Wilson loop [78]

$$W_C = \left\langle \mathrm{Tr}\left[\mathcal{P} e^{ig\oint_C dx^\mu \mathfrak{A}_\mu}\right] \Big/ \mathrm{Tr}\,\mathbb{1} \right\rangle =: \langle \mathcal{W}_C[\mathfrak{A}] \rangle, \tag{2.34}$$

falls off exponentially with the area $|S|$ enclosed by the curve C, $W_C \sim e^{-\sigma|S|}$. $\mathcal{P}$ denotes the path ordering operator and the parameter σ is called string tension. Now, if the Yang-

Mills theory actually becomes effectively Abelian in the infrared, the Abelian projected degrees of freedom must be responsible for the confinement [7]. This phenomenon is known as infrared Abelian dominance. Evidence for this conjecture was given through lattice simulations for $SU(2)$ within the MAG [79] by showing that the string tension obtained by replacing the gauge field in Eq. (2.34) by its diagonal (Abelian) components almost completely recovers the string tension obtained with all components of the gauge field. Moreover, if the Abelian part of the gauge field is decomposed even further into a part identified with the monopoles and a photon part, the Abelian string tension is again almost fully reproduced if only the monopole part is taken into account [80].

Finally, in [8] the two-point functions of the diagonal and off-diagonal gluon propagator have been examined, with the result that off-diagonal components exhibit a rapid exponential fall-off. This indicates that the off-diagonal gluon becomes massive and decouples in the infrared, supporting the picture of an Abelian infrared effective theory.

Despite these promising results, the Abelian projection has some unpleasant features. First of all, it relies on some kind of gauge fixing, which may lead to the impression that the identified monopoles are actually mere gauge artefacts. Also, these gauges break the color symmetry explicitly, which is puzzling if one wants to understand the quark confinement as a special case of color confinement. Fortunately, based on a reformulation of Yang-Mills theory some progress has been made to overcome these flaws.

2.3 Reformulated Yang-Mills theory

The reformulation of the Yang-Mills theory is based on the Cho-Duan-Ge-Faddeev-Niemi-Shabanov decomposition [9–20] for the $SU(2)$ case, which was later extended to the $SU(N)$ case by Cho [12, 13, 21, 22] and Faddeev-Niemi [16–18]. This decomposition represents a gauge-covariant decomposition of the gauge field with respect to the stability subgroup H of $G = SU(N)$ in order to extract monopoles without introducing any singularities in the gauge field and without breaking the color symmetry explicitly. We write

$$\mathfrak{A}_\mu = \mathfrak{X}_\mu + \mathfrak{V}_\mu, \tag{2.35}$$

where $\mathfrak{X}_\mu \in \text{Lie } G/H$ is called the remaining or coset field and the second part $\mathfrak{V}_\mu$ is called the restricted or residual field. The coset field $\mathfrak{X}_\mu$ is supposed to transform homogeneously under gauge transformations, whereas the residual field $\mathfrak{V}_\mu$ carries the inhomogeneous part of the gauge transformations. The decomposition is defined upon the introduction of the so-called color field $\mathfrak{h}(x)$ together with a set of defining equations,

which we will state later.

From a novel viewpoint, however, this decomposition has been regarded as a non-linear change of variables rather than a mere decomposition. The Yang-Mills theory in the new variables has first been established in the $SU(2)$ case [23, 24] and later extended to the general $SU(N)$ case [25]. In particular, a new feature was discovered: In fact, the choice for the stability group H is unique only in the $SU(2)$ case, namely $H = U(1)$. But already in the $SU(3)$ case, for example, there are two options for the stability group,

$$H^{max} = U(1) \times U(1) \quad \text{or} \quad H^{min} = U(2). \tag{2.36}$$

The first case is referred to as maximal option and involves the definition of two color fields. In the second case, the minimal option, we only need one color field to define the decomposition. The maximal option is closely related to the MAG, as will be explained later. The minimal option, corresponding to the choice $H = U(N-1)$ for general N, is of special interest because unlike the maximal option, the stability group is here non-Abelian. We will deal with this option in particular in the third and fourth chapter and will therefore sketch some technical details of the decomposition in this option, following mainly the review article [81]. First, as mentioned earlier, we need only a single color field to define the decomposition in the minimal case. It is taken as a center element of the stability group, $\mathfrak{h} \in \text{Center } (H)$. The defining equations that determine the decomposition uniquely read

$$\mathfrak{X}^H_\mu = 0; \quad \mathfrak{D}_\mu[\mathfrak{V}]\mathfrak{h} = 0. \tag{2.37}$$

Here, we defined the covariant derivative with respect to the residual field alone, $\mathfrak{D}_\mu[\mathfrak{V}] = \partial_\mu - ig\mathfrak{V}_\mu$, as well as the so-called H-commutative part of a Lie algebra-valued field, $\mathfrak{A}^H_\mu := \mathfrak{A}_\mu - \frac{2(N-1)}{N}[\mathfrak{h}, [\mathfrak{h}, \mathfrak{A}_\mu]]$. In this set-up, the decomposition reads

$$\begin{aligned}
\mathfrak{X}_\mu &= -\frac{i}{g}\frac{2(N-1)}{N}[\mathfrak{h}, \mathfrak{D}_\mu[\mathfrak{A}]\mathfrak{h}], \\
\mathfrak{V}_\mu &= \left(\mathfrak{A}_\mu - \frac{2(N-1)}{N}[\mathfrak{h}, [\mathfrak{h}, \mathfrak{A}_\mu]]\right) + \frac{i}{g}\frac{2(N-1)}{N}[\mathfrak{h}, \partial_\mu \mathfrak{h}] \\
&= \mathfrak{c}_\mu + \mathfrak{B}_\mu,
\end{aligned} \tag{2.38}$$

where $\mathfrak{c}_\mu \in \text{Lie } H$ is the H-commutative part of the (full) gauge field $\mathfrak{A}_\mu$ and $\mathfrak{B}_\mu = \mathfrak{V}_\mu - \mathfrak{c}_\mu \in \text{Lie } G/H$ is the remaining (magnetic) part of the residual gauge field $\mathfrak{V}_\mu$.

Next, the coordinate transformation

$$\{\mathfrak{A}_\mu\} \to \{\mathfrak{X}_\mu, \mathfrak{c}_\mu, \mathfrak{h}\} \tag{2.39}$$

should be performed. However, two problems arise. First, if one naively counts the degrees of freedom, the free parameters of the new variables exceed those of the original Yang-Mills theory. Second, the introduction of the color field enlarges the original gauge symmetry by rotations along the axis in color space defined by the color field, $SU(N) \to [SU(N)]_{\mathfrak{A}} \times [SU(N)/H]_{\mathfrak{h}}$. Both is taken care of by imposing a constraint called reduction condition,

$$\mathfrak{D}_\mu[\mathfrak{V}]\mathfrak{X}^\mu = 0 \Longleftrightarrow [\mathfrak{h}, \mathfrak{D}_\mu[\mathfrak{A}]\mathfrak{D}^\mu[\mathfrak{A}]\mathfrak{h}] = 0, \tag{2.40}$$

which corresponds to minimizing the functional

$$\int_x \mathrm{Tr}_{G/H}\left(\mathfrak{X}_\mu \mathfrak{X}^\mu\right). \tag{2.41}$$

The reduction condition can be incorporated into the path integral following the Faddeev-Popov trick. However, it should be emphasized that this procedure is qualitatively different from the usual gauge fixing procedure. Even though the reduction condition is imposed, the theory is still invariant under local $SU(N)$ gauge transformations, i.e., the actual gauge fixing still has to be performed.

Now, the strong advantage of this construction is the following. Upon rewriting the contour integral in the Wilson loop operator into a surface integral via a non-Abelian Stokes theorem [82–85] it is shown that the Wilson loop operator in terms of the full gauge field is rewritten as

$$\mathcal{W}_C[\mathfrak{A}] = \mathcal{W}_C[\mathfrak{V}] = \mathcal{W}_\Sigma[F_V], \tag{2.42}$$

where Σ is the surface bounded by C and $F_V = 2\,\mathrm{Tr}\left(\mathfrak{h}\ \mathfrak{F}_{\mu\nu}[\mathfrak{V}]\right)$. The point is that the quantity F_V is gauge invariant, because $\mathfrak{h}$ as well as $\mathfrak{F}_{\mu\nu}[\mathfrak{V}]$ transform homogeneously. This is the advantage over the usual Abelian projection, which is recovered by choosing a constant, i.e. spacetime-independent, color field.

The relation (2.42) does not immediately imply the equivalent to the Abelian dominance[2], which reads $\langle \mathcal{W}_C[\mathfrak{A}] \rangle = \langle \mathcal{W}_C[\mathfrak{V}] \rangle$. However, within this reformulation not only the "Abelian dominance" has been explicitly confirmed in numerical simulations for the

[2]It is only an equivalent, because in the minimal option the stability group $H = U(N-1)$ is Abelian only in the case of $N = 2$.

$SU(2)$ and $SU(3)$ case, but also the exponential fall-off of the two-point function related to the coset degrees of freedom has been obtained [26–28].

In the upcoming chapters of this thesis, we try to establish analytical arguments for the decoupling of the coset degrees of freedom in the infrared, mainly arguing for a dynamical generation of a mass dimension-two condensate $\langle \mathrm{Tr}_{G/H}(\mathfrak{X}_\mu \mathfrak{X}^\mu - 2i\xi \mathfrak{C}\bar{\mathfrak{C}})\rangle$. Due to the fact that the coset field transforms homogeneously, such a condensate would not be ruled out by gauge invariance [23]. If it exists, it could induce an effective mass term for the coset field through the quartic interaction term coming from the Yang-Mills action.

A first step to approach the question as to whether the condensate really exists or not, are perturbative calculations. However, in practice, an analytical treatment of the color field would be rather difficult due to its non-trivial relation to the gauge field through the reduction condition. For simplicity, we will therefore consider the decomposition for a fixed color field. The consequences of this approximation will be discussed in the next chapter.

Chapter 3

Renormalization of $SU(N)$ Yang-Mills theory with $U(N-1)$ stability group

With the goal of establishing the mass dimension-two condensate within the reformulated Yang-Mills theory in the minimal option in mind, we first perform a perturbative analysis of this theory at one-loop level. Even though formally, a perturbative analysis is only valid for small couplings, it can give insight at least into the principle behavior of the theory. Moreover, any non-perturbative study must correctly reproduce the small coupling regime, and thus the results obtained in this chapter provide a consistency check for upcoming non-perturbative investigations.

In this chapter and throughout this thesis, we only consider the approximation of a fixed color field. While the fixed choice explicitly breaks color symmetry just like in the MAG case, this simplification is reasonable for discussing the existence of the condensate. At this stage, we do not focus on the gauge invariant extraction of the monopoles, which clearly would not be possible in this scenario. The breaking of the color symmetry manifests itself in the fact that the reduction condition no longer preserves the local $SU(N)$ gauge invariance, but breaks the gauge symmetry down to the stability group, $SU(N) \to H = U(N-1)$. However, despite the broken gauge invariance we are still able to define an (on-shell) BRST invariant dimension-two composite operator, which will serve as the candidate for the desired condensate. In this chapter, we explain in detail the decomposition of the Lagrangian in the minimal option for the fixed color field. Then, a one-loop analysis of the obtained theory is performed. Knowledge of the standard renormalization group (RG) functions is required to discuss the multiplicative renormalizability of the composite operator, which in turn is a necessary condition for the existence of the condensate. The results obtained in this chapter are partly published in [86, 87].

3.1 Decomposition of the Lagrangian

3.1.1 Algebra splitting and gauge fixing

In this subsection, we discuss the particular shape of the Lagrangian in the minimal option of the reformulated Yang-Mills theory for the fixed choice of the color field. According to the explanations in the previous chapter, in the minimal option, we take the color field in the center of the stability group $H = U(N-1)$. Therefore,

$$\mathfrak{h} \equiv T^{N^2-1}, \tag{3.1}$$

where T^A is the Ath standard generator of the Lie algebra $\mathfrak{g}$ of $G = SU(N)$ and thus T^{N^2-1} is the last Cartan generator. Considering Eq. (2.38), the fixed choice for the color field ($\partial_\mu \mathfrak{h} = 0$) implies that

$$\mathfrak{V}_\mu = \left(\mathfrak{A}_\mu - \frac{2(N-1)}{N} [\mathfrak{h}, [\mathfrak{h}, \mathfrak{A}_\mu]] \right) = \mathfrak{c}_\mu, \tag{3.2}$$

i.e., $\mathfrak{B}_\mu = 0$. Therefore, our new field variables are the coset field $\mathfrak{X}_\mu$ and the residual field $\mathfrak{V}_\mu$. Next, we choose a convenient basis of the color algebra. Suitable for the decomposition is the following,

$$\begin{aligned} \mathbf{e}_a(x) &= e_a^A(x) T_A \in \text{Lie } G/H, \quad a, b, c, d, e = 1, ..., \dim \text{Lie } G/H, \\ \mathbf{u}_J(x) &= u_J^A(x) T_A \in \text{Lie } H, \quad J, K, L, M, N = 1, ..., \dim \text{Lie } H, \end{aligned} \tag{3.3}$$

with the normalization

$$\text{Tr}[\mathbf{e}_a, \mathbf{e}_b] = \frac{1}{2}\delta_{ab}, \quad \text{Tr}[\mathbf{u}_J, \mathbf{u}_K] = \frac{1}{2}\delta_{JK}, \quad \text{Tr}[\mathbf{e}_a, \mathbf{u}_J] = 0. \tag{3.4}$$

In the specific case of $G = SU(N)$ and $H = U(N-1)$ we furthermore have

$$[\mathbf{e}_a, \mathbf{e}_b] = i f^{abJ} \mathbf{u}_J, \quad [\mathbf{u}_J, \mathbf{e}_a] = i f^{abJ} \mathbf{e}_b, \quad [\mathbf{u}_J, \mathbf{u}_K] = i f^{JKL} \mathbf{u}_L, \tag{3.5}$$

and in particular $f^{abc} = f^{aJK} = 0$. Moreover, we will see later that from the viewpoint of renormalization, we have to further decompose $H = U(N-1) = SU(N-1) \times U(1)$, where the Abelian $U(1)$ sector denotes the center of $U(N-1)$. The corresponding generator is T^{N^2-1}. We manifest this splitting by introducing another index $\gamma \equiv N^2 - 1$ and denoting

the remaining generators within the subgroup H by $i, j, k, l, ...$, such that we find

$$f^{jkl} \neq 0; \quad f^{\gamma JK} = 0. \tag{3.6}$$

In the case of the fixed color field, the basis further simplifies and allows us to expand the coset field $\mathfrak{X}_\mu$ and the residual field $\mathfrak{V}_\mu$ according to

$$\begin{aligned} \mathfrak{X}_\mu &= X^a_\mu T^a \in \mathfrak{su}(N) - \mathfrak{u}(N-1), \\ \mathfrak{V}_\mu &= V^J_\mu T^J = V^j_\mu T^j + V^\gamma_\mu T^\gamma \in \mathfrak{su}(N-1) + \mathfrak{u}(1). \end{aligned} \tag{3.7}$$

In other words, the basis becomes spacetime independent.[1] Having established this basis, the next step is to write down the Lagrangian in this decomposition. The Yang-Mills sector decomposes as

$$\mathfrak{L}_{YM} = -\frac{1}{4} F^a_{\mu\nu} F^{\mu\nu a} - \frac{1}{4} F^j_{\mu\nu} F^{\mu\nu j} - \frac{1}{4} F^\gamma_{\mu\nu} F^{\mu\nu\gamma}, \tag{3.8}$$

where the field strength tensors of the various sectors are given by

$$\begin{aligned} F^a_{\mu\nu} &= D^{ab}_\mu X^b_\nu - D^{ab}_\nu X^b_\mu, \\ F^j_{\mu\nu} &= \partial_\mu V^j_\nu - \partial_\nu V^j_\mu + g f^{jab} X^a_\mu X^b_\nu + g f^{jkl} V^k_\mu V^l_\nu, \\ F^\gamma_{\mu\nu} &= \partial_\mu V^\gamma_\nu - \partial_\nu V^\gamma_\mu + g f^{\gamma ab} X^a_\mu X^b_\nu. \end{aligned} \tag{3.9}$$

The covariant derivative is understood to contain only the residual field,

$$D^{ab}_\mu[V] \equiv \delta^{ab} \partial_\mu + g f^{aJb} V^J_\mu. \tag{3.10}$$

Next, we turn to the gauge fixing of this theory. We introduce ghosts $\mathfrak{C}$, anti-ghosts $\bar{\mathfrak{C}}$, and the Nakanishi-Lautrup field $\mathfrak{N}$, which are decomposed according to the different

[1] As a particular example, in the $SU(2)$ case we have $a \in \{1, 2\}$ and $\gamma = 3$, while the $SU(N-1)$ sector is absent. For $SU(3)$ we have $a \in \{4, 5, 6, 7\}$, $j \in \{1, 2, 3\}$, and $\gamma = 8$.

sectors of the Lie algebra,

$$\begin{aligned}\mathfrak{C} &= \omega^a T^a + C^j T^j + C^\gamma T^\gamma,\\ \bar{\mathfrak{C}} &= \bar{\omega}^a T^a + \bar{C}^j T^j + \bar{C}^\gamma T^\gamma,\\ \mathfrak{N} &= B^a T^a + N^j T^j + N^\gamma T^\gamma.\end{aligned} \tag{3.11}$$

The BRST and anti-BRST transformations are then expressed as follows,

$$\begin{aligned}\delta_B X^a_\mu &= D^{ab}_\mu[V]\omega^b + g f^{abJ} X^b_\mu C^J, & \delta_B C^J &= -\frac{g}{2} f^{JKL} C^K C^L - \frac{g}{2} f^{Jab}\omega^a\omega^b,\\ \delta_B V^J_\mu &= \partial_\mu C^J + g f^{JKL} V^K_\mu C^L + g f^{Jab} X^a_\mu \omega^b, & \delta_B\bar{\omega}^a &= iB^a, \quad \delta_B\bar{C}^J = iN^J,\\ \delta_B\omega^a &= -g f^{abJ}\omega^b C^J, & \delta_B B^a &= \delta_B N^J = 0,\end{aligned} \tag{3.12}$$

and

$$\begin{aligned}\bar{\delta}_B X^a_\mu &= D^{ab}_\mu[V]\bar{\omega}^b + g f^{abJ} X^b_\mu \bar{C}^J, & \bar{\delta}_B \bar{C}^J &= -\frac{g}{2} f^{JKL} \bar{C}^K \bar{C}^L - \frac{g}{2} f^{Jab}\bar{\omega}^a\bar{\omega}^b,\\ \bar{\delta}_B V^J_\mu &= \partial_\mu \bar{C}^J + g f^{JKL} V^K_\mu \bar{C}^L + g f^{Jab} X^a_\mu \bar{\omega}^b, & \bar{\delta}_B\omega^a &= i\bar{B}^a, \quad \bar{\delta}_B C^J = i\bar{N}^J,\\ \bar{\delta}_B\bar{\omega}^a &= -g f^{abJ}\bar{\omega}^b \bar{C}^J, & \bar{\delta}_B \bar{B}^a &= \bar{\delta}_B \bar{N}^J = 0.\end{aligned} \tag{3.13}$$

In the case of the anti-BRST transformations (3.13) we introduced the modified Nakanishi-Lautrup field $\bar{\mathfrak{N}}$

$$\bar{\mathfrak{N}} = -\mathfrak{N} + g[\mathfrak{C}, \bar{\mathfrak{C}}] \tag{3.14}$$

in order to write the anti-BRST transformations in a more symmetric fashion to the standard BRST transformations. Both transformations are found to be nilpotent, $\delta_B^2 = \bar{\delta}_B^2 = 0$, and anticommuting, $\{\delta_B, \bar{\delta}_B\} = 0$. The gauge fixing terms can now be introduced as (anti-)BRST exact terms.

Starting with the fixing of the coset degrees of freedom corresponding to the reduction

condition we firstly calculate

$$\begin{aligned}\mathfrak{L}^{RED}_{GF+FP} &= i\delta_B\bar{\delta}_B \,\mathrm{Tr}_{G/H}\left(\mathfrak{X}_\mu\mathfrak{X}^\mu - i\xi\mathfrak{C}\bar{\mathfrak{C}}\right)\\ &= \frac{\xi}{2}B^aB^a + i\bar{\omega}^a D^{\mu ab}[V]D^{bc}_\mu[V]\omega^c + B^a D^{ab}_\mu[V]X^{\mu b} + igf^{abJ}\bar{\omega}^a(D^{\mu bc}[V]X^c_\mu)C^J\\ &- i\xi g f^{aJb}C^J\bar{\omega}^b B^a + \frac{\xi g^2}{4}f^{abJ}f^{cdJ}\bar{\omega}^a\bar{\omega}^b\omega^c\omega^d + ig^2 f^{abJ}f^{cdJ}X^{\mu a}X^c_\mu\bar{\omega}^b\omega^d\\ &- \frac{\xi g^2}{4}f^{jkl}f^{ajb}\bar{\omega}^a\bar{\omega}^b C^kC^l,\end{aligned} \tag{3.15}$$

with ξ being the related "gauge fixing" parameter. Completing the square for the Nakanishi-Lautrup field B^a and integrating it out we obtain the equation of motion

$$B^a = -\frac{1}{\xi}D^{ab}_\mu X^{\mu b} + igf^{abJ}\bar{\omega}^b C^J, \tag{3.16}$$

and arrive at the coset gauge fixing Lagrangian corresponding to the reduction condition,

$$\begin{aligned}\mathfrak{L}^{RED}_{GF+FP} &= -\frac{1}{2\xi}(D^{ab}_\mu X^\mu_b)^2 + i\bar{\omega}^a D^\mu_{ab}D^{bc}_\mu\omega^c\\ &+ \frac{\xi g^2}{4}f^{cdJ}f^{Jab}\bar{\omega}^a\bar{\omega}^b\omega^c\omega^d - ig^2 f^{aJb}f^{Jcd}\bar{\omega}^b X^\mu_a X^c_\mu\omega^d\\ &- \frac{\xi}{2}g^2 f^{acK}f^{abJ}\bar{\omega}^b\bar{\omega}^c C^JC^K - \frac{\xi g^2}{4}f^{JKL}f^{aJb}\bar{\omega}^a C^K C^L\bar{\omega}^b.\end{aligned} \tag{3.17}$$

Upon careful usage of the Jacobi identity, it is shown that the last two terms cancel, yielding the final result

$$\begin{aligned}\mathfrak{L}^{RED}_{GF+FP} &= -\frac{1}{2\xi}(D^{ab}_\mu[V]X^{\mu b})^2 + i\bar{\omega}^a D^{\mu ab}[V]D^{bc}_\mu[V]\omega^c\\ &+ \frac{\xi g^2}{4}f^{abJ}f^{cdJ}\bar{\omega}^a\bar{\omega}^b\omega^c\omega^d + ig^2 f^{abJ}f^{cdJ}X^{\mu a}X^c_\mu\bar{\omega}^b\omega^d.\end{aligned} \tag{3.18}$$

Let us make a short comment on the unusual four-ghost interaction term appearing in Eq. (3.18). Since the reduction condition is a non-linear constraint, the standard introduction of the corresponding "gauge fixing" term according to

$$\mathfrak{L}'^{\,RED}_{GF+FP} = -i\delta_B\left(\bar{\omega}^a\left[D^{ab}_\mu X^{\mu b} + \frac{\xi}{2}B^a\right]\right) \tag{3.19}$$

will always generate two-gluon-two-ghost interactions, which in turn generate four-ghost interactions at higher loop order. It is therefore necessary to include such interactions at the tree level [88], which explains the choice for our coset gauge fixing construction.

Concerning the gauge fixing of the residual gauge group $H = U(N-1)$, we adopt the

standard Lorenz gauge, respecting the decomposition $U(N-1) = SU(N-1) \times U(1)$ by introducing different gauge fixing parameters λ and α, respectively. Thus, we write

$$\mathfrak{L}^{RES}_{GF+FP} = -i\delta_B \left(\bar{C}^j \left[\partial_\mu V^{\mu j} + \frac{\lambda}{2} N^j \right] \right) - i\delta_B \left(\bar{C}^\gamma \left[\partial_\mu V^{\mu \gamma} + \frac{\alpha}{2} N^\gamma \right] \right), \tag{3.20}$$

which after integrating out the Nakanishi-Lautrup field becomes

$$\begin{aligned} \mathfrak{L}^{RES}_{GF+FP} = &-\frac{1}{2\lambda} \left(\partial_\mu V^{\mu j} \right)^2 - \frac{1}{2\alpha} \left(\partial_\mu V^{\mu \gamma} \right)^2 + i \bar{C}^J \partial^2 C^J \\ &+ i g f^{jkl} \bar{C}^j \partial_\mu (V^{\mu k} C^l) + i g f^{Jab} \bar{C}^J \partial_\mu (X^{\mu a} \omega^b). \end{aligned} \tag{3.21}$$

The corresponding equations of motion for the Nakanishi-Lautrup field read

$$N^j = -\frac{1}{\lambda} \partial_\mu V^{\mu j}, \qquad N^\gamma = -\frac{1}{\alpha} \partial_\mu V^{\mu \gamma}. \tag{3.22}$$

This completes the construction of the gauge-fixed Lagrangian of $SU(N)$ Yang-Mills theory with $U(N-1)$ stability group,

$$\mathfrak{L} = \mathfrak{L}_{YM} + \mathfrak{L}^{RED}_{GF+FP} + \mathfrak{L}^{RES}_{GF+FP}. \tag{3.23}$$

In the next subsection we want to derive some important color algebra relations which are necessary for the (one-)loop calculations, before we close the section with stating the Feynman rules related to the previously defined Lagrangian.

3.1.2 Color algebra relations

Let us denote the full range of color indices by capital letters, i.e., $A, B, C, D, ... = 1, 2, ..., \dim \mathfrak{g}$. Furthermore, we will frequently use that $\dim \text{Lie } G/H = 2(N-1) \equiv d_{G/H}$. Then, starting from the well-known relation for $SU(N)$ structure constants

$$f^{ACD} f^{BCD} = N \delta^{AB}, \tag{3.24}$$

we can derive

$$\begin{aligned} f^{\gamma ab} f^{\gamma ab} &= N, & 2 f^{acj} f^{bcj} + 2 f^{ac\gamma} f^{bc\gamma} &= N \delta^{ab}, \\ f^{\gamma ab} f^{jab} &= 0, & f^{iab} f^{jab} + f^{inm} f^{jnm} &= N \delta^{ij}. \end{aligned} \tag{3.25}$$

Similarly, in the $SU(N-1)$ sector of the residual group $H = U(N-1)$ we must have

$$(N-1)\delta^{ij} = f^{imn} f^{jmn}. \tag{3.26}$$

As a last step, we need a relation for $f^{ac\gamma} f^{bc\gamma}$. This can be obtained by considering the general expression for the residual field, cf. Eq. (2.38):

$$\mathfrak{V}_\mu = \mathfrak{A}_\mu - \frac{2(N-1)}{N}[\mathfrak{h}, [\mathfrak{h}, \mathfrak{A}_\mu]] + \frac{i}{g}\frac{2(N-1)}{N}[\mathfrak{h}, \partial_\mu \mathfrak{h}]. \tag{3.27}$$

Using the fact that $\mathfrak{h} \equiv T^\gamma$ ($\partial_\mu \mathfrak{h} = 0$) and that by construction $\mathfrak{V}_\mu \in \mathfrak{u}(N-1)$, i.e., $V^a_\mu \equiv 0$, we find,

$$0 = V^a_\mu = X^c_\mu \delta^{ac} + \frac{2(N-1)}{N} f^{a\gamma b} f^{b\gamma c} X^c_\mu, \tag{3.28}$$

and therefore $f^{ab\gamma} f^{cb\gamma} = \frac{N}{2(N-1)}\delta^{ac}$. This yields the following base set of color relations,

$$\begin{aligned}
&f^{\gamma ab} f^{\gamma ab} = N, && f^{iab} f^{jab} = \delta^{ij}, && f^{ab\gamma} f^{cb\gamma} = \frac{N}{2(N-1)}\delta^{ac},\\
&f^{imn} f^{jmn} = (N-1)\delta^{ij}, && f^{\gamma ab} f^{jab} = 0, && f^{abj} f^{cbj} = \frac{N(N-2)}{2(N-1)}\delta^{ac}.
\end{aligned} \tag{3.29}$$

To complete the one-loop calculations, however, we will need identities containing three structure constants. They can be obtained by contracting the base relations above with another structure constant and then using the Jacobi identity. In this way, the following relations can be obtained, which turned out to be sufficient for the upcoming calculations,

$$\begin{aligned}
f^{jmn} f^{bmc} f^{anc} &= -\frac{N-1}{2} f^{jab}, & f^{abj} f^{jec} f^{bkc} &= \frac{1}{2(N-1)} f^{aek},\\
f^{jmn} f^{nki} f^{mli} &= -\frac{N-1}{2} f^{jkl}, & f^{abj} f^{jec} f^{b\gamma c} &= -\frac{N(N-2)}{2(N-1)} f^{ae\gamma},\\
f^{jce} f^{eaM} f^{cbM} &= -\frac{1}{2} f^{jab}, & f^{\gamma ab} f^{bcM} f^{aeM} &= -\frac{N}{2} f^{ce\gamma},\\
f^{jec} f^{cmb} f^{enb} &= -\frac{1}{2} f^{jmn}, & f^{jab} f^{bcM} f^{aeM} &= -\frac{1}{2} f^{cej},\\
f^{ab\gamma} f^{jbc} f^{e\gamma c} &= -\frac{N}{2(N-1)} f^{aej}, & f^{ab\gamma} f^{\gamma bc} f^{e\gamma c} &= -\frac{N}{2(N-1)} f^{ae\gamma}.
\end{aligned} \tag{3.30}$$

3.1.3 Feynman rules

As a last step in preparation for the one-loop calculations, we state the Feynman rules derived from the Lagrangian. It is most convenient to express them in momentum space, where we adopt the following convention for the Fourier transformation,

$$\begin{aligned}
\mathfrak{A}_\mu(x) &= \int_p \mathfrak{A}_\mu(p) e^{ipx}, & \mathfrak{A}_\mu(p) &= \int_x \mathfrak{A}_\mu(x) e^{-ipx}, \\
\mathfrak{C}(x) &= \int_p \mathfrak{C}(p) e^{ipx}, & \mathfrak{C}(p) &= \int_x \mathfrak{C}(x) e^{-ipx}, \\
\bar{\mathfrak{C}}(x) &= \int_p \bar{\mathfrak{C}}(p) e^{-ipx}, & \bar{\mathfrak{C}}(p) &= \int_x \bar{\mathfrak{C}}(x) e^{ipx},
\end{aligned} \tag{3.31}$$

with $\int_p \equiv \frac{1}{(2\pi)^d} \int d^d p$. In other words, the momentum of the anti-ghost will be counted as outgoing. Finally, whenever a vertex involves ghosts, they are derived by first varying with respect to the anti-ghost and then with respect to the ghost, $\frac{\vec{\delta}}{\delta\mathfrak{C}} \frac{\vec{\delta}}{\delta\bar{\mathfrak{C}}} \mathfrak{L}$. The induced propagators are then shown in Fig. 3.1,

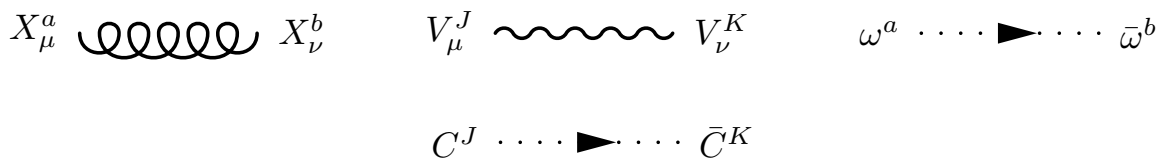

FIGURE 3.1: Propagators

and imply the Feynman rules

$$\begin{aligned}
\langle X^a_\mu X^b_\nu \rangle &= -\delta^{ab} \frac{i}{p^2} \Big(g^{\mu\nu} - (1-\xi) \frac{p_\mu p_\nu}{p^2} \Big), & \langle \omega^a \bar{\omega}^b \rangle &= -\delta^{ab} \frac{1}{p^2}, \\
\langle V^j_\mu V^k_\nu \rangle &= -\delta^{jk} \frac{i}{p^2} \Big(g^{\mu\nu} - (1-\lambda) \frac{p_\mu p_\nu}{p^2} \Big), & \langle C^j \bar{C}^k \rangle &= -\delta^{jk} \frac{1}{p^2}, \\
\langle V^\gamma_\mu V^\gamma_\nu \rangle &= \quad - \frac{i}{p^2} \Big(g^{\mu\nu} - (1-\alpha) \frac{p_\mu p_\nu}{p^2} \Big), & \langle C^\gamma \bar{C}^\gamma \rangle &= \quad - \frac{1}{p^2}.
\end{aligned} \tag{3.32}$$

Furthermore, there exist five three-field vertices, see Fig. 3.2,

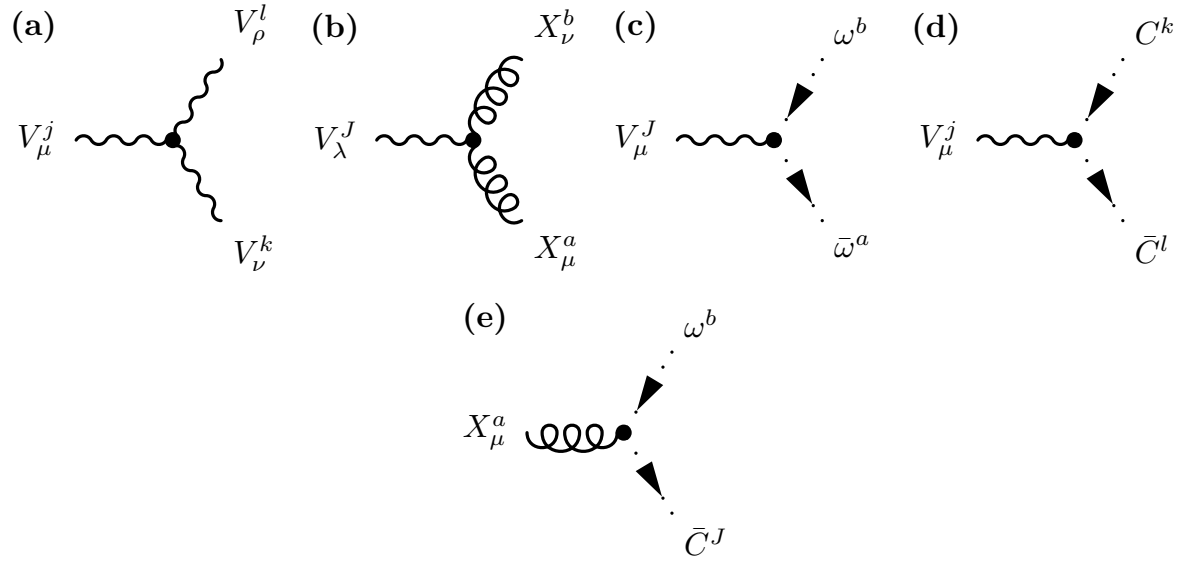

FIGURE 3.2: Three-field vertices.

with the Feynman rules

$$\textbf{(a)}\quad i\langle V_\mu^j(p)V_\nu^k(q)V_\rho^l(r)\rangle = \delta_{p+q+r} g f^{jkl}\left\{g_{\mu\nu}(p-q)_\rho + g_{\mu\rho}(r-p)_\nu + g_{\nu\rho}(q-r)_\mu\right\},$$

$$\textbf{(b)}\quad i\langle X_\mu^a(p)X_\nu^b(q)V_\lambda^J(r)\rangle =$$

$$\delta_{p+q+r} g f^{abJ}\Big\{g_{\mu\nu}(q-p)_\lambda + g_{\lambda\nu}\left(r-q-\xi^{-1}p\right)_\mu - g_{\lambda\mu}\left(r-p-\xi^{-1}q\right)_\nu\Big\},$$

$$\textbf{(c)}\quad i\langle V_\mu^J(r)\omega^b(q)\bar{\omega}^a(p)\rangle = -\delta_{q+r-p} i g f^{aJb}(q+p)_\mu,$$

$$\textbf{(d)}\quad i\langle V_\mu^j(r)C^k(q)\bar{C}^l(p)\rangle = -\delta_{q+r-p} i g f^{jkl} p_\mu,$$

$$\textbf{(e)}\quad i\langle X_\mu^a(r)\omega^b(q)\bar{C}^J(p) = -\delta_{r+q-p} i g f^{abJ} p_\mu. \tag{3.33}$$

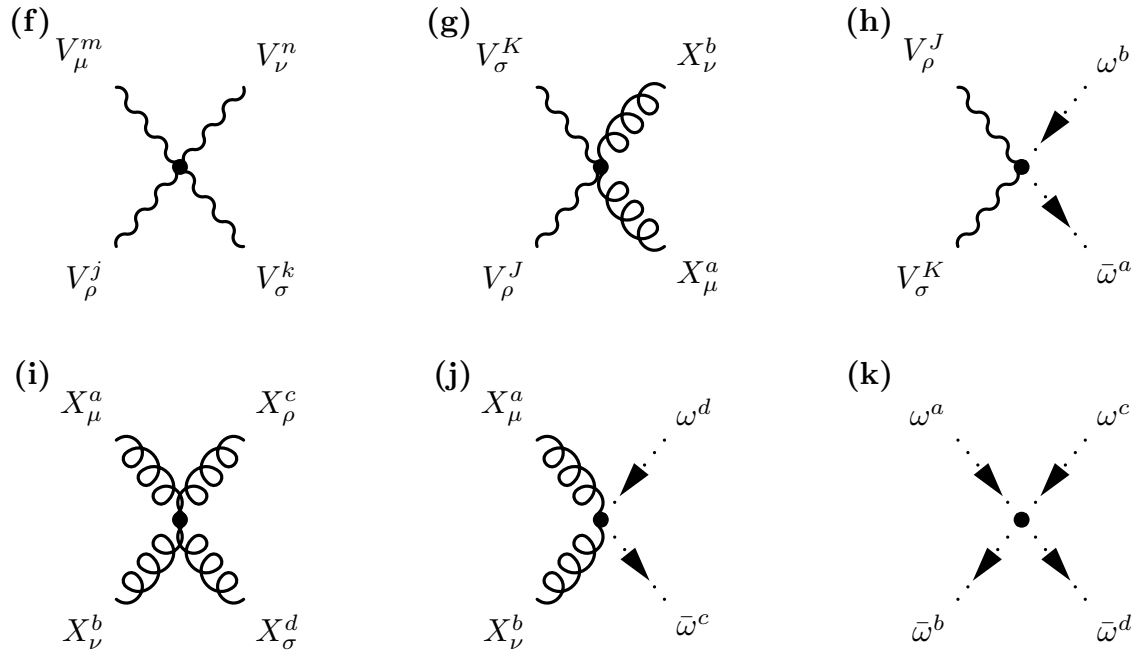

FIGURE 3.3: Four-field vertices.

Moreover, we find six four-field vertices, see Fig. 3.3, and upon defining $I_{\mu\nu,\rho\sigma} = g_{\mu\rho}g_{\nu\sigma} - g_{\mu\sigma}g_{\nu\rho}$ we obtain the Feynman rules

(f) $i\langle V_\mu^m(p)V_\nu^n(q)V_\rho^j(r)V_\sigma^k(s)\rangle =$

$$- ig^2\delta_{p+q+r+s}\{f^{mnl}f^{jkl}I_{\mu\nu,\rho\sigma} + f^{mjl}f^{nkl}I_{\mu\rho,\nu\sigma} + f^{mkl}f^{njl}I_{\mu\sigma,\nu\rho}\},$$

(g) $i\langle X_\mu^a(p)X_\nu^b(q)V_\rho^J(r)V_\sigma^K(s)\rangle = -ig^2\delta_{p+q+r+s}\left\{2f^{abM}f^{JKM}I_{\mu\nu,\rho\sigma}\right.$

$$\left. + f^{cKa}f^{bJc}\left(\left(1-\xi^{-1}\right)g_{\mu\sigma}g_{\rho\nu} - g_{\mu\nu}g_{\rho\sigma}\right) + f^{cJa}f^{bKc}\left(\left(1-\xi^{-1}\right)g_{\mu\rho}g_{\nu\sigma} - g_{\mu\nu}g_{\rho\sigma}\right)\right\},$$

(h) $i\langle V_\rho^J(r)V_\sigma^K(s)\omega^b(q)\bar{\omega}^a(p)\rangle = -g^2\delta_{q-p+r+s}g_{\rho\sigma}(f^{aJc}f^{cKb} + f^{aKc}f^{cJb}),$

$$\textbf{(i)}\quad i\langle X^a_\mu(p)X^b_\nu(q)X^c_\rho(r)X^d_\sigma(s)\rangle =$$

$$-ig^2\delta_{p+q+r+s}\{f^{acJ}f^{bdJ}I_{\mu\rho,\nu\sigma}+f^{adJ}f^{bcJ}I_{\mu\sigma,\nu\rho}+f^{abJ}f^{cdJ}I_{\mu\nu,\rho\sigma}\},$$

$$\textbf{(j)}\quad i\langle X^a_\mu(r)X^b_\nu(s)\omega^d(q)\bar{\omega}^c(p)\rangle = \delta_{r+s+q-p}g^2g_{\mu\nu}\left\{f^{aJc}f^{bdJ}+f^{bJc}f^{adJ}\right\},$$

$$\textbf{(k)}\quad i\langle \omega^a(q)\bar{\omega}^b(p)\omega^c(r)\bar{\omega}^d(s)\rangle = -i\xi g^2\delta_{q+r-p-s}f^{acJ}f^{Jbd}.$$

(3.34)

3.2 One-loop renormalization

Having defined the various kinds of gluon and ghost species and the Feynman rules, we can finally turn to answering the question of one-loop renormalizability. After introducing renormalization factors for the fields $\Phi = Z_\Phi^{1/2}\Phi_R$ and parameters $\zeta = Z_\zeta \zeta_R$, we must show that all divergences resulting from one-loop diagrams can be reabsorbed into these renormalization factors.

3.2.1 Technical preparations

More concrete, we introduce the renormalization factors as follows,

$$\begin{aligned}
X_\mu^a &= Z_X^{1/2} X_{\mu R}^a, & V_\mu^j &= Z_V^{1/2} V_{\mu R}^j, & V_\mu^\gamma &= \tilde{Z}_V^{1/2} V_{\mu R}^\gamma, & g &= Z_g g_R, \\
C^j &= Z_C^{1/2} C_R^j, & \bar{C}^j &= Z_{\bar{C}}^{1/2} \bar{C}_R^j, & C^\gamma &= \tilde{Z}_C^{1/2} C_R^\gamma, & \bar{C}^\gamma &= \tilde{Z}_{\bar{C}}^{1/2} \bar{C}_R^\gamma, \\
\omega^a &= Z_\omega^{1/2} \omega_R^a, & \bar{\omega}^a &= Z_\omega^{1/2} \bar{\omega}_R^a, & \xi &= Z_\xi \xi_R, & \alpha &= Z_\alpha \alpha_R, \\
\lambda &= Z_\lambda \lambda_R.
\end{aligned} \tag{3.35}$$

As mentioned earlier, we introduce different renormalization factors for the $U(1)$ residual field V_μ^γ and the $SU(N-1)$ residual fields V_μ^j, as we are going to see that both types receive different loop corrections. The same distinction must be made for the residual ghosts and anti-ghosts. Moreover, as discussed in [89], only the renormalization constants for the coset ghost and anti-ghost can be chosen to be identical, while in case of the $U(1)$ and $SU(N-1)$ sector, ghost and anti-ghost renormalize in different ways, respectively. Having to respect all these renormalization factors, the counterterm Lagrangian becomes a lengthy expression, containing more than 30 interactions. We therefore present it only in appendix A. The most convenient way of determining all renormalization factors is to calculate the divergences of the following n-point functions,

- 2-point functions: $\langle X_\mu^a X_\nu^b \rangle$, $\langle V_\mu^j V_\nu^k \rangle$, $\langle V_\mu^\gamma V_\nu^\gamma \rangle$, $\langle \omega^a \bar{\omega}^b \rangle$, $\langle C^j \bar{C}^k \rangle$, $\langle C^\gamma \bar{C}^\gamma \rangle$
- 3-point functions: $\langle V_\mu^j C^k \bar{C}^l \rangle$, $\langle X_\mu^a \omega^b \bar{C}^j \rangle$, $\langle X_\mu^a \omega^b \bar{C}^\gamma \rangle$.

In this thesis, we adopt the dimensional regularization scheme [90]. The main task will be to calculate momentum integrals à la

$$\int \frac{d^4q}{(2\pi)^4} f(q,p_i) \left[\prod_n \left((q+e_n)^2 - m_n^2 \right)^{\alpha_n} \right]^{-1}, \tag{3.36}$$

where q is the loop momentum, e_n some sum of the external momenta p_j , m_n are particle masses and $f(q,p_i)$ results from the contraction of the Feynman vertex rules. A comprehensive introduction to solving this kind of integrals in even more complicated settings can be found in [91] and references therein. At this stage, we are only dealing with a massless theory, $m_n = 0$. The strategy to solve such integrals and to extract their divergent part is as follows. First, we promote the integral to d dimensions, $\frac{d^4q}{(2\pi)^4} \to \frac{d^dq}{(2\pi)^d}$. Next, one applies the so-called Feynman parametrization,

$$\begin{aligned} \frac{1}{[q_1^2]^{\alpha_1} \cdots [q_n^2]^{\alpha_n}} = \frac{\Gamma\left(\sum_i \alpha_i\right)}{\prod_i \Gamma(\alpha_i)} \int_0^1 dx_1 \int_0^{1-x_1} dx_2 \cdots \int_0^{1-\ldots-x_{n-1}} dx_n \\ \times \frac{x_1^{\alpha_1-1} x_2^{\alpha_2-1} \cdots (1-x_1-\ldots-x_{n-1})^{\alpha_n-1}}{[x_1 q_1^2 + x_2 q_2^2 + \ldots + (1-x_1-\ldots-x_{n-1}) q_n^2]^{\sum_i \alpha_i}}, \end{aligned} \tag{3.37}$$

where, in the massless case, $q_i = q + e_i$ and $\Gamma(x)$ denotes Euler's Gamma function. The denominator on the right hand side can be combined into $Q^2 - \Delta(p_i, x_i)$, with $Q^2 = \left(q + \sum_i x_i e_i\right)^2$ and the effective mass $\Delta(p_i, x_i)$ is a polynomial of the Feynman parameters x_i, squared momenta p_i^2 and scalar products $p_i \cdot p_j$. Changing the integration variable from q to Q one obtains

$$\begin{aligned} &\int \frac{d^dq}{(2\pi)^d} f(q,p_i) \left[\prod_n \left((q+e_n)^2 - m_n^2 \right)^{\alpha_n} \right]^{-1} \\ &= \frac{\Gamma\left(\sum_i \alpha_i\right)}{\prod_i \Gamma(\alpha_i)} \int_0^1 dx_1 \int_0^{1-x_1} dx_2 \cdots \int_0^{1-\ldots-x_{n-1}} dx_n \int \frac{d^dQ}{(2\pi)^d} \frac{f\left(Q - \sum_i x_i e_i, p_i\right)}{(Q^2-\Delta)^{\sum_i \alpha_i}}. \end{aligned} \tag{3.38}$$

Using the fact that only terms even in Q can contribute, the momentum integral always boils down to the following type and its well-known solution,

$$I[r,m] = \int_Q \frac{(Q^2)^r}{(Q^2-\Delta)^m} = \frac{i}{(4\pi)^{d/2}} (-1)^{r-m} \Delta^{d/2+r-m} \frac{\Gamma[r+d/2]\Gamma[m-r-d/2]}{\Gamma[m]\Gamma[d/2]}. \tag{3.39}$$

Only one more subtlety may arise. The function $f\left(Q - \sum_i x_i e_i, p_i\right)$ can in principle contain scalar products $Q \cdot p_i$, such that on the left hand side of Eq. (3.39) free indices of Q may appear. Throughout this thesis, only two relevant cases occur. The first one reads

$$\int_Q \frac{(Q^2)^r Q^\mu Q^\nu}{(Q^2-\Delta)^m}. \tag{3.40}$$

For symmetry reasons, this can be written as

$$\int_Q \frac{(Q^2)^r Q^\mu Q^\nu}{(Q^2-\Delta)^m} = A_1 g^{\mu\nu} I[r+1,m]. \tag{3.41}$$

Contracting both sides with $g_{\mu\nu}$ yields $A_1 = 1/d$ and thus we obtain

$$\int_Q \frac{(Q^2)^r Q^\mu Q^\nu}{(Q^2-\Delta)^m} = \frac{g^{\mu\nu}}{d} I[r+1,m]. \tag{3.42}$$

The second important case is treated similarly,

$$\int_Q \frac{(Q^2)^r Q^\mu Q^\nu Q^\rho Q^\sigma}{(Q^2-\Delta)^m} = A_1 g^{\mu\nu}g^{\rho\sigma} I[r+2,m] + A_2 g^{\mu\rho}g^{\nu\sigma} I[r+2,m] + A_3 g^{\mu\sigma}g^{\nu\rho} I[r+2,m]. \tag{3.43}$$

Contracting with different metric combinations one obtains a matrix equation for the coefficients A_i,

$$\begin{pmatrix} d & 1 & 1 \\ 1 & d & 1 \\ 1 & 1 & d \end{pmatrix} \vec{A} = \frac{1}{d} \begin{pmatrix} 1 & 1 & 1 \end{pmatrix}^T, \tag{3.44}$$

which is easily solved and yields

$$\int_Q \frac{(Q^2)^r Q^\mu Q^\nu Q^\rho Q^\sigma}{(Q^2-\Delta)^m} = \frac{g^{\mu\nu}g^{\rho\sigma} + g^{\mu\rho}g^{\nu\sigma} + g^{\mu\sigma}g^{\nu\rho}}{d(d+2)} I[r+2,m]. \tag{3.45}$$

In a last step, we want to recover the $d = 4$ case. One therefore writes $d = 4 - 2\epsilon$ and takes the limit $\epsilon \to 0$. The right hand side of Eq. (3.39) is thus expanded in ϵ and the divergent ϵ^{-1} term is extracted, which encodes the UV divergences of the diagram under consideration. Finally, the integral over the Feynman parameters x_i must be performed. The renormalization factors are expanded according to

$$Z = 1 + \hbar\, Z^{(1)} + O(\hbar^2), \tag{3.46}$$

and we require the $Z^{(1)}$ to cancel all appearing one-loop divergences. In the following

subsections, we will determine the $Z^{(1)}$ for our theory.

Before moving on, let us examine one diagram in detail, in order to convince ourselves that this procedure works and to relate the above defined quantities such as f, Q, Δ and so forth to some particular values. We choose a simple example, namely the following contribution to the correction of the two-point function of the $U(1)$ residual field V_μ^γ,

$$= -\int_q iL_\mu^{\gamma ba}(p,q,p+q)\frac{-\delta_{ac}}{(p+q)^2}iL_\nu^{\gamma cd}(-p,p+q,q)\frac{-\delta_{bd}}{q^2}, \tag{3.47}$$

where we already applied the momentum conservation and iL is taken from the Feynman rule **(c)** in Eq. (3.33),

$$iL_\mu^{\gamma ba}(r,q,p) = -igf^{a\gamma b}(q+p)_\mu. \tag{3.48}$$

Performing Feynman parametrization, we can combine the denominators according to

$$x(q+p)^2 + (1-x)q^2 = (q+xp)^2 - x(x-1)p^2 \equiv Q^2 - \Delta, \tag{3.49}$$

with $Q = q + xp$ and $\Delta = x(x-1)p^2$. Shifting the momentum yields

$$= g^2 f^{a\gamma b} f^{b\gamma a} \int_0^1 dx \int_Q \frac{((1-2x)p+2Q)^\mu((1-2x)p+2Q)^\nu}{(Q^2-\Delta)^2}. \tag{3.50}$$

Making use of the fact that only terms even in Q survive and by applying the rules (3.42) and (3.45) we find

$$= g^2 f^{a\gamma b} f^{b\gamma a} \int_0^1 dx \left((1-2x)^2 p^\mu p^\nu I[0,2] + \frac{4g^{\mu\nu}}{d} I[1,2]\right). \tag{3.51}$$

Consequently, we replace $d = 4 - 2\epsilon$ and extract the ϵ^{-1} terms,

$$\begin{aligned} &\cong g^2 f^{a\gamma b} f^{b\gamma a} \int_0^1 dx \frac{i}{(4\pi)^2 \epsilon} \left((1-2x)^2 p^\mu p^\nu + 2\Delta g^{\mu\nu} \right) \\ &= \frac{i g^2 \mu^{-2\epsilon}}{(4\pi)^2 \epsilon} \frac{N}{3} \left[g^{\mu\nu} p^2 - p^\mu p^\nu \right]. \end{aligned} \tag{3.52}$$

Note that in the last step we replaced $g^2 \to \mu^{-2\epsilon} g^2$ in order to keep g dimensionless. This prescription enables us to deal with all one-loop integrals we encounter in our calculations. We proceed with obtaining all necessary renormalization factors, thereby just stating the divergent parts of the involved one-loop corrections to the related n-point functions.

3.2.2 Renormalization of the two-point functions

We begin with the easiest case, the renormalization of $\langle C^\gamma \bar{C}^\gamma \rangle$. In fact, taking a closer look at the Lagrangian, one finds that C^γ does not appear in the interactions. Hence, there are no one-loop corrections and we immediately find[2]

$$\Delta_9^{(1)} = \frac{1}{2} \left(\tilde{Z}_C^{(1)} + \tilde{Z}_{\bar{C}}^{(1)} \right) = 0. \tag{3.53}$$

Next, we turn to the self-energy of the $U(1)$ gauge field, the one-loop corrections are given by the following diagrammatic equation,

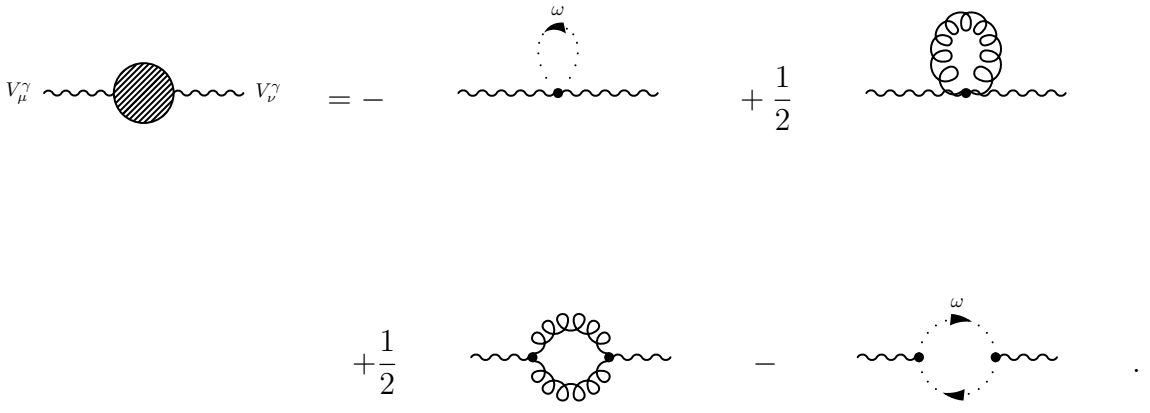

(3.54)

[2]For a definition of the counterterms Δ_i we again refer to appendix A.

Tadpole diagrams with massless propagators do not contribute in dimensional regularization. The last diagram has been calculated in subsection 3.2.1, cf. Eq. (3.52). For the third integral we obtain the divergent part

$$\frac{1}{2}$$ 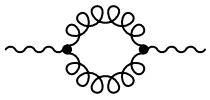 $$= i\frac{g^2\mu^{-2\epsilon}}{(4\pi)^2\epsilon}N\frac{10}{3}\left[g^{\mu\nu}p^2 - p^\mu p^\nu\right]. \tag{3.55}$$

The final result is thus given by

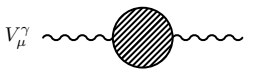 $$= \frac{g^2\mu^{-2\epsilon}}{(4\pi)^2\epsilon}N\frac{11}{3}\left[g^{\mu\nu}p^2 - p^\mu p^\nu\right], \tag{3.56}$$

which is purely transverse. For the related counterterms we consequently obtain

$$\Delta_5^{(1)} = \tilde{Z}_V^{(1)} = \frac{g^2\mu^{-2\epsilon}}{(4\pi)^2\epsilon}N\frac{11}{3}, \tag{3.57}$$

$$\Delta_6^{(1)} = \tilde{Z}_V^{(1)} - Z_\alpha^{(1)} = 0, \tag{3.58}$$

and therefore for the renormalization of the gauge fixing parameter

$$Z_\alpha^{(1)} = \frac{g^2\mu^{-2\epsilon}}{(4\pi)^2\epsilon}N\frac{11}{3}. \tag{3.59}$$

We proceed with the renormalization of the $SU(N-1)$ ghost two-point function. Only one diagram contributes at one-loop level,

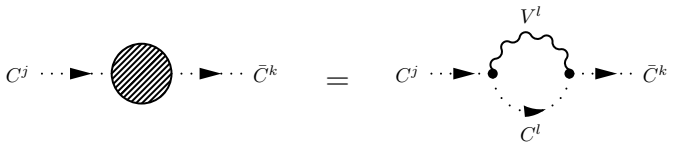 . (3.60)

Calculating the divergent part of this diagram we immediately obtain

$$\Delta_8^{(1)} = \frac{1}{2}\left(Z_C^{(1)} + Z_{\bar{C}}^{(1)}\right) = \frac{g^2\mu^{-2\epsilon}}{(4\pi)^2\epsilon}\frac{N-1}{4}(3-\lambda). \tag{3.61}$$

Next, we turn to the correction of the $SU(N-1)$ residual field two-point function,

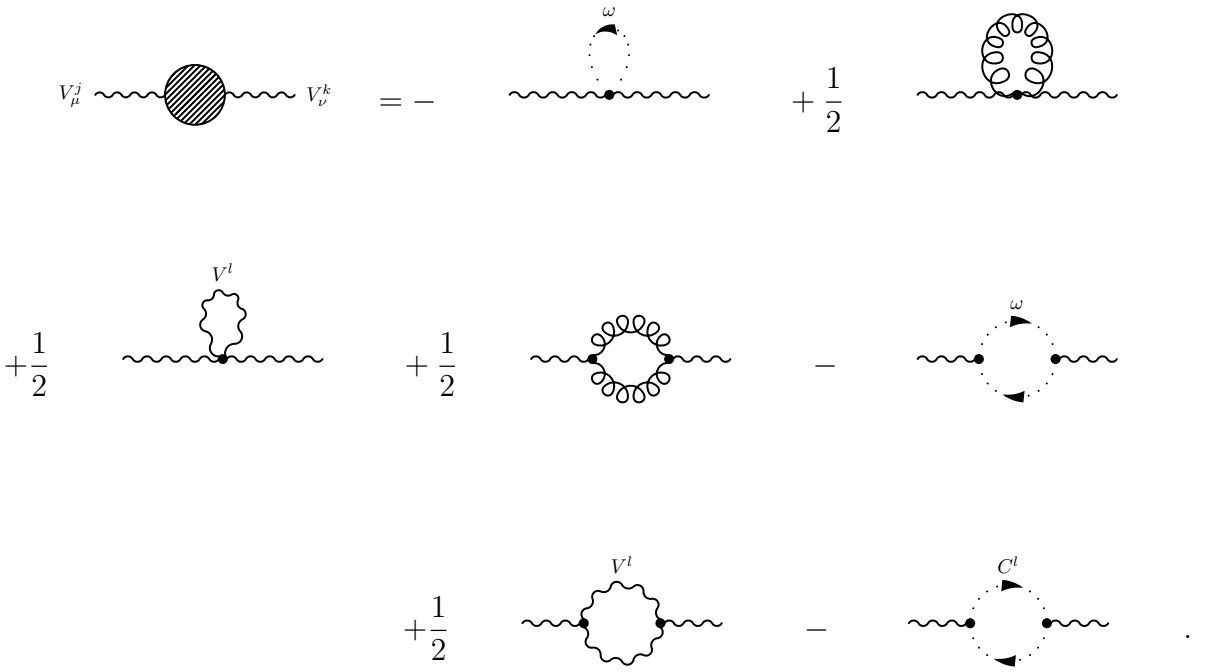

(3.62)

Again, the three tadpole diagrams do not contribute within dimensional regularization. The remaining four diagrams have the divergent parts

$$\frac{1}{2} \quad \text{ 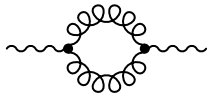 } \quad = i\delta^{jk}\frac{g^2\mu^{-2\epsilon}}{(4\pi)^2\epsilon}\frac{10}{3}\left[p^2 g^{\mu\nu} - p^\mu p^\nu\right], \tag{3.63}$$

$$- \quad \text{  } \quad = i\delta^{jk}\frac{1}{3}\frac{g^2\mu^{-2\epsilon}}{(4\pi)^2\epsilon}\left[g^{\mu\nu}p^2 - p^\mu p^\nu\right], \tag{3.64}$$

$$\frac{1}{2} \quad \text{ 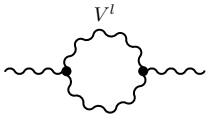 } \quad = i\delta^{jk}\frac{(N-1)}{2}\frac{g^2\mu^{-2\epsilon}}{(4\pi)^2\epsilon}\left[\left(\frac{25}{6}-\lambda\right)p^2 g^{\mu\nu} - \left(\frac{14}{3}-\lambda\right)p^\mu p^\nu\right], \tag{3.65}$$

$$- \quad \text{ 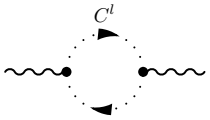 } \quad = i\delta^{jk}\frac{(N-1)}{2}\frac{g^2\mu^{-2\epsilon}}{(4\pi)^2\epsilon}\left[\frac{1}{6}p^2 g^{\mu\nu} + \frac{1}{3}p^\mu p^\nu\right], \tag{3.66}$$

such that the sum is again transverse and one finds

$$\Delta_3^{(1)} = Z_V^{(1)} = \frac{g^2\mu^{-2\epsilon}}{(4\pi)^2\epsilon}\left[\frac{13N+9}{6} - \frac{\lambda}{2}(N-1)\right], \tag{3.67}$$

$$\Delta_4^{(1)} = Z_V^{(1)} - Z_\lambda^{(1)} = 0. \tag{3.68}$$

Thus, the gauge fixing parameter renormalizes according to

$$Z_\lambda^{(1)} = \frac{g^2\mu^{-2\epsilon}}{(4\pi)^2\epsilon}\left[\frac{13N+9}{6} - \frac{\lambda}{2}(N-1)\right]. \tag{3.69}$$

The renormalization of the two-point functions will be completed after taking care of the coset part. First, the correction of the ghost two-point function,

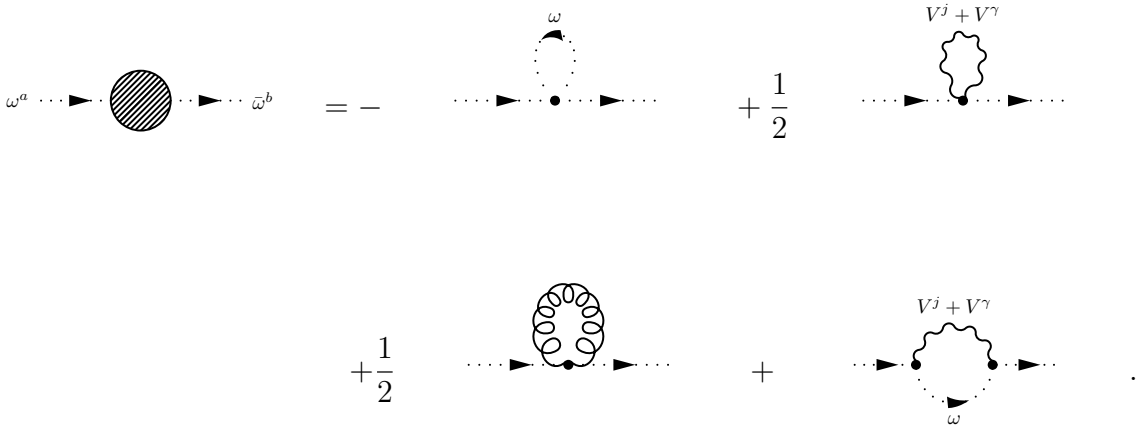

(3.70)

Here, we introduced a new notation. Labelling an internal line as "$V^j + V^\gamma$" means that one actually needs to calculate two diagrams, one with internal $U(1)$ residual field and one with internal $SU(N-1)$ residual field. Since both diagrams will have the exact same momentum integral and differ only in their color factors, it is convenient to combine them. Because tadpoles do not contribute, we only need to calculate the last diagram(s). The divergent part reads

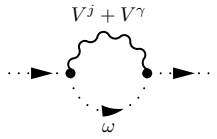

$$= -\frac{g^2\mu^{-2\epsilon}}{(4\pi)^2\epsilon}\frac{N}{2}\left(3 - \frac{\alpha + (N-2)\lambda}{N-1}\right)\delta^{ab}p^2, \tag{3.71}$$

which implies for the renormalization factor

$$\Delta_7^{(1)} = Z_\omega^{(1)} = \frac{g^2\mu^{-2\epsilon}}{(4\pi)^2\epsilon}\frac{N}{2}\left(3 - \frac{\alpha + (N-2)\lambda}{N-1}\right). \tag{3.72}$$

Finally, we turn to the renormalization of the coset gluon two-point function,

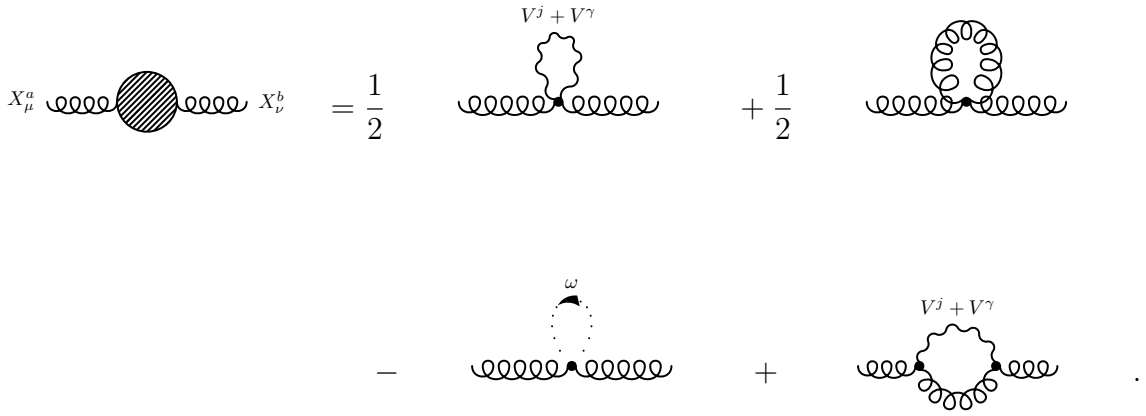

(3.73)

Only the last diagram contributes with the divergent part

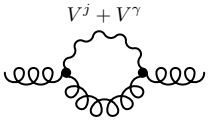

$$= i\delta^{ab}\frac{g^2\mu^{-2\epsilon}}{(4\pi)^2\epsilon}\frac{N}{2}\left[\left(\frac{17-3\xi}{6}-\frac{\alpha+(N-2)\lambda}{N-1}\right)\left[g^{\mu\nu}p^2-p^\mu p^\nu\right]\right.$$

$$\left.+\frac{1}{\xi}\left(\frac{6+\xi(\xi+3)}{2\xi}-\frac{\alpha+(N-2)\lambda}{N-1}\right)p^\mu p^\nu\right]. \tag{3.74}$$

Note that for the coset gluon, the correction is no longer transverse. The transverse part yields the counterterm Δ_1,

$$\Delta_1^{(1)} = Z_X^{(1)} = \frac{g^2\mu^{-2\epsilon}}{(4\pi)^2\epsilon}\frac{N}{2}\left(\frac{17}{6}-\frac{\xi}{2}-\frac{\alpha+(N-2)\lambda}{N-1}\right), \tag{3.75}$$

and from the longitudinal part we infer

$$\Delta_2^{(1)} = Z_X^{(1)} - Z_\xi^{(1)} = \frac{g^2\mu^{-2\epsilon}}{(4\pi)^2\epsilon}\frac{N}{2}\left(\frac{6+\xi(\xi+3)}{2\xi}-\frac{\alpha+(N-2)\lambda}{N-1}\right), \tag{3.76}$$

such that the gauge fixing parameter related to the reduction condition renormalizes as

$$Z_\xi^{(1)} = \frac{g^2\mu^{-2\epsilon}}{(4\pi)^2\epsilon}\frac{N}{2}\left(\frac{4}{3} - \xi - \frac{3}{\xi}\right). \tag{3.77}$$

This completes the renormalization of the two-point functions and we continue with the required three-point vertices.

3.2.3 Renormalization of the three-point functions

We begin this subsection with the renormalization of the $\langle V^j C^k \bar{C}^l \rangle$ vertex, which eventually allows us to obtain the Beta function of the Yang-Mills coupling. The one-loop Beta function is universal and hence independent of the gauge fixing. We should therefore recover the standard result. The one-loop corrections to the vertex are given by the following equation,

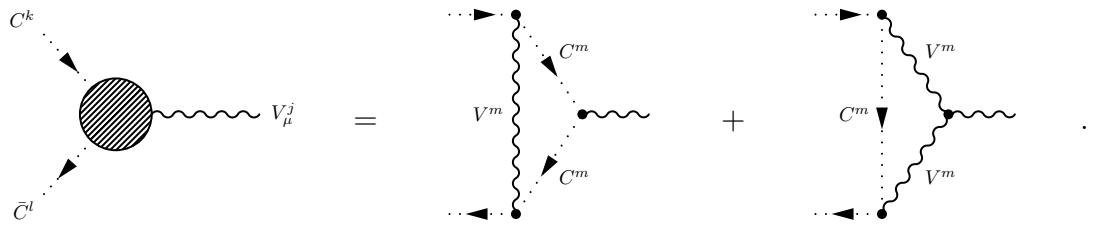

(3.78)

The divergent part of these diagrams is given by

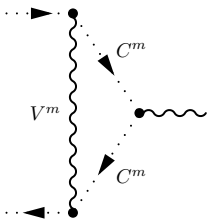

$$= -\frac{g^2\mu^{-2\epsilon}}{(4\pi)^2\epsilon}\frac{N-1}{2}\frac{3\lambda}{4} igf^{jkl}p^\mu, \tag{3.79}$$

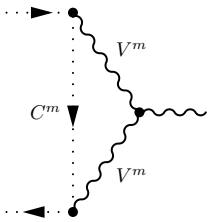

$$= -\frac{g^2\mu^{-2\epsilon}}{(4\pi)^2\epsilon}\frac{N-1}{2}\frac{\lambda}{4} igf^{jkl}p^\mu, \tag{3.80}$$

and yields the following result for the counterterm,

$$\begin{aligned}\Delta_{25}^{(1)} &= \frac{1}{2}\left(Z_V^{(1)} + Z_C^{(1)} + Z_{\bar{C}}^{(1)}\right) + Z_g^{(1)} \\ &= -\frac{g^2\mu^{-2\epsilon}}{(4\pi)^2\epsilon}\frac{N-1}{2}\lambda. \end{aligned} \tag{3.81}$$

Using Eqs. (3.61) and (3.67) we find

$$Z_g^{(1)} = -\frac{g^2\mu^{-2\epsilon}}{(4\pi)^2\epsilon}\frac{11}{6}N. \tag{3.82}$$

The last task is the renormalization of the $\langle X_\mu^a \omega^b \bar{C}^J\rangle$ vertex, once with external $\bar{C}^\gamma$ leg and once with external $\bar{C}^j$ leg, in order to obtain the renormalization factors of the residual ghosts and anti-ghosts. In the first case, the one-loop corrections are given by

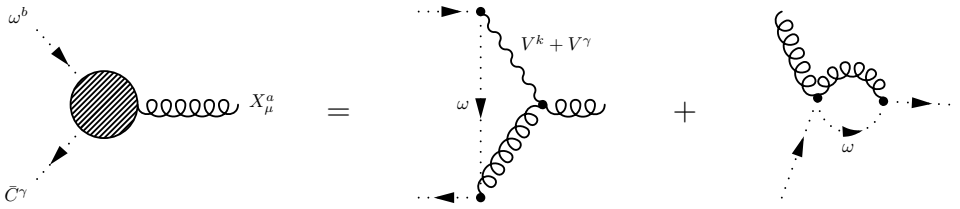

. (3.83)

The first diagram has the following divergent part,

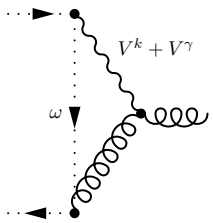

$$= \frac{g^2\mu^{-2\epsilon}}{(4\pi)^2\epsilon} igf^{ce\gamma}\left(\alpha f^{e\gamma b}f^{ca\gamma} + \lambda f^{ekb}f^{cak}\right)p^\mu, \tag{3.84}$$

and for the second diagram we obtain

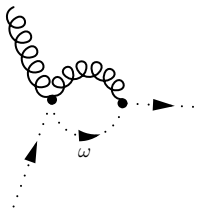

$$= ig\left[\left(f^{eKc}f^{abK} + f^{aKc}f^{ebK}\right)f^{\gamma ec}\right]\frac{\xi+3}{4}\frac{g^2\mu^{-2\epsilon}}{(4\pi)^2\epsilon}p^\mu. \tag{3.85}$$

With the help of the rules established in Eq. (3.30) we can simplify the color factors and find for the related counterterm

$$\Delta_{27}^{(1)} = \left(\frac{1}{2}Z_X^{(1)} + \frac{1}{2}\tilde{Z}_{\bar{C}}^{(1)} + \frac{1}{2}Z_\omega^{(1)} + Z_g^{(1)}\right) = -\frac{g^2\mu^{-2\epsilon}}{(4\pi)^2\epsilon}N\left(\frac{9+3\xi}{8} + \frac{\alpha+(N-2)\lambda}{2(N-1)}\right). \tag{3.86}$$

Applying Eqs. (3.53), (3.72), (3.75), and (3.82) eventually implies

$$\tilde{Z}_{\bar{C}}^{(1)} = -\tilde{Z}_C^{(1)} = -\frac{g^2\mu^{-2\epsilon}}{(4\pi)^2\epsilon}\frac{N}{2}(3+\xi). \tag{3.87}$$

In a last step, we consider the case of an external $\bar{C}^j$ leg. Here, two additional diagrams appear in the one-loop corrections,

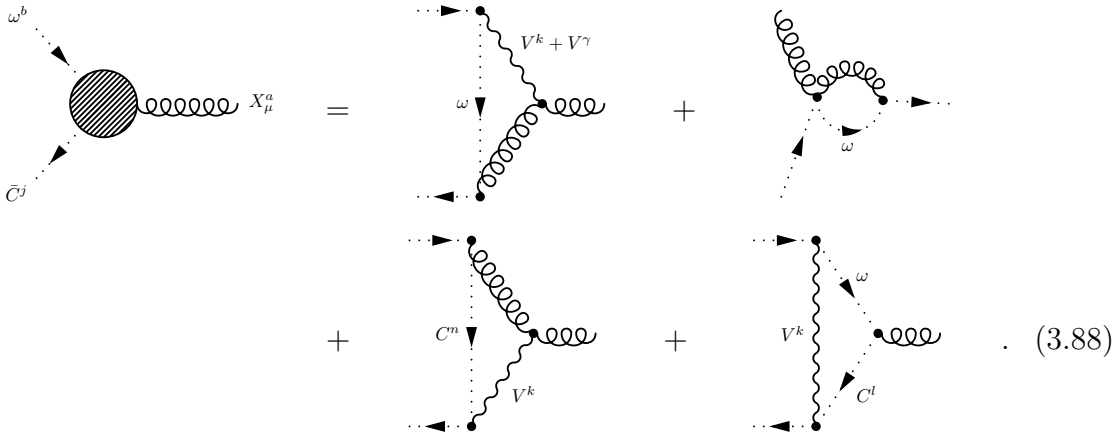

. (3.88)

The various divergent parts read

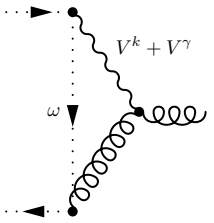

$$= \frac{g^2\mu^{-2\epsilon}}{(4\pi)^2\epsilon} ig f^{cej} \left(\alpha f^{e\gamma b} f^{ca\gamma} + \lambda f^{ekb} f^{cak}\right) p^\mu, \tag{3.89}$$

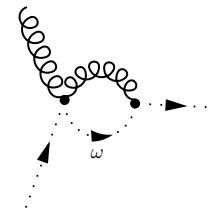

$$= ig \left[\left(f^{eKc} f^{abK} + f^{aKc} f^{ebK}\right) f^{jec}\right] \frac{\xi+3}{4} \frac{g^2\mu^{-2\epsilon}}{(4\pi)^2\epsilon} p^\mu \tag{3.90}$$

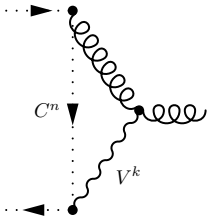

$$= ig \left[f^{ebn} f^{knj} f^{aek}\right] \frac{\lambda + 3(\xi+1)}{4} \frac{g^2\mu^{-2\epsilon}}{(4\pi)^2\epsilon} p_\mu, \tag{3.91}$$

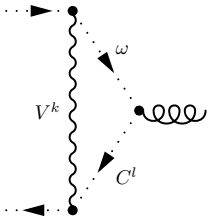

$$= ig \left[f^{ekb} f^{klj} f^{ael}\right] \frac{\lambda}{4} \frac{g^2\mu^{-2\epsilon}}{(4\pi)^2\epsilon} p_\mu, \tag{3.92}$$

such that we infer the counterterm

$$\begin{aligned} \Delta_{26}^{(1)} &= \left(\frac{1}{2} Z_X^{(1)} + \frac{1}{2} Z_{\bar{C}}^{(1)} + \frac{1}{2} Z_\omega^{(1)} + Z_g^{(1)}\right) \\ &= -\frac{g^2}{(4\pi)^2\epsilon} \left(\frac{9+3\xi}{8} + \frac{\alpha N - \lambda}{2(N-1)} + \frac{N-1}{8}[2\lambda + 3(\xi+1)]\right). \end{aligned} \tag{3.93}$$

Finally, with Eqs. (3.61), (3.72), (3.75), and (3.82) we find for the renormalization constants for the $SU(N-1)$ ghosts and anti-ghosts

$$Z_{\bar{C}}^{(1)} = -\frac{g^2\mu^{-2\epsilon}}{(4\pi)^2\epsilon} \frac{1}{2} [N\xi + 3 - \lambda(N-1)], \tag{3.94}$$

$$Z_C^{(1)} = \frac{g^2\mu^{-2\epsilon}}{(4\pi)^2\epsilon} \left[\frac{N}{2}(3+\xi) - \lambda(N-1)\right]. \tag{3.95}$$

This completes the renormalization of the three-point functions and thus the one-loop renormalization. For future application, it is more convenient to work with so-called renormalization group functions rather than the plain renormalization factors. They are introduced in the next subsection.

3.2.4 One-loop renormalization group functions

In this subsection, we summarize the previous results in terms of the renormalization group functions. They are defined in the standard way as follows. For any field Φ we adopt

$$\gamma_\Phi = \frac{1}{2}\mu\frac{\partial}{\partial\mu}\log Z_\Phi = \frac{\hbar}{2}\lim_{\epsilon\to 0}\mu\frac{\partial}{\partial\mu}Z_\Phi^{(1)} + O(\hbar^2). \tag{3.96}$$

For any parameter ζ such as the gauge fixing parameters we define

$$\gamma_\zeta = -\mu\frac{\partial}{\partial\mu}\log Z_\zeta = -\hbar\ \lim_{\epsilon\to 0}\mu\frac{\partial}{\partial\mu}Z_\zeta^{(1)} + O(\hbar^2), \tag{3.97}$$

and finally, for the Beta function of the coupling one has

$$\beta_g = \mu\frac{\partial g_R}{\partial\mu} = -g_R\ \mu\frac{\partial}{\partial\mu}\log Z_g = -\hbar\ g_R\ \lim_{\epsilon\to 0}\mu\frac{\partial}{\partial\mu}Z_g^{(1)} + O(\hbar^2), \tag{3.98}$$

although it will be more convenient to consider the running of g^2,

$$\beta_{g^2} = \mu\frac{\partial g_R^2}{\partial\mu} = -2g_R^2\ \mu\frac{\partial}{\partial\mu}\log Z_g = -2\hbar\ g_R^2\ \lim_{\epsilon\to 0}\mu\frac{\partial}{\partial\mu}Z_g^{(1)} + O(\hbar^2). \tag{3.99}$$

With these conventions the previous results read

$$
\begin{aligned}
\gamma_X &= -\frac{g^2}{(4\pi)^2}\frac{N}{2}\left(\frac{17}{6}-\frac{\xi}{2}-\frac{\alpha+(N-2)\lambda}{N-1}\right), & \gamma_\xi &= \frac{g^2}{(4\pi)^2}N\left(\frac{4}{3}-\xi-\frac{3}{\xi}\right),\\
\gamma_V &= -\frac{g^2}{(4\pi)^2}\left(\frac{13N+9}{6}-\frac{\lambda}{2}(N-1)\right), & \gamma_\lambda &= \frac{g^2}{(4\pi)^2}\left(\frac{13N+9}{3}-\lambda(N-1)\right),\\
\tilde{\gamma}_V &= -\frac{g^2}{(4\pi)^2}N\frac{11}{3}, & \gamma_\alpha &= \frac{g^2}{(4\pi)^2}N\frac{22}{3},\\
\gamma_{\bar{\omega}} &= -\frac{g^2}{(4\pi)^2}\frac{N}{2}\left(3-\frac{\alpha+(N-2)\lambda}{N-1}\right), & \gamma_\omega &= -\frac{g^2}{(4\pi)^2}\frac{N}{2}\left(3-\frac{\alpha+(N-2)\lambda}{N-1}\right),\\
\gamma_{\bar{C}} &= \frac{g^2}{(4\pi)^2}\frac{1}{2}[N\xi+3-\lambda(N-1)], & \gamma_C &= -\frac{g^2}{(4\pi)^2}\left[\frac{N}{2}(3+\xi)-\lambda(N-1)\right],\\
\tilde{\gamma}_{\bar{C}} &= \frac{g^2}{(4\pi)^2}\frac{N}{2}(3+\xi), & \tilde{\gamma}_C &= -\frac{g^2}{(4\pi)^2}\frac{N}{2}(3+\xi),\\
\beta_{g^2} &= -\frac{g^4}{(4\pi)^2}N\frac{22}{3}.
\end{aligned}
\tag{3.100}
$$

We end this section with some comments on the result. First, we stressed earlier that in the case of $N = 2$, our gauge fixing procedure is equivalent to the MAG. In fact, the above results are consistent with the existing literature[3], see, for example, [89, 92–95]. Moreover, as expected, the Beta function of the Yang-Mills coupling is exactly the standard result of pure Yang-Mills theory. In particular, we also observe that $\beta_{g^2} = 2\tilde{\gamma}_V g^2$, or $\tilde{Z}_V^{1/2} = Z_g^{-1}$, at least at one-loop level. Also, we recover a known problem within the MAG. The running of any renormalized parameter ζ in terms of its anomalous dimension is given by $\mu\frac{\partial\zeta}{\partial\mu} = \zeta\gamma_\zeta$. Let us then consider the running of the gauge fixing parameters. First, for the residual gauge fixing parameters we have

$$
\begin{aligned}
\mu\frac{\partial\alpha}{\partial\mu} &= \frac{g^2}{(4\pi)^2}N\frac{22}{3}\alpha,\\
\mu\frac{\partial\lambda}{\partial\mu} &= \frac{g^2}{(4\pi)^2}\left(\frac{13N+9}{3}-\lambda(N-1)\right)\lambda,
\end{aligned}
\tag{3.101}
$$

which implies the existence of two fixed points $(\alpha_*, \lambda_*) \in \left\{(0,0), \left(0, \frac{13N+9}{3(N-1)}\right)\right\}$. On the other hand, the running of the gauge fixing parameter related to the reduction condition

[3]Note that in the $SU(2)$ case, the decompisition reads $SU(2)/U(1)\times U(1)$, i.e., the $SU(N-1)$ sector in the decompisition is absent. Its contribution to other quantities from the coset and the $U(1)$ sector is proportional to $(N-2)$ and therefore vanishes consistently.

causes problems as it does not possess a fixed point at all,

$$\mu\frac{\partial\xi}{\partial\mu} = \frac{g^2}{(4\pi)^2}N\left(\frac{4}{3}\xi - \xi^2 - 3\right). \tag{3.102}$$

This is a rather unpleasant feature for the following reason. Having in mind our reformulation of $SU(N)$ Yang-Mills theory, we would like to impose the reduction condition rigorously. From the viewpoint of the Faddeev-Popov method, this means to incorporate the reduction condition in the path integral as a Delta functional, which corresponds to the limit $\xi \to 0$. However, the running equation for ξ tells us that even if we choose $\xi = 0$ at some scale, it will run towards non-zero values, smearing out the gauge fixing condition. While at present the author is not aware of any possibility to circumvent this problem, we are going to at least take the limit of $\xi \to 0$ in the end, provided that all important quantities remain finite in this limit.

While the standard one-loop renormalization is completed at this stage, special care is necessary concerning composite operators. Under renormalization, such operators may mix with all other composite operators that possess the same quantum numbers, e.g., mass dimension and ghost number. This issue will be considered in the next section.

3.3 Multiplicative renormalizability of the composite operator

In this section, we want to convince ourselves that the composite operator

$$\mathcal{O} = \mathrm{Tr}_{G/H}\left(\mathfrak{X}_\mu\mathfrak{X}^\mu - 2i\xi\mathfrak{C}\bar{\mathfrak{C}}\right) \tag{3.103}$$

is physically meaningful. We specify this statement by the following two criteria. First, even though we broke gauge symmetry through the gauge fixing, the operator should at least be BRST invariant. Second, our operator must be multiplicatively renormalizable. The BRST invariance is shown straightforwardly. Using the BRST transformations (3.12) we find

$$\delta_B\mathcal{O} = X^a_\mu\left(D^{\mu ab}\omega^b + gf^{abJ}X^{\mu b}C^J\right) - i\xi(-gf^{abJ}\omega^b C^J)\bar{\omega}^a + i\xi\omega^a\left(iB^a\right), \tag{3.104}$$

and furthermore, using the equation of motion for the Nakanishi-Lautrup field (3.16) we derive

$$\begin{aligned}\delta_B\mathcal{O} &= X^a_\mu \left(D^{\mu ab}\omega^b + g f^{abJ} X^{\mu b} C^J\right) + i\xi g f^{abJ}\omega^b C^J \bar{\omega}^a \\ &\quad - \xi\omega^a \left(-\frac{1}{\xi} D^{ab}_\mu X^{\mu b} + i g f^{abJ}\bar{\omega}^b C^J\right) \\ &= X^{\mu a} D^{ab}_\mu \omega^b + \omega^a D^{ab}_\mu X^{\mu b} \\ &= \partial^\mu \left(X^a_\mu \omega^a\right). \end{aligned} \tag{3.105}$$

This is nothing but a total derivative and thus we established the (on-shell) BRST invariance of the composite operator.

Proving the multiplicative renormalizability of the composite operator is a more involved task, because we have to consider the mixing of all condensates of the same quantum number. This gives rise to the following mixing matrix,

$$\begin{pmatrix} \left[\frac{1}{2}X^a_\mu X^\mu_a\right]_R \\ \left[\frac{1}{2}V^j_\mu V^\mu_j\right]_R \\ \left[i\omega^a\bar{\omega}^a\right]_R \\ \left[iC^j\bar{C}^j\right]_R \\ \left[\frac{1}{2}V^\gamma_\mu V^\mu_\gamma\right]_R \\ \left[iC^\gamma\bar{C}^\gamma\right]_R \end{pmatrix} = \begin{pmatrix} Z_{11} & Z_{12} & Z_{13} & Z_{14} & Z_{15} & Z_{16} \\ Z_{21} & Z_{22} & Z_{23} & Z_{24} & Z_{25} & Z_{26} \\ Z_{31} & Z_{32} & Z_{33} & Z_{34} & Z_{35} & Z_{36} \\ Z_{41} & Z_{42} & Z_{43} & Z_{44} & Z_{45} & Z_{46} \\ Z_{51} & Z_{52} & Z_{53} & Z_{54} & Z_{55} & Z_{56} \\ Z_{61} & Z_{62} & Z_{63} & Z_{64} & Z_{65} & Z_{66} \end{pmatrix} \begin{pmatrix} \left[\frac{1}{2}X^a_\mu{}_R X^\mu_a{}_R\right] \\ \left[\frac{1}{2}V^j_\mu{}_R V^\mu_j{}_R\right] \\ \left[i\omega^a_R\bar{\omega}^a_R\right] \\ \left[iC^j_R\bar{C}^j_R\right] \\ \left[\frac{1}{2}V^\gamma_\mu{}_R V^\mu_\gamma{}_R\right] \\ \left[iC^\gamma_R\bar{C}^\gamma_R\right] \end{pmatrix}. \tag{3.106}$$

Next, we define the Feynman rules for the operator insertions as shown in Fig. 3.4.

FIGURE 3.4: Feynman rules for operator insertions.

The matrix elements are then calculated by inserting $\mathcal{O}_R$ into the various two-point functions and the renormalization factors are required to cancel the related divergences, following the strategy in [36]. At this point, due to the big number of condensates, the calculation of the mixing matrix becomes quite tedious. Therefore, we postpone the detailed discussion to appendix B. Therein, it is shown that the matrix takes the following

form,

$$\mathcal{Z} = \begin{pmatrix} 1+Z_{11}^{(1)} & 0 & Z_{13}^{(1)} & 0 & 0 & 0 \\ Z_{21}^{(1)} & 1+Z_{22}^{(1)} & Z_{23}^{(1)} & 0 & 0 & 0 \\ Z_{31}^{(1)} & 0 & 1+Z_{33}^{(1)} & 0 & 0 & 0 \\ 0 & Z_{42}^{(1)} & 0 & 1 & 0 & 0 \\ Z_{51}^{(1)} & 0 & Z_{53}^{(1)} & 0 & 1 & 0 \\ 0 & 0 & 0 & 0 & 0 & 1 \end{pmatrix} + O(\hbar^2), \tag{3.107}$$

with entries given by

$$\begin{aligned}
Z_{11}^{(1)} &= -\frac{g^2\mu^{-2\epsilon}}{(4\pi)^2\epsilon}\frac{N}{2}, \left(\frac{3}{2}(\xi+1) + \frac{\alpha+(N-2)\lambda}{N-1}\right), & Z_{31}^{(1)} &= -\frac{g^2\mu^{-2\epsilon}}{(4\pi)^2\epsilon}N, \\
Z_{13}^{(1)} &= \frac{g^2\mu^{-2\epsilon}}{(4\pi)^2\epsilon}N\frac{3+\xi^2}{2}, & Z_{33}^{(1)} &= \frac{g^2\mu^{-2\epsilon}}{(4\pi)^2\epsilon}\frac{N}{2}\left(\xi - \frac{\alpha+(N-2)\lambda}{N-1}\right), \\
Z_{21}^{(1)} &= -\frac{g^2\mu^{-2\epsilon}}{(4\pi)^2\epsilon}\frac{N(N-2)}{2(N-1)}\frac{3}{4}(\xi+3), & Z_{42}^{(1)} &= -\frac{g^2\mu^{-2\epsilon}}{(4\pi)^2\epsilon}\frac{(N-1)}{2}, \\
Z_{22}^{(1)} &= -\frac{g^2\mu^{-2\epsilon}}{(4\pi)^2\epsilon}\frac{3}{4}(N-1)(1+\lambda), & Z_{51}^{(1)} &= -\frac{g^2\mu^{-2\epsilon}}{(4\pi)^2\epsilon}\frac{N}{2(N-1)}\frac{3}{4}(\xi+3), \\
Z_{23}^{(1)} &= -3\frac{g^2\mu^{-2\epsilon}}{(4\pi)^2\epsilon}\frac{N(N-2)}{2(N-1)}, & Z_{53}^{(1)} &= -3\frac{g^2\mu^{-2\epsilon}}{(4\pi)^2\epsilon}\frac{N}{2(N-1)}.
\end{aligned} \tag{3.108}$$

The relation (3.106) is then inverted at one-loop level, which yields

$$\begin{pmatrix} \left[\frac{1}{2}X_\mu^{a\ R}X_a^{\mu\ R}\right] \\ \left[\frac{1}{2}V_\mu^{j\ R}V_j^{\mu\ R}\right] \\ \left[i\omega_R^a\bar{\omega}_R^a\right] \\ \left[iC_R^j\bar{C}_R^j\right] \\ \left[\frac{1}{2}V_\mu^{\gamma\ R}V_\gamma^{\mu\ R}\right] \\ \left[iC_R^\gamma\bar{C}_R^\gamma\right] \end{pmatrix} = \begin{pmatrix} 1-Z_{11}^{(1)} & 0 & -Z_{13}^{(1)} & 0 & 0 & 0 \\ -Z_{21}^{(1)} & 1-Z_{22}^{(1)} & -Z_{23}^{(1)} & 0 & 0 & 0 \\ -Z_{31}^{(1)} & 0 & 1-Z_{33}^{(1)} & 0 & 0 & 0 \\ 0 & -Z_{42}^{(1)} & 0 & 1 & 0 & 0 \\ -Z_{51}^{(1)} & 0 & -Z_{53}^{(1)} & 0 & 1 & 0 \\ 0 & 0 & 0 & 0 & 0 & 1 \end{pmatrix} \begin{pmatrix} \left[\frac{1}{2}X_\mu^a X_a^\mu\right]_R \\ \left[\frac{1}{2}V_\mu^j V_j^\mu\right]_R \\ \left[i\omega^a\bar{\omega}^a\right]_R \\ \left[iC^j\bar{C}^j\right]_R \\ \left[\frac{1}{2}V_\mu^\gamma V_\gamma^\mu\right]_R \\ \left[iC^\gamma\bar{C}^\gamma\right]_R \end{pmatrix}. \tag{3.109}$$

This finally enables us to discuss the multiplicative renormalizability of the composite

operator,

$$\begin{aligned}
\mathcal{O} &= \left(1+Z_X^{(1)}\right)\frac{1}{2}X^\mu_{a\,R}X^a_{\mu R} - \left(1+Z_\xi^{(1)}\right)\left(1+Z_\omega^{(1)}\right)\xi i\omega^a_R\bar{\omega}^a_R \\
&= \left(1+Z_X^{(1)}\right)\left\{\left(1-Z_{11}^{(1)}\right)\left[\frac{1}{2}X^a_\mu X^\mu_a\right]_R - Z_{13}^{(1)}\left[i\omega^a\bar{\omega}^a\right]_R\right\} \\
&- \left(1+Z_\xi^{(1)}\right)\left(1+Z_\omega^{(1)}\right)\xi\left\{-Z_{31}^{(1)}\left[\frac{1}{2}X^a_\mu X^\mu_a\right]_R\right. \\
&\qquad\left. + \left(1-Z_{33}^{(1)}\right)\left[i\omega^a\bar{\omega}^a\right]_R\right\} \\
&\stackrel{!}{=} \left(1+\frac{1}{2}Z_\mathcal{O}^{(1)}\right)\left(\left[\frac{1}{2}X^a_\mu X^\mu_a\right]_R - \xi\left[i\omega^a\bar{\omega}^a\right]_R\right).
\end{aligned} \tag{3.110}$$

We infer the condition

$$-Z_{11}^{(1)} + Z_X^{(1)} + \xi Z_{31}^{(1)} = Z_\xi^{(1)} - Z_{33}^{(1)} + Z_\omega^{(1)} + \frac{1}{\xi}Z_{13}^{(1)}, \tag{3.111}$$

and indeed find

$$\begin{aligned}
-Z_{11}^{(1)} + Z_X^{(1)} + \xi Z_{31}^{(1)} &= \frac{g^2\mu^{-2\epsilon}}{(4\pi)^2\epsilon}\left[\frac{N}{6}(13-3\xi)\right], \\
Z_\xi^{(1)} - Z_{33}^{(1)} + Z_\omega^{(1)} + \frac{1}{\xi}Z_{13}^{(1)} &= \frac{g^2\mu^{-2\epsilon}}{(4\pi)^2\epsilon}\left[\frac{N}{6}(13-3\xi)\right].
\end{aligned} \tag{3.112}$$

Thus, the composite operator is one-loop multiplicatively renormalizable, $\mathcal{O} = Z_\mathcal{O}^{1/2}\mathcal{O}_R$, with the renormalization factor

$$\begin{aligned}
Z_\mathcal{O}^{(1)} &= 2\left(-Z_{11}^{(1)} + Z_X^{(1)} + \xi Z_{31}^{(1)}\right) \\
&= 2\left(Z_\xi^{(1)} - Z_{33}^{(1)} + Z_\omega^{(1)} + \frac{1}{\xi}Z_{13}^{(1)}\right) \\
&= \frac{g^2\mu^{-2\epsilon}}{(4\pi)^2\epsilon}\frac{N}{3}(13-3\xi).
\end{aligned} \tag{3.113}$$

Again, this is in agreement with the existing $N=2$ MAG results, e.g., [41]. According to Eq. (3.109), the existence of the coset gluon condensate seems to induce a residual field condensate $V^j_\mu V^{\mu j}$ ($V^\gamma_\mu V^{\mu\gamma}$) due to a non-vanishing of the matrix entries $Z_{21}^{(1)}$ and $Z_{23}^{(1)}$ ($Z_{51}^{(1)}$ and $Z_{53}^{(1)}$). However, no BRST invariant combination of mass dimension-two operators including the residual field condensate can be constructed. This renders such a condensate non-physical and therefore we continue to discuss the composite operator

$\mathcal{O}$ only.

Finally, for later use we furthermore introduce the composite operator anomalous dimension

$$\gamma_{\mathcal{O}} = \frac{\mu}{\mathcal{O}_R}\frac{\partial \mathcal{O}_R}{\partial \mu} = -\frac{1}{2}\mu\frac{\partial}{\partial \mu}\log Z_{\mathcal{O}}, \tag{3.114}$$

which reads at one-loop level

$$\gamma_{\mathcal{O}} = \frac{g^2}{(4\pi)^2}\frac{N}{3}(13 - 3\xi). \tag{3.115}$$

Note that $\gamma_{\mathcal{O}}$ does not contain the residual gauge fixing parameters α and λ. This is reasonable, as the composite operator respects the local $U(N-1)$ symmetry, and is also invariant under the local transformations corresponding to the $U(1)$ and $SU(N-1)$ sectors of the $U(N-1)$ stability group, respectively. This follows from the fact that for infinitesimal gauge transformations δ_ϑ with $\vartheta = \vartheta^J T^J$ we find

$$\begin{aligned}\delta_\vartheta \mathcal{O} &= X^a_\mu \Big\{\delta^{aJ}\partial^\mu + g f^{abJ} X^\mu_b\Big\}\vartheta^J - i\xi g\Big\{f^{abJ}\omega^b\bar{\omega}^a + f^{baJ}\omega^b\bar{\omega}^a\Big\}\vartheta^J \\ &= 0.\end{aligned} \tag{3.116}$$

Within this chapter, we explicitly performed the decomposition of the $SU(N)$ Yang-Mills in the minimal option and with fixed color field. In particular, we discussed the gauge-fixing procedure and the role of the reduction condition in this situation. Consequently, we showed that the obtained theory is one-loop renormalizable. In particular, a special consideration related to the composite operator $\mathcal{O}$ was necessary, namely we had to prove its multiplicative renormalizability. Yet, these results just have preliminary character regarding the existence of the condensate $\langle\mathcal{O}\rangle$. To investigate the existence of this object, we must follow a more involved procedure called local composite operator formalism. This will be the content of the next chapter.

Chapter 4

LCO formalism and perturbative existence of the condensate

With the results of the previous chapter, we are ready to discuss whether the condensate related to our composite operator exists. However, introducing a composite operator to a theory via a source term $\int J\mathcal{O}$ will always introduce new divergences to the theory which are quadratic in the source J. To treat these divergences, the so-called LCO formalism has been developed in [52, 53]. It has already been applied to various gluon-ghost composite operators, for example in the usual Lorenz gauge and even in the MAG [29, 30, 41], giving a positive answer to the question as to whether the condensate exists or not. While our construction is equivalent to the MAG for $N = 2$, it is *a priori* not clear if the condensate exists in the new case of a $U(N-1)$ stability group for $N > 2$. In this chapter, we are going to follow the lines of [41], where the MAG was considered, and check if the condensate exists in our case as well. Since the anomalous dimension of the composite operator is independent of the residual gauge fixing parameters α and λ, and because we already showed that $\alpha = \lambda = 0$ is a fixed point, at least at one-loop level, we set them to zero throughout this chapter. The content of this chapter is partly published in [86].

4.1 Introduction to the LCO formalism

In order to cure the aforementioned divergences we extend the Lagrangian by adding the following additional piece,

$$\mathfrak{L}_{LCO} = \frac{1}{2}\zeta J^2 + \frac{1}{2}\delta\zeta J^2, \tag{4.1}$$

where ζ is an *a priori* arbitrary auxiliary parameter and the second term is understood to be a pure counterterm. At first sight, the introduction of an additional parameter to the theory might be strange. However, it can be shown that ζ can be uniquely determined through its running, up to integration constants, if we assume that ζ runs with the RG scale μ only implicitly through its dependence on the Yang-Mills coupling and the gauge fixing parameter ξ. First, since we already proved the multiplicative renormalizability of the composite operator we define $J_0 = Z_{\mathcal{O}}^{-1/2} J$ such that $J_0 \mathcal{O}_0 = J\mathcal{O}$. From the RG invariance of the generating functional we then obtain

$$\left[\mu\frac{\partial}{\partial\mu} + \beta_{g^2}\frac{\partial}{\partial g^2} + \xi\gamma_\xi\frac{\partial}{\partial\xi} - \gamma_{\mathcal{O}} J\frac{\partial}{\partial J} + \eta\frac{\partial}{\partial\zeta}\right] W[J] = 0; \quad \eta = \mu\frac{\partial}{\partial\mu}\zeta. \tag{4.2}$$

Next, we note that ζ and $\delta\zeta$ have mass dimension $[\zeta] = [\delta\zeta] = d - 4 = -2\epsilon$ and require $\mathfrak{L}_{LCO}$ to respect RG invariance as well,

$$0 = \mu\frac{\partial}{\partial\mu}\left[\frac{1}{2}(\zeta + \delta\zeta) J^2 \mu^{-2\epsilon}\right]. \tag{4.3}$$

Therefore, the running of ζ can be expressed as

$$\eta = \mu\frac{\partial\zeta}{\partial\mu} = (2\epsilon + 2\gamma_{\mathcal{O}})\zeta + \delta, \tag{4.4}$$

with the inhomogeneity

$$\delta = (2\epsilon + 2\gamma_{\mathcal{O}})\delta\zeta - \mu\frac{\partial}{\partial\mu}\delta\zeta. \tag{4.5}$$

Now, we make use of the assumption that the auxiliary parameter ζ depends on μ only implicitly via $g^2(\mu)$ and $\xi(\mu)$, i.e., $\zeta = \zeta(g^2(\mu), \xi(\mu))$. The Eq. (4.4) thus becomes

$$\left[2\epsilon + 2\gamma_{\mathcal{O}} - \beta_{g^2}\frac{\partial}{\partial g^2} - \xi\gamma_\xi\frac{\partial}{\partial\xi}\right](\zeta + \delta\zeta) = 0. \tag{4.6}$$

Upon expanding in $\hbar$, this differential equation can be solved order by order if

$$\zeta(g^2, \xi) = \frac{\zeta_0}{g^2} + \hbar\zeta_1 + \hbar^2\zeta_2 g^2 + \ldots, \tag{4.7}$$

where we temporarily introduced $\hbar$. At this stage, it becomes obvious that we unfortunately need to perform $(n+1)$-loop calculations in order to determine ζ at n-loop level. For example, consider the following expansion of all involved quantities to two-loop or-

der[1],

$$\begin{aligned}\beta_{g^2} &= -2\epsilon g^2 + \beta_1\, g^4 + \beta_2\, g^6,\\ \delta\zeta &= \frac{\delta\zeta_1}{\epsilon} + \left(\frac{\delta\zeta_{2,1}}{\epsilon} + \frac{\delta\zeta_{2,2}}{\epsilon^2}\right) g^2,\\ \gamma_{\mathcal{O}} &= \gamma_{\mathcal{O},1}\, g^2 + \gamma_{\mathcal{O},2}\, g^4,\\ \gamma_{\xi} &= \gamma_{\xi,1}\, g^2 + \gamma_{\xi,2}\, g^4.\end{aligned} \tag{4.8}$$

Note, that the one-loop part of $\delta\zeta$ is $O(g^0)$. Inserting these expansions into Eq. (4.6) one finds order by order

$$\begin{aligned} g^{-2}: &\quad 2\epsilon\zeta_1 - 2\epsilon\zeta_1 = 0,\\ g^{0}: &\quad 2\gamma_{\mathcal{O},1}\,\zeta_0 + \zeta_0\beta_1 - \xi\gamma_{\xi,1}\,\partial_\xi\zeta_0 + 2\delta\zeta_1 = 0,\\ g^{2}: &\quad \xi\gamma_{\xi,1}\,\partial_\xi\zeta_1 - 2\gamma_{\mathcal{O},1}\,\zeta_1 = \delta_1,\end{aligned} \tag{4.9}$$

where

$$\delta_1 = -\xi\gamma_{\xi,2}\,\partial_\xi\zeta_0 + 2\gamma_{\mathcal{O},2}\,\zeta_0 + \beta_2\zeta_0 + 4\delta\zeta_{2,1} + \frac{1}{\epsilon}[4\delta\zeta_{2,2} + 2\gamma_{\mathcal{O},1}\,\delta\zeta_0 - \xi\gamma_{\xi,1}\,\partial_\xi\delta\zeta_1]. \tag{4.10}$$

The $O(g^{-2})$ equation is satisfied identically while the $O(g^0)$ equation implies the ordinary differential equation (ODE) for ζ_0,

$$[\xi\gamma_{\xi,1}\,\partial_\xi - 2\gamma_{\mathcal{O},1} - \beta_1]\,\zeta_0 = 2\delta\zeta_1. \tag{4.11}$$

Therefore, knowledge of the one-loop quantities $\gamma_{\xi,1}$, $\gamma_{\mathcal{O},1}$, β_1, and $\delta\zeta_1$ is necessary to obtain the tree-level part ζ_0. The solution of this ODE is plugged into the second equation of (4.9) to obtain ζ_1. However, one comment needs to be made about the inhomogeneity δ_1. When taking the limit $\epsilon \to 0$, the last term in Eq. (4.10) can only be finite if the bracket vanishes identically. This is guaranteed from the fact that if the theory is renormalizable, the finiteness of Eqs. (4.2)-(4.4) implies the finiteness of δ and therefore there is no need to consider the terms proportional to $1/\epsilon$ in δ, as they must vanish by construction [96]. In fact, based on the results in [30] for the case of the "full" gluon composite operator $A^A_\mu A^\mu_A$ and in Lorenz gauge with arbitrary gauge parameter this

[1]Note the term $-2\epsilon g^2$, which is often neglected because in the end one usually takes the limit $\epsilon \to 0$. For the LCO, however, we must take it into account because it will render some ϵ^{-1} terms finite.

condition can be explicitly checked and is found to be satisfied. It should be remarked on the other hand that if one is interested in the mere existence of the condensate, knowledge of ζ_0 is sufficient, thus avoiding this subtlety in determining ζ_1.

Before we turn to the calculation of the last ingredient for the ODE (4.11), namely the one-loop part of $\delta\zeta$, let us note that there actually exist two ways of calculating this quantity and also $\gamma_{\mathcal{O}}$, depending on the interpretation of the composite operator source J. One possibility is to regard J as a constant parameter and therefore treat $\gamma_{\mathcal{O}}$ as a mass renormalization. Hence, all calculations are performed using a massive gluon propagator, which is quite cumbersome especially in higher loop calculations. This has been adopted in the original version of the LCO formalism. Alternatively, in [97], it has been suggested to treat J as a non-dynamical field that interacts with the gluon. In this case, the calculations can be performed using massless propagators and the renormalization is done by inserting the composite operator into two-point functions in order to obtain $\gamma_{\mathcal{O}}$, while $\delta\zeta$ is obtained by inserting the composite operator into the vacuum bubbles, requiring the quantity $\langle\mathcal{O}(x)\mathcal{O}(y)\rangle$ to be finite. It actually was the second viewpoint that we used to prove the one-loop multiplicative renormalizability of our composite operator in section 3.3. Both approaches seem to be equivalent as for example the results derived in [97] agree with those in [29].

Getting back to the calculation of $\delta\zeta_1$, it is convenient to return to the viewpoint of J being a mass. Thus, the quadratic divergences can be obtained by calculating the standard one-loop corrections $-\frac{i}{2}\,\mathrm{STr}\log S^{(2)}$ to the Schwinger functional $W[J]$, where $S^{(2)}$ is the Hessian of our action including the source term for the composite operator,

$$S_{\text{source}} = \int_x J\,\mathrm{Tr}_{G/H}\left(\mathfrak{X}_\mu\mathfrak{X}^\mu - 2i\xi\mathfrak{C}\bar{\mathfrak{C}}\right). \tag{4.12}$$

Since we are only interested in the J-dependent terms, we can use the projection

$$\begin{aligned}-\frac{i}{2}\,\mathrm{STr}_{G/H}\log S^{(2)}\Big|_{\mathfrak{A}_\mu=\mathfrak{C}=\bar{\mathfrak{C}}=0}\\ = -\frac{i}{2}\,\mathrm{Tr}\log\left[\delta^{ab}\left(-p^2g_{\mu\nu}+(1-\xi^{-1})p_\mu p_\nu + g_{\mu\nu}J\right)\right] + i\,\mathrm{Tr}\log\left[\delta^{ab}\left(-p^2+\xi J\right)\right].\end{aligned} \tag{4.13}$$

Let us start with the gluon sector. We rewrite it in terms of

$$D^{-1}_{\mu\nu} = -p^2\left(\Pi^T_{\mu\nu}(p) + \frac{1}{\xi}\Pi^L_{\mu\nu}(p)\right), \tag{4.14}$$

with the orthonormal transverse and longitudinal projectors

$$\Pi^T_{\mu\nu}(p) = g_{\mu\nu} - \frac{p_\mu p_\nu}{p^2}; \quad \Pi^L_{\mu\nu}(p) = \frac{p_\mu p_\nu}{p^2}. \tag{4.15}$$

Then we write symbolically

$$\begin{aligned} -\frac{i}{2}\,\mathrm{Tr}\log\left[\delta^{ab}\left(-p^2 g_{\mu\nu} + (1-\xi^{-1})p_\mu p_\nu + g_{\mu\nu}J\right)\right] &= -i\frac{2(N-1)}{2}\,\mathrm{Tr}\log\left[D^{-1}+J\right] \\ &= -i\frac{2(N-1)}{2}\,\mathrm{Tr}\log\left[D^{-1}(1+DJ)\right] \\ &\cong -i\frac{2(N-1)}{2}\,\mathrm{Tr}\log\left[(1+DJ)\right], \end{aligned} \tag{4.16}$$

where in the last line we dropped the J-independent term. Next, we expand the logarithm,

$$\begin{aligned} \mathrm{Tr}\log\left[(1+DJ)\right] &= -\int_p \sum_k (-1)^k \frac{J^k}{k}\,\mathrm{Tr}\,D^k \\ &= -\int_p \sum_k \frac{1}{k}\left(\frac{J}{p^2}\right)^k \left[(d-1)+\xi^k\right] \\ &= \int_p (d-1)\log\left[1-\frac{J}{p^2}\right] + \int_p \log\left[1-\frac{\xi J}{p^2}\right], \end{aligned} \tag{4.17}$$

where the second line is obtained using the orthonormality of the transverse and longitudinal projectors. For convenience, we add the J-independent term $-i\frac{2(N-1)}{2}\log[-p^2]$ and perform a Wick rotation, such that the gluonic part becomes

$$\begin{aligned} &-\frac{i}{2}\,\mathrm{Tr}\log\left[\delta^{ab}\left(-p^2 g_{\mu\nu} + (1-\xi^{-1})p_\mu p_\nu + g_{\mu\nu}J\right)\right] \\ &\qquad \cong \frac{2(N-1)}{2}\int_{p_E}\left((d-1)\log[p_E^2+J] + \log[p_E^2+\xi J]\right), \end{aligned} \tag{4.18}$$

with the Euclidean momentum $p_E^2 = -p^2 > 0$. The momentum integral can be solved within dimensional regularization, using

$$\begin{aligned} \int_{p_E}\log[p_E^2+m^2] &= -\frac{\partial}{\partial t}\frac{1}{(p_E^2+m^2)^t}\Big|_{t=0} \\ &= -\frac{\Gamma[-d/2]}{(4\pi)^{d/2}}(m^2)^{d/2}. \end{aligned} \tag{4.19}$$

We first apply Eq. (4.19) to Eq. (4.18), then take the derivative with respect to J twice

and send ϵ to 0. The result reads

$$-\frac{2(N-1)}{2}\frac{(3+\xi^2)}{(4\pi)^2\epsilon} + \text{finite}. \tag{4.20}$$

The ghost sector can be treated in the same way, yielding

$$i\,\mathrm{Tr}\log\left[\delta^{ab}\left(-p^2+\xi J\right)\right] = \frac{2(N-2)}{2}\frac{\xi^2}{8\pi^2\epsilon} + \text{finite}, \tag{4.21}$$

such that we obtain the counterterm

$$\frac{\delta\zeta_1}{\epsilon} = -\frac{2(N-1)}{2}\frac{(3-\xi^2)}{(4\pi)^2\epsilon}. \tag{4.22}$$

We are now ready to solve the differential Eq. (4.11) for ζ_0. A particular solution is given by

$$\zeta_0^{(p)} = \frac{2(N-1)}{N}\xi. \tag{4.23}$$

The homogeneous part is solved as

$$\begin{aligned}\int\frac{d\zeta_0}{\zeta_0} &= \int\frac{2\gamma_{\mathcal{O},1}+\beta_1}{\xi\gamma_{\xi,1}} \\ &= \int\frac{4-6\xi}{4\xi-3\xi^2-9}d\xi = \int\frac{\frac{d}{d\xi}[4\xi-3\xi^2-9]}{4\xi-3\xi^2-9}d\xi,\end{aligned} \tag{4.24}$$

and therefore

$$\zeta_0^{(h)} = C(4\xi-3\xi^2-9), \tag{4.25}$$

which implies the general solution

$$\zeta_0 = \frac{2(N-1)}{N}\xi + C(4\xi-3\xi^2-9). \tag{4.26}$$

For $N=2$, this is again in agreement with the MAG result [41]. The choice of the integration constant C will be discussed in the next section.

With this result, we succeeded to remove the (one-loop) divergences in our decomposition as well, finding a non-zero value for the tree-level part of the auxiliary parameter. This means that indeed, a term ζJ^2 enters our action, which spoils the usual construction of the generating functional or more precisely, we can no longer interpret it as an energy density [53]. Still, a procedure to circumvent this problem is well-known. By a

Hubbard-Stratonovich transformation [98, 99], an auxiliary field is introduced in such a way that the quadratic source term is eliminated. This procedure will be discussed in the next section.

4.2 Perturbative existence of the condensate

We begin with the announced Hubbard-Stratonovich transformation, introducing the auxiliary field σ as

$$1 = \int \mathcal{D}\sigma \ \ \exp\left[-i\frac{1}{2g^2\zeta}(\sigma + A\mathcal{O} + BJ)^2\right]. \tag{4.27}$$

Here, a normalization constant was absorbed into the path integral measure. The parameters A and B are chosen such that the J^2 term and the composite operator source term $J\mathcal{O}$ in the original Lagrangian are cancelled, i.e., $A = -g$ and $B = -g\zeta$. The modified Lagrangian then reads

$$\mathfrak{L}_{\text{mod}} = \mathfrak{L}_{YM} + \mathfrak{L}^{RED}_{GF+FP} + \mathfrak{L}^{RES}_{GF+FP} + \mathfrak{L}_{\sigma} + \frac{\sigma}{g}J, \tag{4.28}$$

where

$$\mathcal{L}_{\sigma} = -\frac{\sigma^2}{2g^2\zeta} + \frac{1}{\zeta}\frac{\sigma}{g}\mathcal{O} - \frac{1}{2\zeta}\mathcal{O}^2. \tag{4.29}$$

From Eq. (4.27) we also find that the vacuum expectation values of $\mathcal{O}$ and the auxiliary field σ at $J = 0$ are related as

$$\langle\sigma\rangle = g\langle\mathcal{O}\rangle. \tag{4.30}$$

Provided the auxiliary field has a non-zero vacuum expectation value and using

$$\frac{1}{g^2\zeta} = \frac{1}{\zeta_0} - \hbar\frac{\zeta_1}{\zeta_0^2}g^2 + O(g^4, \hbar^2), \tag{4.31}$$

we observe that $\mathfrak{L}_{\sigma}$ contains the mass term for the coset gluon and ghosts, with the tree-level masses

$$m_X^2 = \frac{g\langle\sigma\rangle}{\zeta_0}; \qquad m_{\omega}^2 = \frac{\xi g\langle\sigma\rangle}{\zeta_0}. \tag{4.32}$$

Thus, to answer whether the condensate exists or not, we need to calculate the effective potential for the auxiliary field, hoping for a non-trivial minimum at $\sigma \neq 0$. Such a

physical quantity should be independent of the choice of the gauge fixing parameter, but as we will see, in practice they do depend on ξ. As discussed in [41], this is due to the mixing between different orders of perturbation theory and could only be avoided if one knew the potential up to infinite order. In particular, the integration constant C in the solution of the tree-part ζ_0 of the auxiliary parameter, cf. Eq. (4.26), will enter the expressions. We will motivate a reasonable choice in the course of this section.

Let us proceed with the calculation of the one-loop effective potential for σ. Decomposing the potential into $V = V_0 + V_1$ with the tree part V_0 and the one-loop part V_1, we immediately find the tree-level part

$$V_0(\sigma) = \frac{\sigma^2}{2\zeta_0}. \tag{4.33}$$

For the one-loop correction we have

$$\begin{aligned} V_1(\sigma) = &-\frac{\zeta_1}{2\zeta_0^2} g^2\sigma^2 + i\,\mathrm{Tr}\log\left[\delta^{ab}\left(-p^2 + \frac{\xi g\sigma}{\zeta_0}\right)\right] \\ &- \frac{i}{2}\,\mathrm{Tr}\log\left[\delta^{ab}\left(-p^2 g_{\mu\nu} + (1-\xi^{-1})p_\mu p_\nu + g_{\mu\nu}\frac{g\sigma}{\zeta_0}\right)\right]. \end{aligned} \tag{4.34}$$

Within dimensional regularization, the calculation of the logarithms can be done analogously to section 4.1. Adopting the $\overline{MS}$-scheme we arrive at

$$\begin{aligned} V_1(\sigma) = &-\frac{\zeta_1}{2\zeta_0^2} g^2\sigma^2 - \frac{3}{64\pi^2} 2(N-1)\frac{g^2\sigma^2}{\zeta_0^2}\left(\frac{5}{6} - \log\left[\frac{g\sigma}{\zeta_0\bar{\mu}^2}\right]\right) \\ &+ \frac{1}{64\pi^2} 2(N-1)\frac{\xi^2 g^2\sigma^2}{\zeta_0^2}\left(\frac{3}{2} - \log\left[\frac{\xi g\sigma}{\zeta_0\bar{\mu}^2}\right]\right), \end{aligned} \tag{4.35}$$

where $\bar{\mu}^2 = 4\pi\mu^2 e^{-\gamma}$. Next, we are looking for the stationary points, thus considering the first derivative:

$$\begin{aligned} \frac{dV}{d\sigma} = &\frac{\sigma}{\zeta_0}\left(1 - \frac{g^2\zeta_1}{\zeta_0}\right) - \frac{3}{32\pi^2} 2(N-1)\frac{g^2\sigma}{\zeta_0^2}\left(\frac{1}{3} - \log\left[\frac{g\sigma}{\zeta_0\bar{\mu}^2}\right]\right) \\ &+ \frac{1}{32\pi^2} 2(N-1)\frac{\xi^2 g^2\sigma}{\zeta_0^2}\left(1 - \log\left[\frac{\xi g\sigma}{\zeta_0\bar{\mu}^2}\right]\right). \end{aligned} \tag{4.36}$$

Besides the solution $\sigma = 0$, we find another stationary point σ_*, providing the squared mass m_X^2 given by

$$m_X^2 = \frac{g\sigma_*}{\zeta_0} = \bar{\mu}^2\ \mathrm{Exp}\left[\frac{H_1}{g^2} + H_2\right], \tag{4.37}$$

with

$$H_1(\xi,\zeta_0) = -\frac{1}{(3-\xi^2)}\frac{32\pi^2}{2(N-1)}\zeta_0,$$
$$H_2(\xi,\zeta_1) = \frac{1}{(3-\xi^2)}\left(\frac{32\pi^2}{2(N-1)}\zeta_1 + 1 + \frac{1}{2}\xi^2\log\xi^2 - \xi^2\right). \tag{4.38}$$

Based on these results, we want to discuss the open issue of fixing the integration constant C in the solution for $\zeta_0(\xi)$, cf. Eq. (4.26). First of all, we learn from the tree potential (4.33) that ζ_0 should be positive in order to have a bounded-from-below tree part. In addition, we need to recover the correct UV limit, $\sigma_* \to 0$ as $g^2 \to 0$, which implies that H_1 must be negative. Hence, together with $\zeta_0 > 0$ we conclude $\xi^2 < 3$. This condition is consistent with our picture of the reduction condition, namely rigorously imposing it through a Delta functional in the Faddeev-Popov formalism, corresponding to the limit $\xi \to 0$. The choice

$$C_0 = -\frac{1}{11}\frac{N-1}{N}, \tag{4.39}$$

guarantees that ζ_0 is positive for all ξ within the close vicinity of $\xi = 0$.

Let us finally enforce $\xi = 0$. Assuming that the at this loop-level undetermined one-loop part ζ_1 of the auxiliary parameter remains finite, the function H_2 becomes an irrelevant constant, while for H_1 we obtain

$$H_1\left(\xi = 0, \zeta_0 = -9C_0\right) = -(4\pi)^2\frac{3}{11N} = \frac{1}{\beta_1}. \tag{4.40}$$

Introducing the experimentally accessible and RG invariant QCD scale Λ_{QCD} in the usual way,

$$\Lambda_{QCD} = \bar{\mu}\ \mathrm{Exp}\left[-\int^g \frac{dg'}{\beta_g(g')}\right], \tag{4.41}$$

we find that at $\xi = 0$ and to one-loop order the coset gluon mass becomes proportional to Λ^2_{QCD},

$$m_X^2 = e^{H_2(\xi=0,\zeta_1)}\Lambda^2_{QCD}. \tag{4.42}$$

Therefore, assuming that ξ only changes marginally with $\bar{\mu}$ around $\xi = 0$ we obtain an

RG invariant coset gluon mass. More explicitly, to one-loop order,

$$\bar{\mu}\frac{d}{d\bar{\mu}}m_X^2 \cong \text{const.} \times \bar{\mu}\frac{d}{d\bar{\mu}}\left(\bar{\mu}^2 \text{ Exp}\left[-\frac{3}{11N}\frac{(4\pi)^2}{g^2}\right]\right) = 0. \tag{4.43}$$

Consequently, the vacuum energy is calculated,

$$\begin{aligned} V(\sigma_*) = \frac{\sigma_*^2}{2\zeta_0}\left(1-\frac{g^2\zeta_1}{\zeta_0}\right) - \frac{3\cdot 2(N-1)}{64\pi^2}\frac{g^2\sigma_*^2}{\zeta_0^2}\left(\frac{5}{6}-\log\left[\frac{g\sigma_*}{\zeta_0\bar{\mu}^2}\right]\right) \\ + \frac{2(N-1)}{64\pi^2}\frac{g^2\sigma_*^2\xi^2}{\zeta_0^2}\left(\frac{3}{2}-\frac{1}{2}\log\xi^2-\log\left[\frac{g\sigma_*}{\zeta_0\bar{\mu}^2}\right]\right). \end{aligned} \tag{4.44}$$

The first term in Eq. (4.44) is replaced using $\frac{dV}{d\sigma}\Big|_{\sigma_*} = 0$, which yields

$$\begin{aligned} \frac{\sigma_*^2}{2\zeta_0}\left(1-\frac{g^2\zeta_1}{\zeta_0}\right) = \frac{3\cdot 2(N-1)}{64\pi^2}\frac{g^2\sigma_*^2}{\zeta_0^2}\left(\frac{1}{3}-\log\left[\frac{g\sigma_*}{\zeta_0\bar{\mu}^2}\right]\right) \\ - \frac{2(N-1)}{64\pi^2}\frac{g^2\sigma_*^2\xi^2}{\zeta_0^2}\left(1-\log\left[\frac{\xi g\sigma_*}{\zeta_0\bar{\mu}^2}\right]\right). \end{aligned} \tag{4.45}$$

Plugging this into Eq. (4.44) we obtain

$$V(\sigma_*) = -(3-\xi^2)\frac{2(N-1)}{128\pi^2}\frac{g^2\sigma_*^2}{\zeta_0^2} = -(3-\xi^2)\frac{2(N-1)}{128\pi^2}m_X^4, \tag{4.46}$$

where in the last line we used that the gluon mass is given by $m_X^2 = \frac{g\sigma_*}{\zeta_0}$ and the result is in full agreement with the $N = 2$ MAG case [41]. Together with the condition $\xi^2 < 3$ we indeed find that the energy for this vacuum is negative and therefore the condensate is energetically favored. As mentioned before, the fact that in this one-loop approximation the vacuum energy as well as the position of the minimum depend on the parameter ξ cannot be avoided. However, the condition $\xi^2 < 3$, which is simply a consequence of asymptotic freedom, already guarantees the existence of the condensate. Even though at this stage no further quantitative conclusions can be drawn, the existence of the condensate within $SU(N)$ Yang-Mills theory with $U(N-1)$ stability group has been shown qualitatively at one-loop level. At this point, we also mention [100], where the condensate was found to be energetically favored as well, however, only for $SU(2)$ and based on a background field approach, rather than the LCO formalism.

As explained earlier, the motivation for this study came from lattice simulations performed within this novel reformulation in the $SU(3)$ case, i.e., with the non-Abelian stability group $U(2)$ [27, 28]. These investigations suggested a new type of "infrared Abelian dominance" in the sense that some gluon degrees of freedom become dominant

in the infrared region. However, here these degrees of freedom are not Abelian, as $U(2)$ is a non-Abelian group. In particular, the monopole degrees of freedom carried by the restricted field $\mathfrak{V}_\mu \in \text{Lie } H$ are of non-Abelian type, in contrast to the conventional approach of the Abelian projection. The effective mass term for the remaining degrees of freedom $\mathfrak{X}_\mu \in \text{Lie } G/H$, which we established in this chapter, represents at least qualitatively an analytical explanation for the lattice observations. This marks an important step towards a non-Abelian dual superconductivity picture.

Chapter 5

Condensates within the functional renormalization group

The results obtained so far are based on one-loop perturbation theory. While this is surely a good starting point and important to understand basic mechanisms, the application of perturbation theory towards generically non-pertubative questions like the generation of a gluon mass in the strongly coupled infrared regime of Yang-Mills theory has to be treated with care. We therefore want to reconsider this problem with a non-perturbative tool, the so-called functional renormalization group (FRG). In this chapter, we will first briefly introduce this method. Second, based on the example of the derivation of lower Higgs mass bounds we demonstrate how perturbative calculations may lead to wrong conclusions and how the FRG is able to cure them. This part represents a short digression from the present research, but will familiarize us with key concepts of the FRG and introduces techniques that can be applied equally well to our case. Consequently, in the end, we apply the FRG to the problem of how an effective mass term for the coset gluon may be generated.

As it is common within the FGR framework, throughout this chapter, we will adopt Euclidean spacetime $g_{\mu\nu} = \delta_{\mu\nu}$.

5.1 The concept of the functional renormalization group

The idea behind the functional renormalization group is the Wilsonian concept of integrating out quantum fluctuations momentum shell by momentum shell [101, 102], rather than treating the fluctuations the same at all scales. Several flow equations have been derived on the basis of this approach, e.g., [103–105]. In this thesis, we will adopt a formulation in terms of an object called effective average action Γ_k [106]. Here, k denotes

an intermediate scale, up to which the quantum fluctuations are integrated out, starting from the cutoff Λ. It interpolates between the classical action S at $k = \Lambda$, $\Gamma_\Lambda = S$, where no fluctuations have been integrated out, and the full quantum effective action, $\Gamma_{k\to 0} = \Gamma$, which is recovered once all fluctuations are included. The flow is controlled by introducing a k-dependent regulator term to the classical term according to

$$S \to S_k = S + \Delta S_k[\chi] = S + \frac{1}{2}\int_p \chi^T(-q)R_k(q)\chi(q), \tag{5.1}$$

where χ denotes the collective field variable for the classical fields and the so-called regulator R_k is supposed to satisfy the following three limits,

$$i)\ \lim_{\frac{q^2}{k^2}\to 0} R_k > 0, \quad ii)\ \lim_{\frac{k^2}{q^2}\to 0} R_k = 0, \quad iii)\ \lim_{k^2\to\Lambda^2\to\infty} R_k = \infty. \tag{5.2}$$

Together with the construction of the scale dependent Schwinger functional and the effective average action being its Legendre transformation modified by the regulator term,

$$e^{W_k[J]} = Z_k[J] = \int \mathcal{D}\chi\ e^{-S_k + \int_p J\cdot\chi}; \quad \Gamma_k[\Phi] = \sup_J \{J\cdot\Phi - \log Z_k\} - \Delta S_k[\Phi], \tag{5.3}$$

the three conditions guarantee that

i) the regulator term serves as a k-dependent mass term for the fields,

ii) in the limit $k \to 0$, the effective action Γ is recovered from Γ_k,

iii) in the limit $k \to \Lambda \to \infty$, the classical action S is recovered from Γ_k.

The flow of the effective average action Γ_k is given by the Wetterich equation,

$$\partial_t \Gamma_k = \frac{1}{2}\,\mathrm{STr}\left[\frac{\partial_t R_k}{\Gamma_k^{(2)} + R_k}\right], \quad t = \log\frac{k}{\Lambda}, \tag{5.4}$$

where $\Gamma_k^{(2)}[\Phi]$ denotes the Hessian of the effective average action. Its derivation can be found in the original work [106] or in several reviews, e.g., [107–109]. The Wetterich equation has a one-loop structure and closely resembles the equation for the one-loop corrections to effective action, see Eq. (2.20). The crucial difference, however, is that the loops contain dressed propagators and vertices rather than classical ones, which leads in particular to resummation effects. Therefore, the Wetterich equation is exact at this stage, no approximation has been made. Moreover, in its form (5.4), the effect of the

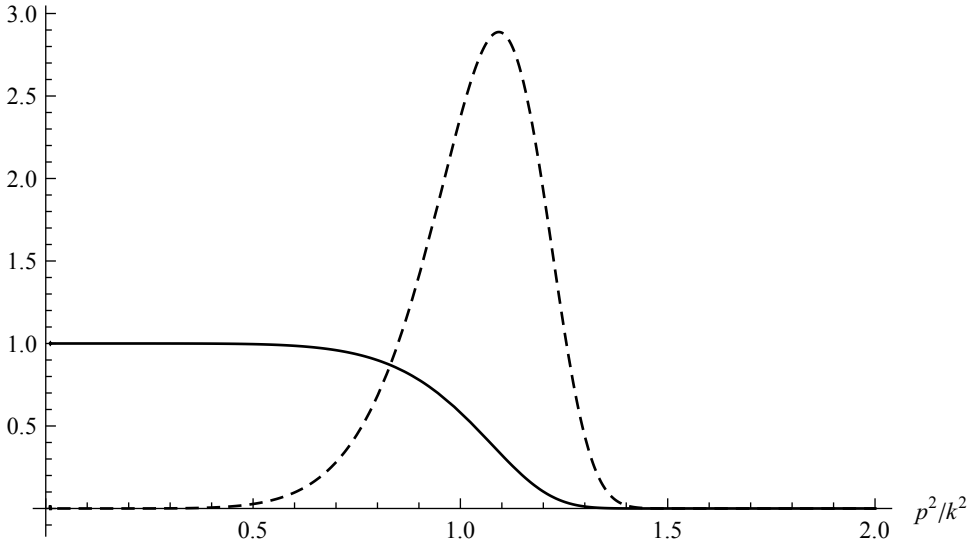

FIGURE 5.1: Typical shape of the regulator (plain) and its scale derivative (dashed), normalized by k^2.

regulator term can be easily understood. Consider a typical shape of the regulator and its scale derivative as shown in Fig. 5.1.

The regulator itself appearing in the denominator of Eq. (5.4) serves as an effective mass term proportional to k^2, yielding infrared regularization. On the other hand, the scale derivative in the numerator is peaked around $p \approx k$, incorporating the idea of integrating out the momentum shell centred around k^2 and at the same time, providing the UV regularization. Let us next mention some advantages of the simple form of the Wetterich equation. First, unlike in Eq. (2.19), where the effective action is determined from a functional integro-differential equation, the Wetterich equation is "just" a differential equation in the intermediate scale k and thus easier to handle. Second, the concept does not involve any expansions in small parameters, making this tool applicable to a wide range of problems. Third, the one-loop form circumvents technical difficulties related to overlapping loop calculations, as they appear for example in perturbation theory at higher loop level or in the Dyson-Schwinger equations. Nevertheless, there is an important fact that needs to be taken care of in the practical use of the FRG. Consider the infinite-dimensional "theory space", spanned by all interactions and their corresponding couplings as the coordinate axes. During the flow of the effective average action through this theory space, in principle *all* of the interactions that respect the symmetry of the theory could be excited, even if they were absent at the cutoff. Of course, it is impossible to take an infinite number of interactions into account. One therefore must truncate the effective average action, making an ansatz including only a finite subset of all possible operators. Common approximation schemes are for example the derivative expansion or the vertex expansion. The fact that one has to truncate also leads to another problem concerning the regulator. As discussed earlier, the starting and endpoint of the flow are fixed by the conditions $\Gamma_\Lambda = S$ and $\Gamma_{k\to 0} = \Gamma$, independently of the chosen regulator. Different regulators will only lead to different "paths" in the theory space, cf. Fig. 5.2.

By truncating, however, the choice of different regulators, while keeping Γ_Λ fixed, may lead to a deviation from the correct infrared effective action. A chosen truncation could for example be tested by investigating how results change when higher order terms are included or by making contact with experimental data.

5.2 Application to the lower Higgs mass bound problem

This section marks a digression from the current line of research, namely the examination of the composite operator condensate. Instead, we consider a different issue related to lower Higgs mass bounds within the standard model. A central role is played by the Higgs condensate and its Yukawa interaction with the quarks and we will acquire techniques that

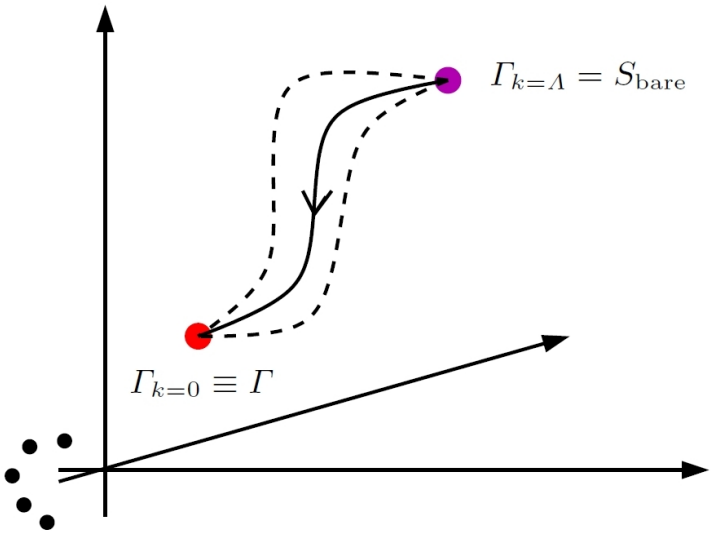

FIGURE 5.2: Schematic flow of the effective average action in theory space. This figure is taken from [109].

will turn out useful when we later handle the interplay between the Hubbard-Stratonovich auxiliary field and the composite operator in a very similar way. Moreover, the Higgs mass bound problem also illustrates how shortcomings of perturbative calculations can be overcome with the help of the FRG. A nice summary related to this kind of research can be found in [110].

5.2.1 Introduction to the problem

Within the standard model, a naive mass term for quarks is forbidden as the left- and right-handed components show a different behavior under gauge transformations of the electroweak sector $SU(2)_L \times U(1)_Y$. This is very similar to how a gluon mass term in Yang-Mills theory is forbidden due to gauge invariance. On the other hand, experiments clearly show that quarks are massive particles. The situation is saved by the Higgs field, which is already responsible for the gauge bosons of the electroweak sector, the $W^{\pm}$ and Z bosons, to become massive. The related mechanism [111–114] also allows for an explanation for the quark masses, as one can introduce gauge invariant Yukawa-type interactions between quark, antiquark and the Higgs field. Simply speaking, if the Higgs field develops a non-vanishing vacuum expectation value, a mass term for the quarks is induced.

Historically the derivation of lower Higgs mass bounds was based on the perturbative analysis of the effective potential for the Higgs field. In particular, within these investigations typically the renormalizable ϕ^4-type potential is used. To discuss the usual line

of arguments, consider the following one-loop Beta functions [115–118],

$$\begin{aligned}
\beta_{\lambda_2} &= \frac{1}{(4\pi)^2}\left[12\lambda_2^2\left(1+\frac{h^2}{\lambda_2}\right) - 12h^4 - 3\lambda_2(3g^2+g'^2) + \frac{9}{4}g^4 + \frac{3}{4}g'^2 + \frac{3}{2}g^2g'^2\right], \\
\beta_{h^2} &= \frac{h^2}{8\pi^2}\left[\frac{9}{2}h^2 - 8g_s^2 - \frac{9}{4}g^2 - \frac{17}{12}g'^2\right], \\
\beta_{g_s^2} &= -7\frac{g_s^4}{8\pi^2}, \quad \beta_{g^2} = -\frac{19}{6}\frac{g^4}{8\pi^2}, \quad \beta_{g'^2} = \frac{41}{6}\frac{g'^4}{8\pi^2}.
\end{aligned} \tag{5.5}$$

Here, $g_s(SU(3))$ is the strong coupling, $g(SU(2))$ and $g'(U(1))$ are the couplings of the electroweak sector, λ_2 is the quartic Higgs coupling with normalization $\frac{\lambda_2}{4}\phi^4$, and finally, h is the top Yukawa coupling. In the above expressions, we neglected already all contributions coming from other fermions, since the top quark is by far the heaviest fermion and thus its coupling to the Higgs field has the dominant effect. Let us take a look at the running of the Beta function of λ_2. For small values of the quartic coupling, its running is dominated by the negative top quark fluctuations proportional to $-h^4$. The coupling therefore may turn negative if running towards large scales, depending on the ratio $\frac{h^2}{\lambda_2}$. On the other hand, the electroweak coupling g'^2 grows towards the UV, potentially turning λ_2 positive again, seeding a meta- or instability in the potential. The lower Higgs mass bound is then derived by requiring the potential to be at least metastable, see, for example, [115–117, 119, 120]. However, there are a few problems in this picture. First, depending on the input of external parameters such as the top mass, the experimental value of the Higgs mass is found to be close to or even violates the perturbatively derived lower mass bounds. Second, lattice simulations actually showed no sign of instabilities for the case of quartic Higgs potentials [121–123]. Third, based on a simple Higgs-Yukawa model used to mimic the Yukawa sector of the standard model, it was shown that the instabilities only occur at scales where the perturbative approximation actually does no longer hold [124].

These facts initiated a series of works that tackled this issue within the FRG framework. As indicated by [124], the qualitative effects could already be understood by a simple Higgs-Yukawa toy model, which, as suggested by the name, only takes into account the interplay between Higgs field and quarks, in particular neglecting the gauge sector. A first attempt in the FRG analysis [125] thus took the following ansatz for the

effective average action,[1]

$$\Gamma_k = \int \frac{Z_{\phi,k}}{2}(\partial_\mu \phi)^2 + U_k(\phi^2) + Z_{\psi,k}\bar{\psi} i\partial\!\!\!/ \psi + i h_k \phi \bar{\psi}\psi. \tag{5.6}$$

The symmetries respected by this ansatz are a $\mathbb{Z}_2$ symmetry for the scalar field (Higgs field) ϕ as well as a chiral symmetry for the Dirac fermion (quark), $\psi \to e^{i\frac{\pi}{2}\gamma_5}\psi$, $\bar{\psi} \to \bar{\psi}e^{i\frac{\pi}{2}\gamma_5}$. The latter symmetry excludes a naive fermionic mass term, while in combination with the $\mathbb{Z}_2$ symmetry, a Yukawa interaction remains invariant. The flowing quantities are U_k, h_k, as well as the anomalous dimensions $\eta_\phi = -\partial_t \log Z_{\phi,k}$ and $\eta_\psi = -\partial_t \log Z_{\psi,k}$. Denoting the vacuum expectation value of ϕ by v_k, the flow is fixed in the infrared by requiring

$$\begin{aligned} v_0 &= \lim_{k\to 0} v_k = 246 \text{ GeV} \\ m_t &= \lim_{k\to 0} (v_k h_k) = 173 \text{ GeV}. \end{aligned} \tag{5.7}$$

In other words, the vacuum expectation value v_k should take the infrared value of the electroweak minimum v_0, and the fermion mass should arrive at the top quark mass m_t. This is achieved by fine-tuning the bare values of the ϕ^2 operator in the effective potential as well as the bare value h_Λ of the Yukawa coupling. On the other hand, the Higgs mass, defined as the curvature of the effective potential evaluated at the minimum, will be considered as a function of the cutoff and the bare potential, $m_H = m_H[\Lambda, U_\Lambda]$. The flow usually is initiated in the symmetric phase and the breaking is triggered dynamically during the flow. For simplicity, the potential is approximated by polynomial expansions around the minimum $v_k = 0$ in the symmetric phase and $v_k \neq 0$ in the broken regime. Thus, in the simplest setting of the perturbatively renormalizable quartic bare potentials,

$$U_\Lambda = \lambda_{1,\Lambda}\rho + \frac{\lambda_{2,\Lambda}}{2}\rho^2, \rho = \frac{1}{2}\phi^2, \tag{5.8}$$

the Higgs mass becomes a function of Λ and $\lambda_{2,\Lambda}$. Two important facts are now observed. First, during the flow no instabilities occur in the effective potential. This agrees with lattice calculations. Second, for fixed cutoff the Higgs mass is increasing with $\lambda_{2,\Lambda}$, i.e., the lower bound is obtained for the choice $\lambda_{2,\Lambda} = 0$. This is also in agreement with lattice results. A negative bare value is not allowed, as the bare potential would no

[1]Here and in the following, we use the same symbols for the microscopic fields χ appearing in the classical action $S_\Lambda[\chi]$ and the macroscopic field $\Phi = \frac{\delta W_k[J]}{\delta J}$, appearing in the effective average action $\Gamma_k[\Phi]$, as it is always clear from the context about which type of field we are talking.

longer be bounded from below and thus the theory ill-defined. Still, a new twist has been added in these investigations, namely the consideration of generalized bare potentials, in the easiest case by adding a $\frac{\lambda_3}{3}\rho^3$ operator. Even though such Higgs interactions of higher canonical dimension are non-renormalizable and therefore vanish in the infrared by simple power counting arguments, they might affect the flow itself considerably in the UV regime where they are still sizeable. In particular, if the corresponding bare value is positive, $\lambda_{3,\Lambda} > 0$, it could stabilize the potential against a negative value of $\lambda_{2,\Lambda}$, which may lead to lower Higgs masses. Indeed, this behavior was exactly observed and therefore a mechanism was presented which can relax the lower Higgs mass bounds, potentially resolving the issue of the near criticality of the experimental Higgs mass value with respect to the perturbative mass bounds. Yet, the simple Higgs-Yukawa model of course can only be used for qualitative statements rather than quantitative ones, as it only represents a rudimentary version of the standard model Yukawa sector. Effort has thus been made to improve the truncation, adding more field content in order to get closer to the standard model. In [126] for example, a chiral Higgs-top-bottom model has been considered. However, recalling the one-loop Beta function for the top coupling of the full standard model,

$$\beta_{h^2} = \frac{h^2}{8\pi^2}\left[\frac{9}{2}h^2 - 8g_s^2 - \frac{9}{4}g^2 - \frac{17}{12}g'^2\right], \tag{5.9}$$

it becomes clear in what direction we should move: The inclusion of the gauge sector, at least the strong interaction, as g and g' remain smaller than g_s at least up to the GUT scale, cf. Fig. 5.3.

Indeed, estimating the top coupling by its infrared value $h = \frac{173}{246}$ and the strong coupling by its value at the Z mass scale, $g_s^2(m_Z) = 4\pi\ 0.118$, one finds that the top fluctuations enter the Beta function with $\frac{9}{2}h^2 \approx 2.226$, while the gluon fluctuations contribute with $-8g_s^2 \approx -11.863$. Additionally, we will extend the truncation by including higher Yukawa interactions of the type $h(\phi)\phi\bar{\psi}\psi$.

5.2.2 Gauged Higgs-Yukawa model

The results in this section are based on collaboration with H. Gies and R. Sondenheimer. They have partial overlap with [127] and lead to the publication [128].

The ansatz for the classical action reads,

$$S_\Lambda = \int_x \left[\frac{1}{2}(\partial_\mu\phi)^2 + U(\rho) + \bar{\psi}^I i\not{D}^{IJ}\psi^J + \frac{1}{4}(F^A_{\mu\nu})^2 + ih(\rho)\phi\bar{\psi}^I\psi^I\right]. \tag{5.10}$$

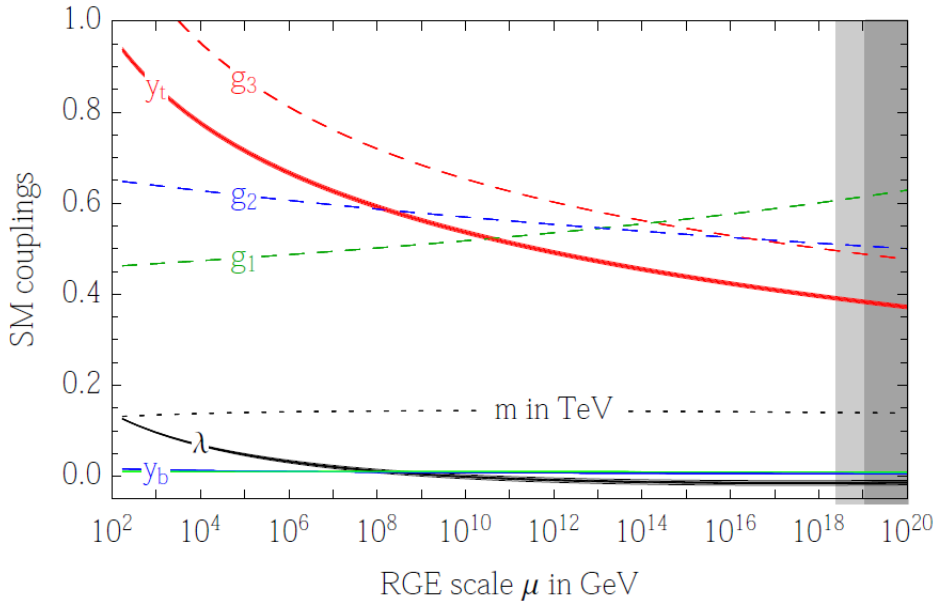

FIGURE 5.3: Running of the couplings $g_3 = g_s$, $g_2 = g$, $g_1 = \sqrt{\frac{5}{3}}g'$, $y_t = h$ as well as the Beta functions for the bottom quark y_b and the τ-lepton y_τ. Moreover, the running of the quartic coupling $\lambda = \frac{\lambda_2}{2}$ is plotted. This figure is taken from [118].

Here, the functions $U(\rho)$ and $h(\rho)$ are functions of the $\mathbb{Z}_2$ invariant $\rho = \frac{1}{2}\phi^2$. The indices $A, B, .. = 1, ..., N^2 - 1$ label the indices of the generators of the Lie algebra of $SU(N)$, while $I, J, ... = 1, ..., N$ label the fundamental representation of the Dirac fermion ψ. The gluon couples to the fermions via a covariant derivative in the fundamental representation, $D_\mu^{IJ} = \delta^{IJ}\partial_\mu - igA_\mu^A[T_A]^{IJ}$. Regarding the truncation for the effective average action, for practical calculations it is more convenient to use a gauge fixed version. In particular, we adopt the common Landau gauge, $\partial_\mu A_\mu^A = 0$, obtaining

$$\Gamma_k = \int_x \Bigg[\frac{Z_{\phi,k}}{2}(\partial_\mu \phi)^2 + U_k(\rho) + Z_{\psi,k}\bar{\psi}^I i\not{D}^{IJ}\psi^J + \frac{Z_{G,k}}{4}(F_{\mu\nu}^A)^2 + ih_k(\rho)\phi\bar{\psi}^I\psi^I + \frac{Z_{G,k}}{2\xi}(\partial_\mu A_A^\mu)^2 + Z_C\bar{C}_A\partial_\mu D_{AB}^\mu C_B \Bigg], \tag{5.11}$$

where the ghosts are taken in the adjoint representation and ξ is the gauge fixing parameter, which will be set to zero in the end. Dirac indices are suppressed throughout this thesis. The clifford algebra in Euclidean spacetime respects $\{\gamma_\mu, \gamma_\nu\} = 2\delta_{\mu\nu}\mathbb{1}_{d_\gamma}$, where $d_\gamma = 2^{\left[\frac{d}{2}\right]}$ and $[n]$ denotes the integer part of n. The ansatz is based on a derivative expansion and is valid as long as the anomalous dimensions $\eta = -\partial_t \log Z$ remain sufficiently small.

Technical set-up

In general, it is more convenient to work in momentum space. We adopt the same conventions on the Fourier transformation as in Eq. (3.31). Furthermore, before deriving the flow equations, we adopt the following conventions. First, the field variations of the effective average action are defined in terms of left-handed and right-handed derivatives,

$$\begin{aligned}\Gamma_k^{(2)}(p,q) &= \frac{\overrightarrow{\delta}}{\delta\Phi^T(-p)}\Gamma_k\frac{\overleftarrow{\delta}}{\delta\Phi(q)} \\ &:= \begin{pmatrix} \frac{\overrightarrow{\delta}}{\delta\phi(-p)} \\ \frac{\overrightarrow{\delta}}{\delta A_\mu^A(-p)} \\ \frac{\overrightarrow{\delta}}{\delta\psi^{TI}(-p)} \\ \frac{\overrightarrow{\delta}}{\delta\bar{\psi}^I(p)} \\ \frac{\overrightarrow{\delta}}{\delta C^A(-p)} \\ \frac{\overrightarrow{\delta}}{\delta\bar{C}^A(p)} \end{pmatrix} \Gamma_k \begin{pmatrix} \frac{\overleftarrow{\delta}}{\delta\phi(q)} & \frac{\overleftarrow{\delta}}{\delta A_\nu^B(q)} & \frac{\overleftarrow{\delta}}{\delta\psi^J(q)} & \frac{\overleftarrow{\delta}}{\delta\bar{\psi}^{TJ}(-q)} & \frac{\overleftarrow{\delta}}{\delta C^B(q)} & \frac{\overleftarrow{\delta}}{\delta\bar{C}^B(-q)} \end{pmatrix}, \end{aligned} \tag{5.12}$$

with the collective field vector Φ. Whenever a superscript "T" is attached to a spinor it refers to transposition with respect to the Dirac indices. Now, the regulator term within this convention is expressed as

$$\Delta S_k[\Phi] = \frac{1}{2}\int_p \Phi^T(-p)R_k(p)\Phi(p), \tag{5.13}$$

with the matrix valued regulator

$$R_k(p) = \begin{pmatrix} R_\phi(p) & 0 & 0 & 0 & 0 & 0 \\ 0 & R_A(p) & 0 & 0 & 0 & 0 \\ 0 & 0 & 0 & -R_\psi^T(-p) & 0 & 0 \\ 0 & 0 & R_\psi(p) & 0 & 0 & 0 \\ 0 & 0 & 0 & 0 & 0 & R_C(-p) \\ 0 & 0 & 0 & 0 & R_C(p) & 0 \end{pmatrix}. \tag{5.14}$$

A typical choice for the regulator of a certain field type is to take the related kinetic part of the effective average action and modify it by the dimensionless shape function $r_k = r_k(p^2/k^2)$, which we will choose identically for all field species, except for the Dirac fermion. In more detail, we write

$$
\begin{aligned}
R_A(p) &= \delta_{AB} Z_{G,k} p^2 \left(\Pi^T_{\mu\nu}(p) + \frac{1}{\xi} \Pi^L_{\mu\nu}(p) \right) r_k, & R_\phi(p) &= Z_{\phi,k} p^2 \; r_k, \\
R_C(p) &= \delta_{AB} Z_{C,k} p^2 \; r_k, & R_\psi(p) &= -\delta_{IJ} Z_{\psi,k} \not{p} \; r_{\psi,k},
\end{aligned}
\tag{5.15}
$$

with the transverse projector Π^T and longitudinal projector Π^L as defined in Eq. (4.15). Next, we derive the flow equations based on the Wetterich equation

$$
\partial_t \Gamma_k = \frac{1}{2} \, \mathrm{STr} \left[\frac{\partial_t R_k}{\Gamma_k^{(2)} + R_k} \right]. \tag{5.16}
$$

Deriving the flow equations

To derive the flow equation for a particular quantity one has to apply projection rules onto the right hand side of the Wetterich equation. In our case, we can distinguish three different cases, which require slightly different techniques in evaluating the projection rule.

The first and probably easiest one is the projection onto the flow of the effective potential. One simply has

$$
\delta_0 \partial_t U_k(\phi) = \frac{1}{2} \, \mathrm{STr} \left[\frac{\partial_t R_k}{\Gamma_k^{(2)} + R_k} \right] \Bigg|_\phi, \tag{5.17}
$$

where δ_0 is the spacetime volume and the right hand side is evaluated at constant ϕ with all other fields set to zero. The calculation is straightforward and one obtains

$$
\partial_t U_k = \frac{1}{2} \int_q \frac{q^2 \partial_t (Z_{\phi,k} r_k(q)}{Z_{\phi,k} P_\phi(q) + U_k''(\phi)} - d_\gamma N \int_q \frac{q^2 Z_{\psi,k} (1 + r_{k,\psi}(q)) \partial_t (Z_{\psi,k} r_{k,\psi}(q))}{Z_{\psi,k}^2 P_\psi(q) + \phi^2 h_k^2(\phi)}. \tag{5.18}
$$

Here, we introduced the generalized momenta $P_\psi(q) = q^2 (1 + r_{k,\psi}(q))^2$ for the fermion and $P_\phi(q) = q^2 (1 + r_k(q))$ for the scalar field. The derivatives of the potential are here defined with respect to ϕ. Diagrammatically, this corresponds to contributions of the following diagrams,

$\partial_t U :$ 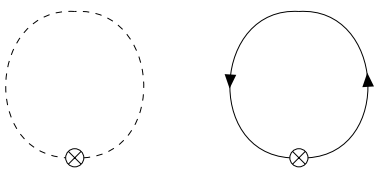 . (5.19)

The dashed line corresponds to the Higgs scalar and the solid line including the arrows represents the fermion. The crossed dot is the regulator insertion $\partial_t R$. As mentioned before, the internal lines and all appearing vertices are understood to be dressed. There are no contributions from gluon or ghost loops included, because they are independent of ϕ and therefore irrelevant for the upcoming discussions. It is convenient to introduce renormalized and dimensionless fields and couplings according to

$$\begin{aligned} \tilde{\psi} &= Z_{\psi,k}^{1/2} k^{(1-d)/2} \psi, & \tilde{C} &= Z_{C,k}^{1/2} k^{1-d/2} C, \\ \tilde{\phi} &= Z_{\phi,k}^{1/2} k^{1-d/2} \phi, & u(\tilde{\phi}) &= k^{-d} U_k(\phi), \\ \tilde{g}^2 &= Z_{G,k}^{-1} k^{4-d} \bar{g}^2, & \tilde{h}(\tilde{\phi}) &= Z_{\phi,k}^{-\frac{1}{2}} Z_{\psi,k}^{-1} k^{2-d/2} h_k(\phi). \end{aligned} \tag{5.20}$$

Moreover, the flow equations are typically expressed in terms of so-called threshold functions, which are listed in appendix C. With the running anomalous dimensions $\eta_\phi = -\partial_t \log Z_{\phi,k}$ and $\eta_\psi = -\partial_t \log Z_{\psi,k}$, the flow equation for the potential becomes

$$\partial_t u = -\, d\, u + (d - 2 + \eta_\phi)\rho u' + 2 v_d \Big[l_0^{(B)d}(u' + 2\rho u''; \eta_\phi) - d_\gamma N\, l_0^{(F)d}(2\rho h^2; \eta_\psi) \Big], \tag{5.21}$$

where now primes denote derivatives with respect to the field invariant ρ and $v_d^{-1} = 2^{d+1} \pi^{\frac{d}{2}} \Gamma(d/2)$ stems from the angle integration over d-dimensional spherical coordinates.

Next, we describe how to obtain the anomalous dimensions. For the scalar field, for example, one uses the projection

$$-\delta_0 \eta_\phi = \frac{Z_{\phi,k}^{-1}}{2d} \partial_{p_\mu} \partial_{p_\mu} \frac{\delta}{\delta\sigma(p)} \frac{\delta}{\delta\sigma(-p)} \frac{1}{2}\, \mathrm{STr} \left[\frac{\partial_t R_k}{\Gamma_k^{(2)} + R_k} \right] \Bigg|_{v_k}. \tag{5.22}$$

A few comments are in order. First, we introduced the fluctuations σ of the Higgs scalar around a vacuum expectation value v_k, $\phi(x) = \sigma(x) + v_k$, which in addition is allowed to be scale dependent. The evaluation of the right hand side at v_k stands for setting to zero all fields except $\phi = v_k$ after taking the field variations with respect to σ. The external momentum p is set to zero at the final stage, once the momentum derivatives have been performed. We only take derivatives with respect to the fluctuations σ in order to account for operators such as $v_k \bar{\psi}\psi$. The fact that we need to perform field derivatives calls for a more convenient form of the Wetterich equation, which is derived as follows.

Let us firstly split the matrix $\Gamma_k^{(2)} + R_k$ into a field-independent part $\Gamma_{k,0}^{(2)} + R_k$ and the

field-dependent (interaction) part $\Delta\Gamma_k^{(2)}$. Upon introducing the modified scale derivative

$$\tilde{\partial}_t = \sum_i \int_q \frac{\partial_t (Z_i r_k)}{Z_i} \frac{\delta}{\delta r_i(q)} = \sum_i \int_q (\partial_t r_i - \eta_i r_i) \frac{\delta}{\delta r_i(q)}, \tag{5.23}$$

we can rewrite

$$\begin{aligned} \left(\Gamma_k^{(2)} + R_k\right)^{-1} \partial_t R_k &= \tilde{\partial}_t \log\left[\Gamma_k^{(2)} + R_k\right] \\ &= \tilde{\partial}_t \log\left[\Gamma_{k,0}^{(2)} + R_k\right] + \tilde{\partial}_t \log\left[1 + \left(\Gamma_{k,0}^{(2)} + R_k\right)^{-1} \Delta\Gamma_k^{(2)}\right]. \end{aligned} \tag{5.24}$$

The first term can be omitted, as the projection rule contains variations with respect to the fields. The logarithm is expanded according to $\log(1+x) = \sum_n (-)^{n+1} \frac{x^n}{n}$ and only those orders are taken into account, that match the number of field variations. In the current case of the anomalous dimensions, one needs to expand up to second order, leading to bubble diagrams in the graphical representation. One typically ends up with terms of the form

$$\partial_{p_\mu} \partial_{p_\mu} \tilde{\partial}_t \int_q \frac{1}{P_1(q)} \frac{1}{P_2(q+p)} \bigg|_{p=0}, \tag{5.25}$$

before taking the derivatives with respect to the external momentum p. One expands the integrand in the external momentum,

$$\partial_{p_\mu} \partial_{p_\mu} \tilde{\partial}_t \int_q \frac{1}{P_1(q)} \left[\frac{1}{P_2(q)} + \partial_{q_\rho} \frac{1}{P_2(q)} p_\rho + \frac{1}{2} \partial_{q_\rho} \partial_{q_\sigma} \frac{1}{P_2(q)} p_\rho p_\sigma + O(p^3)\right] \bigg|_{p=0}, \tag{5.26}$$

performs the momentum derivative, and finally uses the fact that the generalized momenta $P_i(q)$ are actually functions of q^2 to rewrite

$$\partial_{q_\mu} f(q^2) = 2 q_\mu \partial_{q^2} f(q^2). \tag{5.27}$$

For our example, this finally leads to

$$\partial_{p_\mu} \partial_{p_\mu} \tilde{\partial}_t \int_q \frac{1}{P_1(q)} \frac{1}{P_2(q+p)} \bigg|_{p=0} = \tilde{\partial}_t \int_q \frac{1}{P_1(q)} \left[4q^2 \partial_{q^2} \partial_{q^2} + 2d \partial_{q^2}\right] \frac{1}{P_2(q)}. \tag{5.28}$$

Following this line of calculation, we arrive at the anomalous dimension of the Higgs field, conveniently expressed in terms of the renormalized dimensionless quantities and

the threshold functions,

$$\begin{aligned}\eta_\phi =&\frac{8v_d}{d}\Big[\kappa\big(3u''(\kappa)+2\kappa u'''(\kappa)\big)^2 m_2^{(\mathrm{B})d}(m_\phi^2;\eta_\phi)\\ &+d_\gamma N\big(h(\kappa)+2\kappa h'(\kappa)\big)^2\Big(m_4^{(\mathrm{F})d}(m_t^2;\eta_\psi)-2\kappa h^2(\kappa)\,m_2^{(\mathrm{F})d}(m_t^2;\eta_\psi)\Big)\Big].\end{aligned} \tag{5.29}$$

Here, we defined $\kappa=\frac{1}{2}v^2$ and the mass parameters in the threshold functions are $m_\phi^2=u'(\kappa)+2\kappa u''(\kappa)$ and $m_t^2=2\kappa h^2(\kappa)$. Similarly, one obtains the anomalous dimension of the quark,

$$\begin{aligned}\eta_\psi =&\frac{8v_d}{d}\Big[(h(\kappa)+2\kappa h'(\kappa))^2 m_{1,2}^{(\mathrm{FB})d}(m_t^2,m_\phi^2;\eta_\psi,\eta_\phi)\\ &-\frac{N^2-1}{2N}g^2\Big[(1-d+\xi)m_{1,2}^{(\mathrm{FB})d}(m_t^2,0;\eta_\psi,\eta_\mathrm{G})\\ &+(1-d)(\xi-1)\tilde{m}_{1,1}^{(\mathrm{FB})d}(m_t^2,0;\eta_\psi,\eta_\mathrm{G})\Big]\Big].\end{aligned} \tag{5.30}$$

Here, the anomalous dimension η_G appears, on which we comment later. These flow equations correspond to the diagrammatic contributions of the following graphs,

$\eta_\phi:\quad \tilde{\partial}_t\Big\{$ 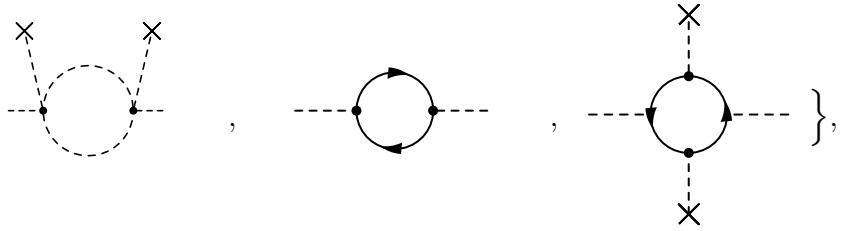 $\Big\},$ (5.31)

and

$\eta_\psi:\quad \tilde{\partial}_t\Big\{$  $\Big\}.$ (5.32)

The curly line stands for the gluon. External lines with a cross at the end correspond to insertions of the condensate $\propto v_k$. Moreover, the operator $\tilde{\partial}_t$ acts onto the diagrams by inserting $\partial_t R_k$ into an internal line, one at a time.

A representative of the third case is the flow of the Yukawa function. As the corresponding vertex is momentum independent, we can give the fields zero external momen-

tum in the projection rule,

$$\delta_0 \partial_t(\phi h_k)\mathbb{1}_{d_\gamma} = \frac{1}{iN}\frac{\overrightarrow{\delta}}{\delta\bar{\psi}^I(0)}\frac{1}{2}\,\mathrm{STr}\left[\frac{\partial_t R_k}{\Gamma_k^{(2)}+R_k}\right]\frac{\overleftarrow{\delta}}{\delta\psi^I(0)}\bigg|_\phi . \tag{5.33}$$

Here, the evaluation at ϕ means that after applying the field variations, all fields except ϕ are set to zero. The calculation can be performed in the same way as described above, yielding the final result

$$\begin{aligned}\partial_t h =& \frac{1}{2}(d-4+\eta_\phi+2\eta_\psi)h + (d-2+\eta_\phi)\rho h' \\ &+ 2v_d\Big[2h(h+2\rho h')^2 l_{1,1}^{(\mathrm{FB})d}(2\rho h^2, u'+2\rho u''; \eta_\psi, \eta_\phi) - (3h'+2\rho h'')l_1^{(\mathrm{B})d}(u'+2\rho u''; \eta_\phi) \\ &- 2g^2 h\frac{N^2-1}{2N}(d-1+\xi)\, l_{1,1}^{(\mathrm{FB})d}(2\rho h^2, 0; \eta_\psi, \eta_\mathrm{G})\Big].\end{aligned} \tag{5.34}$$

Note that here, the argument of u and h is understood to be ρ and consequently, the primes also denote derivatives with respect to ρ. They are *not* evaluated at κ, according to the projection rule. It should be remarked that once the right hand side of Eq. (5.33) has been expressed in terms of ρ and derivatives with respect to ρ, a global factor ϕ has been cancelled with the ϕ on the left hand side. On the other hand, having in mind the standard Yukawa interaction $h\phi\bar{\psi}\psi$, one might be tempted to take a third field derivative with respect to the scalar field. This is actualy how the equation for the standard Yukawa coupling in the more simple truncation was obtained. While the flow is in general independent from the projection, the situation may become different if one deals with truncations such as the polynomial expansion we will adopt later. As it turns out, the projection rule without the additional ϕ-derivative shows better convergence properties and is more suitable for the application to polynomial truncations of h_k. For the details, we refer to [128].

The last open task is to derive the flow equations of the gauge sector. However, due to the fact that the electroweak scale is sufficiently far away from the QCD scale, we are in the position to approximate the flow in this sector by one-loop perturbation theory results. Indeed, we will observe that all relevant quantities in the scalar and fermionic sector decouple from the flow long before the strong coupling runs into its Landau pole. Therefore, we may use

$$\partial_t g^2 = \eta_G g^2; \quad \eta_G = -\frac{g^2}{(4\pi)^2}\left(\frac{22}{3}N - \frac{4}{3}N_f\right), \tag{5.35}$$

where N_f denotes the number of flavors. To mimic the correct standard model running,

we will adopt $N_f = 6$, even though the flow equations we derived before only hold for $N_f = 1$, corresponding to the top quark. However, we could imagine adding five more kinetic terms for the remaining quarks together with corresponding Yukawa couplings, but then set the latter effectively to zero as they are negligible in comparison to the top Yukawa coupling. That this is a reasonable approximation is discussed in [129].

Having completed the set of flow equations, let us mention some consistency checks. First of all, in the case $g^2 = 0$ and $N = 1$ and with $h(\phi) \equiv h$ we recover the flow equations of the simple Higgs-Yukawa system discussed in the previous subsection, except for the flow of h itself due to the projection rule we adopted in this subsection. Moreover, generalized Yukawa interactions have also been studied in an ungauged model in [130] with respect to quark-meson models at finite temperature, and also in the context of Higgs physics in [131]. Furthermore, investigations with respect to the parametrization $\tilde{h}_\phi \equiv \phi h(\phi)$, i.e., $\tilde{h}_\phi$ is not necessarily subject to the symmetry constraints, and concerning gravitational corrections to Higgs-Yukawa systems can be found in [132, 133]. By now, there also exist investigations within the gauged model dealing with asymptotic safety, but with the standard Yukawa coupling [134].

Numerical results

Having completed the set of flow equations within this novel truncation, we start the numerical analysis. First, we finally need to fix our choice for the regulator. The form we adopted in Eq. (5.15) actually is already part of a specific choice for the regulator, which has been optimized with respect to the derivative expansion scheme [135, 136]. It specifies the shape function r_k for the bosons, i.e., the scalar field, gauge field, and ghosts to be

$$r_k(q^2) = \left(\frac{k^2}{q^2} - 1\right) \Theta[k^2 - q^2], \tag{5.36}$$

with the Heaviside step function $\Theta(x)$. On the other hand, for the Dirac fermion we choose

$$(1 + r_{k,\psi})^2 = 1 + r_k. \tag{5.37}$$

The simple form of this so-called Litim regulator [136] allows to analytically solve the momentum integrals that are encoded in the threshold functions. The threshold functions evaluated for this regulator are listed in appendix C. We initiate the flows in the symmetric phase, expanding the effective potential and the Yukawa function around $\kappa_k = 0$

according to

$$u = \sum_{n=1}^{N_u} \frac{\lambda_n}{n!}\rho^n; \quad h = \sum_{\ell=0}^{N_h} \frac{y_\ell}{\ell!}\rho^\ell. \tag{5.38}$$

The flow of the coefficients is easily obtained from the flow equations of the full functions. The switching to the spontaneously broken phase is signaled by λ_1 becoming zero. We then expand according to

$$u = \sum_{n=2}^{N_u} \frac{\lambda_n}{n!}(\rho - \kappa_k)^n; \quad h = \sum_{\ell=0}^{N_h} \frac{y_\ell}{\ell!}(\rho - \kappa_k)^\ell, \tag{5.39}$$

with $u'(\kappa_k) = 0$. As mentioned in the previous subsection, the flow is fixed such that the infrared mass of the fermion coincides with the top quark mass of 173 GeV, while the vacuum expectation value of the Higgs must arrive at 246 GeV,

$$\begin{aligned} v_0 &= \lim_{k\to 0} v_k = 246 \text{ GeV}, \\ m_t &= \lim_{k\to 0} (v_k y_0) = 173 \text{ GeV}. \end{aligned} \tag{5.40}$$

These constraints are achieved by fine-tuning the bare values $\lambda_{1,\Lambda}$ and $y_{0,\Lambda}$. The infrared Higgs mass

$$m_H^2 = \lim_{k\to 0} 2\kappa_k u_k''(\kappa_k), \tag{5.41}$$

is then a function of the remaining bare parameters $\lambda_{n,\Lambda}$ and $y_{\ell,\Lambda}$, with $n > 1$ and $\ell > 0$. We observed that $N_u = 4$ and $N_h = 2$ are sufficient in regard of the quality of the truncation. Taking even higher order operators into account does not have a significant impact on the infrared Higgs mass.

The first thing to check is whether the new terms coming from the gluonic sector change the important features that have already been present in the simple Higgs-Yukawa model. For that purpose, we set the bare values of the higher Yukawa interactions to zero, $y_{1,\Lambda} = y_{2,\Lambda} = 0$, and restrict ourselves to quartic bare potentials, leaving $\lambda_{2,\Lambda}$ as the only free parameter. In fact, as shown in Fig. 5.4 the exact same behavior is observed, namely for fixed cut-off, m_H is again a monotonically growing function of $\lambda_{2,\Lambda}$. In particular, the

effective potential does not develop any instabilities during the flow.

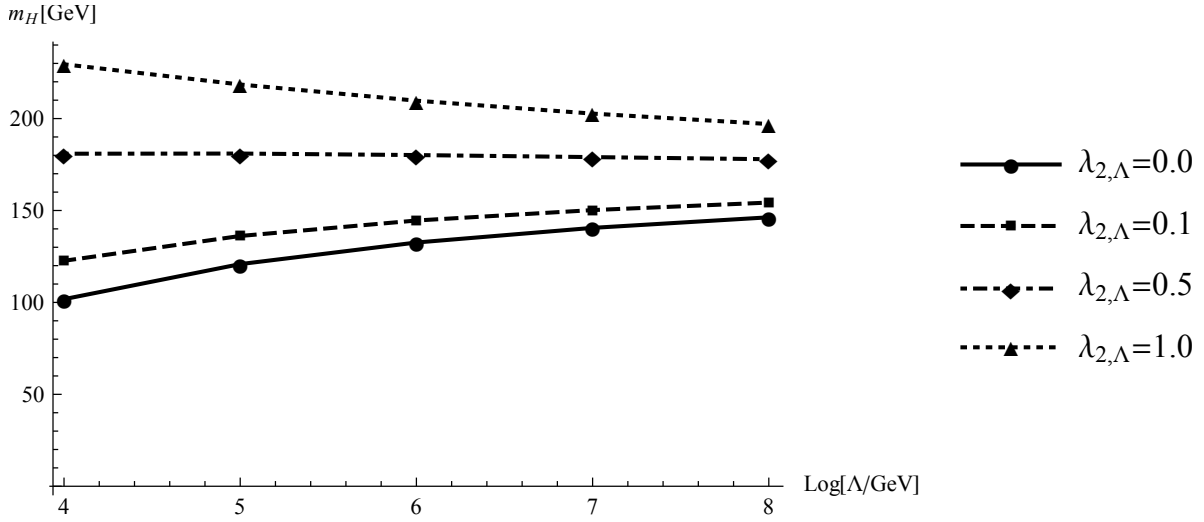

FIGURE 5.4: Higgs masses over the cutoff for quartic bare potentials. As in the simple Higgs-Yukawa system, the Higgs mass is a monotonic function in $\lambda_{2,\Lambda}$ for fixed cutoff, yielding the conventional lower bound at $\lambda_{2,\Lambda} = 0$.

Moreover, if we allow for non-quartic bare potentials in the gauged model, we are in the position to choose negative bare values for the quartic coupling, which generates Higgs masses below the conventional bound just as in the case of the simple model, see Fig. 5.5.

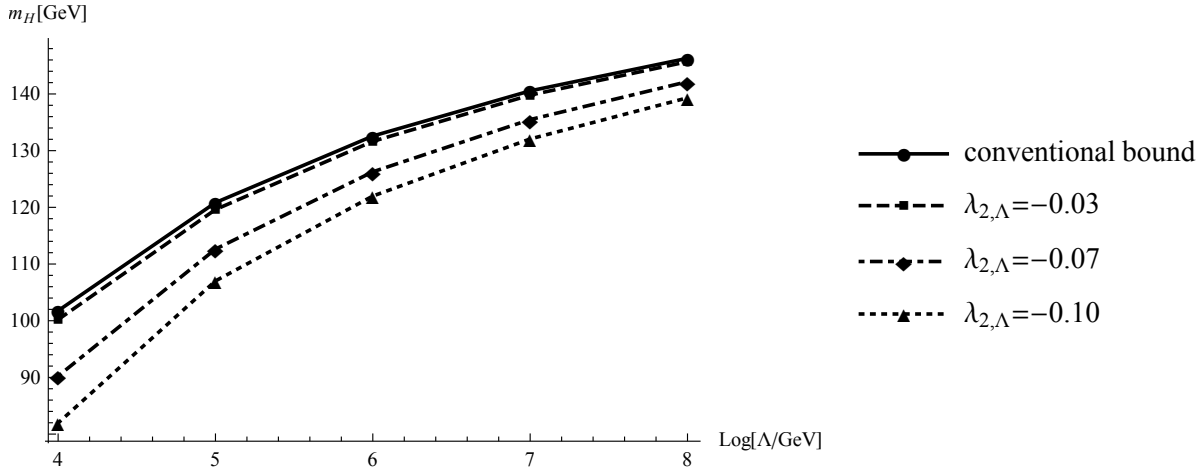

FIGURE 5.5: Higgs masses over the cutoff for non-quartic bare potentials. Already in the easiest case of a non-vanishing bare value of the ρ^3 operator, here $\lambda_{3,\Lambda} = 3$, we are free to choose negative initial values for the quartic coupling, yielding Higgs masses below the conventional bound.

Considering higher polynomials in our expansion can naturally seed instabilities in the potential. In our argumentation, we only take flows into account, where the potential

is stable on all scales, since we cannot decide whether additional minima are artefacts of the truncation. The lower bound naturally emerges from the FRG from the fact that λ_2 must become positive before the system switches to the spontaneously broken phase, otherwise non-physical imaginary Higgs masses are obtained.

This confirms that the main lessons learned from the ungauged model still hold in the gauged model. One difference, however, is the running of the standard top Yukawa coupling y_0. While in the ungauged model, it approaches its infrared value from above, in the gauged model it approaches it from below, see Fig. 5.6.

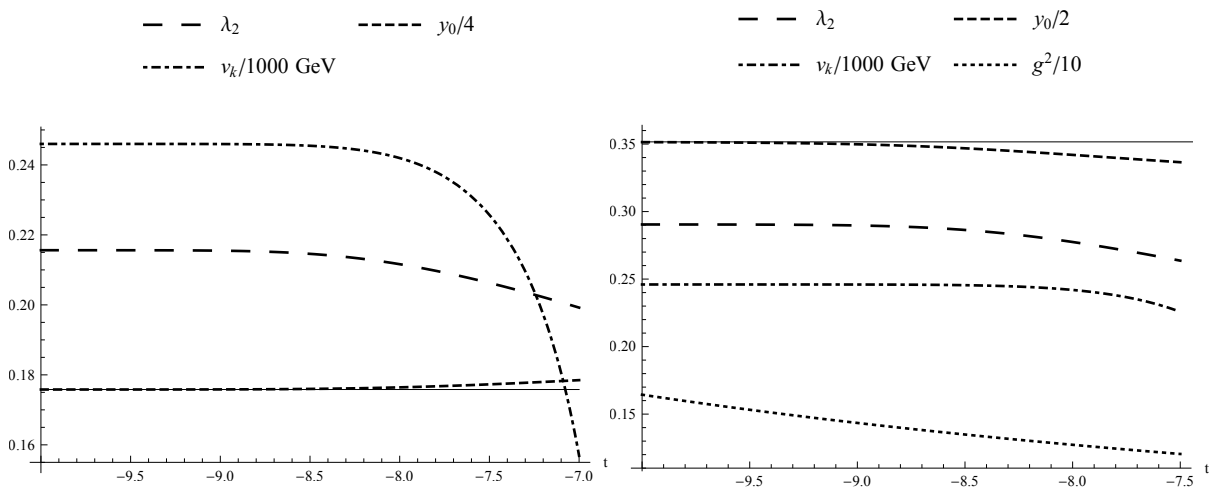

(A) ungauged model

(B) gauged model

FIGURE 5.6: Freezeout of a variety of relevant quantities of the ungauged and the gauged model. Some are rescaled such that they can be presented in one plot. The shallow plain line corresponds to the infrared value of y_0. While y_0 approaches this value from the top in the ungauged model, it approaches it from below in the gauged model. The plot of the gauged model additionally contains the one-loop running of the strong coupling. As can be seen, all relevant quantities decoupled from the flow before the strong coupling runs into the Landau pole.

This behavior can be understood already from the one-loop Beta function in Eq. (5.5). The gluon fluctuations that are now included in the running come with a different sign than the top fluctuations. In particular, the standard top Yukawa coupling becomes asymptotically free.

Next, we examine the impact of the generalized Yukawa operators y_1 and y_2. If their bare value is chosen to be negative, the Higgs mass increases. Since we are interested in the lower bounds, we focus on positive bare values. Moreover, the y_1 operator is found to have the dominant effect, hence we include y_2 in the flow but leave its bare value at zero. Indeed, we again can generate Higgs masses below the conventional bound, as shown in Fig. 5.7. There is an upper limit to the bare value of the Yukawa operators, as they

trigger the switching to the symmetry broken phase. If they are too large, the system switches too early and the infrared Higgs expectation value always exceeds 246 GeV.

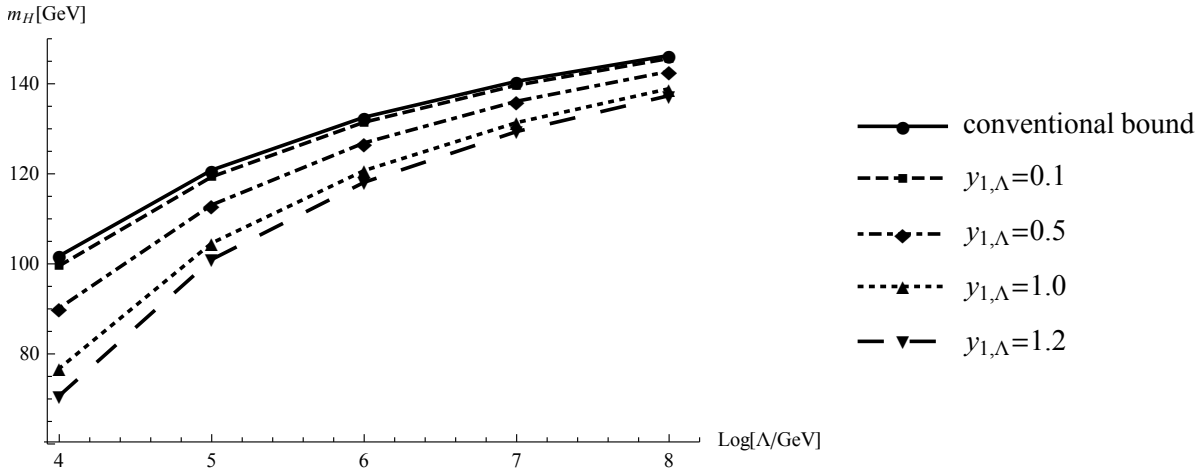

FIGURE 5.7: Higgs masses over the cutoff for quartic bare potentials but including the operator $y_1\phi^3\bar{\psi}\psi$. Choosing positive bare values for this operator can generate masses below the conventional bound.

Concerning the mass bounds, however, we find that the mechanism leading to the lower Higgs masses is essentially the same as for the non-quartic bare potentials. While the latter directly allow to choose negative bare quartic couplings, the higher order Yukawa couplings force the quartic coupling to flow to smaller values, before the behavior changes again as the influence of the operators of higher canonical dimension becomes weaker towards the infrared. The effect is shown in Fig. 5.8.

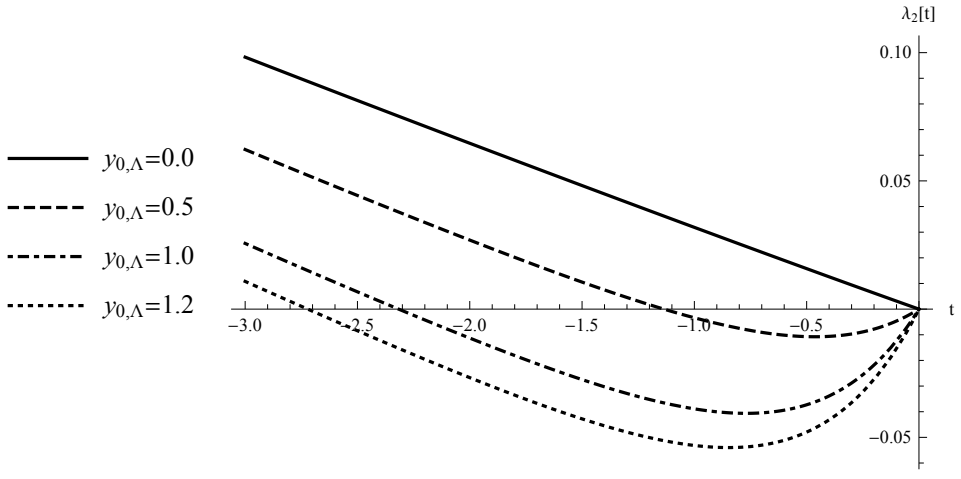

FIGURE 5.8: Effect of the inclusion of higher Yukawa operators on the flow of the quartic coupling λ_2. At the initial scale $t = 0$, these operators lead to a diminishing of the quartic coupling, before it flows back to positive values.

Consequently, the lowest masses obtained in this manner are close to the mass bounds obtained from considering non-quartic bare potentials of the scalar field, see Fig. 5.9.

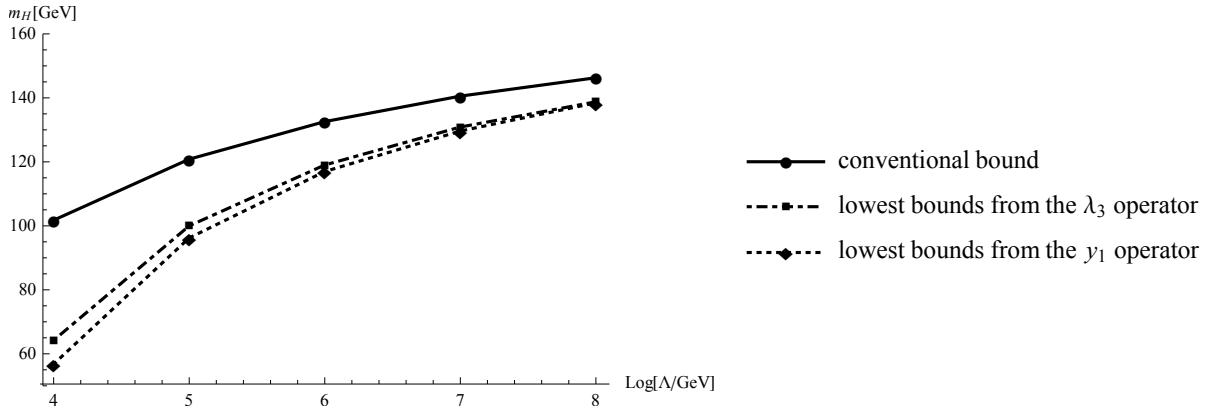

FIGURE 5.9: Comparison of the lower bounds obtained upon inclusion of the ρ^3 operator λ_3 and those obtained upon inclusion of the $\phi^3\bar{\psi}\psi$ operator y_1.

In this subsection, we investigated an improved truncation of a Higgs-Yukawa system with Dirac fermions coupled to the gauge sector and generalized Yukawa interactions. The model exhibits all known features of the simple Higgs-Yukawa system. For quartic bare potentials, the flow of the effective potential is stable on all scales, in contrast to the common perturbative arguments and in accordance with lattice simulations. Allowing for non-quartic bare potentials, flows can be generated that are stable on all scales and that yield Higgs masses below the conventional bound, just like in the ungauged model. This provides a possible mechanism to resolve the puzzling observation of near-criticality of the experimental value of the Higgs mass with respect to perturbatively obtained lower Higgs mass bounds.

Turning to the generalized Yukawa interactions we showed that they can lower the Higgs mass in the same way and that the mechanism behind the lowering is basically the same as for the non-quartic bare potentials. A combination of both effects cannot lead to a further diminishing of the mass bound.

Nevertheless, at this stage the toy model is still a significant simplification of the standard model, we are thus only able to make qualitative statements rather that quantitative ones. This leaves further room for improvement. By now, further progress has been made concerning the treatment of the functions $u(\phi)$ and $h(\phi)$. Solvers for the flow of the full potential have been developed [137], that do not rely on the expansions adopted in this work. It is consistent in the sense that whenever instabilities in the flow have been observed in our case of expanding the potential, the full flow developed the instabilities as well and vice versa. Moreover, in [138] non-polynomial potentials have been considered. For a summary in the progress of the FRG flow studies of the Higgs

potential, see [110].

5.3 Towards establishing the gluon-ghost condensate within the FRG

In the previous section, we gained experience in the application of the FRG and with the examination of the near-criticality of the experimentally obtained Higgs mass in relation to perturbatively obtained Higgs mass bounds, we presented an example of how the FRG can improve perturbation theory. With this knowledge, we return to our original problem regarding the condensate corresponding to the composite operator, trying to improve the perturbative results of chapter 4. For the sake of simplicity, we initially restrict ourselves to the $SU(2)$ case. Even though this corresponds to the conventional MAG, the main focus in this section is to establish the generation of the mass for the remaining field $\mathfrak{X}_\mu \in \text{Lie } G/H$ in a non-perturbative way. The extension towards general N and thus to our new scheme of "non-Abelian infrared dominance" is just a technical matter, if the mass term for the remaining field is generated for $SU(2)$ then the mechanism certainly is present for general N as well.

5.3.1 Defining the truncation

As we learned from the general introduction to the FRG, we firstly have to fix our ansatz for the effective average action. Let us consider the Euclidean version of the classical $SU(2)$ action,

$$S_\Lambda = \int_x \frac{1}{4}(F^a_{\mu\nu})^2 + \frac{1}{4}(F^\gamma_{\mu\nu})^2 + S^{RED}_{GF+FP} + S^{RES}_{GF+FP}, \tag{5.42}$$

where in analogy to chapter 3 the field strength tensors are given by

$$\begin{aligned} F^a_{\mu\nu} &= D^{ab}_\mu X^b_\nu - D^{ab}_\nu X^b_\mu, \\ F^\gamma_{\mu\nu} &= \partial_\mu V^\gamma_\nu - \partial_\nu V^\gamma_\mu + g f^{\gamma ab} X^a_\mu X^b_\nu, \end{aligned} \tag{5.43}$$

with the covariant derivative $D^{ab}_\mu = \delta^{ab}\partial_\mu + g f^{a\gamma b} V^\gamma_\mu$. The indices take value in $a, b \in \{1, 2\}$ and $\gamma \equiv 3$. The coset gauge fixing part reads

$$S^{RED}_{GF+FP} = -\int_x i\delta_B \bar{\delta}_B \,\mathrm{Tr}_{G/H}\left(\mathfrak{X}_\mu \mathfrak{X}_\mu - i\xi \mathfrak{C}\bar{\mathfrak{C}}\right). \tag{5.44}$$

After integrating out the Nakanishi-Lautrup field we obtain

$$= \int_x \Big[\frac{1}{2\xi} (D^{ab}_\mu[V] X^b_\mu)^2 - i\bar{\omega}^a D^{ab}_\mu[V] D^{bc}_\mu[V] \omega^c \\ - \frac{\xi g^2}{4} f^{abJ} f^{cdJ} \bar{\omega}^a \bar{\omega}^b \omega^c \omega^d - i g^2 f^{ab\gamma} f^{cd\gamma} X^a_\mu X^c_\mu \bar{\omega}^b \omega^d \Big]. \tag{5.45}$$

On the other hand, for the residual gauge fixing we only need to take the $U(1)$ part into account,

$$S^{RES}_{GF+FP} = i \int_x \delta_B \left(\bar{C}^\gamma \left[\partial_\mu V^\gamma_\mu + \frac{\alpha}{2} N^\gamma \right] \right), \tag{5.46}$$

which after integrating out the Nakanishi-Lautrup field becomes

$$S^{RES}_{GF+FP} = \int_x \left[\frac{1}{2\alpha} \left(\partial_\mu V^\gamma_\mu \right)^2 - i\bar{C}^\gamma \partial^2 C^\gamma - i g f^{\gamma ab} \bar{C}^\gamma \partial_\mu (X^a_\mu \omega^b) \right]. \tag{5.47}$$

Having the LCO formalism in mind, we next perform a Hubbard-Stratonovich transformation,

$$1 = \int \mathcal{D}\varphi \; e^{-\frac{m^2_\varphi}{2} \left(\varphi + \frac{h}{m^2_\varphi} \mathcal{O} \right)^2}; \quad \mathcal{O} = \frac{1}{2} X^a_\mu X^a_\mu - i\xi \omega^a \bar{\omega}^a, \tag{5.48}$$

introducing new interactions between the auxiliary field φ and the composite operator $\mathcal{O}$,

$$S_{\text{aux}} = \int_x \frac{m^2_\varphi}{2} \varphi^2 + h\varphi\mathcal{O} + \frac{h^2}{2m^2_\varphi} \mathcal{O}^2. \tag{5.49}$$

From Eq. (5.48) we infer that the auxiliary field inherits the (on-shell) BRST invariance of the composite operator,

$$\delta_B \varphi = 0. \tag{5.50}$$

Therefore, the action $S' = S_\Lambda + S_{\text{aux}}$ is BRST invariant. The idea is that the Yukawa-like interaction between the auxiliary field and the composite operator will generate the mass term for the coset gluon and ghosts, very similar to the LCO formalism, provided that the auxiliary field develops a non-zero expectation value. Such investigations based on a combination of the FRG with the Hubbard-Stratonovich already exist, cf. [139–142].

We take the following naive ansatz for the corresponding effective average action,

$$\begin{aligned}\Gamma_k &= \Gamma_{YM} + \Gamma^{RED}_{GF+FP} + \Gamma^{RES}_{GF+FP} + U_k(\varphi) + \frac{Z_{\varphi,k}}{2}\partial_\mu\varphi\partial_\mu\varphi \\ &+ \frac{h_{X,k}}{2}\varphi X^a_\mu X^a_\mu - ih_{\omega,k}\xi\varphi\omega^a\bar{\omega}^a + \frac{\zeta_{1,k}}{8}X^a_\mu X^a_\mu X^b_\nu X^b_\nu - i\xi\frac{\zeta_{2,k}}{2}X^a_\mu X^a_\mu\omega^b\bar{\omega}^b - \frac{\zeta_{3,k}}{2}\xi^2\bar{\omega}^a\omega^a\bar{\omega}^b\omega^b,\end{aligned} \tag{5.51}$$

where we absorbed the mass term $\frac{1}{2}m^2_\varphi\varphi^2$ for the auxiliary field φ into the effective potential $U_k(\varphi)$. The potential is just a function of φ rather than φ^2, because φ is already the invariant with respect to the BRST symmetry. In addition, a kinetic term for the auxiliary field has been added. The parts Γ_{YM}, Γ^{RED}_{GF+FP}, and Γ^{RES}_{GF+FP} are obtained from their classical counterparts by modifying them with flowing renormalization factors, for example,

$$F^\gamma_{\mu\nu} \to \tilde{Z}^{1/2}_{V,k}\left(\partial_\mu V^\gamma_\nu - \partial_\nu V^\gamma_\mu\right) + gf^{\gamma ab}Z_{X,k}X^a_\mu X^b_\nu. \tag{5.52}$$

The Yang-Mills coupling g as well as the gauge fixing parameters ξ and α are considered to be running as well. The Yukawa-like interaction term as well as the $\mathcal{O}^2$ term are split according to

$$\begin{aligned} h\varphi\mathcal{O} &\to \frac{h_{X,k}}{2}\varphi X^a_\mu X^a_\mu - ih_{\omega,k}\xi\varphi\omega^a\bar{\omega}^a, \\ \frac{h^2}{2m^2_\varphi}\mathcal{O}^2 &\to \frac{\zeta_{1,k}}{8}X^a_\mu X^a_\mu X^b_\nu X^b_\nu - i\xi\frac{\zeta_{2,k}}{2}X^a_\mu X^a_\mu\omega^b\bar{\omega}^b - \frac{\zeta_{3,k}}{2}\xi^2\bar{\omega}^a\omega^a\bar{\omega}^b\omega^b.\end{aligned} \tag{5.53}$$

The reasons for this splitting will be discussed in more detail in subsection 5.3.3.

It should be remarked that within a similar ansatz, it was shown that the existence of $\langle\varphi\rangle \neq 0$ can stabilize the Savvidy vacuum [143], i.e., the condensate can lead to the disappearance of the imaginary part present in the one-loop effective potential for the magnetic condensate [42, 43]. However, in the related work, only the flow of the effective potential under certain approximations was considered and in particular not the dynamical generation of the condensate $\langle\varphi\rangle$.

Having defined our ansatz for the effective average action, we proceed with the derivation of the corresponding flow equations.

5.3.2 Deriving the flow equations

Similar to the previous section, we will present all flow equations in terms of dimensionless and renormalized fields and couplings,

$$\begin{aligned}
\tilde{\varphi} &= Z_{\varphi,k}^{1/2} k^{1-d/2} \varphi, & \tilde{\mathfrak{A}}_\mu &= Z_{\mathcal{A},k}^{1/2} k^{1-d/2} \mathfrak{A}_\mu, \\
\tilde{\mathfrak{C}} &= Z_{\mathcal{C},k}^{1/2} k^{1-d/2} \mathfrak{C}, & \tilde{\bar{\mathfrak{C}}} &= Z_{\bar{\mathcal{C}},k}^{1/2} k^{1-d/2} \bar{\mathfrak{C}}, \\
\tilde{h}_X &= k^{d/2-3} Z_{\varphi,k}^{-1/2} Z_{X,k}^{-1} h_{X,k}, & \tilde{h}_\omega &= k^{d/2-3} Z_{\varphi,k}^{-1/2} Z_{\omega\bar{\omega}}^{-1} h_{\omega,k}, \\
\tilde{\zeta}_1 &= k^{d-4} Z_{X,k}^{-2} \zeta_{1,k}, & \tilde{\zeta}_2 &= k^{d-4} Z_{X,k}^{-1} Z_{\omega\bar{\omega}}^{-1} \zeta_{2,k}, \\
\tilde{\zeta}_3 &= k^{d-4} Z_{\omega\bar{\omega}}^{-2} \zeta_{3,k}, & \tilde{g}^2 &= k^{4-d} g^2, \\
u(\tilde{\varphi}) &= k^{-d} U_k(\varphi).
\end{aligned} \tag{5.54}$$

Here, we have $\mathfrak{A}_\mu = \left(X_\mu^a, V_\mu^\gamma\right)$, $\mathfrak{C} = (\omega^a, C^\gamma)$, $\bar{\mathfrak{C}} = \left(\bar{\omega}^a, \bar{C}^\gamma\right)$ and similarly for the related renormalization factors. Moreover, we introduce the symbols $Z_{\omega\bar{\omega}} := \left(Z_{\omega,k} Z_{\bar{\omega},k}\right)^{1/2}$ and $\tilde{Z}_{C\bar{C}} := \left(\tilde{Z}_{C,k} \tilde{Z}_{\bar{C},k}\right)^{1/2}$, as only these combinations will appear in the flow equations. The tilde for the renormalized fields and couplings will be dropped hereafter again. Accordingly, we define the running anomalous dimensions,[2]

$$\begin{aligned}
\eta_X &= -\partial_t \log Z_{X,k}, & \eta_\omega &= -\partial_t \log Z_{\omega\bar{\omega}}, \\
\tilde{\eta}_V &= -\partial_t \log \tilde{Z}_{V,k}, & \tilde{\eta}_C &= -\partial_t \log \tilde{Z}_{C\bar{C}}, \\
\eta_\varphi &= -\partial_t \log Z_{\varphi,k}.
\end{aligned} \tag{5.55}$$

We use similar conventions for the regulators as in subsection 5.2.2, just with small adjustments,

[2]Note, that we maintain the tilde for the quantities related to the residual $U(1)$ sector, in accordance with the notation in chapter 3.

$$
\begin{aligned}
R_X(p) &= \delta_{ab} Z_{X,k} p^2 \left(\Pi^T_{\mu\nu}(p) + \frac{1}{\xi} \Pi^L_{\mu\nu}(p) \right) r_k(p), & R_\omega(p) &= i Z_{\omega\bar{\omega}} p^2 \; r_k(p), \\
\tilde{R}_V(p) &= \tilde{Z}_{V,k} p^2 \left(\Pi^T_{\mu\nu}(p) + \frac{1}{\alpha} \Pi^L_{\mu\nu}(p) \right) r_k(p), & \tilde{R}_C(p) &= i \tilde{Z}_{C\bar{C}} p^2 \; r_k(p), \\
R_\varphi(p) &= Z_{\varphi,k} p^2 \; r_k(p).
\end{aligned}
\tag{5.56}
$$

Note that, even though we regulate the transverse and longitudinal parts of the gluons identically, the mass term for the coset gluon will lead to the following inverse propagator in the coset gluon sector,

$$
\begin{aligned}
\left(\Gamma^{(2)}_k + R_k \right)^{-1}_{XX} \Big|_{\varphi=\text{const.}} &= \frac{\delta^{ab}}{Z_{X,k}} \left(\frac{1}{P_X(p) + k^2 h_X \varphi} \Pi^T_{\mu\nu}(p) + \frac{\xi}{P_X(p) + k^2 \xi h_X \varphi} \Pi^L_{\mu\nu}(p) \right) \\
&=: \delta^{ab} Z^{-1}_{X,k} G_{X\,\mu\nu}(p),
\end{aligned}
\tag{5.57}
$$

where one has to distinguish between the transverse and the longitudinal part. On the other hand, for the $U(1)$ field we have

$$
\left(\Gamma^{(2)}_k + R_k \right)^{-1}_{\tilde{V}\tilde{V}} \Big|_{\varphi=\text{const.}} = \frac{1}{\tilde{Z}_{V,k} \tilde{P}_V(p)} \left(\Pi^T_{\mu\nu}(p) + \alpha \; \Pi^L_{\mu\nu}(p) \right) =: \tilde{Z}^{-1}_{V,k} \; G_{V\,\mu\nu}(p). \tag{5.58}
$$

G_X and $\tilde{G}_V$ are the regularized full propagators of the coset and the residual gluon, respectively. The generalized momenta $P(p) = p^2(1 + r_k(p))$ are defined as usual.

Flow of the effective potential

We apply the same simple projection rule as in section 5.2.2, namely set the fields to constants on the right hand side of the Wetterich equation. As usual, it is most convenient to express the flow equation in terms of the threshold functions. Consequently, the flow for the effective potential reads

$$
\begin{aligned}
\dot{u} = &- d \; u + \left(\frac{1}{2}(d + \eta_\varphi) - 1 \right) u'(\varphi) \; \varphi + 2 v_d d_{G/H} (d-1) l_0^{(B)d}[h_X \varphi; \eta_X] \\
&+ 2 v_d d_{G/H} l_0^{(B)d}[\xi h_X \varphi; \eta_X] - 4 v_d d_{G/H} l_0^{(B)d}[\xi h_\omega \varphi; \eta_\omega] + 2 v_d l_0^{(B)d}[u''(\varphi); \eta_\varphi].
\end{aligned}
\tag{5.59}
$$

Here, primes denote derivatives with respect to φ. The definitions for the threshold functions are given in appendix C. As a reminder, $d_{G/H}$ denotes the dimension of the

coset, $d_{G/H} = 2(N-1)$. The existence of the condensate corresponds to φ developing a non-zero vacuum expectation value, thus we write $\varphi = v_k + \sigma$ just like in the previous section. Moreover, we follow the strategy of local polynomial expansions around v_k defined by $u'(v_k) = 0$, writing,

$$u = \sum_{n=2}^{N_u} \frac{\lambda_n}{n!}(\varphi - v_k)^n. \tag{5.60}$$

From the classical or bare action (5.49) we infer $u_\Lambda = \frac{\lambda_{2,\Lambda}}{2}\varphi^2$, which means $v_{k=0} = 0$ and we assume to be at the borderline to the generation of a non-trivial minimum associated with the vacuum expectation value. The flow of v_k and the couplings λ_n is then calculated in the usual manner,

$$\dot{\lambda}_n = \partial_\varphi^{(n)} \dot{u}\Big|_{\varphi=v_k} + \lambda_{n+1}\dot{v}_k; \quad \lambda_{N_u+1} \equiv 0, \qquad \dot{v}_k = -\frac{1}{\lambda_2}\partial_\varphi \dot{u}\Big|_{\varphi=v_k}. \tag{5.61}$$

The contributions result from the following diagrams,

$\dot{u}$: 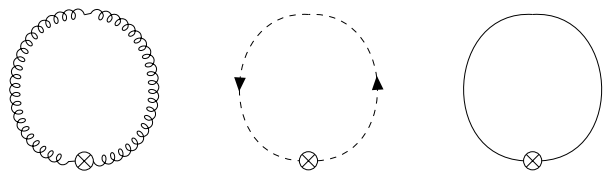 , (5.62)

where in this section the plain line corresponds to the scalar field and the ghost loop in the middle stems from the coset ghosts only. The curly line represents the coset gluon.

Flow of the anomalous dimensions

We begin with the anomalous dimensions of the gluons, in particular of the coset gluon. As we already saw in the one-loop perturbative renormalization (3.74), the longitudinal part and the transverse part of the coset gluon renormalize in a different way. We therefore must project onto the transverse and the longitudinal part independently,

$$\begin{aligned}
-\eta_X d_{G/H}(d-1)\delta_0 &= Z_{X,k}^{-1}\partial_{p^2}\left\{\Pi^T_{\mu\nu}(p)\frac{\delta}{\delta X^a_\mu(p)}\frac{\delta}{\delta X^a_\nu(-p)}\frac{1}{2}\,\mathrm{STr}\left[\frac{\partial_t R_k}{\Gamma_k^{(2)}+R_k}\right]\right\}\Bigg|_{v_k}, \\
\frac{d_{G/H}}{\xi^2}\left(-\eta_X\xi - \dot{\xi}\right)\delta_0 &= Z_{X,k}^{-1}\partial_{p^2}\left\{\Pi^L_{\mu\nu}(p)\frac{\delta}{\delta X^a_\mu(p)}\frac{\delta}{\delta X^a_\nu(-p)}\frac{1}{2}\,\mathrm{STr}\left[\frac{\partial_t R_k}{\Gamma_k^{(2)}+R_k}\right]\right\}\Bigg|_{v_k}.
\end{aligned} \tag{5.63}$$

The evaluation at v_k means that φ is set to v_k and all other fields are set to zero after performing the field variations. Moreover, after performing the momentum derivative, the external momentum p is set to zero. The following diagrams must be taken into account,

∂_t $:\ \tilde{\partial}_t\Big\{$ 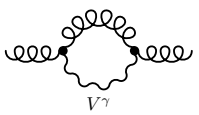 , 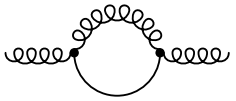 $\Big\}.$

(5.64)

Here, wavy lines represent the residual gluon. Each diagram has to be transversally and longitudinally projected, according to the rules above. Tadpoles do not contribute, as they are found to be independent of the external momentum p. The calculations are rather tedious, for example the gluon loop gives rise to the integral,

$$\begin{aligned}
&\int_q \tilde{G}_{V\,\mu\alpha}(q) G_{X\,\nu\beta}(q+p) \\
&\times \left\{-\delta_{\alpha\nu}(2q+(1-\xi^{-1})p)_\rho + \delta_{\alpha\rho}((1+\xi^{-1})q+(\xi^{-1}-1)p)_\nu + \delta_{\nu\rho}(2p+q)_\alpha\right\} \\
&\times \left\{\delta_{\beta\mu}(2q+(1-\xi^{-1})p)_\rho + \delta_{\beta\rho}(-q-2p)_\mu + \delta_{\mu\rho}(-(1+\xi^{-1})q+(1-\xi^{-1})p)_\beta\right\} \\
&+ (p \to -p).
\end{aligned} \tag{5.65}$$

Next, we have to expand the coset gluon propagator in the external momentum p,

$$\begin{aligned}
&G_{X\nu\beta}(q+p) = G_{X\nu\beta} + \left[\partial_{q_\sigma} T\ \Pi^T_{\nu\beta} + \xi\partial_{q_\sigma} L\ \Pi^L_{\nu\beta} + (T-\xi L)\partial_{q_\sigma}\Pi^T_{\nu\beta}\right] p_\rho \\
&+ \frac{1}{2}\left[\partial_{q_\sigma}\partial_{q_\rho} T\ \Pi^T_{\nu\beta} + \xi\partial_{q_\sigma}\partial_{q_\rho} L\ \Pi^L_{\nu\beta} + (\partial_{q_\rho} T - \xi\partial_{q_\rho} L)\partial_{q_\sigma}\Pi^T_{\nu\beta} + (\partial_{q_\sigma} T - \xi\partial_{q_\sigma} L)\partial_{q_\rho}\Pi^T_{\nu\beta}\right] p_\sigma p_\rho \\
&+ \frac{1}{2}\left[(T-\xi L)\partial_{q_\sigma}\partial_{q_\rho}\Pi^T_{\nu\beta}\right] p_\sigma p_\rho + O(p^3), \qquad T \equiv \frac{1}{P_X + k^2 m_X^2}, \quad L \equiv \frac{1}{P_X + k^2\xi m_X^2},
\end{aligned} \tag{5.66}$$

where $m_X^2 := v_k h_X$ and all arguments of the functions on the right hand side are understood to be q. Finally, one applies the transverse or longitudinal projector, contracts the spacetime indices and applies the p^2 derivative. The transverse projection yields

$$-\eta_X d_{G/H}(d-1) =$$

$$
\begin{aligned}
&g^2 N\Big\{ -4v_d X_1^T[\alpha] l_{1,1}^{(BB)d}[0,m_X^2;\tilde{\eta}_V,\eta_X] - 4v_d X_2^T[\alpha] l_{1,1}^{(BB)d}[0,\xi m_X^2;\tilde{\eta}_V,\eta_X] \\
&+ 4v_d X_3^T[\alpha] m_{1,1}^{(BB)d}[0,m_X^2;\tilde{\eta}_V,\eta_X] + 4v_d X_4^T[\alpha] m_{1,1}^{(BB)d}[0,\xi m_X^2;\tilde{\eta}_V,\eta_X] \\
&+ 4v_d X_5^T[\alpha] n_{1,1}^{(BB)d}[0,m_X^2;\tilde{\eta}_V,\eta_X] + 4v_d X_6^T[\alpha] n_{1,1}^{(BB)d}[0,\xi m_X^2;\tilde{\eta}_V,\eta_X]\Big\} \\
&- h_X^2 d_{G/H}\Big\{ -8v_d \bar{X}_1^T \bar{l}_{1,1}^{(BB)d}[u''(v_k),m_X^2;\eta_\varphi,\eta_X] - 8v_d \bar{X}_2^T \bar{l}_{1,1}^{(BB)d}[u''(v_k),\xi m_X^2;\eta_\varphi,\eta_X] \\
&+ 4v_d \bar{X}_3^T \bar{m}_{1,1}^{(BB)d}[u''(v_k),m_X^2;\eta_\varphi,\eta_X] + 4v_d \bar{X}_4^T \bar{m}_{1,1}^{(BB)d}[u''(v_k),\xi m_X^2;\eta_\varphi,\eta_X] \\
&+ 4v_d \bar{X}_5^T \bar{n}_{1,1}^{(BB)d}[u''(v_k),m_X^2;\eta_\varphi,\eta_X] + 4v_d \bar{X}_6^T \bar{n}_{1,1}^{(BB)d}[u''(v_k),\xi m_X^2;\eta_\varphi,\eta_X]\Big\},
\end{aligned}
\tag{5.67}
$$

while for the longitudinal projection we obtain

$$
\frac{d_{G/H}}{\xi^2}\left(-\eta_X \xi - \dot{\xi}\right) =
$$

$$
\begin{aligned}
&g^2 N\Big\{ -4v_d X_1^L[\alpha] l_{1,1}^{(BB)d}[0,m_X^2;\tilde{\eta}_V,\eta_X] - 4v_d X_2^L[\alpha] l_{1,1}^{(BB)d}[0,\xi m_X^2;\tilde{\eta}_V,\eta_X] \\
&+ 4v_d X_3^L[\alpha] m_{1,1}^{(BB)d}[0,m_X^2;\tilde{\eta}_V,\eta_X] + 4v_d X_4^L[\alpha] m_{1,1}^{(BB)d}[0,\xi m_X^2;\tilde{\eta}_V,\eta_X] \\
&+ 4v_d X_5^L[\alpha] n_{1,1}^{(BB)d}[0,m_X^2;\tilde{\eta}_V,\eta_X] + 4v_d X_6^L[\alpha] n_{1,1}^{(BB)d}[0,\xi m_X^2;\tilde{\eta}_V,\eta_X]\Big\} \\
&- h_X^2 d_{G/H}\Big\{ -8v_d \bar{X}_1^L \bar{l}_{1,1}^{(BB)d}[u''(v_k),m_X^2;\eta_\varphi,\eta_X] - 8v_d \bar{X}_2^L \bar{l}_{1,1}^{(BB)d}[u''(v_k),\xi m_X^2;\eta_\varphi,\eta_X] \\
&+ 4v_d \bar{X}_3^L \bar{m}_{1,1}^{(BB)d}[u''(v_k),m_X^2;\eta_\varphi,\eta_X] + 4v_d \bar{X}_4^L \bar{m}_{1,1}^{(BB)d}[u''(v_k),\xi m_X^2;\eta_\varphi,\eta_X] \\
&+ 4v_d \bar{X}_5^L \bar{n}_{1,1}^{(BB)d}[u''(v_k),m_X^2;\eta_\varphi,\eta_X] + 4v_d \bar{X}_6^L \bar{n}_{1,1}^{(BB)d}[u''(v_k),\xi m_X^2;\eta_\varphi,\eta_X]\Big\}.
\end{aligned}
\tag{5.68}
$$

The coefficients $X_i^T[\theta]$, $X_i^L[\theta]$, $\bar{X}_i^T$, and $\bar{X}_i^L$ are listed in appendix D.

In a similar way, we obtain the flow of the transversally and longitudinally projected flow equations for the residual gluon. First, for the transverse projection we find

$$
-\tilde{\eta}_V(d-1) =
$$

$$
\begin{aligned}
&-\frac{g^2 N}{2}\Big\{ -4v_d V_1^T l_{1,1}^{(BB)d}[m_X^2,m_X^2;\eta_X,\eta_X] - 4v_d V_2^T l_{1,1}^{(BB)d}[m_X^2,\xi m_X^2;\eta_X,\eta_X] \\
&- 4v_d V_3^T l_{1,1}^{(BB)d}[\xi m_X^2,\xi m_X^2;\eta_X,\eta_X] + 4v_d V_4^T m_{1,1}^{(BB)d}[m_X^2,m_X^2;\eta_X,\eta_X] \\
&+ 4v_d V_5^T m_{1,1}^{(BB)d}[m_X^2,\xi m_X^2;\eta_X,\eta_X] + 4v_d V_6^T m_{1,1}^{(BB)d}[\xi m_X^2,m_X^2;\eta_X,\eta_X] \\
&+ 4v_d V_7^T m_{1,1}^{(BB)d}[\xi m_X^2,\xi m_X^2;\eta_X,\eta_X] + 4v_d V_8^T n_{1,1}^{(BB)d}[m_X^2,m_X^2;\eta_X,\eta_X]
\end{aligned}
$$

$$
\begin{aligned}
&+ 4v_d V_9^T n_{1,1}^{(BB)d}[m_X^2, \xi m_X^2; \eta_X, \eta_X] + 4v_d V_{10}^T n_{1,1}^{(BB)d}[\xi m_X^2, m_X^2; \eta_X, \eta_X] \\
&+ 4v_d V_{11}^T n_{1,1}^{(BB)d}[\xi m_X^2, \xi m_X^2; \eta_X, \eta_X] \Big\} \\
&+ g^2 N \Bigg\{ 4v_d \left(4 - \frac{4}{d}\right) m_{1,1}^{(BB)d}[m_\omega^2, m_\omega^2; \eta_\omega, \eta_\omega] \\
&+ 4v_d \left(\frac{8}{d} - \frac{24}{d(d+2)}\right) n_{1,1}^{(BB)d}[m_\omega^2, m_\omega^2; \eta_\omega, \eta_\omega] \Bigg\},
\end{aligned} \tag{5.69}
$$

where we defined $m_\omega^2 = \xi h_\omega v_k$, and the longitudinally projected equation reads

$$
\frac{1}{\alpha^2}\left(-\tilde{\eta}_V \alpha - \dot{\alpha}\right) =
$$

$$
\begin{aligned}
&- \frac{g^2 N}{2} \Big\{ - 4v_d V_1^L l_{1,1}^{(BB)d}[m_X^2, m_X^2; \eta_X, \eta_X] - 4v_d V_2^L l_{1,1}^{(BB)d}[m_X^2, \xi m_X^2; \eta_X, \eta_X] \\
&- 4v_d V_3^L l_{1,1}^{(BB)d}[\xi m_X^2, \xi m_X^2; \eta_X, \eta_X] + 4v_d V_4^L m_{1,1}^{(BB)d}[m_X^2, m_X^2; \eta_X, \eta_X] \\
&+ 4v_d V_5^L m_{1,1}^{(BB)d}[m_X^2, \xi m_X^2; \eta_X, \eta_X] + 4v_d V_6^L m_{1,1}^{(BB)d}[\xi m_X^2, m_X^2; \eta_X, \eta_X] \\
&+ 4v_d V_7^L m_{1,1}^{(BB)d}[\xi m_X^2, \xi m_X^2; \eta_X, \eta_X] + 4v_d V_8^L n_{1,1}^{(BB)d}[m_X^2, m_X^2; \eta_X, \eta_X] \\
&+ 4v_d V_9^L n_{1,1}^{(BB)d}[m_X^2, \xi m_X^2; \eta_X, \eta_X] + 4v_d V_{10}^L n_{1,1}^{(BB)d}[\xi m_X^2, m_X^2; \eta_X, \eta_X] \\
&+ 4v_d V_{11}^L n_{1,1}^{(BB)d}[\xi m_X^2, \xi m_X^2; \eta_X, \eta_X] \Big\} \\
&+ g^2 N \Big\{ - 4v_d l_{1,1}^{(BB)d}[m_\omega^2, m_\omega^2; \eta_\omega, \eta_\omega] + 4v_d \frac{12}{d} m_{1,1}^{(BB)d}[m_\omega^2, m_\omega^2; \eta_\omega, \eta_\omega] \\
&+ 4v_d \frac{24}{d(d+2)} n_{1,1}^{(BB)d}[m_\omega^2, m_\omega^2; \eta_\omega, \eta_\omega] \Big\}.
\end{aligned} \tag{5.70}
$$

The contributing graphs are listed below,

∂_t $:\ \tilde{\partial}_t \Big\{$ 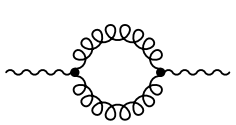 , 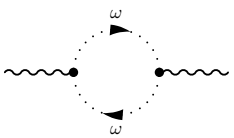 $\Big\}.$

(5.71)

Obtaining the remaining anomalous dimensions is less technical. For the coset ghosts we

have contributions coming from

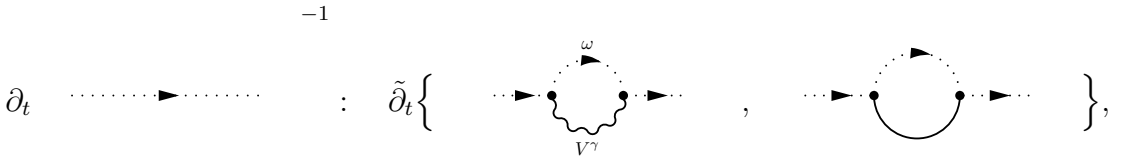

(5.72)

and the flow equation in terms of the threshold functions reads

$$\begin{aligned}\eta_\omega =&\frac{g^2 N}{2d_{G/H}d}\Big\{-32v_d(d-1+\alpha)l_{1,1}^{(BB)d}[0,m_\omega^2;\tilde{\eta}_V,\eta_\omega]+8v_d(8\alpha+d)m_{1,1}^{(BB)d}[0,m_\omega^2;\tilde{\eta}_V,\eta_\omega]\\&+16v_d\;\alpha\;n_{1,1}^{(BB)d}[0,m_\omega^2;\tilde{\eta}_V,\eta_\omega]\Big\}+\frac{\xi^2h_\omega^2}{2d}\Big\{16v_dN_{1,1}^{(BB)d}[m_\omega^2,u''(v_k);\eta_\omega,\eta_\varphi]\Big\}.\end{aligned}\tag{5.73}$$

The flow of the anomalous dimension for the $U(1)$ ghost is trivial, because C^γ does not appear in any interaction. Thus, $\tilde{\eta}_C = 0$. Finally, the contributions to the flow of the two-point function of the auxiliary field are obtained from

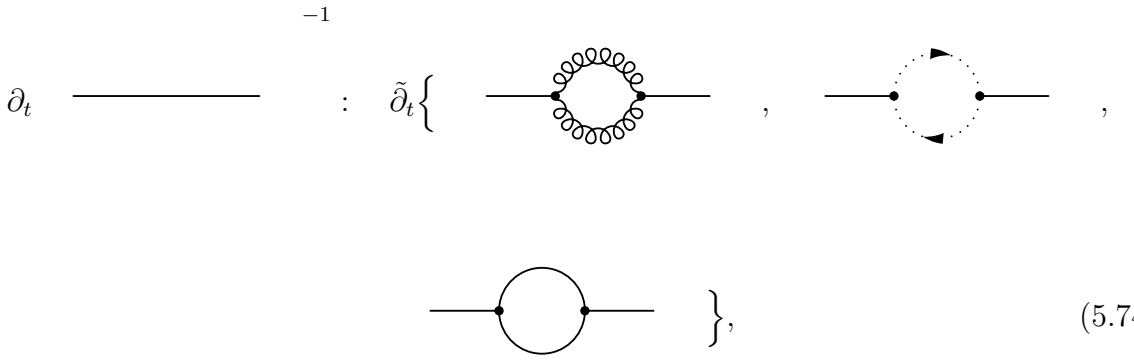

(5.74)

which yields the flow equation

$$\begin{aligned}\eta_\varphi =&4v_dh_X^2d_{G/H}\frac{d-1}{d}\Big\{\bar{l}_{1,1}^{(BB)d}[m_X^2,m_X^2;\eta_X,\eta_X]-2\xi\;\bar{l}_{1,1}^{(BB)d}[m_X^2,\xi m_X^2;\eta_X,\eta_X]\\&+\xi^2\bar{l}_{1,1}^{(BB)d}[\xi m_X^2,\xi m_X^2;\eta_X,\eta_X]\Big\}+4v_dh_X^2d_{G/H}\frac{d-1}{d}m_2^{(B)d}[m_X^2;\eta_X]\\&+4v_dh_X^2d_{G/H}\frac{\xi^2}{d}m_2^{(B)d}[\xi m_X^2;\eta_X]-8v_dd_{G/H}\frac{\xi^2h_\omega^2}{d}m_2^{(B)d}[m_\omega^2;\eta_\omega]\\&+\frac{4v_d}{d}[u^{(3)}(v_k)]^2m_2^{(B)d}[u''(v_k);\eta_\varphi].\end{aligned}\tag{5.75}$$

This completes the set of anomalous dimensions. The set consisting of the Eqs. (5.67), (5.69), (5.73), and (5.75) is a closed algebraic system for the anomalous dimensions and can be solved analytically. The expressions are very long and will not be presented in this

thesis. One observes that $\tilde{\eta}_V$ remains finite if we set α to zero, which means according to Eq. (5.70), that $\alpha = 0$ is a fixed point in the flow. On the other hand, this is not true for η_X and the gauge fixing parameter ξ, which is in accordance with our perturbative calculations in chapter 3. In fact, the perturbative calculation can provide a non-trivial consistency check for the previous equations. This is due to the one-loop structure of the Wetterich equation. The perturbative results should be recovered if we apply the following prescription. First, we identify our FRG scale k with the scale μ introduced in the course of dimensional regularization, $k = \mu$. Next, keeping in mind the anomalous dimensions already represent higher order effects, we must set them to zero in the arguments of the threshold functions, because the latter ones already encode a loop integral. Finally, because the standard perturbation theory does not include threshold effects, we also have to set the mass parameters in the threshold functions to zero. Moreover, to make contact with the results of chapter 3, we set all quantities coming from the auxiliary action to zero,

$$\{h_X, h_\omega, \zeta_i, \lambda_i, v_k\} \to \{0\}, \tag{5.76}$$

as well as $d = 4$. For more information about how certain limits can emerge from the FRG equations, see, for example, [144, 145]. Under the described projections, the equations in this paragraph read

$$\begin{aligned}
&-\eta_X = \frac{g^2}{(4\pi)^2}\left(\frac{17}{3} - 2\alpha - \xi\right) && \Longrightarrow \eta_X = 2\gamma_X,\\
&\left(-\frac{\eta_X}{\xi} - \frac{\dot{\xi}}{\xi^2}\right) = \frac{g^2}{(4\pi)^2}\left(-\frac{2\alpha}{\xi} + \frac{3}{\xi} + \frac{6}{\xi^2} + 1\right) && \Longrightarrow \dot{\xi} = \xi\gamma_\xi,\\
&-\tilde{\eta}_V = \frac{g^2}{(4\pi)^2}\frac{44}{3} && \Longrightarrow \tilde{\eta}_V = 2\tilde{\gamma}_V,\\
&\left(-\frac{\tilde{\eta}_V}{\alpha} - \frac{\dot{\alpha}}{\alpha^2}\right) = 0 && \Longrightarrow \dot{\alpha} = \alpha\gamma_\alpha,\\
&\eta_\omega = \frac{g^2}{(4\pi)^2}(-6 + 2\alpha) && \Longrightarrow \eta_\omega = 2\gamma_\omega,\\
&\tilde{\eta}_C = 0 && \Longrightarrow \tilde{\gamma}_C = -\tilde{\gamma}_{\bar{C}}.
\end{aligned} \tag{5.77}$$

The factor 2 between η and γ with respect to the fields comes from the fact that we defined $\gamma \propto \frac{1}{2}\mu\frac{\partial}{\partial\mu}\log Z$. Hence, we have recovered the correct perturbative limit for the anomalous dimensions and the running of the gauge fixing parameters. Because we

already found that $\alpha = 0$ is a fixed point, we restrict ourselves to this case hereafter.

Flow of the Yukawa operators

We begin with the Yukawa operator related to the coset gluon,

$$d_{G/H}\; d\; \dot{h}_X\; \delta_0 = \frac{\delta}{\delta\sigma(0)} \frac{\delta}{\delta X^a_\mu(0)} \frac{\delta}{\delta X^a_\mu(0)} \frac{1}{2}\, \mathrm{STr} \left[\frac{\partial_t R_k}{\Gamma^{(2)}_k + R_k} \right] \Bigg|_{v_k} . \tag{5.78}$$

This relates to contributions from the following graphs,

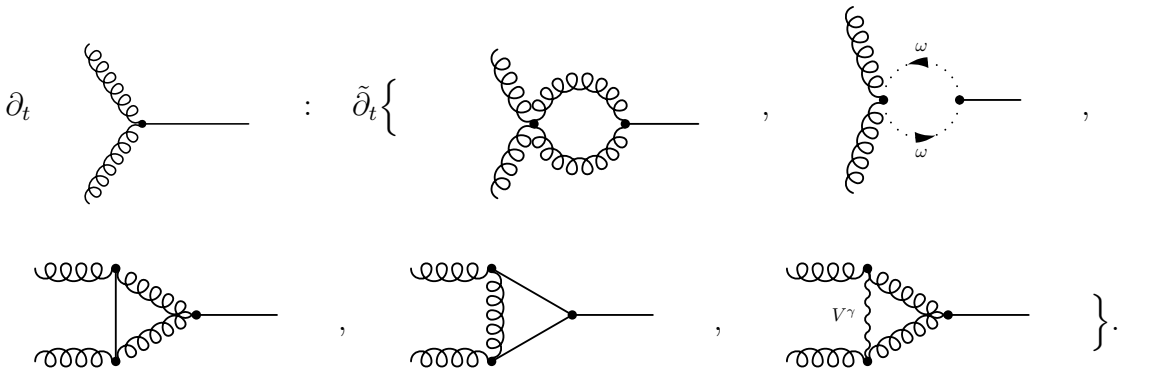

(5.79)

The flow equation in terms of the threshold functions reads

$$\begin{aligned}
\dot{h}_X = &\left(\frac{d}{2} - 3 + \eta_X + \frac{\eta_\varphi}{2} \right) h_X + 2 v_d h_X \left(\frac{d-1}{d} N g^2 + \zeta_1 \left[d_{G/H} + \frac{2}{d} \right] \right) \times \\
&\Big\{ (d-1) l^{(BB)d}_{1,1}[m_X^2, m_X^2; \eta_X, \eta_X] + \xi^2 l^{(BB)d}_{1,1}[\xi m_X^2, \xi m_X^2; \eta_X, \eta_X] \Big\} \\
&- 4 v_d\; \xi\; h_\omega \left(\frac{\zeta_2}{2}\; \xi\; d_{G/H} - g^2 N \right) l^{(BB)d}_{1,1}[m_\omega^2, m_\omega^2; \eta_\omega, \eta_\omega] \\
&- 4 v_d \frac{h_X^3}{d} \Big\{ (d-1) T^{(BBB)d}_{1,1,1}[u''(v_k), m_X^2, m_X^2; \eta_\varphi, \eta_X, \eta_X] \\
&+ \xi^2 T^{(BBB)d}_{1,1,1}[u''(v_k), \xi m_X^2, \xi m_X^2; \eta_\varphi, \eta_X, \eta_X] \Big\} \\
&- 4 v_d \frac{h_X^2 u^{(3)}(v_k)}{d} \Big\{ (d-1) T^{(BBB)d}_{1,1,1}[u''(v_k), u''(v_k), m_X^2; \eta_\varphi, \eta_\varphi, \eta_X] \\
&+ \xi T^{(BBB)d}_{1,1,1}[u''(v_k), u''(v_k), \xi m_X^2; \eta_\varphi, \eta_\varphi, \eta_X] \Big\} \\
&- 8 v_d\; g^2 N \frac{h_X}{d\; d_{G/H}} \Big\{ (4+\alpha)(d-1) \bar{T}^{(BBB)d}_{1,1,1}[0, m_X^2, m_X^2; \tilde{\eta}_V, \eta_X, \eta_X] \\
&+ ((\xi+1)^2 (d-1) + \alpha) \bar{T}^{(BBB)d}_{1,1,1}[0, \xi m_X^2, \xi m_X^2; \tilde{\eta}_V, \eta_X, \eta_X] \Big\} .
\end{aligned} \tag{5.80}$$

Concerning the flow of the Yukawa coupling related to the coset ghosts, we project onto the combination (ξh_ω),

$$id_{G/H}\left(h_\omega\dot{\xi}+\dot{h}_\omega\xi\right)\ \delta_0=\frac{\delta}{\delta\sigma(0)}\frac{\delta}{\delta\omega^a(0)}\frac{\delta}{\delta\bar{\omega}^a(0)}\frac{1}{2}\,\mathrm{STr}\left[\frac{\partial_t R_k}{\Gamma_k^{(2)}+R_k}\right]\Bigg|_{v_k}. \tag{5.81}$$

Contributions stem from the following graphs,

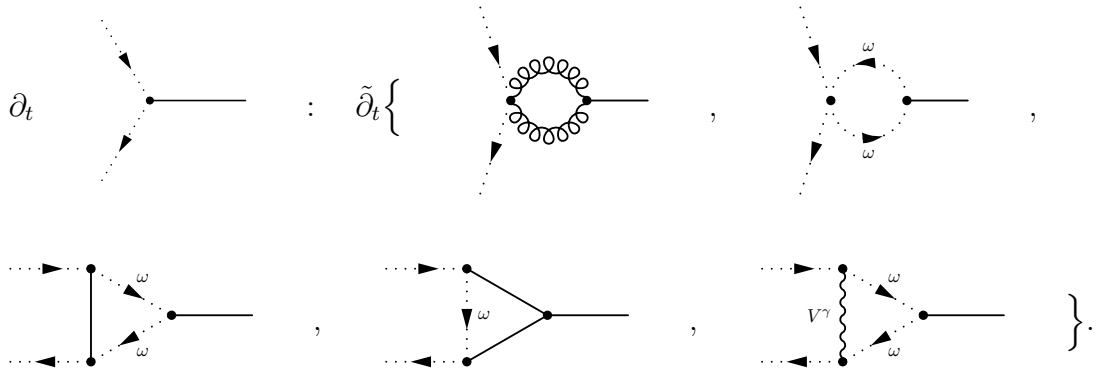

(5.82)

The last diagram is actually found to vanish under the projection, i.e., when the external momenta are set to zero. The remaining diagrams yield the flow equation

$$\begin{aligned}
h_\omega\dot{\xi}+\dot{h}_\omega\xi=&\left(\frac{d}{2}-3+\eta_\omega+\frac{\eta_\varphi}{2}\right)\xi h_\omega+2v_d h_X\left(\xi\frac{\zeta_2}{2}d_{G/H}-g^2N\right)\times\\
&\Big\{(d-1)l_{1,1}^{(BB)d}[m_X^2,m_X^2;\eta_X,\eta_X]+\xi^2 l_{1,1}^{(BB)d}[\xi m_X^2,\xi m_X^2;\eta_X,\eta_X]\Big\}\\
&+4v_d\ \xi\ h_\omega(\xi\ g^2\frac{N}{2}+(1-d_{G/H})\zeta_3\xi^2)l_{1,1}^{(BB)d}[m_\omega^2,m_\omega^2;\eta_\omega,\eta_\omega]\\
&-4v_d\xi^3h_\omega^3\Big\{T_{1,1,1}^{(BBB)d}[u''(v_k),m_\omega^2,m_\omega^2;\eta_\varphi,\eta_\omega,\eta_\omega]\Big\}\\
&-4v_d\xi^2h_\omega^2u^{(3)}(v_k)\Big\{T_{1,1,1}^{(BBB)d}[u''(v_k),u''(v_k),m_\omega^2;\eta_\varphi,\eta_\varphi,\eta_\omega]\Big\}.
\end{aligned} \tag{5.83}$$

We immediately find from Eqs. (5.80) and (5.83) that $h_X=h_\omega=0$ is a fixed point. This is expected because we introduced these interactions by hand through the Hubbard-Stratonovich transformation. Whether or not a non-trivial infrared fixed point exists will be seen later.

Flow of the Yang-Mills coupling

We will obtain the flow of the Yang-Mills coupling from the $V^\gamma\omega\bar{\omega}$ vertex. The adopted projection rule reads

$$\delta_0\ 2dN\ g\ \partial_t\left(\tilde{Z}_V^{1/2}Z_{\omega\bar{\omega}}\ g\right) = gf^{a\gamma b}\partial_{p_\mu}\frac{\delta}{\delta V_\mu^\gamma(p-p')}\frac{\delta}{\delta\omega^b(p')}\frac{\delta}{\delta\bar{\omega}^a(p)}\frac{1}{2}\,\mathrm{STr}\left[\frac{\partial_t R_k}{\Gamma_k^{(2)}+R_k}\right]\Bigg|_{v_k}, \tag{5.84}$$

where the evaluation at v_k is defined as usual and after performing the field variations, we set $p'=p$, perform the momentum derivative and then evaluate at $p=0$. An additional factor g was multiplied in order to receive the running of g^2 rather than g. The following diagrams can in principle contribute,

$\beta_{g^2}:\quad \tilde{\partial}_t\Big\{$ 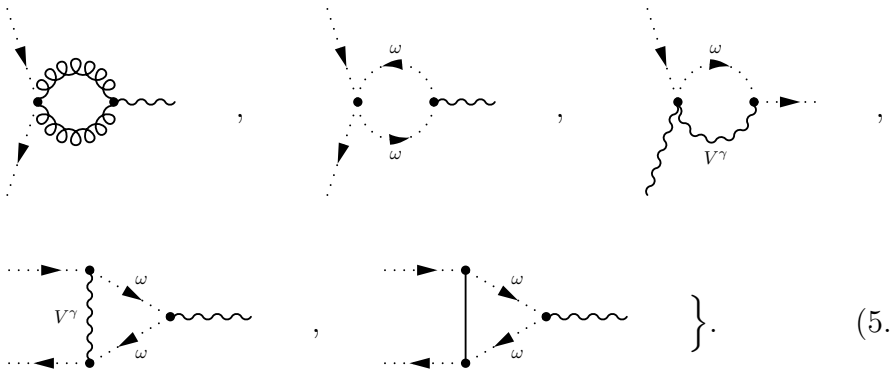 $\Big\}.$ (5.85)

However, the first and second diagram are found to be independent from the external momentum, such that both diagrams vanish under the projection ∂_{p_μ}. In terms of the threshold functions we find

$$\begin{aligned}
\beta_{g^2} &= (\tilde{\eta}_V+2\eta_\omega)g^2+(d-4)g^2\\
&\quad+16v_d g^4\frac{N}{d(N-1)}\Big\{(d-1+\alpha)l_{1,1}^{(BB)d}[0,m_\omega^2;\tilde{\eta}_V,\eta_\omega]-\alpha\ m_{1,1}^{(BB)d}[0,m_\omega^2;\tilde{\eta}_V,\eta_\omega]\Big\}\\
&\quad-4v_d g^4\frac{N}{d(N-1)}\ \alpha\Big\{2(4+d)\bar{T}_{1,1,1}^{(BBB)d}[0,m_\omega^2,m_\omega^2;\tilde{\eta}_V,\eta_\omega,\eta_\omega]\\
&\qquad\qquad-4\ \bar{D}_{1,1,1}^{(BBB)d}[0,m_\omega^2,m_\omega^2;\tilde{\eta}_V,\eta_\omega,\eta_\omega]\Big\}\\
&\quad-4v_d g^2\frac{(\xi h_\omega)^2}{d}\Big\{2d\ T_{1,1,1}^{(BBB)d}[u''(v_k),m_\omega^2,m_\omega^2;\eta_\varphi,\eta_\omega,\eta_\omega]\\
&\qquad\qquad-8\ D_{1,1,1}^{(BBB)d}[u''(v_k),m_\omega^2,m_\omega^2;\eta_\varphi,\eta_\omega,\eta_\omega]\Big\}.
\end{aligned}\tag{5.86}$$

Note that we temporarily reintroduced the residual gauge fixing parameter α. This is in order to perform a consistency check with the one-loop perturbative result. In fact, all dependence on gauge fixing parameters must vanish in this limit. With the description

we explained in the previous paragraphs, Eq. (5.86) reduces to

$$\beta_{g^2} = -\frac{44}{3}\frac{g^4}{(4\pi)^2}, \tag{5.87}$$

which is indeed in agreement with the standard result for $SU(2)$.

Flow of the auxiliary four-point couplings ζ_i

At the level of our truncation, the auxiliary four-point interactions corresponding to the couplings ζ_i are momentum independent, i.e., we can use the projection rules

$$\begin{aligned}
d\ d_{G/H}(2+d\ d_{G/H})\partial_t\left(\zeta_1+\frac{N(d-1)}{(2+d\ d_{G/H})}g^2\right)\delta_0 = \\
\frac{\delta}{\delta X^a_\mu(0)}\frac{\delta}{\delta X^a_\mu(0)}\frac{\delta}{\delta X^b_\nu(0)}\frac{\delta}{\delta X^b_\nu(0)}\frac{1}{2}\,\mathrm{STr}\left[\frac{\partial_t R_k}{\Gamma^{(2)}_k+R_k}\right]\Bigg|_{v_k}, \\
i\ d\ d^2_{G/H}\partial_t\left(\xi\frac{\zeta_2}{2}-\frac{N}{d_{G/H}}g^2\right)\delta_0 = \\
\frac{\delta}{\delta X^a_\mu(0)}\frac{\delta}{\delta X^a_\mu(0)}\frac{\delta}{\delta \omega^b(0)}\frac{\delta}{\delta \bar\omega^b(0)}\frac{1}{2}\,\mathrm{STr}\left[\frac{\partial_t R_k}{\Gamma^{(2)}_k+R_k}\right]\Bigg|_{v_k}, \\
d_{G/H}(1-d_{G/H})\partial_t\left(\xi^2\zeta_3+\frac{N}{2}\frac{1}{1-d_{G/H}}g^2\xi\right)\delta_0 = \\
\frac{\delta}{\delta \omega^a(0)}\frac{\delta}{\delta \bar\omega^a(0)}\frac{\delta}{\delta \omega^b(0)}\frac{\delta}{\delta \bar\omega^b(0)}\frac{1}{2}\,\mathrm{STr}\left[\frac{\partial_t R_k}{\Gamma^{(2)}_k+R_k}\right]\Bigg|_{v_k}.
\end{aligned} \tag{5.88}$$

As usual, evaluation at v_k means that after performing the field variations, all fields are set to zero except $\varphi = v_k$. However, the flow equations become rather involved due to a big number of diagrams. They could in principle be obtained using computer algebra systems, see, for example, the powerful *Mathematica* packages "*doFun*" [146] and "*FormTracer*" [147]. For the sake of simplicity, we refrain from obtaining their flow equations explicitly, but approximate their flow as explained in the next subsection.

5.3.3 Mimicking BRST invariant flows

In this subsection, we explain in more detail the reason for the operator splitting we performed in Eq. (5.53), as well as a certain approximation we adopt when solving the

flow equations. First, due to its composite nature, the two "pieces" of the $\varphi\mathcal{O}$ interaction, φXX and $\varphi\omega\bar{\omega}$, will *a priori* flow differently, and similarly the parts $XXXX$, $XX\omega\bar{\omega}$, and $\omega\bar{\omega}\omega\bar{\omega}$ of the $\mathcal{O}^2$ interaction. This is realized by introducing the independent couplings h_X, h_ω and the ζ_i. Second, the regulator term for the fields will generally break the BRST invariance,

$$\delta_B \Delta S_k[\Phi] \neq 0, \tag{5.89}$$

leading to modified Slavnov-Taylor identities. In particular, if calculated in terms of the effective average action, the master equation (2.26) will receive non-zero corrections on the right hand side. The modified Slavnov-Taylor identities lead to constraints on the bare action and consequently limit the set of truncations of the effective average action that would be compatible with BRST invariant flows. As one would expect, these identities are highly involved, especially in non-Abelian field theories, and would be very complicated to solve. We therefore refrain from dealing explicitly with these identities and instead take a much simpler approach explained below. We do not discuss the issues related to the modified Slavnov-Taylor identities any further and refer to the literature for more details [108, 109, 148–153]. Let us now explain our simplified picture. Knowing that by construction, the regulator term vanishes at $k = 0$, the standard Slavnov-Taylor identities have to be recovered in the infrared, leaving us again with a BRST invariant action. Instead of solving the very complicated modified Slavnov-Taylor identities and calculating the bare action that is compatible with this fact, we could instead fine-tune the bare values of our operators exactly such that in the limit $k \to 0$, a BRST invariant action is obtained. In our particular case, this means matching the following conditions,

$$\lim_{k\to 0} h_X = \lim_{k\to 0} h_\omega; \qquad \lim_{k\to 0} \zeta_1 = \lim_{k\to 0} \zeta_2 = \lim_{k\to 0} \zeta_3 = \lim_{k\to 0} \frac{h_\omega^2}{\lambda_2} = \lim_{k\to 0} \frac{h_X^2}{\lambda_2}. \tag{5.90}$$

Hence, we would have only one free bare parameter, say $h_{X,\Lambda}$, and must fine-tune the bare values of h_ω and the ζ_i such that the conditions (5.90) are satisfied. Regarding our initial analysis, however, we will go even one step further. We replace h_X and h_ω from the beginning by a unique operator h, and let it flow according to one of the three choices

$$\dot{h} = \left\{ \dot{h}_X, \dot{h}_\omega, \frac{1}{2}\left(\dot{h}_X + \dot{h}_\omega\right) \right\}. \tag{5.91}$$

Similarly, we replace the quartic auxiliary couplings by a unique ζ and let it run according to $\frac{h^2}{\lambda_2}$. For example, if we choose $\dot{h} = \dot{h}_X$ the running of ζ obeys

$$\begin{aligned}\dot{\zeta} = &(d - 4 + 2\eta_X)\,\frac{h_X^2}{\lambda_2} + 2\frac{h_X}{\lambda_2}\left\{\left(3 - \frac{d}{2} - \eta_X - \frac{\eta_\varphi}{2}\right) h_X + \dot{h}_X\right\} \\ &- \frac{h_X^2}{\lambda_2^2}\Big\{(2 - \eta_\varphi)\lambda_2 + \dot{\lambda}_2\Big\}. \end{aligned} \tag{5.92}$$

The terms in curly brackets are just the Beta functions of the dimensionless quantities h_X and λ_2 minus their canonical running[3]. The canonical running of ζ is covered by the first term. In this way, we forced our action to become BRST invariant in the limit $k \to 0$, or more precisely, we forced it to remain BRST invariant on all scales. Moreover, testing different running behaviors (5.91) for the unified Yukawa operator h provides a good consistency check for the flow equations in the sense that no qualitative feature should occur for one choice but not the other.

5.3.4 Numerical results

For the cutoff, we choose the Z mass scale $\Lambda = 91.2$ GeV. Let us for a moment reintroduce the tilde for the renormalized and dimensionless quantities. According to Eq. (5.49), we take the following initial condition for the effective potential,

$$u_\Lambda = \frac{\tilde{\lambda}_{2,\Lambda}}{2}\tilde{\varphi}^2 \equiv \frac{\tilde{m}^2_{\Lambda,\varphi}}{2}\varphi^2. \tag{5.93}$$

For the renormalization factors we adopt

$$Z_{X,\Lambda} = Z_{V,\Lambda} = Z_{\omega\bar{\omega},\Lambda} = Z_{C\bar{C},\Lambda} = 1; \quad Z_{\varphi,\Lambda} = 10^{-5}. \tag{5.94}$$

The initial renormalization factor $Z_{\varphi,\Lambda}$ for the auxiliary field is chosen much smaller compared to the other ones, because we assume the original degrees of freedom related to the standard fields to be dominant at the initial scale. This corresponds to the fact that the kinetic term of the auxiliary field, which is proportional to Z_φ, is approximately zero at the initial scale, in accordance with its absence in the classical theory. Moreover, this choice essentially means that the renormalized mass $\bar{\lambda}_2 = \frac{\lambda_2}{Z_\varphi}$ becomes large in the UV and the propagator therefore effectively momentum independent [141, 142]. This is reasonable, because the two-point function of φ is effectively related to the $\mathcal{O}^2$ interactions

[3]Consider a coupling Y of mass dimension d_m which renormalizes with renormalization factor Z, i.e., the dimensionless and renormalized quantity is given by $\tilde{Y} = Z^{-1}k^{d_m}Y$. The running $\partial_t\tilde{Y}$ thus includes contributions from Z and the scaling factor k^{-d_m}. We refer to them as the canonical running.

and thus to the $XXXX$, $XX\omega\bar{\omega}$, and the $\omega\bar{\omega}\omega\bar{\omega}$ interactions. These are all momentum independent at the cutoff scale. In particular, we choose the initial values corresponding to the unrenormalized and dimensionful quantities according to

$$\lambda_{2,\Lambda} = 1 \text{ GeV}^2; \quad h_{X,\Lambda} = h_{\omega,\Lambda} \equiv h_\Lambda = 1 \text{ GeV}. \tag{5.95}$$

We furthermore include the λ_3 and λ_4 operators into the flow as well and set their initial values to zero. Apart from the flow of the effective potential, the operator λ_3 also appears in the flow equation for η_φ and the Yukawa operators through the $u^{(3)}(v_k)$ term and λ_4 thus corresponds to the first term beyond these non-trivial contributions. Furthermore, we assume that at the cutoff, the Yukawa interactions between the auxiliary field and the coset fields are weak in comparison to the scalar mass term. Hereafter, we drop the tilde and only talk about the dimensionless and renormalized quantities again. The only parameter left to be discussed is the initial value of ξ. Of course, following previous discussions we would like to choose $\xi_\Lambda = 0$. However, the flow equations contain terms proportional to ξ^{-1} and prevent us from adopting this choice. Moreover, let us have a look at the flow for the effective potential, cf. Eq. (5.59), with the threshold functions evaluated for the Litim regulator and at $d = 4$,

$$\begin{aligned}\dot{u} = &-4\, u(\varphi) + \left(1 + \frac{\eta_\varphi}{2}\right) u'(\varphi)\, \varphi + \frac{3\left(1 - \frac{\eta_X}{6}\right)}{16\pi^2\,(1 + \varphi\, h_X)} + \frac{1 - \frac{\eta_X}{6}}{16\pi^2\,(1 + \varphi\, \xi\, h_X)} \\ &- \frac{1 - \frac{\eta_\omega}{6}}{8\pi^2\,(1 + \varphi\, \xi\, h_w)} + \frac{1 - \frac{\eta_\varphi}{6}}{32\pi^2\,(1 + u''(\varphi))}.\end{aligned} \tag{5.96}$$

The first two terms are just a consequence of the transition to dimensionless and renormalized quantities, in other words, the canonical running mentioned before. The third and fourth terms come from the coset gluon loop, the fifth term represents the coset ghost loop and finally, the sixth term originates from the auxiliary field loop. Now, generally speaking, a non-zero value for the minimum we expand around is triggered by terms entering the flow equation with a negative sign. Assuming that the anomalous dimensions remain small in accordance with the validity of the derivative expansion, only the ghost loop term can generate such a non-zero expectation value, as it comes with the for anti-commuting fields expected negative sign. However, for $\xi = 0$ this term would become independent of φ and could be neglected. This emphasizes again that the gauge fixing parameter ξ plays an unusual role. This line of argument somewhat contradicts the line of argument presented in chapter 4, which was based on perturbation theory. The one-loop running of ξ predicted that it will always grow to infinity, as no fixed point exists. We therefore argued that in the end it should be set to zero by hand in order to

rigorously incorporate the reduction condition by means of a Delta functional through the Faddeev-Popov trick. Now, within the FRG set-up, the situation is different. Even though the FRG flow equations still imply that $\xi = 0$ is not a fixed point, just like in the perturbative predictions, they also imply that a non-zero value of ξ is necessary to generate the condensate. The FRG calculations could be regarded as an improvement if we would observe that ξ approaches a non-zero infrared fixed point instead of growing to infinity, and if we could manage to find initial conditions where the infrared value is sufficiently small, so that at $k = 0$ we could regard the reduction condition as approximately satisfied. Therefore, a first natural try is to choose a very small initial value for ξ. In Fig. 5.10, we report the flow of the various quantities for the choice $\xi_\Lambda = 0.01$. If not stated otherwise, within this and all following plots, we use plain, dashed, and dotted lines for the choices $\dot{h} = \dot{h}_X$, $\dot{h}_\omega$, and $\frac{1}{2}\left(\dot{h}_X + \dot{h}_\omega\right)$, respectively.

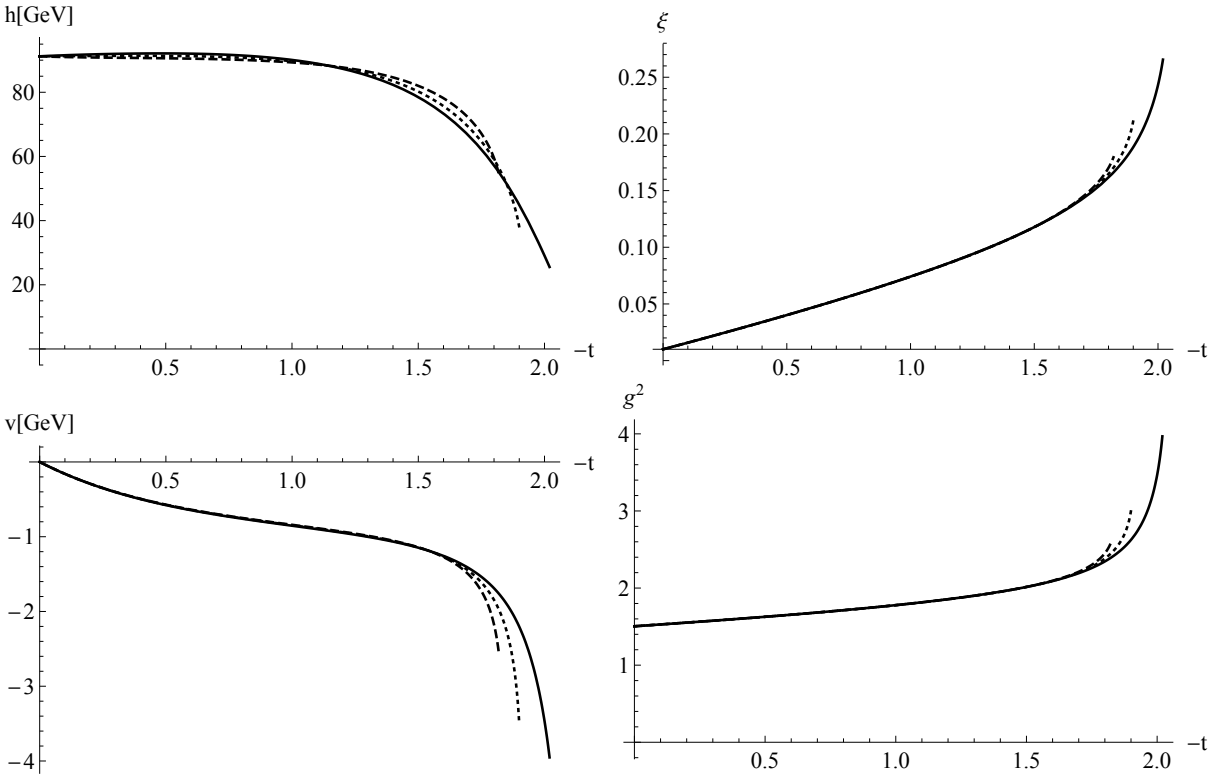

FIGURE 5.10: Running of the various quantities for the initial value $\xi_\Lambda = 0.01$. The minimum v_k runs towards negative values instead of the desired positive values. This would lead to the non-physical situation of tachyonic gluon and ghost masses.

We find that v_k immediately flows to negative values and the integration already stops after $t \simeq -2$. This is due to the fact that the squared masses become negative (tachyonic) and hence at some point, the threshold terms $\propto \frac{1}{1+m^2}$ diverge. While the scale where the integration stops varies with the choices for the Beta function $\dot{h} =$

$\left\{\dot{h}_X, \dot{h}_\omega, \frac{1}{2}\left(\dot{h}_X + \dot{h}_\omega\right)\right\}$, the qualitative behavior is the same in all three cases. Let us take a look at the Beta function of the minimum, $\dot{v}_k$. Inserting the initial values mentioned above and keeping only the initial value of ξ arbitrary, we plot $\dot{v}_\Lambda(\xi_\Lambda)$ in Fig. 5.11. To obtain positive values, we look for regions where $\dot{v}_\Lambda < 0$. We notice a pole for very small $\xi \simeq 10^{-3}$ which should be avoided. After the pole, $\dot{v}_\Lambda$ remains positive, until it switches sign at $\xi_\Lambda \simeq 3$. Indeed, for $\xi_\Lambda = 2$ we still observe the same behavior as above, see Fig. 5.12.

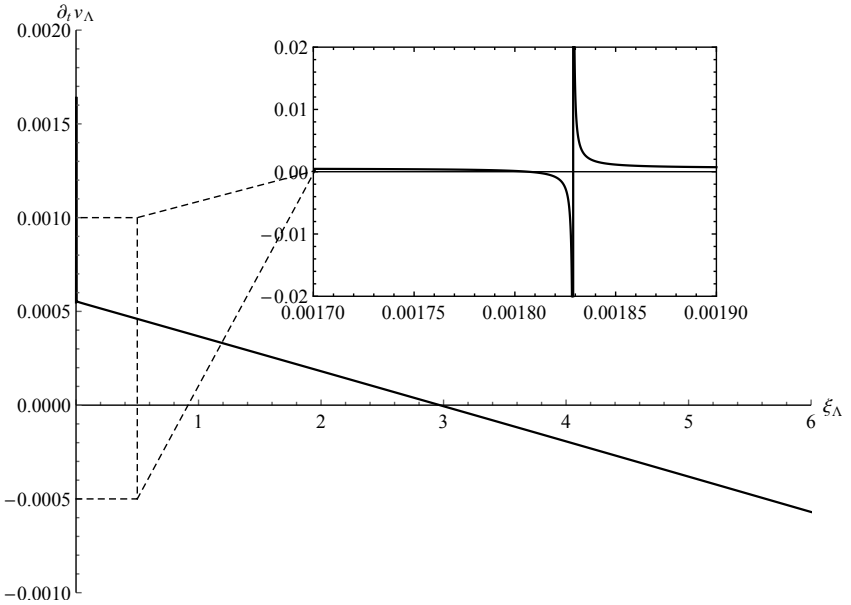

FIGURE 5.11: Beta function $\dot{v}_k$ evaluated at the cutoff over the bare value ξ_Λ. For very small bare values exists a pole. The interesting region is defined by $\partial_t v_\Lambda < 0$, because v_k then flows to positive values when integrating towards the infrared.

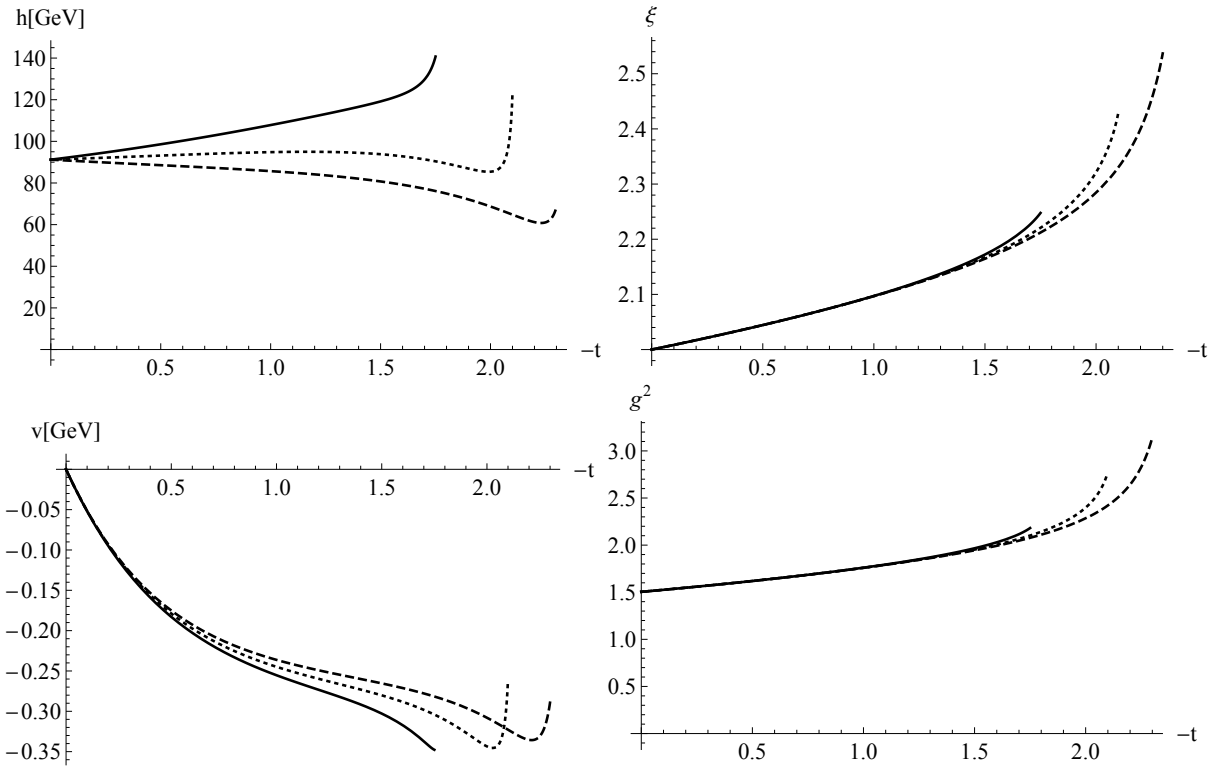

FIGURE 5.12: Running of the various quantities for the initial value $\xi_\Lambda = 2$. The minimum still runs towards negative values according to the analysis of the Beta function.

On the other hand, if we go to the region where $\dot{v}_\Lambda < 0$, say $\xi_\Lambda = 3.5$, the picture changes as expected. As shown in Fig. 5.13, we indeed flow to positive values of v_k. The masses m_X^2 and m_ω^2 remain positive, avoiding the previously encountered divergences and we can integrate over several orders of magnitude, until all quantities decouple and freeze out. In particular, we find that the parameter ξ related to reduction condition runs into an infrared fixed point, in contrast to the one-loop perturbative predictions. Moreover, despite the brute force ansatz for the effective average action, the Yang-Mills coupling defined through the running of the $\langle V^\gamma \omega \bar{\omega} \rangle$ vertex also freezes out, although the infrared value of $\frac{g_*^2}{4\pi} \sim 0.3$ is very small compared to the value of $\frac{g_*^2}{4\pi} = 11.3$, which was obtained through FRG studies in the background field formalism [154]. The Yang-Mills coupling thus even remains close to the perturbative regime. Also, we note that for the choice $\dot{h} = \dot{h}_X$, the unified Yukawa operator grows, while in the other cases it decreases in the course of the flow. This is desirable because once we consider an independent flow of h_X and h_ω, we must obtain a slightly different flow behavior in order to tune the system such that $h_X = h_\omega$ at $k = 0$. Also, differences in the running of the Yang-Mills coupling are only found once the running deviates from the one-loop running indicated by the gray

line. In fact, the (non-perturbative) Beta function in the one-loop limit is given by

$$\beta_{g^2} = -\frac{g^4}{(4\pi)^2}\frac{44}{3}, \tag{5.97}$$

but this expression is obtained *without* setting the auxiliary quantities to zero by hand. Different choices for $\dot{h}$ only influence the running of g^2 in the non-perturbative regime. Based on the last plot, we conclude that the mechanism of generating the non-zero condensate of the auxiliary field φ and thus of the composite operator $\mathcal{O}$ is present, leading to non-zero coset gluon and ghost masses.

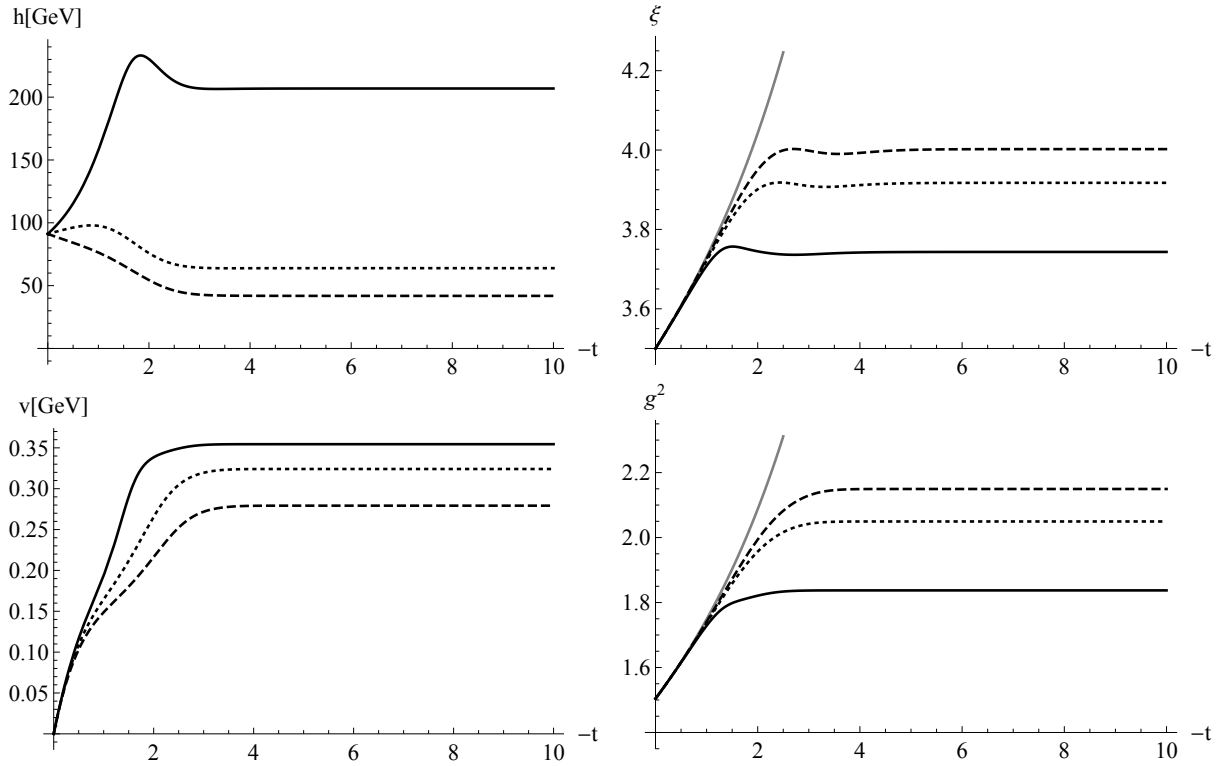

FIGURE 5.13: Running of the various quantities for the initial value $\xi_\Lambda = 3.5$. As expected, the minimum runs towards positive values. Consequently, the flow can be integrated over a large range of t and all quantities eventually freeze out. The gray lines in the plots of ξ and g^2 correspond to their respective one-loop flows.

However, as discussed earlier, we want to achieve a very small infrared value for the parameter ξ, whereas for the current parameter combination it is even growing from the already large initial value $\xi_\Lambda = 3.5$. This is already expected from the one-loop running of ξ. In the current set-up, the one-loop limit including the auxiliary terms reads

$$\dot{\xi} = \frac{g^2}{(4\pi)^2}\left(\frac{8}{3}\xi - 2\xi^2 - 6\right) + \frac{h^2}{24\pi^2}\xi(\xi - 1). \tag{5.98}$$

The first term is the standard term, which is negative for all values of ξ and therefore leads to a growing of ξ. The second term has a positive sign at least for $\xi > 1$, which includes the relevant initial values according to the analysis of the Beta function of v_k. The overall sign is then determined by the ratio h^2/g^2. Due to the importance of the Yukawa coupling in this discussion, let us further improve our approximation by considering the running of the Yukawa couplings h_X and h_ω independently. The quartic couplings ζ_i will still be kept at the simplified level, $\zeta_i = \frac{h^2}{\lambda_2}$, choosing $h^2 = h_X^2$, h_ω^2, or $\frac{1}{2}(h_X^2 + h_\omega^2)$. The initial values of h_X and h_ω must then be tuned such that both quantities merge in the infrared, yielding a BRST invariant effective action. To determine reasonable choices for the initial values of the Yukawa operators, we proceed as follows. We make contact with the numerical data from the lattice which state a coset gluon mass of $m_X = 1.2$ GeV [8]. Since $m_X^2 = h_X\, v$, this fixes the initial value of h_X. At the same time, h_ω or rather the ratio h_ω/h_X is tuned such that in the infrared, the condition $h_X = h_\omega$ is realized. In Fig. 5.14, we present the RG flow within such a setting with $\lambda_{2,\Lambda} = \frac{10}{\Lambda^2 Z_{\varphi,\Lambda}}$ and $Z_{\varphi,\Lambda} = 10^{-5}$, while Fig. 5.15 shows the corresponding flow of the masses. We find that the ratio of the Yukawa operators at the cutoff must satisfy $h_\omega/h_X > 1$ in order to guarantee the merging. Moreover, the desired gluon mass is achieved for an initial value of $h_{X,\Lambda} \sim \frac{0.5}{\sqrt{\Lambda^2 Z_{\varphi,\Lambda}}}$. In terms of the renormalized and dimensionless couplings we thus obtain $\lambda_{2,\Lambda} >> h_\Lambda$, as expected earlier. However, the order of magnitude of h_X and h_ω is not enough to lead to a diminishing of the gauge fixing parameter ξ, such that it still increases to values larger than 1 before finally decoupling from the flow. In particular, this implies that the coset ghost mass is even larger than the obtained coset gluon mass.

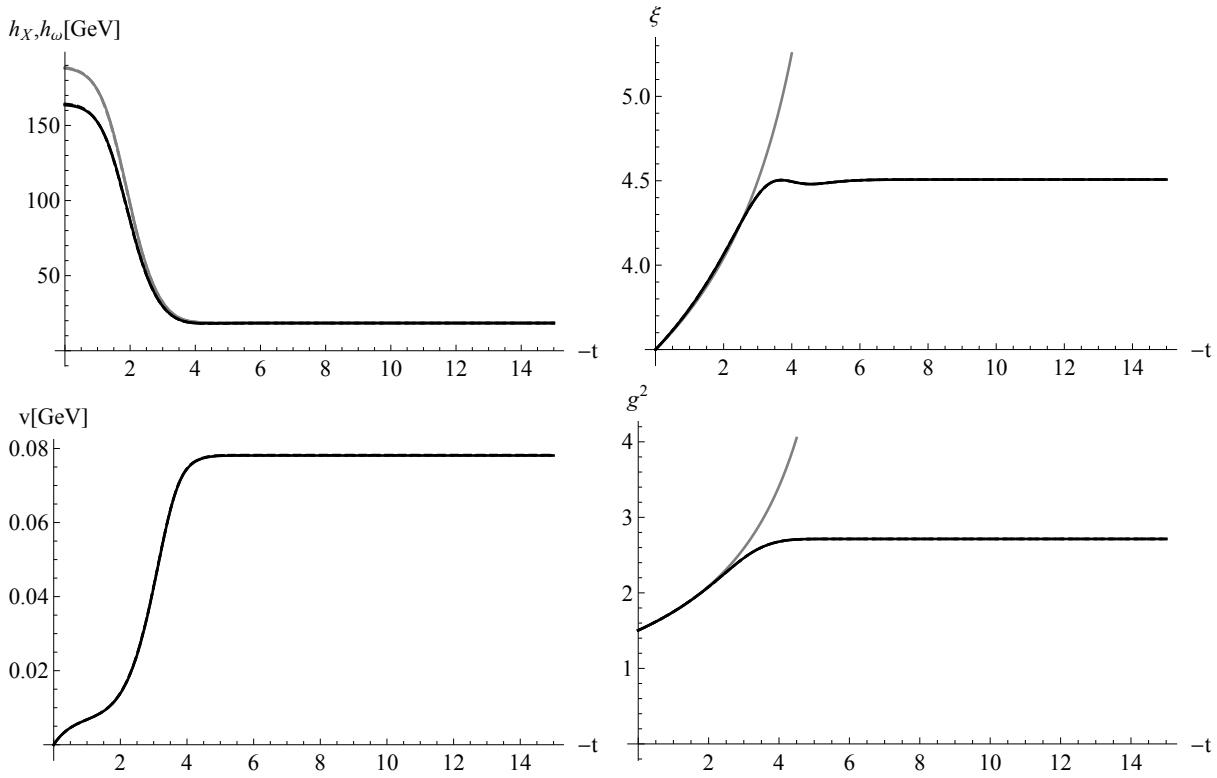

FIGURE 5.14: RG flow in the case of independent Yukawa operators h_X and h_ω. Each panel shows three plots corresponding to the choices $\zeta_i = \left\{\frac{h_X^2}{\lambda_2}, \frac{h_X^2}{\lambda_2}, \frac{1}{2\lambda_2}(h_X^2 + h_\omega^2)\right\}$ represented by plain, dashed, and dotted lines, respectively. However, all three cases lie on top of each other. The top left panel shows the merging of h_X (black) and h_ω (gray). In order to achieve the merging, the bare value of h_ω must be chosen larger than h_X. In the top right and bottom right panel, the gray line corresponds to the one-loop flow of ξ and g^2, respectively.

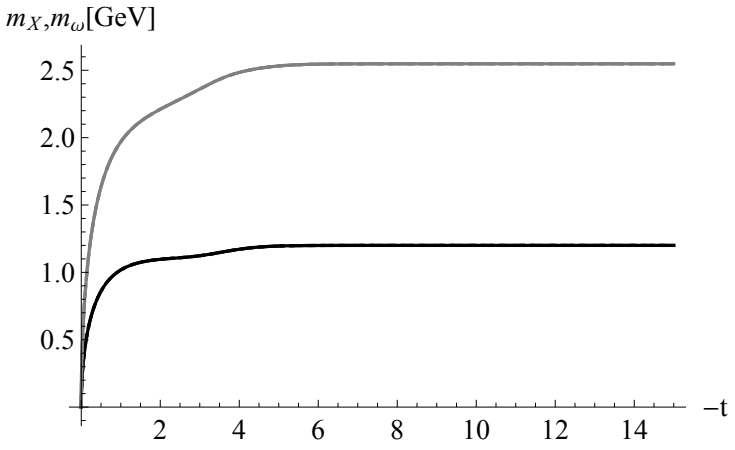

FIGURE 5.15: Flow of the coset gluon mass $m_X = \sqrt{h_X\, v}$ (black) and the coset ghost mass $m_\omega = \sqrt{\xi\, h_\omega\, v}$ (gray) corresponding to the setting of Fig. 5.14.

So far, in this section, we showed by strictly non-perturbative methods that the

minimum of the effective potential for the auxiliary field and associated with the vacuum expectation value flows to non-zero and positive values, implying the generation of the desired mass term for the coset field $\mathfrak{X}_\mu$. We were able to tune the initial values of the flow to make contact with lattice simulations of the coset gluon mass, our ansatz can therefore be mapped to the physical region by means of the FRG flow. In particular, we also tuned the Yukawa operators such that in the limit $k \to 0$, the obtained effective action is BRST invariant. However, the gauge fixing parameter ξ decouples at values $\xi >> 1$. This implies a non-vanishing coset ghost mass, which in addition is larger than the coset gluon mass by the factor $\sqrt{\xi}$. Moreover, in the sense of the Faddeev-Popov trick, the related reduction condition also is not strictly incorporated as desired from the viewpoint of the reformulated Yang-Mills theory, even though the perturbative picture is at least improved as ξ takes a finite value.

5.3.5 Extension to $SU(N)$

In this subsection, we extend the flow equations of the $SU(2)$ case to general $SU(N)$. In particular, this will enable us to consider the gauge group $SU(3)$, where our construction of a $U(N-1) = U(2)$ stability group really differs from the conventional MAG. If we consider general N, we have to take into account the new sector $SU(N-1)$ within the decomposition of the stability group, $U(N-1) = SU(N-1) \times U(1)$. First, we calculate the anomalous dimensions of the corresponding residual field and residual ghosts. The diagrams contributing to the two-point function of the $SU(N-1)$ residual field are given by

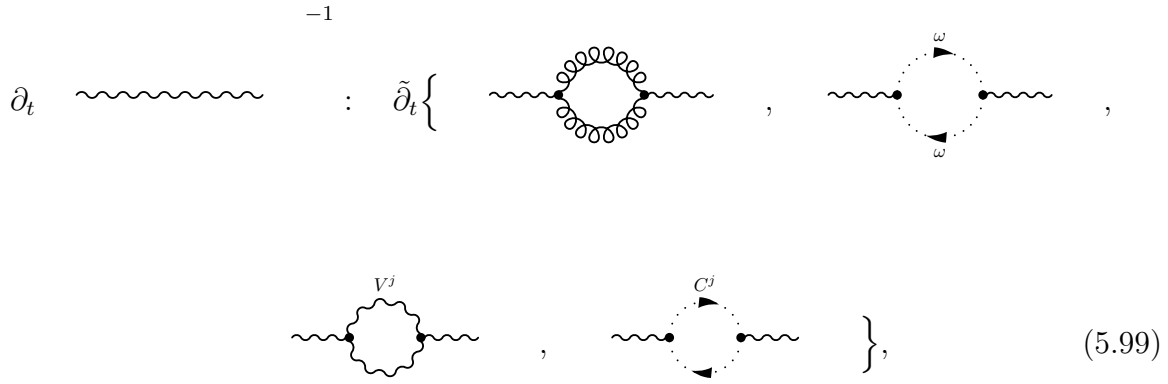

(5.99)

where in the last two diagrams the loop consists of $SU(N-1)$ residual fields and residual ghosts, respectively. The transversally projected flow equation yields

$$-\eta_V(d-1) =$$

$$\begin{aligned}
&-\frac{g^2}{2}\Big\{-4v_d V_1^T l_{1,1}^{(BB)d}[m_X^2,m_X^2;\eta_X,\eta_X]-4v_d V_2^T l_{1,1}^{(BB)d}[m_X^2,\xi m_X^2;\eta_X,\eta_X]\\
&-4v_d V_3^T l_{1,1}^{(BB)d}[\xi m_X^2,\xi m_X^2;\eta_X,\eta_X]+4v_d V_4^T m_{1,1}^{(BB)d}[m_X^2,m_X^2;\eta_X,\eta_X]\\
&+4v_d V_5^T m_{1,1}^{(BB)d}[m_X^2,\xi m_X^2;\eta_X,\eta_X]+4v_d V_6^T m_{1,1}^{(BB)d}[\xi m_X^2,m_X^2;\eta_X,\eta_X]\\
&+4v_d V_7^T m_{1,1}^{(BB)d}[\xi m_X^2,\xi m_X^2;\eta_X,\eta_X]+4v_d V_8^T n_{1,1}^{(BB)d}[m_X^2,m_X^2;\eta_X,\eta_X]\\
&+4v_d V_9^T n_{1,1}^{(BB)d}[m_X^2,\xi m_X^2;\eta_X,\eta_X]+4v_d V_{10}^T n_{1,1}^{(BB)d}[\xi m_X^2,m_X^2;\eta_X,\eta_X]\\
&+4v_d V_{11}^T n_{1,1}^{(BB)d}[\xi m_X^2,\xi m_X^2;\eta_X,\eta_X]\Big\}\\
&-g^2 N\Bigg\{4v_d\left(4-\frac{4}{d}\right)m_{1,1}^{(BB)d}[m_\omega^2,m_\omega^2;\eta_\omega,\eta_\omega]\\
&+4v_d\left(\frac{8}{d}-\frac{24}{d(d+2)}\right)n_{1,1}^{(BB)d}[m_\omega^2,m_\omega^2;\eta_\omega,\eta_\omega]\Bigg\}\\
&-\frac{g^2(N-1)}{2}\Big\{-4v_d E_1^T l_{1,1}^{(BB)}[0,0;\eta_V,\eta_V]+4v_d E_2^T m_{1,1}^{(BB)}[0,0;\eta_V,\eta_V]\\
&+4v_d E_3^T n_{1,1}^{(BB)}[0,0;\eta_V,\eta_V]\Big\}\\
&+g^2(N-1)4v_d\Big\{\bar{E}_1^T m_{1,1}^{(BB)}[0,0;\eta_C,\eta_C]+\bar{E}_2^T n_{1,1}^{(BB)}[0,0;\eta_C,\eta_C]\Big\},
\end{aligned}\tag{5.100}$$

with the anomalous dimensions

$$\eta_V=-\partial_t\log Z_{V,k},\quad \eta_C=-\partial_t\log\left(Z_{C,k}Z_{\bar{C},k}\right)^{1/2},\tag{5.101}$$

and the coefficients E_i^T and $\bar{E}_i^T$ are defined in appendix D. For the transversally projected flow, we obtain

$$\frac{1}{\lambda^2}\left(-\eta_V\lambda-\dot{\lambda}\right)=$$

$$
\begin{aligned}
&- \frac{g^2}{2}\Big\{ - 4v_d V_1^L l_{1,1}^{(BB)d}[m_X^2, m_X^2; \eta_X, \eta_X] - 4v_d V_2^L l_{1,1}^{(BB)d}[m_X^2, \xi m_X^2; \eta_X, \eta_X] \\
&- 4v_d V_3^L l_{1,1}^{(BB)d}[\xi m_X^2, \xi m_X^2; \eta_X, \eta_X] + 4v_d V_4^L m_{1,1}^{(BB)d}[m_X^2, m_X^2; \eta_X, \eta_X] \\
&+ 4v_d V_5^L m_{1,1}^{(BB)d}[m_X^2, \xi m_X^2; \eta_X, \eta_X] + 4v_d V_6^L m_{1,1}^{(BB)d}[\xi m_X^2, m_X^2; \eta_X, \eta_X] \\
&+ 4v_d V_7^L m_{1,1}^{(BB)d}[\xi m_X^2, \xi m_X^2; \eta_X, \eta_X] + 4v_d V_8^L n_{1,1}^{(BB)d}[m_X^2, m_X^2; \eta_X, \eta_X] \\
&+ 4v_d V_9^L n_{1,1}^{(BB)d}[m_X^2, \xi m_X^2; \eta_X, \eta_X] + 4v_d V_{10}^L n_{1,1}^{(BB)d}[\xi m_X^2, m_X^2; \eta_X, \eta_X] \\
&+ 4v_d V_{11}^L n_{1,1}^{(BB)d}[\xi m_X^2, \xi m_X^2; \eta_X, \eta_X]\Big\}
\end{aligned}
$$

$$
\begin{aligned}
&- g^2 N\Bigg\{ 4v_d \left(4 - \frac{4}{d}\right) m_{1,1}^{(BB)d}[m_\omega^2, m_\omega^2; \eta_\omega, \eta_\omega] \\
&+ 4v_d \left(\frac{8}{d} - \frac{24}{d(d+2)}\right) n_{1,1}^{(BB)d}[m_\omega^2, m_\omega^2; \eta_\omega, \eta_\omega]\Bigg\} \\
&- \frac{g^2(N-1)}{2}\Big\{ - 4v_d E_1^L l_{1,1}^{(BB)}[0, 0; \eta_V, \eta_V] + 4v_d E_2^L m_{1,1}^{(BB)}[0, 0; \eta_V, \eta_V] \\
&+ 4v_d E_3^L n_{1,1}^{(BB)}[0, 0; \eta_V, \eta_V]\Big\} \\
&+ g^2(N-1) 4v_d \Big\{ \bar{E}_1^L m_{1,1}^{(BB)}[0, 0; \eta_C, \eta_C] + \bar{E}_2^L n_{1,1}^{(BB)}[0, 0; \eta_C, \eta_C]\Big\}. \qquad (5.102)
\end{aligned}
$$

Again, the coefficients E_i^T and $\bar{E}_i^T$ are defined in appendix D. Regarding the anomalous dimension of the residual $SU(N-1)$ ghosts, only one diagram contributes,

$$
\partial_t \quad \overset{-1}{\cdots\!\blacktriangleright\!\cdots} \quad : \quad \tilde{\partial}_t \Big\{ \quad
\begin{array}{c}
\overset{V^j}{\frown} \\
\cdots\!\blacktriangleright\!\bullet\!\blacktriangleright\!\cdots \\
\underset{C^j}{\blacktriangleleft}
\end{array}
\quad \Big\}. \qquad (5.103)
$$

The corresponding flow equation is given by

$$
\eta_C = \frac{g^2(N-1)}{d}\Big\{ - 4v_d(d - 1 + \lambda) l_{1,1}^{(BB)}[0, 0; \eta_V, \eta_C] + 2\lambda\, m_{1,1}^{(BB)}[0, 0; \eta_V, \eta_C]\Big\}. \qquad (5.104)
$$

In the one-loop limit, we recover the perturbative results given in Eq. (3.100),

$$
\eta_V \Longrightarrow 2\gamma_V, \quad \eta_C \Longrightarrow \gamma_C + \gamma_{\bar{C}}. \qquad (5.105)
$$

Concerning the remaining flow equations, the expressions given in subsection 5.3.2 are valid for all N but must be extended by diagrams that now can contain internal $SU(N-1)$

lines. In particular, the following terms must be added. For the coset gluon two-point functions, the additional diagram

$$\tilde{\partial}_t \Big\{ \quad \Big\} \tag{5.106}$$

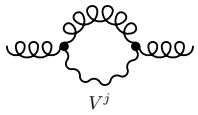

gives rise to

$$\begin{aligned}
&-\eta_X(d-1) \sim \\
&g^2 N(N-2)\Big\{ -4v_d X_1^T[\lambda] l_{1,1}^{(BB)d}[0, m_X^2; \eta_V, \eta_X] - 4v_d X_2^T[\lambda] l_{1,1}^{(BB)d}[0, \xi m_X^2; \eta_V, \eta_X] \\
&+ 4v_d X_3^T[\lambda] m_{1,1}^{(BB)d}[0, m_X^2; \eta_V, \eta_X] + 4v_d X_4^T[\lambda] m_{1,1}^{(BB)d}[0, \xi m_X^2; \eta_V, \eta_X] \\
&+ 4v_d X_5^T[\lambda] n_{1,1}^{(BB)d}[0, m_X^2; \eta_V, \eta_X] + 4v_d X_6^T[\lambda] n_{1,1}^{(BB)d}[0, \xi m_X^2; \eta_V, \eta_X] \Big\}, \\
&\frac{1}{\xi^2}\left(-\eta_X \xi - \dot{\xi}\right) \sim \\
&g^2 N(N-2)\Big\{ -4v_d X_1^L[\lambda] l_{1,1}^{(BB)d}[0, m_X^2; \eta_V, \eta_X] - 4v_d X_2^L[\lambda] l_{1,1}^{(BB)d}[0, \xi m_X^2; \eta_V, \eta_X] \\
&+ 4v_d X_3^L[\lambda] m_{1,1}^{(BB)d}[0, m_X^2; \eta_V, \eta_X] + 4v_d X_4^L[\lambda] m_{1,1}^{(BB)d}[0, \xi m_X^2; \eta_V, \eta_X] \\
&+ 4v_d X_5^L[\lambda] n_{1,1}^{(BB)d}[0, m_X^2; \eta_V, \eta_X] + 4v_d X_6^L[\lambda] n_{1,1}^{(BB)d}[0, \xi m_X^2; \eta_V, \eta_X] \Big\},
\end{aligned} \tag{5.107}$$

where the first term corresponds to the new contribution to the transversally projected equation, cf. Eq. (5.67), and the second one is the new addition to the longitudinally part, cf. Eq. (5.68). Regarding the two-point function of the $U(1)$ residual field, there is no new contribution for $N > 2$. The coset ghost two-point function receives a new contribution from the diagram

$$\tilde{\partial}_t \Big\{ \quad \Big\}, \tag{5.108}$$

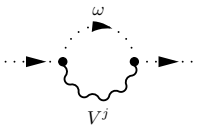

which reads

$$\eta_\omega \sim \frac{g^2 N(N-2)}{2 d_{G/H} d}\Big\{ -32 v_d (d-1+\lambda) l_{1,1}^{(BB)d}[0, m_\omega^2; \eta_V, \eta_\omega] + 8 v_d (8\lambda + d) m_{1,1}^{(BB)d}[0, m_\omega^2; \eta_V, \eta_\omega] + 16 v_d \ \lambda \ n_{1,1}^{(BB)d}[0, m_\omega^2; \eta_V, \eta_\omega]\Big\}. \tag{5.109}$$

The flow of the residual $U(1)$ ghosts remains trivial, $\tilde{\eta}_C = 0$, and the flow of the two-point function for the auxiliary field as well as the flow equation for the effective potential receive no new contributions. Regarding the flow of h_X, we have a new diagram

$\tilde{\partial}_t \Big\{$ 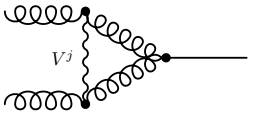 $\Big\}$, (5.110)

leading to a new term

$$\dot{h}_X \sim -8 v_d \ g^2 N(N-2) \frac{h_X}{d \ d_{G/H}} \Big\{ (4+\lambda)(d-1) \bar{T}_{1,1,1}^{(BBB)d}[0, m_X^2, m_X^2; \eta_V, \eta_X, \eta_X] + ((\xi+1)^2 (d-1) + \lambda) \bar{T}_{1,1,1}^{(BBB)d}[0, \xi m_X^2, \xi m_X^2; \eta_V, \eta_X, \eta_X] \Big\}. \tag{5.111}$$

The flow of h_ω would obtain new terms coming from the diagram

$\tilde{\partial}_t \Big\{$ 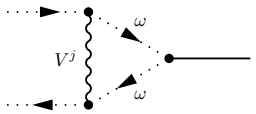 $\Big\}$. (5.112)

However, just like in the case with an internal $U(1)$ residual field, this diagram vanishes under the projection rule. Finally, the $\langle V^\gamma \omega \bar{\omega} \rangle$ vertex and thus the running of the Yang-Mills coupling receives new terms coming from the diagrams

$\tilde{\partial}_t \Big\{$ 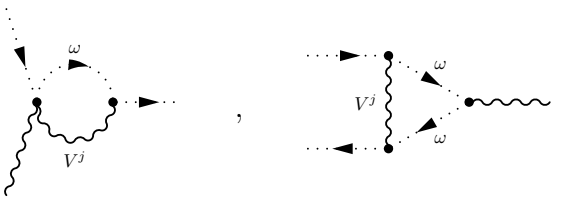 $\Big\}$, (5.113)

which read

$$\begin{aligned}\beta_{g^2} \sim\ & 16 v_d g^4 \frac{N(N-2)}{d(N-1)} \Big\{ (d-1+\lambda) l_{1,1}^{(BB)d}[0, m_\omega^2; \eta_V, \eta_\omega] - \lambda m_{1,1}^{(BB)d}[0, m_\omega^2; \eta_V, \eta_\omega] \Big\} \\ & - 4 v_d g^4 \frac{N(N-2)}{d(N-1)}\ \lambda \Big\{ 2(4+d) \bar{T}_{1,1,1}^{(BBB)d}[0, m_\omega^2, m_\omega^2; \eta_V, \eta_\omega, \eta_\omega] \\ & \qquad - 4 \bar{D}_{1,1,1}^{(BBB)d}[0, m_\omega^2, m_\omega^2; \eta_V, \eta_\omega, \eta_\omega] \Big\}. \end{aligned} \tag{5.114}$$

Note that all these additional contributions vanish for $N = 2$, as one would expect. Moreover, in the one-loop limit and with the auxiliary quantities set to zero, all extended flow equations agree with the perturbative one-loop results for general N, cf. Eq. (3.100). This completes the set of extended flow equations, since the quartic auxiliary couplings are approximated in the same way as before. Solving the extended algebraic system for the anomalous dimension, we find that the solution for η_V remains finite for $\lambda = 0$. Thus, we conclude from the flow equation (5.102) that $\lambda = 0$ is a fixed point, which we will adopt in the numerical calculations. We examined the new equation system for the $SU(3)$ case. As before, we tuned h_ω such that in the limit $k \to 0$ it takes the same value as h_X, while h_X is tuned such that the infrared target mass is achieved. In the $SU(3)$ case in the minimal option, reference [28] reports a value of $m_X = 1.15$ GeV from the lattice. Figs. 5.16 – 5.18 show the results in comparison with the $SU(2)$ case.

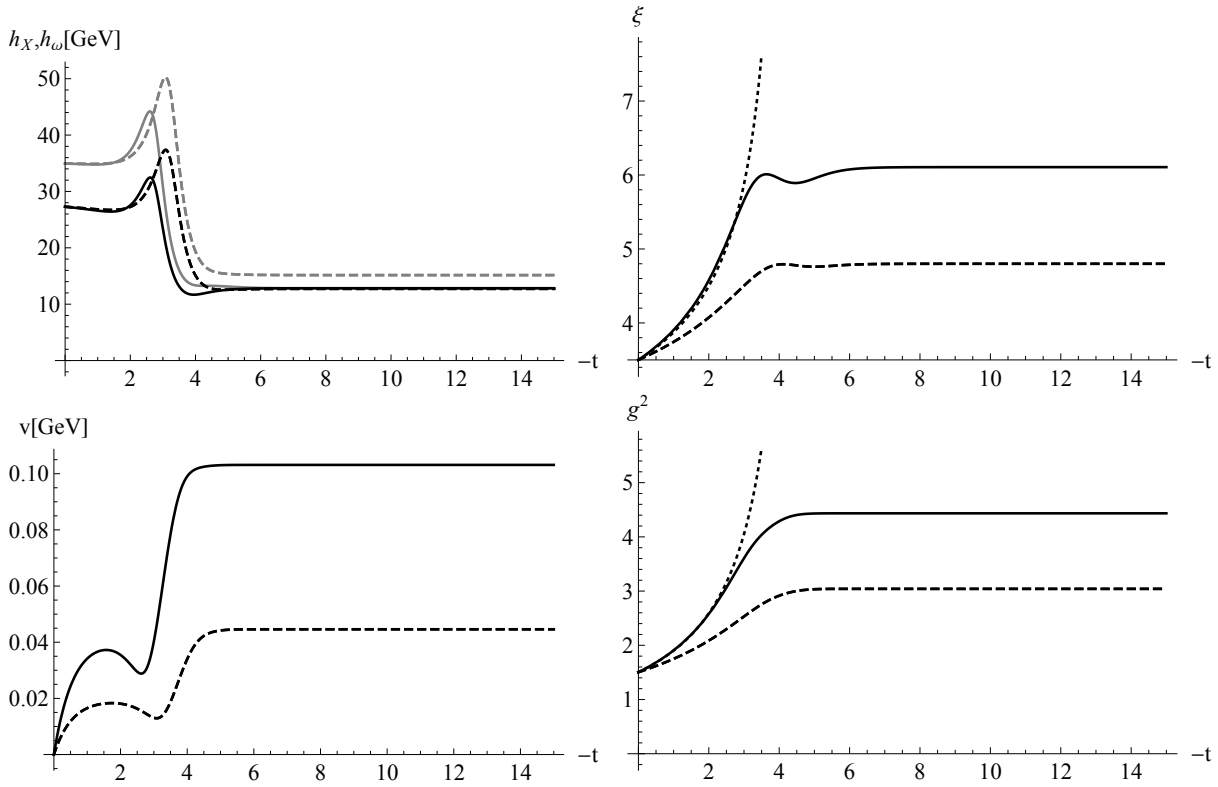

FIGURE 5.16: RG flow of the tuned $SU(3)$ system. For comparison, the dashed lines correspond to the flow in the $SU(2)$ case with the same initial values. Consequently, the Yukawa operators do not merge in the latter case. In the top left panel, the gray lines correspond to h_ω and the black lines correspond to h_X. Additionally, the plots of g^2 and ξ contain their respective $SU(3)$ one-loop running as dotted lines. The data are obtained using $\zeta_i = \frac{h_X^2}{\lambda_2}$ and $\lambda_{2,\Lambda} = 1$.

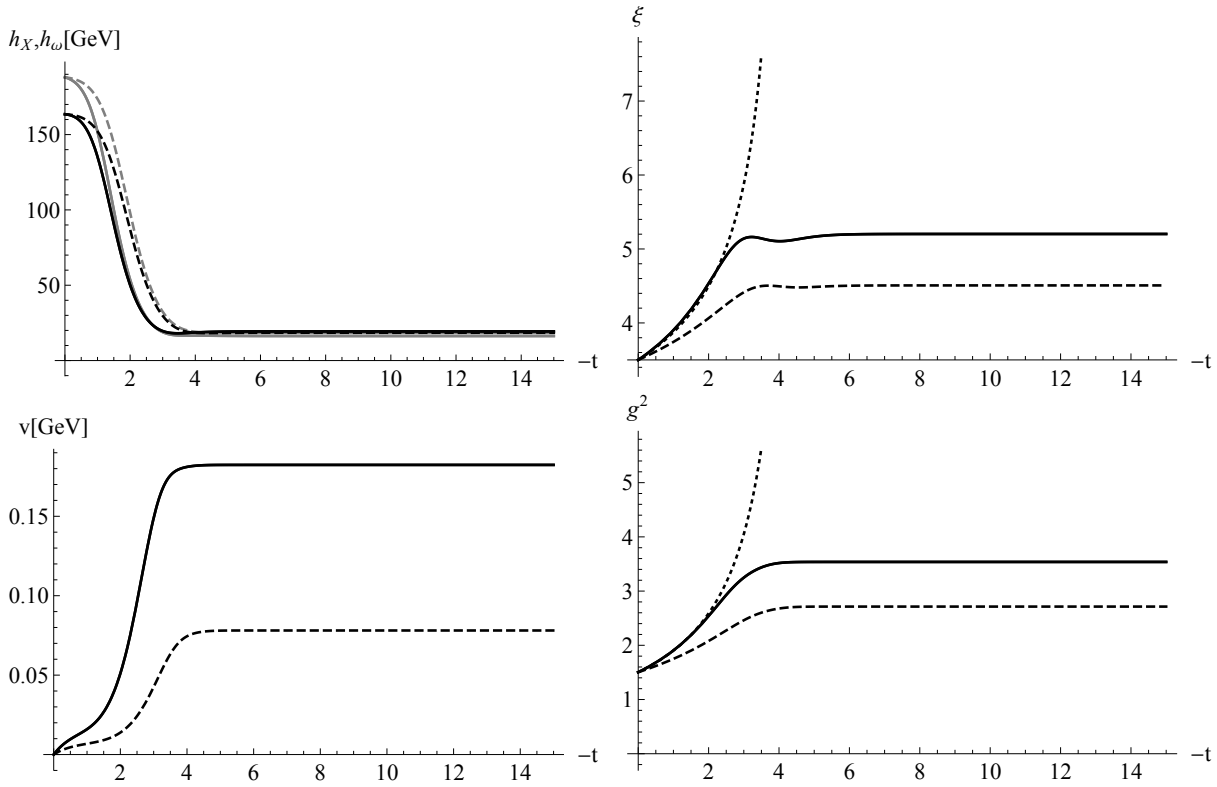

FIGURE 5.17: The nomenclature of this plot is the same as in Fig. 5.16, however, here the $SU(2)$ data are tuned and the $SU(3)$ case is just plotted with the same initial values for comparison. For this data set, we used $\lambda_{2,\Lambda} = 10$.

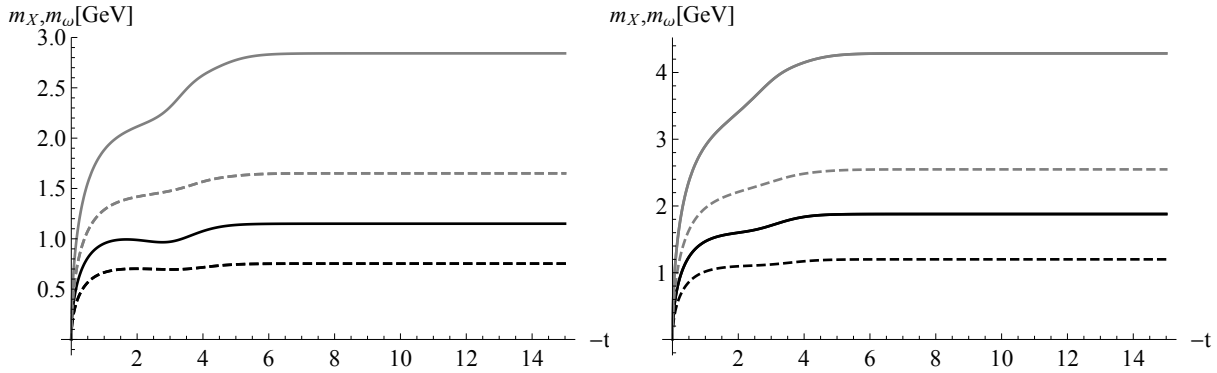

(A) $SU(3)$ tuned (B) $SU(2)$ tuned

FIGURE 5.18: (Left panel): Flow of the coset gluon mass m_X (black) and ghost mass m_ω (gray) corresponding to the set-up in Fig. 5.16. (Right panel): Flow corresponding to the set-up in Fig. 5.17.

For the $SU(3)$ system, we observe in principle the same behavior as for $SU(2)$, as expected. The system can be tuned in such a way that $h_X = h_\omega$ in the infrared as well as $m_X = 1.15$ GeV. As before, a rather large initial value for ξ is necessary. Generally

speaking, for the same set of initial data the infrared values for v_k and the obtained coset masses are larger for $SU(3)$ and the same holds for ξ and the Yang-Mills coupling. In Fig. 5.17, we observe a difference to the previously presented flow data in the sense that the Yukawa operators do not decrease monotonically at the beginning of the flow, but undergo a phase of increasing. Similarly v_k does not grow monotonically but undergoes a phase of decreasing again. This comes from the fact that the fine-tuned initial ratio $\frac{h_\omega}{h_X}\Big|_\Lambda$ for $SU(3)$ is close to the upper bound before the system yields non-physical flows and collapses. This upper bound exists because as mentioned earlier, the positive value for v_k is triggered by the ghost loop contribution in the effective potential. If h_ω becomes too large in comparison to h_X, the suppression of the ghost loop by $m_\omega^2 = \xi h_\omega v_k$ becomes too strong compared to the suppression of the gluon loop. Apart from that, the same conclusions as in the $SU(2)$ case still hold. We can tune the action to be BRST invariant in the infrared and we can match our truncation to the correct infrared physics in the sense that the FRG flow maps it onto the coset gluon mass reported on the lattice. Yet, we need large initial ξ values that grow to even larger values than those in the $SU(2)$ case, and consequently, the ratio between coset ghost and coset gluon mass is even bigger. Still, the coset gluon becomes massive, implying that in $SU(3)$, the non-Abelian residual $U(2)$ degrees of freedom are infrared dominant which can be regarded as evidence for the non-Abelian infrared dominance within a non-Abelian dual superconductivity picture.

Chapter 6

Summary and outlook

In the present work, we investigated the existence of a certain mass dimension-two gluon-ghost condensate by means of perturbative and non-perturbative techniques. Such condensates play an important role when it comes to explaining how infrared "Abelian" dominance occurs within the dual superconductivity picture for quark confinement, i.e., how the "non-Abelian" degrees of freedom decouple from the theory. Such condensates could in principle generate mass terms for these degrees of freedom, coming from the quartic gluon-interaction of the Yang-Mills action.

A common attempt to realize the Abelian infrared effective theory is through a procedure called Abelian projection, with the most famous variant being the maximal Abelian gauge. It corresponds to a decomposition of the gauge group into $SU(N)/H \times H$ with $H = U(1)^{N-1}$ being the Abelian maximal torus subgroup. The coset degrees of freedom are then fixed by a certain gauge fixing condition that corresponds to minimizing the functional $\int \mathrm{Tr}_{G/H}\, \mathfrak{A}_\mu \mathfrak{A}^\mu$. Within this theory, it was shown on the lattice that the related degrees of freedom acquire a mass dynamically. An analytical explanation for this mass was provided by the existence of the mentioned condensates and examined in many subsequent works, especially in the course of perturbative calculations. A criticism that the results derived in this set-up, especially the existence of for the dual superconductivity crucial magnetic monopoles, may just be artefacts of the adopted gauge fixing, was improved through recent studies on a reformulation of $SU(N)$ Yang-Mills theory. The maximal Abelian gauge is then just a special case of this more general approach. The reformulation also revealed that there are actually several options for the decomposition of the gauge group. A particularly interesting candidate appears in the previously overlooked decomposition with respect to the stability group $H = U(N-1)$, which agrees with the maximal Abelian gauge only for $N = 2$. The related condensate was the object of interest in this thesis.

In chapter 2, we set the theoretical foundations including a very brief introduction to Yang-Mills theory as well as explanations with regard to the dual superconductivity picture and the mentioned reformulation of $SU(N)$ Yang-Mills theory. The reformulation in particular is based on the Cho-Faddeev-Niemi decomposition of the gauge field, which is defined in terms of an object called color field. Concerning the discussion whether the condensate in this novel decomposition exists or not, it is sufficient to restrict this in general space-time dependent color field to a fixed value, which simplifies the calculations in an adequate way as the color field is difficult to handle analytically.

In chapter 3, we discussed the consequences of this approximation and performed a one-loop analysis of the decomposed theory. We found that the stability group must further be decomposed according to $U(N-1) = SU(N-1) \times U(1)$ and for the first time obtained all relevant one-loop renormalization group functions. Especially, the $SU(N-1)$ sector, which is absent in the maximal Abelian gauge case, was carefully examined. Yet, for $N = 2$ the maximal Abelian gauge case must be recovered, which provided an excellent cross-checking opportunity. Indeed, all results are in agreement with the existing literature. In particular, we also encountered a well-known problem concerning the gauge fixing parameter ξ related to the gauge fixing condition of the coset degrees of freedom, namely that its running lacks a fixed point. In the second part of this chapter, we furthermore discussed a necessary condition for the existence of the condensate, namely that the related composite operator $\mathcal{O} = \mathrm{Tr}_{G/H}\left(\mathfrak{A}_\mu \mathfrak{A}^\mu - 2i\xi \mathfrak{C}\bar{\mathfrak{C}}\right)$ is multiplicatively renormalizable. This is *a priori* not clear, as in principle all condensates with the same quantum numbers can mix under renormalization. Upon inserting them into the various two-point functions, the mixing matrix was obtained and the condition of multiplicative renormalizability was found to be satisfied, in accordance with the $N = 2$ maximal Abelian gauge case.

In chapter 4, we used these results to discuss the existence of the condensate by means of the local composite operator formalism. Consequently, after performing a Hubbard-Stratonovich transformation, we obtained the one-loop effective potential $V(\sigma)$ for the auxiliary field σ, where the vacuum expectation values of σ and $\mathcal{O}$ are related as $\langle\sigma\rangle = g\langle\mathcal{O}\rangle$. Indeed, we found a non-zero stationary point σ_* away from the origin. However, the corresponding vacuum energy $V(\sigma_*)$ explicitly depends on the parameter ξ. This would be a problem in the usual gauge fixing framework, but in our case the gauge fixing condition has a different meaning. In the original reformulation of the Yang-Mills theory, it reduces the enlarged color field extended gauge symmetry back to the theory equipollent to the $SU(N)$ Yang-Mills theory. We therefore refer to it as reduction condition. In other words, even though the reduction condition is imposed, the full $SU(N)$ gauge symmetry is preserved. Due to our approximation of fixing the color field, however,

the situation changes. The reduction condition appears as a gauge fixing-like term for the coset gluon. Nevertheless, we took the standpoint that according to the previous argument, we should adopt the "physical" choice $\xi = 0$ in order to incorporate the reduction condition in a Delta function like manner within the Faddeev-Popov framework. In this case, the value $V(\sigma_*)$ is negative and a non-zero coset gluon condensate is energetically favored. This is a remarkable result because in particular for $SU(3)$, the effective mass term for the remaining field $\mathfrak{X}_\mu$ renders the residual degrees of freedom corresponding to the non-Abelian stability group $U(2)$ to be infrared dominant. As pointed out earlier, this is in sharp contrast to the conventional MAG, where the residual degrees of freedom are of the Abelian type. Therefore, we defined a novel scheme, the non-Abelian dual superconductivity, where the inherent monopoles would be non-Abelian as the corresponding degrees of freedom are exactly encoded in the infrared dominant field $\mathfrak{V}_\mu \in \text{Lie } U(2)$. Hence, the analytical analysis performed in this chapter supports the lattice simulations that predicted exactly this fact. A possible way to extend the analysis is the transition to higher loop orders. Especially the behavior of the parameter ξ is interesting in that regard. Still, we should keep in mind that performing the local composite operator formalism to n-loop order requires the knowledge of all other RG functions up to $(n+1)$-loop level. This renders especially the renormalization of the composite operator a very difficult task, already at two-loop level.

In chapter 5, we attempted to improve these perturbative results within the framework of the functional renormalization group, calculating the renormalization group flow by means of the Wetterich equation. After a brief introduction to this technique, we applied the FRG to a slightly different problem in order to demonstrate the usefulness of this tool and how it can overcome shortcomings of perturbative approaches. In particular, the problem under investigation was the derivation of lower Higgs mass bounds within a Higgs-Yukawa toy model. Previous works applying perturbative methods, and using the perturbatively renormalizable quartic bare Higgs effective potential, predicted instabilities. Consequently, from the (meta-)stability requirement, lower Higgs mass bounds were originally deduced. These were in tension with the experimental value for the Higgs mass as well as with lattice simulations. Previous studies within the FRG then showed that the class of quartic potentials does not exhibit any instabilities at all, in accordance with lattice simulations, and even more, presented a mechanism that can lead to a diminishing of the lower mass bound by generalizing the bare potentials to higher order self-interactions. Roughly speaking, the inclusion of higher order operators in the effective bare potential allows to choose negative bare values for the quartic coupling, such that the latter ends up with smaller infrared values and therefore with smaller Higgs masses, as both quantities are directly related. In this work, we further developed this line of research by consider-

ing a gauged Higgs-Yukawa model together with another potential mechanism to further diminish the mass bounds, the inclusion of generalized Yukawa interactions $\sim \phi^{2n+1}\bar{\psi}\psi$. Gauging the model by coupling the Dirac fermions (quarks) of the Higgs-Yukawa model to the color $SU(N)$ gauge fields was an important step towards closing the gap between the actual standard model and the simplified Higgs-Yukawa toy model. This is because the gauge field fluctuations have a significant impact on the Yukawa coupling, which relates to the fermionic fluctuations that trigger the symmetry breaking. In particular, we demonstrated that all the key features observed in the simple Higgs-Yukawa model, such as the diminishing of the lower Higgs mass bound through the inclusion of higher order Higgs self-interactions, are still present in the gauged model - the gauging does not spoil any of those effects. Concerning the higher Yukawa interactions, they indeed represented another possibility to obtain Higgs masses below the conventional bound. However, the mechanism behind the lowering was found to be the same, namely the higher order operators lead to an initial decrease of the quartic Higgs coupling which in turn yields lower Higgs masses. Therefore, both effects coming from the generalized bare potentials and the higher Yukawa operators do not stack.

In the second part of chapter 5, the FRG tools were applied to the original question concerning the existence of the gluon-ghost condensate. We generated a situation quite similar to the first part of this chapter by performing a Hubbard-Stratonovich transformation, introducing a scalar field φ representing the condensate together with a Yukawa-like interaction $\varphi\mathcal{O}$ and a $\mathcal{O}^2$ interaction term. This enabled us to apply the lessons learned from the gauged Higgs-Yukawa model in a similar fashion, i.e., if the effective potential for the scalar field developed a non-trivial minimum, the Yukawa-like interaction would generate the desired mass term for the coset gluon. For simplicity, we firstly restricted ourselves to the $SU(2)$ case, in other words to the maximal Abelian gauge case. Working with a gauge-fixed version of the effective average action, the symmetry we wanted to preserve was the BRST symmetry. This usually translates into a series of highly involved modified Slavnov-Taylor identities. In practical calculations, it is more reasonable to ignore these identities and instead mimic BRST invariant flows in the sense that the action at the initial scale is fine-tuned in order to recover an BRST invariant action at least in the infrared. Following this path, we were able to show that the effective potential can develop a non-trivial minimum associated with the condensate and thus to a non-zero mass for the coset gluon and ghosts. The gauge fixing parameter was observed to decouple from the flow as well, taking a finite infrared value in contrast to the perturbative one-loop predictions. Moreover, despite the straightforward choice for the truncation of the effective average action, the Yang-Mills coupling defined through the running of the $V\omega\bar{\omega}$-vertex also exhibited a finite infrared fixed point, even though the value was much

smaller than reported in other studies, for example in the more involved background field formalism. Furthermore, it was possible to fix the bare values of the Yukawa operators such that the infrared gluon mass takes the value reported in lattice studies. Yet, a downside of our setting is always present. The described situation could only be achieved for rather large values of the gauge fixing parameter, which is even growing a little further before eventually freezing out. This is problematic for two reasons. First of all, we wanted to achieve very small infrared values for the parameter ξ related to the reduction condition, because this corresponds to incorporating the latter in the path integral as a Delta functional within the Faddeev-Popov framework. Second, the ratio m_ω/m_X is exactly given by $\sqrt{\xi}$. The freezing values of the parameter ξ we found in our simulations were all larger than 1, which implies that the obtained ghost mass is larger than the gluon mass. The large initial value for ξ is necessary to obtain the non-trivial positive value for the minimum v_k. At the same time, we were not able to tune other initial values such that ξ may decrease in the course of the flow. The situation did not change notably after extending the analysis to the $SU(3)$ gauge group, where the decomposition according to the minimal option is qualitatively different from the MAG. Still, the fact that the mechanism can be in principle observed within this approach marks a small step towards a non-perturbative establishment of the condensate and a non-Abelian dual superconductivity pciture, since especially in the $SU(3)$ case, the infrared dominant residual degrees of freedom are non-Abelian and so are the related monopoles. The encountered situation may be improved if one considers a more refined ansatz for the effective average action, for example by incorporating the flow of the quartic auxiliary couplings ζ_i with their true flow behavior rather than the approximation through $\frac{h^2}{\lambda_2}$. Another possibility could be to further resolve the interplay between the auxiliary field and the composite operator in the Yukawa-like interaction term in the sense of allowing for field dependent Yukawa couplings, just like in the case of the Higgs-Yukawa model investigated in the first part of this chapter. Moreover, the fact that the last diagram in the flow equation of the h_ω operator, cf. Eq. (5.82), actually vanished under the projection of zero external momenta suggests that momentum dependent terms may be generated, and thus derivative terms should be included, i.e., $h_\omega = h_\omega(\varphi, p)$. Finally, in the future it may be interesting to leave the color field spacetime dependent instead of fixing it, as we did in our approximation. Results alongside this direction can be found, for example, in [155].

Appendix A

Counterterm Lagrangian

In this appendix, we set up the counterterm Lagrangian corresponding to

$$\mathfrak{L} = \mathfrak{L}_{YM} + i\delta_B\bar{\delta}_B\left(\frac{1}{2}X^a_\mu X^{\mu a} - i\frac{\xi}{2}\omega^a\bar{\omega}^a\right) - i\delta_B\left[\bar{C}^j\left(\partial_\mu V^{\mu j} + \frac{\lambda}{2}N^j\right)\right] - i\delta_B\left[\bar{C}^\gamma\left(\partial_\mu V^{\mu\gamma} + \frac{\alpha}{2}N^\gamma\right)\right]. \tag{A.1}$$

Upon defining the following set of counterterms,

$$\begin{aligned}
&\Delta_1 = Z_X - 1, && \Delta_2 = Z_X Z_\xi^{-1} - 1, && \Delta_3 = Z_V - 1,\\
&\Delta_4 = Z_V Z_\lambda^{-1} - 1, && \Delta_5 = \tilde{Z}_V - 1, && \Delta_6 = \tilde{Z}_V Z_\alpha^{-1} - 1,\\
&\Delta_7 = Z_\omega - 1, && \Delta_8 = Z_C^{1/2} Z_{\bar{C}}^{1/2} - 1, && \Delta_9 = \tilde{Z}_C^{1/2} \tilde{Z}_{\bar{C}}^{1/2} - 1,\\
&\Delta_{10} = Z_V^{3/2} Z_g - 1, && \Delta_{11} = Z_X Z_V^{1/2} Z_g Z_\xi^{-1} - 1, && \Delta_{12} = Z_X \tilde{Z}_V^{1/2} Z_g Z_\xi^{-1} - 1,\\
&\Delta_{13} = Z_X Z_V^{1/2} Z_g - 1, && \Delta_{14} = Z_X \tilde{Z}_V^{1/2} Z_g - 1, && \Delta_{15} = Z_g^2 Z_X^2 - 1,\\
&\Delta_{16} = Z_V^2 Z_g^2 - 1, && \Delta_{17} = Z_X Z_V Z_g^2 - 1, && \Delta_{18} = Z_X \tilde{Z}_V Z_g^2 - 1,\\
&\Delta_{19} = Z_X Z_V^{1/2} \tilde{Z}_V^{1/2} Z_g^2 - 1, && \Delta_{20} = Z_X Z_V Z_g^2 Z_\xi^{-1} - 1, && \Delta_{21} = Z_X \tilde{Z}_V Z_g^2 Z_\xi^{-1} - 1,\\
&\Delta_{22} = Z_X Z_V^{1/2} \tilde{Z}_V^{1/2} Z_g^2 Z_\xi^{-1} - 1, && \Delta_{23} = Z_\omega Z_V^{1/2} Z_g - 1, && \Delta_{24} = Z_\omega \tilde{Z}_V^{1/2} Z_g - 1,\\
&\Delta_{25} = Z_C^{1/2} Z_{\bar{C}}^{1/2} Z_V^{1/2} Z_g - 1, && \Delta_{26} = Z_\omega^{1/2} Z_{\bar{C}}^{1/2} Z_X^{1/2} Z_g - 1, && \Delta_{27} = Z_\omega^{1/2} \tilde{Z}_{\bar{C}}^{1/2} Z_X^{1/2} Z_g - 1,\\
&\Delta_{28} = Z_\omega Z_V Z_g^2 - 1, && \Delta_{29} = Z_\omega \tilde{Z}_V Z_g^2 - 1, && \Delta_{30} = Z_\omega Z_V^{1/2} \tilde{Z}_V^{1/2} Z_g^2 - 1,\\
&\Delta_{31} = Z_\omega Z_X Z_g^2 - 1, && \Delta_{32} = Z_\omega^2 Z_g^2 Z_\xi - 1,
\end{aligned} \tag{A.2}$$

we write the counterterm Lagrangian in the form

$$
\begin{aligned}
&\mathfrak{L}_{c.t.} = \\
&\Delta_1 \frac{1}{2} X^a_\mu \left(g^{\mu\nu}\partial^2 - \partial^\mu\partial^\nu\right) X^a_\nu + \Delta_2 \frac{1}{2\xi} X^a_\mu \partial^\mu\partial^\nu X^a_\nu + \Delta_3 \frac{1}{2} V^j_\mu \left(g^{\mu\nu}\partial^2 - \partial^\mu\partial^\nu\right) V^j_\nu + \Delta_4 \frac{1}{2\lambda} V^j_\mu \partial^\mu\partial^\nu V^j_\nu \\
&+ \Delta_5 \frac{1}{2} V^\gamma_\mu \left(g^{\mu\nu}\partial^2 - \partial^\mu\partial^\nu\right) V^\gamma_\nu + \Delta_6 \frac{1}{2\alpha} V^\gamma_\mu \partial^\mu\partial^\nu V^\gamma_\nu + \Delta_7 i\bar\omega^a \partial^2 \omega^a + \Delta_8 i\bar C^j \partial^2 C^j + \Delta_9 i\bar C^\gamma \partial^2 C^\gamma \\
&- \Delta_{10} \frac{g}{2} f^{jkl} (\partial_\mu V^j_\nu - \partial_\nu V^j_\mu) V^{\mu k} V^{\nu l} - \Delta_{11} \frac{g}{\xi} f^{ajb} \partial_\mu X^{\mu a} V^j_\nu X^{\nu b} - \Delta_{12} \frac{g}{\xi} f^{a\gamma b} \partial_\mu X^{\mu a} V^\gamma_\nu X^{\nu b} \\
&+ \Delta_{13} \frac{g}{2} f^{ajb} \left\{ X^{\mu a} X^{\nu b} (\partial_\mu V^j_\nu - \partial_\nu V^j_\mu) + V^{\mu j} X^{\nu b} (\partial_\nu X^a_\mu - \partial_\mu X^a_\nu) + V^{\nu j} X^{\mu b} (\partial_\mu X^a_\nu - \partial_\nu X^a_\mu) \right\} \\
&+ \Delta_{14} \frac{g}{2} f^{a\gamma b} \left\{ X^{\mu a} X^{\nu b} (\partial_\mu V^\gamma_\nu - \partial_\nu V^\gamma_\mu) + V^{\mu\gamma} X^{\nu b} (\partial_\nu X^a_\mu - \partial_\mu X^a_\nu) + V^{\nu\gamma} X^{\mu b} (\partial_\mu X^a_\nu - \partial_\nu X^a_\mu) \right\} \\
&- \Delta_{15} \frac{g^2}{4} f^{abJ} f^{cdJ} X^a_\mu X^b_\nu X^{\mu c} X^{\nu d} - \Delta_{16} \frac{g^2}{4} f^{jkl} f^{jmn} V^k_\mu V^l_\nu V^{\mu m} V^{\nu n} \\
&+ \Delta_{17} g^2 \left\{ \frac{1}{2} f^{akc} f^{cjb} \left(X^a_\mu X^{\mu b} V^k_\nu V^{\nu j} - X^a_\mu X^b_\nu V^{\mu k} V^{\nu j} \right) - f^{abj} f^{jkl} V^k_\mu V^l_\nu X^{\mu a} X^{\nu b} \right\} \\
&+ \Delta_{18} g^2 \left\{ \frac{1}{2} f^{a\gamma c} f^{c\gamma b} \left(X^a_\mu X^{\mu b} V^\gamma_\nu V^{\nu\gamma} - X^a_\mu X^b_\nu V^{\mu\gamma} V^{\nu\gamma} \right) \right\} \\
&+ \Delta_{19} g^2 f^{akc} f^{c\gamma b} \left\{ X^a_\mu X^{\mu b} V^k_\nu V^{\nu\gamma} - \frac{1}{2} X^a_\mu X^{\nu b} V^{\mu k} V^\gamma_\nu - \frac{1}{2} X^b_\mu X^{\nu a} V^{\mu\gamma} V^k_\nu \right\} \\
&- \Delta_{20} \frac{g^2}{2\xi} f^{ajb} f^{akc} V^{\mu j} X^b_\mu V^k_\nu X^{\nu c} - \Delta_{21} \frac{g^2}{2\xi} \frac{N}{2(N-1)} V^{\mu\gamma} X^a_\mu V^\gamma_\nu X^{\nu a} \\
&- \Delta_{22} \frac{g^2}{2\xi} f^{a\gamma b} f^{akc} \left\{ V^{\mu\gamma} X^b_\mu V^k_\nu X^{\nu c} + V^{\mu k} X^c_\mu X^b_\nu V^{\nu\gamma} \right\} + \Delta_{23} i g f^{ajb} \left\{ \bar\omega^a \partial_\mu (V^{\mu j} \omega^b) + \bar\omega^a V^{\mu j} \partial_\mu \omega^b \right\} \\
&+ \Delta_{24} i g f^{a\gamma b} \left\{ \bar\omega^a \partial_\mu (V^{\mu\gamma} \omega^b) + \bar\omega^a V^{\mu\gamma} \partial_\mu \omega^b \right\} + \Delta_{25} i g f^{jkl} \bar C^j \partial_\mu (V^{\mu k} C^l) + \Delta_{26} i g f^{jab} \bar C^j \partial_\mu (X^{\mu a} \omega^b) \\
&+ \Delta_{27} i g f^{\gamma ab} \bar C^\gamma \partial_\mu (X^{\mu a} \omega^b) + \Delta_{28} i g^2 f^{akc} f^{cjb} \bar\omega^a \omega^b V^{\mu k} V^j_\mu - i \Delta_{29} g^2 \frac{N}{2(N-1)} \bar\omega^a \omega^a V^{\mu\gamma} V^\gamma_\mu \\
&+ \Delta_{30} i g^2 f^{akc} f^{c\gamma b} V^k_\mu V^{\mu\gamma} \left\{ \bar\omega^a \omega^b + \bar\omega^b \omega^a \right\} + \Delta_{31} i g^2 f^{abJ} f^{cdJ} \bar\omega^b \omega^d X^a_\mu X^\mu_c \\
&+ \Delta_{32} \frac{\xi g^2}{4} f^{abJ} f^{cdJ} \bar\omega^a \bar\omega^b \omega^c \omega^d. \qquad \text{(A.3)}
\end{aligned}
$$

Appendix B

Derivation of the mass mixing matrix

In this appendix, we briefly explain how to determine the renormalization matrix of the composite operator renormalization, deriving the diagrammatic equations for the renormalization matrix elements. Let us write the mixing matrix (3.106) symbolically as

$$[\Phi_R]_A = \mathcal{Z}_{AB}[\Phi_B]_R. \tag{B.1}$$

To obtain the entries of the mixing matrix $\mathcal{Z}$, we have to insert each condensate $[\Phi_B]_R$ into each two-point function and require cancellation of the emerging divergences.

Insertion into $\langle XX \rangle$

For the insertion into $\langle XX \rangle$ we obtain

$\delta^{1B}\cdot$  $\equiv \langle XX[\Phi_B]_R\rangle =$

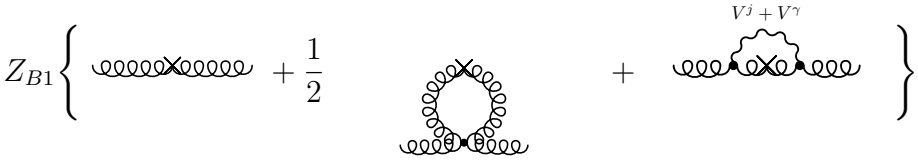

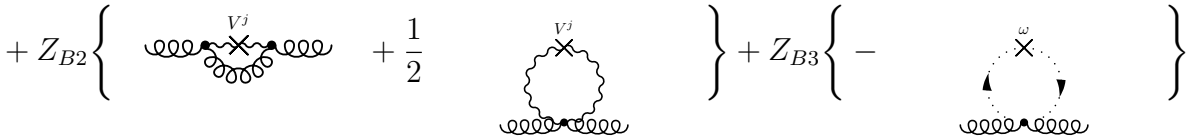

$$+ Z_{B4}\{0\} + Z_{B5}\Bigg\{ \quad + \frac{1}{2} \quad \Bigg\} + Z_{B6}\{0\}. \qquad \text{(B.2)}$$

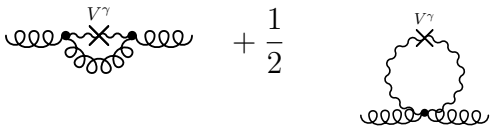

Note that due to the insertions, also tadpole diagrams must be taken into account, as they also become divergent. By construction, an insertion of $[\Phi_B]_R$ into the two-point function only yields non-zero contributions if the XX condensate is inserted. This explains the δ^{1B} on the left hand side. The right hand side can only generate such a tree level term for $B = 1$ if Z_{11} possesses a tree part. On the other hand, this also implies that for $B \neq 1$ the renormalization factors Z_{B1} do not have a tree part.

Insertion into $\langle V^j V^k \rangle$

For the insertion into $\langle V^j V^k \rangle$ we obtain

$$\delta^{2B}\cdot$$

$$\equiv \langle V^j V^k [\Phi_B]_R \rangle = Z_{B1}\Bigg\{ \frac{1}{2}$$ 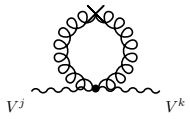

$$+$$ 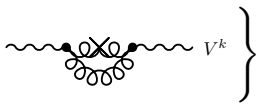

$$\Bigg\}$$

$$+ Z_{B2}\Bigg\{$$ 

$$+ \frac{1}{2}$$ 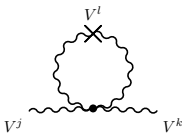

$$+$$ 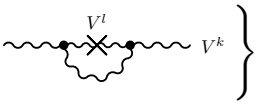

$$\Bigg\}$$

$$+ Z_{B3}\Bigg\{ -$$ 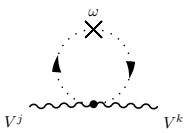

$$- 2$$ 

$$\Bigg\}$$

$$+ Z_{B4}\Bigg\{ - 2$$ 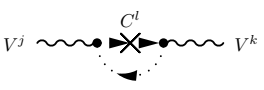

$$\Bigg\} + Z_{B5}\{0\} + Z_{B6}\{0\}. \qquad \text{(B.3)}$$

By the same arguments as before, only Z_{22} has the tree part, while all Z_{B2} with $B \neq 2$ do not possess a tree part.

Insertion into $\langle\omega\bar{\omega}\rangle$

For the insertion into $\langle\omega\bar{\omega}\rangle$ we obtain

$$\delta^{3B} \cdot \quad \equiv \langle\omega\bar{\omega}[\Phi_B]_R\rangle =$$

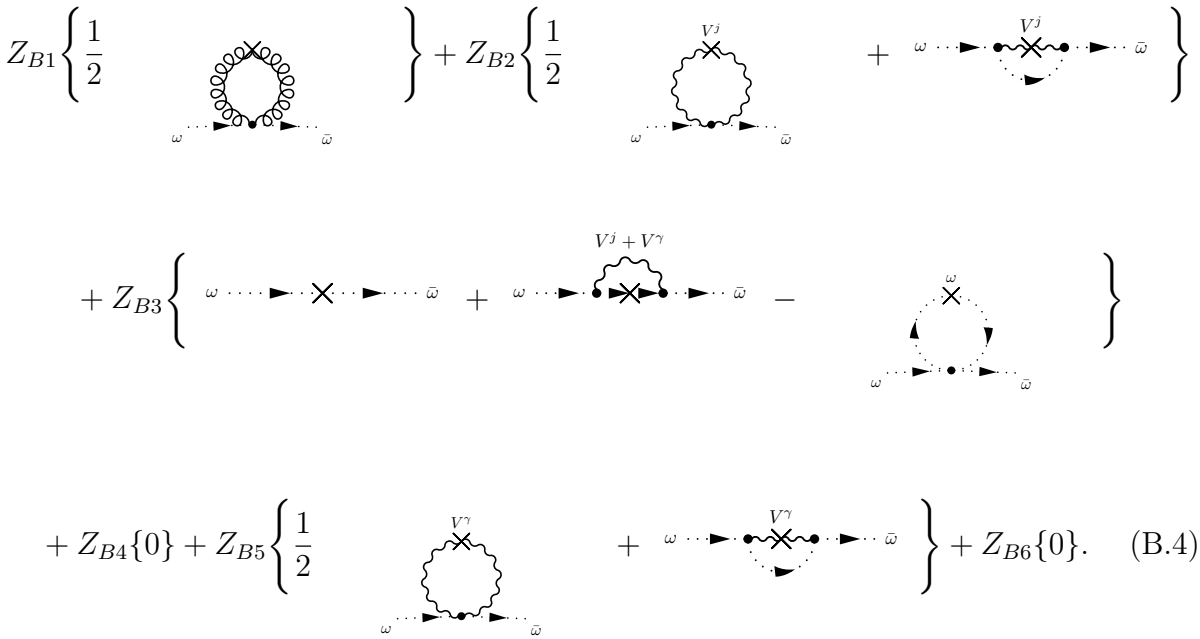

(B.4)

By the same arguments as before, only Z_{33} has the tree part, while all Z_{B3} with $B \neq 3$ do not possess a tree part.

Insertion into $\langle C^j \bar{C}^k \rangle$

For the insertion into $\langle C^j \bar{C}^k \rangle$ we obtain

$$\delta^{4B} \cdot \; C^j \cdots\!\blacktriangleright\!\cdots\times\cdots\!\blacktriangleright\!\cdots \bar{C}^k \;\equiv\; \langle C^j \bar{C}^k [\Phi_B]_R \rangle =$$

$$Z_{B1}\{0\} + Z_{B2}\Big\{ \; C^j \cdots\!\blacktriangleright\!\cdots \overset{V^l}{\times} \cdots\!\blacktriangleright\!\cdots \bar{C}^k \; \Big\} + Z_{B3}\{0\}$$

$$+ Z_{B4}\Big\{ \; C^j \cdots\!\blacktriangleright\!\cdots\times\cdots\!\blacktriangleright\!\cdots \bar{C}^k \; + \; C^j \cdots\!\blacktriangleright\!\cdots \overset{C^l}{\times} \cdots\!\blacktriangleright\!\cdots \bar{C}^k \; \Big\} + Z_{B5}\{0\} + Z_{B6}\{0\}. \qquad \text{(B.5)}$$

By the same arguments as before, only Z_{44} has the tree part, while all Z_{B4} with $B \neq 4$ do not possess a tree part.

Insertion into $\langle V^\gamma V^\gamma \rangle$

For the insertion into $\langle V^\gamma V^\gamma \rangle$ we obtain

$$\delta^{5B} \cdot \; V^\gamma \sim\!\sim\!\times\!\sim\!\sim V^\gamma \;\equiv\; \langle V^\gamma V^\gamma [\Phi_B]_R \rangle =$$

$$Z_{B1}\Big\{ \frac{1}{2} \quad \overset{V^\gamma}{\underset{V^\gamma}{\circlearrowright}} \quad + \; V^\gamma \sim\!\sim\!\overset{}{\times}\!\sim\!\sim V^\gamma \; \Big\} + Z_{B2}\{0\}$$

$$+ Z_{B3}\Big\{ - \quad \overset{\omega}{\underset{V^\gamma}{\circlearrowright}} \quad + \; V^\gamma \sim\!\sim\!\overset{\omega}{\times}\!\sim\!\sim V^\gamma \; \Big\}$$

$$+ Z_{B4}\{0\} + Z_{B5}\left\{ \right. \quad \left. \right\} + Z_{B6}\{0\}. \tag{B.6}$$

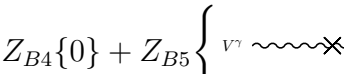

By the same arguments as before, only Z_{55} has the tree part, while all Z_{B5} with $B \neq 5$ do not possess a tree part.

Insertion into $\langle C^\gamma \bar{C}^\gamma \rangle$

For the insertion into $\langle C^\gamma \bar{C}^\gamma \rangle$ we obtain

$$\delta^{6B} \cdot \quad \equiv \langle C^\gamma \bar{C}^\gamma [\Phi_B]_R \rangle =$$

$$Z_{B1}\{0\} + Z_{B2}\{0\} + Z_{B3}\{0\} + Z_{B4}\{0\} + Z_{B5}\{0\} + Z_{B6}\left\{ \right. \quad \left. \right\}. \tag{B.7}$$

By the same arguments as before, only Z_{66} has the tree part, while all Z_{B6} with $B \neq 6$ do not possess a tree part.

At this point, we established the following shape of the mixing matrix,

$$\mathcal{Z}_{AB} = \delta_{AB} + \mathcal{Z}^{(1)}_{AB}. \tag{B.8}$$

With this knowledge, we can reconsider the Eqs. (B.2) - (B.7) and derive the following diagrammatic equations for the $Z^{(1)}_{AB}$, including their divergent parts,

$$Z^{(1)}_{11} = -\left\{ \frac{1}{2} \right.$$

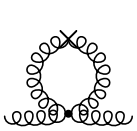

$$+$$

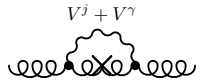

$$\left. \right\}$$

$$= -\frac{g^2 \mu^{-2\epsilon}}{(4\pi)^2 \epsilon} \frac{N}{2} \left(\frac{3}{2}(\xi + 1) + \frac{\alpha + (N-2)\lambda}{N-1} \right),$$

$$Z_{21}^{(1)} = -\Bigg\{ \quad + \frac{1}{2} \quad \Bigg\} = -\frac{g^2\mu^{-2\epsilon}}{(4\pi)^2\epsilon}\frac{N(N-2)}{2(N-1)}\frac{3}{4}(\xi+3),$$

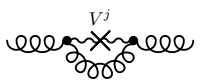

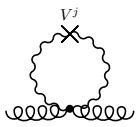

$$Z_{31}^{(1)} = -\Bigg\{ - \quad \Bigg\} = -\frac{g^2\mu^{-2\epsilon}}{(4\pi)^2\epsilon}N,$$

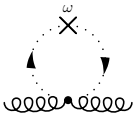

$$Z_{51}^{(1)} = -\Bigg\{ \quad + \frac{1}{2} \quad \Bigg\} = -\frac{g^2\mu^{-2\epsilon}}{(4\pi)^2\epsilon}\frac{N}{2(N-1)}\frac{3}{4}(\xi+3),$$

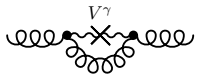

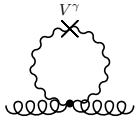

$$Z_{12}^{(1)} = -\Bigg\{ \frac{1}{2} \quad + \quad \Bigg\} = 0,$$

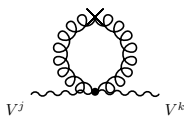

$$Z_{22}^{(1)} = -\Bigg\{ \frac{1}{2} \quad + \quad \Bigg\} = -\frac{g^2\mu^{-2\epsilon}}{(4\pi)^2\epsilon}\frac{3}{4}(N-1)(1+\lambda),$$

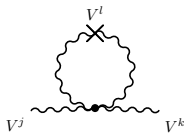

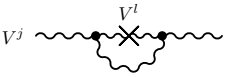

$$Z_{32}^{(1)} = -\Bigg\{ - \quad - 2 \quad \Bigg\} = 0,$$

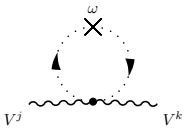

$$Z_{42}^{(1)} = -\Bigg\{ -2 \quad \text{  } \quad \Bigg\} = -\frac{g^2\mu^{-2\epsilon}}{(4\pi)^2\epsilon}\frac{(N-1)}{2},$$

$$Z_{13}^{(1)} = -\Bigg\{ \frac{1}{2} \quad \text{ 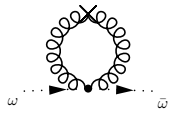 } \quad \Bigg\} = \frac{g^2\mu^{-2\epsilon}}{(4\pi)^2\epsilon} N \frac{3+\xi^2}{2},$$

$$Z_{23}^{(1)} = -\Bigg\{ \frac{1}{2} \quad \text{ 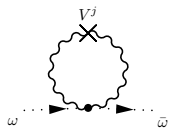 } \quad + \quad \text{  } \quad \Bigg\} = -3\frac{g^2\mu^{-2\epsilon}}{(4\pi)^2\epsilon}\frac{N(N-2)}{2(N-1)},$$

$$Z_{33}^{(1)} = -\Bigg\{ \quad \text{ 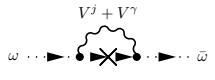 } \quad - \quad \text{ 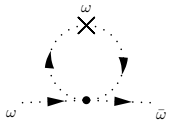 } \quad \Bigg\} = \frac{g^2\mu^{-2\epsilon}}{(4\pi)^2\epsilon}\frac{N}{2}\left(\xi - \frac{\alpha+(N-2)\lambda}{N-1}\right),$$

$$Z_{53}^{(1)} = -\Bigg\{ \frac{1}{2} \quad \text{ 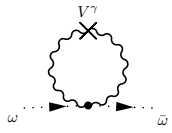 } \quad + \quad \text{  } \quad \Bigg\} = -3\frac{g^2\mu^{-2\epsilon}}{(4\pi)^2\epsilon}\frac{N}{2(N-1)},$$

$$Z_{24}^{(1)} = -\Bigg\{ \quad \text{ 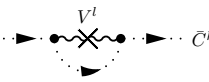 } \quad \Bigg\} = 0,$$

$$Z_{44}^{(1)} = -\Bigg\{ \quad \text{ 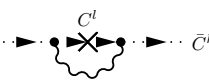 } \quad \Bigg\} = 0,$$

$$Z_{15}^{(1)} = -\Bigg\{ \frac{1}{2} \quad \text{ 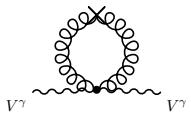 } \quad + \text{  } \Bigg\} = 0,$$

$$Z_{35}^{(1)} = -\Bigg\{ - \quad \text{ 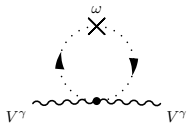 } \quad + \text{  } \Bigg\} = 0.$$

(B.9)

With these results, we arrive exactly at the mixing matrix stated in Eq. (3.107).

Appendix C

Threshold functions

In this appendix, we summarize the definitions of the threshold functions appearing in the flow equations of chapter 5. Recalling the modified scale derivative

$$\tilde{\partial}_t = \sum_{i=F,B} \int_q \frac{\partial_t (Z_{i,k}\, r_{k,i}(q))}{Z_{i,k}} \frac{\delta}{\delta r_{k,i}(q)}, \tag{C.1}$$

where $F = \psi$ stands for the Dirac fermion, while B stands for the bosonic fields, namely the scalar field, gluon, and ghosts, as well as the generalized momenta

$$P_F(q) = q^2(1 + r_{F,k})^2; \quad P_B = q^2(1 + r_{B,k}), \tag{C.2}$$

the threshold functions relevant for subsection 5.2.2 are defined according to

$$\begin{aligned}
l_n^{(\mathrm{B})d}[\omega; \eta_\mathrm{B}] &= \frac{n + \delta_{n,0}}{4v_d} k^{2n-d} \int_q \left[\frac{\partial_t R_{\mathrm{B},k}(q)}{Z_{\mathrm{B},k}} (P_\mathrm{B}(q) + \omega k^2)^{-(n+1)} \right], \\
l_n^{(\mathrm{F})d}[\omega; \eta_\mathrm{F}] &= \frac{n + \delta_{n,0}}{2v_d} k^{2n-d} \int_q \left[\frac{P_\mathrm{F}(q)\, \partial_t (Z_{\mathrm{F},k}\, r_{\mathrm{F},k}(q))}{Z_{\mathrm{F},k}(1 + r_{\mathrm{F},k})} (P_\mathrm{F}(q) + \omega k^2)^{-(n+1)} \right], \\
l_{n_1,n_2}^{(\mathrm{FB})d}[\omega_1, \omega_2; \eta_\mathrm{F}, \eta_\mathrm{B}] &= -\frac{1}{4v_d} k^{2(n_1+n_2)-d} \int_q \tilde{\partial}_t \left[\frac{1}{(P_\mathrm{F}(q) + k^2\omega_1)^{n_1} (P_\mathrm{B}(q) + k^2\omega_2)^{n_2}} \right], \\
m_4^{(\mathrm{F})d}[\omega; \eta_\mathrm{F}] &= -\frac{1}{4v_d} k^{4-d} \int_q q^4 \tilde{\partial}_t \left[\frac{\partial}{\partial q^2} \frac{1 + r_{\mathrm{F},k}(q)}{P_\mathrm{F}(q) + k^2\omega} \right]^2, \\
m_2^{(\mathrm{F})d}[\omega; \eta_\mathrm{F}] &= -\frac{1}{4v_d} k^{6-d} \int_q q^2 \tilde{\partial}_t \left[\frac{\left(\frac{\partial}{\partial q^2} P_\mathrm{F}(q) \right)}{(P_\mathrm{F}(q) + k^2\omega)^2} \right]^2,
\end{aligned}$$

$$
\begin{aligned}
m_2^{(\mathrm{B})d}[\omega;\eta_\mathrm{B}] &= -\frac{1}{4v_d}k^{6-d}\int_q q^2\tilde{\partial}_t\left[\frac{\left(\frac{\partial}{\partial q^2}P_\mathrm{B}(q)\right)}{(P_\mathrm{B}(q)+k^2\omega)^2}\right]^2,\\
m_{n_1,n_2}^{(\mathrm{FB})d}[\omega_1,\omega_2;\eta_\mathrm{F},\eta_\mathrm{B}] &= -\frac{1}{4v_d}k^{2(n_1+n_2-1)-d}\int_q q^2\tilde{\partial}_t\left[\frac{1+r_{\mathrm{F},k}(q)}{(P_\mathrm{F}(q)+k^2\omega_1)^{n_1}}\frac{\left(\frac{\partial}{\partial q^2}P_\mathrm{B}(q)\right)}{(P_\mathrm{B}(q)+k^2\omega_2)^{n_2}}\right],\\
\tilde{m}_{n_1,n_2}^{(\mathrm{FB})d}[\omega_1,\omega_2;\eta_\mathrm{F},\eta_\mathrm{B}] &= -\frac{1}{4v_d}k^{2(n_1+n_2)-d}\int_q \tilde{\partial}_t\left[\frac{1+r_{\mathrm{F},k}(q)}{(P_\mathrm{F}(q)+k^2\omega_1)^{n_1}}\frac{1}{(P_\mathrm{B}(q)+k^2\omega_2)^{n_2}}\right].
\end{aligned}
\tag{C.3}
$$

The threshold functions additionally appearing in section 5.3 read

$$
\begin{aligned}
l_{1,1}^{(BB)d}[\omega_1,\omega_2;\eta_{B1},\eta_{B2}] &= -\frac{1}{4v_d}k^{4-d}\int_q\tilde{\partial}_t\left[\frac{1}{P_{B1}+k^2\omega_1}\frac{1}{P_{B2}+k^2\omega_2}\right],\\
m_{1,1}^{(BB)d}[\omega_1,\omega_2;\eta_{B1},\eta_{B2}] &= \frac{1}{4v_d}k^{4-d}\int_q\tilde{\partial}_t\left[\frac{1}{P_{B1}+k^2\omega_1}\frac{-q^2\partial_{q^2}P_{B2}}{(P_{B2}+k^2\omega_2)^2}\right],\\
n_{1,1}^{(BB)d}[\omega_1,\omega_2;\eta_{B1},\eta_{B2}] &= \frac{1}{4v_d}k^{4-d}\int_q\tilde{\partial}_t\left[\frac{1}{P_{B1}+k^2\omega_1}q^4\partial_{q^2}\partial_{q^2}\left(\frac{1}{P_{B2}+k^2\omega_2}\right)\right],\\
\bar{l}_{1,1}^{(BB)d}[\omega_1,\omega_2;\eta_{B1},\eta_{B2}] &= -\frac{1}{8v_d}k^{6-d}\int_q\frac{1}{q^2}\tilde{\partial}_t\left[\frac{1}{P_{B1}+k^2\omega_1}\frac{1}{P_{B2}+k^2\omega_2}\right],\\
\bar{m}_{1,1}^{(BB)d}[\omega_1,\omega_2;\eta_{B1},\eta_{B2}] &= \frac{1}{4v_d}k^{6-d}\int_q\frac{1}{q^2}\tilde{\partial}_t\left[\frac{1}{P_{B1}+k^2\omega_1}\frac{-q^2\partial_{q^2}P_{B2}}{(P_{B2}+k^2\omega_2)^2}\right],\\
\bar{n}_{1,1}^{(BB)d}[\omega_1,\omega_2;\eta_{B1},\eta_{B2}] &= \frac{1}{4v_d}k^{6-d}\int_q\frac{1}{q^2}\tilde{\partial}_t\left[\frac{1}{P_{B1}+k^2\omega_1}q^4\partial_{q^2}\partial_{q^2}\left(\frac{1}{P_{B2}+k^2\omega_2}\right)\right],\\
N_{1,1}^{(BB)d}[\omega_1,\omega_2;\eta_{B1},\eta_{B2}] &= -\frac{1}{4v_d}k^{6-d}\int_q q^2\tilde{\partial}_t\left[\frac{\partial_{q^2}P_{B1}}{(P_{B1}+k^2\omega_1)^2}\frac{\partial_{q^2}P_{B2}}{(P_{B2}+k^2\omega_2)^2}\right],\\
T_{1,1,1}^{(BBB)d}[\omega_1,\omega_2,\omega_3;\eta_{B1},\eta_{B2},\eta_{B3}] &= -\frac{1}{4v_d}k^{6-d}\int_q\tilde{\partial}_t\left[\frac{1}{P_{B1}+k^2\omega_1}\frac{1}{P_{B2}+k^2\omega_2}\frac{1}{P_{B3}+k^2\omega_3}\right],\\
\bar{T}_{1,1,1}^{(BBB)d}[\omega_1,\omega_2,\omega_3;\eta_{B1},\eta_{B2},\eta_{B3}] &= -\frac{1}{8v_d}k^{8-d}\int_q q^2\tilde{\partial}_t\left[\frac{1}{P_{B1}+k^2\omega_1}\frac{1}{P_{B2}+k^2\omega_2}\frac{1}{P_{B3}+k^2\omega_3}\right],\\
D_{1,1,1}^{(BBB)d}[\omega_1,\omega_2,\omega_3;\eta_{B1},\eta_{B2},\eta_{B3}] &= \frac{1}{4v_d}k^{6-d}\int_q\tilde{\partial}_t\left[\frac{1}{P_{B1}+k^2\omega_1}\frac{1}{P_{B2}+k^2\omega_2}\frac{-q^2\partial_{q^2}P_{B3}}{(P_{B3}+k^2\omega_3)^2}\right],\\
\bar{D}_{1,1,1}^{(BBB)d}[\omega_1,\omega_2,\omega_3;\eta_{B1},\eta_{B2},\eta_{B3}] &= \frac{1}{4v_d}k^{4-d}\int_q q^2\tilde{\partial}_t\left[\frac{1}{P_{B1}+k^2\omega_1}\frac{1}{P_{B2}+k^2\omega_2}\frac{-q^2\partial_{q^2}P_{B3}}{(P_{B3}+k^2\omega_3)^2}\right].
\end{aligned}
\tag{C.4}
$$

With the Litim regulator [136]

$$r_{\mathrm{B},k}(q) = \left(\frac{k^2}{q^2} - 1\right)\Theta(k^2 - q^2); \quad (1 + r_{\mathrm{F},k}(q))^2 = (1 + r_{\mathrm{B},k}(q)), \tag{C.5}$$

the momentum integrals can be solved analytically, yielding for the first set of threshold functions

$$\begin{aligned}
l_n^{(\mathrm{B})d}[\omega;\eta_{\mathrm{B}}] &= \frac{2(n+\delta_{n,0})}{d}\left(1 - \frac{\eta_{\mathrm{B},k}}{d+2}\right)\frac{1}{(1+\omega)^{n+1}},\\
l_n^{(\mathrm{F})d}[\omega;\eta_{\mathrm{F}}] &= \frac{2(n+\delta_{n,0})}{d}\left(1 - \frac{\eta_{\mathrm{F},k}}{d+1}\right)\frac{1}{(1+\omega)^{n+1}},\\
l_{n_1,n_2}^{(\mathrm{FB})d}[\omega_1,\omega_2;\eta_{\mathrm{F}},\eta_{\mathrm{B}}] &= \frac{2}{d}\frac{1}{(1+\omega_1)^{n_1}(1+\omega_2)^{n_2}}\left[\frac{n_1}{1+\omega_1}\left(1 - \frac{\eta_{\mathrm{F},k}}{d+1}\right) + \frac{n_2}{1+\omega_2}\left(1 - \frac{\eta_{\mathrm{B},k}}{d+2}\right)\right],\\
m_4^{(\mathrm{F})d}[\omega;\eta_{\mathrm{F}}] &= \frac{1}{(1+\omega)^4} + \frac{1-\eta_{\mathrm{F},k}}{d-2}\frac{1}{(1+\omega)^3} - \left(\frac{1-\eta_{\mathrm{F},k}}{2d-4} + \frac{1}{4}\right)\frac{1}{(1+\omega)^2},\\
m_2^{(\mathrm{F})d}[\omega;\eta_{\mathrm{F}}] &= \frac{1}{(1+\omega)^4},\\
m_2^{(\mathrm{B})d}[\omega;\eta_{\mathrm{B}}] &= \frac{1}{(1+\omega_1)^4},\\
m_{n_1,n_2}^{(\mathrm{FB})d}[\omega_1,\omega_2;\eta_{\mathrm{F}},\eta_{\mathrm{B}}] &= \left(1 - \frac{\eta_{\mathrm{B},k}}{d+1}\right)\frac{1}{(1+\omega_1)^{n_1}(1+\omega_2)^{n_2}},\\
\tilde{m}_{n_1,n_2}^{(\mathrm{FB})d}[\omega_1,\omega_2;\eta_{\mathrm{F}},\eta_{\mathrm{B}}] &= \frac{2n_2}{(d-1)}\left(1 - \frac{\eta_{\mathrm{B},k}}{d+1}\right)\frac{1}{(1+\omega_1)^{n_1}(1+\omega_2)^{n_2+1}},\\
&\quad - \frac{1+\omega_1-2n_1}{d-1}\left(1 - \frac{\eta_{\mathrm{F},k}}{d}\right)\frac{1}{(1+\omega_1)^{n_1+1}(1+\omega_2)^{n_2}}.
\end{aligned} \tag{C.6}$$

For the second set we find

$$\begin{aligned}
l_{1,1}^{(BB)d}[\omega_1,\omega_2;\eta_{B1},\eta_{B2}] &= \frac{2}{d}\frac{1}{1+\omega_1}\frac{1}{1+\omega_2}\left(\frac{1}{1+\omega_1}\left[1 - \frac{\eta_{B1}}{d+2}\right] + \frac{1}{1+\omega_2}\left[1 - \frac{\eta_{B2}}{d+2}\right]\right),\\
m_{1,1}^{(BB)d}[\omega_1,\omega_2;\eta_{B1},\eta_{B2}] &= \frac{1}{1+\omega_1}\frac{1}{(1+\omega_2)^2}\left[1 - \frac{\eta_{B2}}{d+2}\right],\\
n_{1,1}^{(BB)d}[\omega_1,\omega_2;\eta_{B1},\eta_{B2}] &= \frac{1}{1+\omega_1}\frac{1}{(1+\omega_2)^2}\left(\frac{1}{1+\omega_1} - \left(1 + \frac{d}{2}\right)\left[1 - \frac{\eta_{B2}}{d+2}\right]\right),\\
\bar{l}_{1,1}^{(BB)d}[\omega_1,\omega_2;\eta_{B1},\eta_{B2}] &= \frac{1}{d-2}\frac{1}{1+\omega_1}\frac{1}{1+\omega_2}\left(\frac{1}{1+\omega_1}\left[1 - \frac{\eta_{B1}}{d}\right] + \frac{1}{1+\omega_2}\left[1 - \frac{\eta_{B2}}{d}\right]\right),\\
\bar{m}_{1,1}^{(BB)d}[\omega_1,\omega_2;\eta_{B1},\eta_{B2}] &= \frac{1}{1+\omega_1}\frac{1}{(1+\omega_2)^2}\left[1 - \frac{\eta_{B2}}{d}\right],
\end{aligned}$$

$$
\begin{aligned}
\bar{n}^{(BB)d}_{1,1}[\omega_1,\omega_2;\eta_{B1},\eta_{B2}] &= \frac{1}{1+\omega_1}\frac{1}{(1+\omega_2)^2}\left(\frac{1}{1+\omega_1}-\frac{d}{2}\left[1-\frac{\eta_{B2}}{d}\right]\right),\\
N^{(BB)d}_{1,1}[\omega_1,\omega_2;\eta_{B1},\eta_{B2}] &= \frac{1}{(1+\omega_1)^2}\frac{1}{(1+\omega_2)^2},\\
T^{(BBB)d}_{1,1,1}[\omega_1,\omega_2,\omega_3;\eta_{B1},\eta_{B2},\eta_{B3}] &= \frac{2}{d}\frac{1}{1+\omega_1}\frac{1}{1+\omega_2}\frac{1}{1+\omega_3}\left(\frac{1}{1+\omega_1}\left[1-\frac{\eta_{B1}}{d+2}\right]\right.\\
&\quad\left.+\frac{1}{1+\omega_2}\left[1-\frac{\eta_{B2}}{d+2}\right]+\frac{1}{1+\omega_3}\left[1-\frac{\eta_{B3}}{d+2}\right]\right),\\
\bar{T}^{(BBB)d}_{1,1,1}[\omega_1,\omega_2,\omega_3;\eta_{B1},\eta_{B2},\eta_{B3}] &= \frac{1}{d+2}\frac{1}{1+\omega_1}\frac{1}{1+\omega_2}\frac{1}{1+\omega_3}\left(\frac{1}{1+\omega_1}\left[1-\frac{\eta_{B1}}{d+4}\right]\right.\\
&\quad\left.+\frac{1}{1+\omega_2}\left[1-\frac{\eta_{B2}}{d+4}\right]+\frac{1}{1+\omega_3}\left[1-\frac{\eta_{B3}}{d+4}\right]\right),\\
D^{(BBB)d}_{1,1,1}[\omega_1,\omega_2,\omega_3;\eta_{B1},\eta_{B2},\eta_{B3}] &= \frac{1}{1+\omega_1}\frac{1}{1+\omega_2}\frac{1}{(1+\omega_3)^2}\left[1-\frac{\eta_{B3}}{d+2}\right],\\
\bar{D}^{(BBB)d}_{1,1,1}[\omega_1,\omega_2,\omega_3;\eta_{B1},\eta_{B2},\eta_{B3}] &= \frac{1}{1+\omega_1}\frac{1}{1+\omega_2}\frac{1}{(1+\omega_3)^2}\left[1-\frac{\eta_{B3}}{d+4}\right].
\end{aligned}
\tag{C.7}
$$

Appendix D

Coefficients in the FRG flow equations

We present the coefficients appearing in the flow equations of section 5.3. First, the coefficients of the flow equations within the transversally projected two-point function of the coset gluon, cf. Eq. (5.67), read

$$\begin{aligned}
\bar{X}_1^T &= \frac{12}{(d+2)d} - \frac{5}{d} + 1, & \bar{X}_2^T &= \frac{5\xi}{d} - \frac{12\xi}{d(d+2)} - \xi, \\
\bar{X}_3^T &= d - \frac{12}{(d+2)d} + \frac{5}{d} - 2, & \bar{X}_4^T &= -\frac{5\xi}{d} + \frac{12\xi}{d(d+2)} + \xi, \\
\bar{X}_5^T &= \frac{6}{(d+2)d} - \frac{4}{d} + 2, & \bar{X}_6^T &= \frac{2\xi}{d} - \frac{6\xi}{d(d+2)},
\end{aligned} \tag{D.1}$$

and

$$\begin{aligned}
X_1^T[\theta] &= -\frac{(d-1)\left(8d^2 + d(5\theta+4) + 10(\theta-2)\right)}{d(d+2)}, \\
X_2^T[\theta] &= \frac{(d-1)\left(d^2\left(3\xi^2+2\xi-1\right) - d\left(\theta+\xi^2-2(\theta+1)\xi+1\right) - 2\left(\theta+5\xi^2-2(\theta-1)\xi-1\right)\right)}{d(d+2)\xi}, \\
X_3^T[\theta] &= -\frac{(d-1)\left(d^2(\theta+4) + d(9\theta+4) + 10\theta - 8\right)}{d(d+2)}, \\
X_4^T[\theta] &= -\frac{(d-1)\left(d^2(\xi+1)^2 + d\left(\theta - 3\xi^2 + 2\xi + 5\right) + 6\theta - 6\xi^2 - 4\xi + 2\right)}{d(d+2)\xi}, \\
X_5^T[\theta] &= -\frac{2(d-1)(d(\theta+4)+\theta-4)}{d(d+2)}, \\
X_6^T[\theta] &= -\frac{2(d-1)\left(d(\xi+1)^2 + \theta + \xi^2 + 2\xi + 1\right)}{d(d+2)\xi}.
\end{aligned} \tag{D.2}$$

Next, we present the coefficients in the longitudinally projected two-point function of the coset gluon, cf. Eq. (5.68),

$$\begin{aligned}
\bar{X}_1^L &= -\frac{12}{(d+2)d} + \frac{5}{d} - 1, & \bar{X}_2^L &= -\frac{5\xi}{d} + \frac{12\xi}{d(d+2)} + \xi, \\
\bar{X}_3^L &= \frac{12}{(d+2)d} - \frac{5}{d} + 1, & \bar{X}_4^L &= \frac{5\xi}{d} - \frac{12\xi}{d(d+2)}, \\
\bar{X}_5^L &= \frac{2}{d} - \frac{6}{d(d+2)}, & \bar{X}_6^L &= \frac{6\xi}{d(d+2)},
\end{aligned} \tag{D.3}$$

and

$$\begin{aligned}
X_1^L[\theta] &= -\frac{(d-1)\left(d^2(\xi-1)^2 + d\left((\theta+2)\xi^2 - 2(\theta+2)\xi + 2\right) + 2\xi((\theta-2)\xi - 2\theta)\right)}{d(d+2)\xi^2}, \\
X_2^L[\theta] &= \frac{d^2\left(-\theta + \xi^2 - 2\xi - 3\right) - d\left(5\theta + 3\xi^2 + 2\xi + 3\right) + 2\left(-3\theta + \xi^2 + 2\xi + 3\right)}{d(d+2)\xi}, \\
X_3^L[\theta] &= -\frac{(d-1)(d((\theta+12)\xi - 8) + 6(\theta+4)\xi - 16)}{d(d+2)\xi}, \\
X_4^L[\theta] &= \frac{-d^2(\xi+1)^2 + d\left(-5(\theta+1) + 3\xi^2 - 2\xi\right) - 22\theta - 2\xi^2 + 4\xi + 6}{d(d+2)\xi}, \\
X_5^L[\theta] &= -\frac{2(d-1)(\theta+12)}{d(d+2)}, \\
X_6^L[\theta] &= -\frac{2\left(d(\xi+1)^2 + 3\theta - \xi^2 - 2\xi - 1\right)}{d(d+2)\xi}.
\end{aligned} \tag{D.4}$$

We proceed with the coefficients in the transversally projected two-point function of the residual gluon, cf. Eq. (5.69),

$$\begin{aligned}
V_1^T &= 4\left(\frac{4d+5}{d^2+2d} + 2d - 5\right), \\
V_2^T &= -\frac{(d-1)\left(d^2\left(3\xi^2 - 2\xi - 1\right) - 2d\left(3\xi^2 + 1\right) - 20\xi^2 + 8\xi + 4\right)}{d(d+2)\xi}, \\
V_3^T &= \frac{4(d-1)((d+2)\xi + 1)}{d(d+2)},
\end{aligned}$$

$$
\begin{aligned}
V_4^T &= 4\left(d+\frac{1}{d}-2\right),\\
V_5^T &= \frac{8(d-1)^2}{d(d+2)},\\
V_6^T &= \frac{(d-1)(\xi-1)\left(d^2(\xi-1)-d(3\xi+5)-6\xi-2\right)}{d(d+2)\xi},\\
V_7^T &= \frac{2\left(d^2-1\right)(\xi-1)^2}{d(d+2)\xi},\\
V_8^T &= \frac{(d-1)(\xi-1)\left(d^2(\xi-1)+d(9\xi-1)+10\xi-2\right)}{d(d+2)\xi},\\
V_9^T &= \frac{2\left(d^2-1\right)(\xi-1)^2}{d(d+2)\xi},\\
V_{10}^T &= 4-\frac{4}{d},\\
V_{11}^T &= \frac{8(d-1)}{d(d+2)}.
\end{aligned}
\tag{D.5}
$$

In the longitudinally projected case, cf. Eq. (5.70), we find

$$
\begin{aligned}
V_1^L &= \frac{d^3+d^2-6d+4}{d^2+2d}, & V_2^L &= \frac{4(d-1)\left(\xi^2+1\right)}{d(d+2)\xi},\\
V_3^L &= \frac{d^2-2d+4}{d^2+2d}, & V_4^L &= \frac{12(d-1)}{d},\\
V_5^L &= \frac{24(d-1)}{d(d+2)}, & V_6^L &= \frac{(d-1)(\xi-1)(d(\xi-1)-2(\xi+3))}{d(d+2)\xi},\\
V_7^L &= \frac{2(d-1)(\xi-1)^2}{d(d+2)\xi}, & V_8^L &= \frac{(d-1)(\xi-1)(d(\xi-1)+6\xi+2)}{d(d+2)\xi},\\
V_9^L &= \frac{2(d-1)(\xi-1)^2}{d(d+2)\xi}, & V_{10}^L &= \frac{12}{d},\\
V_{11}^L &= \frac{24}{d(d+2)}.
\end{aligned}
\tag{D.6}
$$

Finally, the coefficients related to the flow of the $SU(N-1)$ residual field, cf. Eqs. (5.100) and (5.102), are given by

$$\begin{aligned} \bar{E}_1^T &= 1 - \frac{1}{d}, & \bar{E}_2^T &= \frac{2}{d} - \frac{6}{d(d+2)}, \\ \bar{E}_1^L &= \frac{3}{d}, & \bar{E}_2^L &= \frac{6}{d(d+2)}, \end{aligned} \tag{D.7}$$

and

$$\begin{aligned} E_1^T &= -3d\lambda + \frac{12\lambda}{(d+2)d} - \frac{16\lambda}{d} + 8d - \frac{12}{(d+2)d} + \frac{16}{d} + 15\lambda - 20, \\ E_2^T &= 2d\lambda - \frac{2\lambda}{d} + 4d + \frac{4}{d} - 8, \\ E_3^T &= -\frac{8\lambda}{d} + \frac{12\lambda}{d(d+2)} - \frac{8}{d} + \frac{24}{d(d+2)} - \frac{24}{d+2} + 4\lambda + 8, \\ E_1^L &= -\frac{12\lambda}{(d+2)d} + \frac{4\lambda}{d} + d + \frac{12}{(d+2)d} - \frac{4}{d} - 1, \\ E_2^L &= -\frac{2\lambda}{d} - \frac{12}{d} + 2\lambda + 12, \\ E_3^L &= \frac{4\lambda}{d} - \frac{12\lambda}{d(d+2)} - \frac{24}{d(d+2)} + \frac{24}{d+2}. \end{aligned} \tag{D.8}$$

Bibliography

[1] Yoichiro Nambu. Strings, monopoles, and gauge fields. *Physical Review D*, 10(12): 4262, 1974.

[2] High-Energy Physics. Bologna, Italy, 1976. G. 't Hooft in: A.Zichichi (Ed.), High Energy Physics, Editorice Compositori, Compositori.

[3] S. Mandelstam. Vortices and Quark Confinement in Nonabelian Gauge Theories. *Phys. Rept.*, 23:245–249, 1976.

[4] Gerard 't Hooft. Topology of the Gauge Condition and New Confinement Phases in Nonabelian Gauge Theories. *Nucl. Phys.*, B190:455–478, 1981.

[5] Andreas S Kronfeld, ML Laursen, G Schierholz, and U-J Wiese. Monopole condensation and color confinement. *Physics Letters B*, 198(4):516–520, 1987.

[6] Andreas S Kronfeld, Gerrit Schierholz, and U-J Wiese. Topology and dynamics of the confinement mechanism. *Nuclear Physics B*, 293:461–478, 1987.

[7] Z. F. Ezawa and A. Iwazaki. Abelian dominance and quark confinement in yang-mills theories. *Phys. Rev. D*, 25:2681–2689, May 1982.

[8] Kazuhisa Amemiya and Hideo Suganuma. Off-diagonal gluon mass generation and infrared abelian dominance in the maximally abelian gauge in lattice qcd. *Phys. Rev. D*, 60:114509, Nov 1999.

[9] Yi-Shi Duan and Mo-Lin Ge. Su (2) gauge theory and electrodynamics of n moving magnetic monopoles. *Sci. Sinica*, 11:1072, 1979.

[10] YM Cho. Restricted gauge theory. *Physical Review D*, 21(4):1080, 1980.

[11] YM Cho. Extended gauge theory and its mass spectrum. *Physical Review D*, 23 (10):2415, 1981.

[12] YM Cho. Extended qcd and its mass spectrum. *Unpublished preprint, MPI-PAE/PTh 14/80*, 1980.

[13] YM Cho. Colored monopoles. *Physical Review Letters*, 44(17):1115, 1980.

[14] Ludvig Faddeev and Antti J Niemi. Partially dual variables in su (2) yang-mills theory. *Physical Review Letters*, 82(8):1624, 1999.

[15] Ludvig Faddeev and Antti J Niemi. Spin-charge separation, conformal covariance and the su (2) yang–mills theory. *Nuclear Physics B*, 776(1):38–65, 2007.

[16] Ludvig Faddeev and Antti J Niemi. Partial duality in su (n) yang-mills theory. *Physics Letters B*, 449(3):214–218, 1999.

[17] Ludvig Faddeev and Antti J Niemi. Decomposing the yang-mills field. *Physics Letters B*, 464(1):90–93, 1999.

[18] Timur Anatol'evich Bolokhov and Lyudvig Dmitrievich Faddeev. Infrared variables for the su (3) yang–mills field. *Theoretical and mathematical physics*, 139(2):679–692, 2004.

[19] Sergei V Shabanov. An effective action for monopoles and knot solitons in yang–mills theory. *Physics Letters B*, 458(2):322–330, 1999.

[20] S. V. Shabanov. Yang-Mills theory as an Abelian theory without gauge fixing. *Physics Letters B*, 463:263–272, September 1999.

[21] WS Bae, YM Cho, and SW Kimm. Extended qcd versus skyrme-faddeev theory. *Physical Review D*, 65(2):025005, 2001.

[22] YM Cho. Color reflection invariance and monopole condensation in qcd. *arXiv preprint hep-th/0301013*, 2003.

[23] K. I. Kondo, T. Murakami, and T. Shinohara. Yang-Mills theory constructed from Cho-Faddeev-Niemi decomposition. *Prog. Theor. Phys.*, 115:201–216, 2006.

[24] K. I. Kondo, T. Murakami, and T. Shinohara. BRST symmetry of SU(2) Yang-Mills theory in Cho-Faddeev-Niemi decomposition. *Eur. Phys. J.*, C42:475–481, 2005.

[25] Kei-Ichi Kondo, Toru Shinohara, and Takeharu Murakami. Reformulating SU(N) Yang-Mills theory based on change of variables. *Prog. Theor. Phys.*, 120:1–50, 2008.

[26] A Shibata, S Kato, K-I Kondo, T Murakami, T Shinohara, and S Ito. Compact lattice formulation of cho–faddeev–niemi decomposition: Gluon mass generation and infrared abelian dominance. *Physics Letters B*, 653(1):101–108, 2007.

[27] Kei-Ichi Kondo, Akihiro Shibata, Toru Shinohara, and Seikou Kato. Non-Abelian Dual Superconductor Picture for Quark Confinement. *Phys. Rev.*, D83:114016, 2011.

[28] Akihiro Shibata, Kei-Ichi Kondo, Seikou Kato, and Toru Shinohara. Non-abelian dual superconductivity in su (3) yang-mills theory: Dual meissner effect and type of the vacuum. *Physical Review D*, 87(5):054011, 2013.

[29] Henri Verschelde, Kenny Knecht, Karel Van Acoleyen, and M Vanderkelen. The non-perturbative groundstate of qcd and the local composite operator a 2 μ. *Physics Letters B*, 516(3):307–313, 2001.

[30] David Dudal, Henri Verschelde, John A Gracey, Vitor ER Lemes, Marcelo S Sarandy, Rodrigo F Sobreiro, and Silvio P Sorella. Dynamical gluon mass generation from$<$ aμ2$>$ in linear covariant gauges. *Journal of High Energy Physics*, 2004(01):044, 2004.

[31] Martin Schaden. Mass generation in continuum SU(2) gauge theory in covariant Abelian gauges. *arXiv hep-th/9909011*, 1999.

[32] Kei-Ichi Kondo and Toru Shinohara. Abelian dominance in low-energy gluodynamics due to dynamical mass generation. *Physics Letters B*, 491(3):263 – 274, 2000. ISSN 0370-2693.

[33] David Dudal and Henri Verschelde. On ghost condensation, mass generation and abelian dominance in the maximal abelian gauge. *Journal of Physics A: Mathematical and General*, 36(31):8507, 2003.

[34] H. Sawayanagi. Ghost condensation in nonlinear gauges: Euclidean space, minkowski space, and high temperature. *Phys. Rev. D*, 67:045002, Feb 2003.

[35] Kei-Ichi Kondo. Vacuum condensate of mass dimension 2 as the origin of mass gap and quark confinement. *Physics Letters B*, 514(3):335–345, 2001.

[36] K-I Kondo, T Murakami, T Shinohara, and T Imai. Renormalizing a becchi-rouet-stora-tyutin-invariant composite operator of mass dimension 2 in yang-mills theory. *Physical Review D*, 65(8):085034, 2002.

[37] G Curci and R Ferrari. On a class of lagrangian models for massive and massless yang-mills fields. *Il Nuovo Cimento A (1971-1996)*, 32(2):151–168, 1976.

[38] G Curci and R Ferrari. Slavnov transformations and supersummetry. *Physics Letters B*, 63(1):91–94, 1976.

[39] David Dudal, Henri Verschelde, VER Lemes, MS Sarandy, R Sobreiro, SP Sorella, M Picariello, and JA Gracey. The anomalous dimension of the gluon-ghost mass operator in yang–mills theory. *Physics Letters B*, 569(1):57–66, 2003.

[40] David Dudal, Henri Verschelde, VER Lemes, MS Sarandy, SP Sorella, and M Picariello. Gluon–ghost condensate of mass dimension 2 in the curci–ferrari gauge. *Annals of Physics*, 308(1):62–77, 2003.

[41] David Dudal, JA Gracey, VER Lemes, MS Sarandy, RF Sobreiro, SP Sorella, and Henri Verschelde. Analytic study of the off-diagonal mass generation for yang-mills theories in the maximal abelian gauge. *Physical Review D*, 70(11):114038, 2004.

[42] G.K. Savvidy. Infrared instability of the vacuum state of gauge theories and asymptotic freedom. *Physics Letters B*, 71(1):133 – 134, 1977. ISSN 0370-2693.

[43] N.K. Nielsen and P. Olesen. An unstable yang-mills field mode. *Nuclear Physics B*, 144(2):376 – 396, 1978. ISSN 0550-3213.

[44] Kei-Ichi Kondo. Gauge-invariant gluon mass, infrared abelian dominance, and stability of magnetic vacuum. *Physical Review D*, 74(12):125003, 2006.

[45] Kei-Ichi Kondo. Stability of chromomagnetic condensation and mass generation for confinement in su (2) yang-mills theory. *Physical Review D*, 89(10):105013, 2014.

[46] L. D. Faddeev. Quantization of Solitons. In *Proceedings, 18th International Conference on High Energy Physics, Tbilisi, USSR, Jul 15-21, 1976*, 1975.

[47] L. D. Faddeev and Antti J. Niemi. Knots and particles. *Nature*, 387:58, 1997.

[48] Kei-Ichi Kondo. Magnetic condensation, abelian dominance, and instability of savvidy vacuum. *Physics Letters B*, 600(3):287–296, 2004.

[49] Kei-Ichi Kondo. Magnetic condensation, abelian dominance, and instability of savvidy vacuum in yang-mills theory. *International Journal of Modern Physics A*, 20(19):4609–4614, 2005.

[50] Kei-Ichi Kondo, Akihito Ono, Akihiro Shibata, Toru Shinohara, and Takeharu Murakami. Glueball mass from quantized knot solitons and gauge-invariant gluon mass. *Journal of Physics A: Mathematical and General*, 39(44):13767, 2006.

[51] Kei-Ichi Kondo. Confinement–deconfinement phase transition and gauge-invariant gluonic mass in yang-mills theory. *arXiv preprint arXiv:1508.02656*, 2015.

[52] Henri Verschelde. Perturbative calculation of non-perturbative effects in quantum field theory. *Physics Letters B*, 351(1):242–248, 1995.

[53] Kenny Knecht and Henri Verschelde. New start for local composite operators. *Physical Review D*, 64(8):085006, 2001.

[54] Michael E. Peskin and Daniel V. Schroeder. *An Introduction to quantum field theory*. Addison-Wesley, Reading, USA, 1995. ISBN 9780201503975, 0201503972.

[55] T. Muta. Foundations of quantum chromodynamics. Second edition. *World Sci. Lect. Notes Phys.*, 57:1–409, 1998.

[56] Jean Zinn-Justin. Quantum field theory and critical phenomena. *Int. Ser. Monogr. Phys.*, 113:1–1054, 2002.

[57] L.D. Faddeev and V.N. Popov. Feynman diagrams for the yang-mills field. *Physics Letters B*, 25(1):29 – 30, 1967. ISSN 0370-2693.

[58] V. N. Gribov. Quantization of Nonabelian Gauge Theories. *Nucl. Phys.*, B139:1, 1978. [,1(1977)].

[59] I. M. Singer. Some remarks on the gribov ambiguity. *Communications in Mathematical Physics*, 60(1):7–12, Feb 1978. ISSN 1432-0916.

[60] C Becchi, A Rouet, and R Stora. Renormalization of gauge theories. *Annals of Physics*, 98(2):287 – 321, 1976. ISSN 0003-4916.

[61] M. Z. Iofa and I. V. Tyutin. Gauge Invariance of Spontaneously Broken Nonabelian Theories in the Bogolyubov-Parasiuk-HEPP-Zimmerman Method. *Teor. Mat. Fiz.*, 27:38–47, 1976. [Theor. Math. Phys.27,316(1976)].

[62] G. Curci and R. Ferrari. Slavnov Transformations and Supersymmetry. *Phys. Lett.*, 63B:91–94, 1976.

[63] Izumi Ojima. Another brs transformation. *Progress of Theoretical Physics*, 64(2): 625–638, 1980.

[64] Luis Alvarez-Gaumé and Laurent Baulieu. The two quantum symmetries associated with a classical symmetry. *Nuclear Physics B*, 212(2):255 – 267, 1983. ISSN 0550-3213.

[65] Stephen Hwang. Properties of the anti-brs symmetry in a general framework. *Nuclear Physics B*, 231(3):386 – 396, 1984. ISSN 0550-3213.

[66] F. De Jonghe, R. Siebelink, W. Troost, S. Vandoren, P. van Nieuwenhuizen, and Antoine Van Proeyen. The Regularized BRST Jacobian of pure Yang-Mills theory. *Phys. Lett.*, B289:354–360, 1992.

[67] J.C. Taylor. Ward identities and charge renormalization of the yang-mills field. *Nuclear Physics B*, 33(2):436 – 444, 1971. ISSN 0550-3213.

[68] A. A. Slavnov. Ward Identities in Gauge Theories. *Theor. Math. Phys.*, 10:99–107, 1972. [Teor. Mat. Fiz.10,153(1972)].

[69] Taichiro Kugo and Izumi Ojima. Local covariant operator formalism of non-abelian gauge theories and quark confinement problem. *Progress of Theoretical Physics Supplement*, 66:1–130, 1979.

[70] Taichiro Kugo. The Universal renormalization factors Z(1) / Z(3) and color confinement condition in nonAbelian gauge theory. In *BRS symmetry. Proceedings, International Symposium on the Occasion of its 20th Anniversary, Kyoto, Japan, September 18-22, 1995*, pages 107–119, 1995.

[71] Daniel Zwanziger. Fundamental modular region, boltzmann factor and area law in lattice theory. *Nuclear Physics B*, 412(3):657 – 730, 1994. ISSN 0550-3213.

[72] Georges Ripka. Dual superconductor models of color confinement. *Lect. Notes Phys.*, 639:pp.1–135, 2004.

[73] P. A. M. Dirac. Quantised singularities in the electromagnetic field. *Proc. Roy. Soc. London A*, 133(821):60–72, 1931. ISSN 0950-1207.

[74] A.M. Polyakov. Compact gauge fields and the infrared catastrophe. *Physics Letters B*, 59(1):82 – 84, 1975. ISSN 0370-2693.

[75] A.M. Polyakov. Quark confinement and topology of gauge theories. *Nuclear Physics B*, 120(3):429 – 458, 1977. ISSN 0550-3213.

[76] N. Seiberg and E. Witten. Electric-magnetic duality, monopole condensation, and confinement in n=2 supersymmetric yang-mills theory. *Nuclear Physics B*, 426(1): 19 – 52, 1994. ISSN 0550-3213.

[77] N. Seiberg and Edward Witten. Electric - magnetic duality, monopole condensation, and confinement in N=2 supersymmetric Yang-Mills theory. *Nucl. Phys.*, B426:19–52, 1994. [Erratum: Nucl. Phys.B430,485(1994)].

[78] Kenneth G. Wilson. Confinement of quarks. *Phys. Rev. D*, 10:2445–2459, Oct 1974.

[79] Tsuneo Suzuki and Ichiro Yotsuyanagi. Possible evidence for abelian dominance in quark confinement. *Phys. Rev. D*, 42:4257–4260, Dec 1990.

[80] John D. Stack, Steven D. Neiman, and Roy J. Wensley. String tension from monopoles in su(2) lattice gauge theory. *Phys. Rev. D*, 50:3399–3405, Sep 1994.

[81] Kei-Ichi Kondo, Seikou Kato, Akihiro Shibata, and Toru Shinohara. Quark confinement: Dual superconductor picture based on a non-abelian stokes theorem and reformulations of yang–mills theory. *Physics Reports*, 579:1 – 226, 2015. ISSN 0370-1573.

[82] D.I. Diakonov and V.Yu. Petrov. A formula for the wilson loop. *Physics Letters B*, 224(1):131 – 135, 1989. ISSN 0370-2693.

[83] Manfried Faber, A. N. Ivanov, N. I. Troitskaya, and M. Zach. On the path integral representation for the Wilson loop and the nonAbelian Stokes theorem. *Phys. Rev.*, D62:025019, 2000.

[84] Kei-Ichi Kondo. Abelian magnetic monopole dominance in quark confinement. *Phys. Rev.*, D58:105016, 1998.

[85] Kei-Ichi Kondo. Wilson loop and magnetic monopole through a non-Abelian Stokes theorem. *Phys. Rev.*, D77:085029, 2008.

[86] Matthias Warschinke, Ryutaro Matsudo, Shogo Nishino, Toru Shinohara, and Kei-Ichi Kondo. Composite operator and condensate in the $su(n)$ yang-mills theory with $u(n-1)$ stability group. *Phys. Rev. D*, 97:034029, Feb 2018.

[87] Matthias Warschinke, Ryutaro Matsudo, Shogo Nishino, Toru Shinohara, and Kei-Ichi Kondo. Erratum: Composite operator and condensate in the $su(n)$ yang-mills theory with $u(n-1)$ stability group [phys. rev. d 97, 034029 (2018)]. *Phys. Rev. D*, 98:059901, Sep 2018.

[88] Hyunsoo Min, Taehoon Lee, and PY Pac. Renormalization of yang-mills theory in the abelian gauge. *Physical Review D*, 32(2):440, 1985.

[89] Toru Shinohara, Takahito Imai, and Kei-Ichi Kondo. The most general and renormalizable maximal abelian gauge. *International Journal of Modern Physics A*, 18 (31):5733–5756, 2003.

[90] Gerard 't Hooft and M. J. G. Veltman. Regularization and Renormalization of Gauge Fields. *Nucl. Phys.*, B44:189–213, 1972.

[91] R. Keith Ellis, Zoltan Kunszt, Kirill Melnikov, and Giulia Zanderighi. One-loop calculations in quantum field theory: from Feynman diagrams to unitarity cuts. *Phys. Rept.*, 518:141–250, 2012.

[92] Kei-Ichi Kondo and Toru Shinohara. Renormalizable abelian-projected effective gauge theory derived from quantum chromodynamics. *Progress of theoretical physics*, 105(4):649–665, 2001.

[93] Toru Shinohara. Renormalizable abelian-projected effective gauge theory derived from quantum chromodynamics ii. *Modern Physics Letters A*, 18(20):1403–1412, 2003.

[94] Ulrich Ellwanger and Nicolas Wschebor. Massive yang–mills theory in abelian gauges. *International Journal of Modern Physics A*, 18(09):1595–1612, 2003.

[95] K-I Kondo. Implications of analyticity to mass gap, color confinement and infrared fixed point in yang–mills theory. *arXiv preprint hep-th/0303251*, 2003.

[96] Private correspondence with D. Dudal.

[97] Ruth E Browne and John A Gracey. Two loop effective potential for$<$ a2$\mu>$ in the landau gauge in quantum chromodynamics. *Journal of High Energy Physics*, 2003 (11):029, 2003.

[98] R. L. Stratonovich. A method for the computation of quantum distribution functions. *Dokl. Akad. Nauk SSSR*, 115(6):1097–1100, 1957.

[99] J. Hubbard. Calculation of partition functions. *Phys. Rev. Lett.*, 3:77–78, Jul 1959.

[100] Kei-Ichi Kondo. Gauge-invariant gluon mass, infrared abelian dominance, and stability of magnetic vacuum. *Phys. Rev. D*, 74:125003, Dec 2006.

[101] Kenneth G. Wilson. Renormalization group and critical phenomena. i. renormalization group and the kadanoff scaling picture. *Phys. Rev. B*, 4:3174–3183, Nov 1971.

[102] Kenneth G. Wilson. Renormalization group and critical phenomena. ii. phase-space cell analysis of critical behavior. *Phys. Rev. B*, 4:3184–3205, Nov 1971.

[103] Franz J. Wegner and Anthony Houghton. Renormalization group equation for critical phenomena. *Phys. Rev. A*, 8:401–412, Jul 1973.

[104] Kenneth G. Wilson and J. Kogut. The renormalization group and the epsilon expansion. *Physics Reports*, 12(2):75 – 199, 1974. ISSN 0370-1573.

[105] Joseph Polchinski. Renormalization and effective lagrangians. *Nuclear Physics B*, 231(2):269 – 295, 1984. ISSN 0550-3213.

[106] Christof Wetterich. Exact evolution equation for the effective potential. *Physics Letters B*, 301(1):90 – 94, 1993. ISSN 0370-2693.

[107] Juergen Berges, Nikolaos Tetradis, and Christof Wetterich. Nonperturbative renormalization flow in quantum field theory and statistical physics. *Phys. Rept.*, 363: 223–386, 2002.

[108] Jan M. Pawlowski. Aspects of the functional renormalisation group. *Annals Phys.*, 322:2831–2915, 2007.

[109] Holger Gies. Introduction to the functional RG and applications to gauge theories. *Lect. Notes Phys.*, 852:287–348, 2012.

[110] Holger Gies and René Sondenheimer. Renormalization Group Flow of the Higgs Potential. *Phil. Trans. Roy. Soc. Lond.*, A376(2114):20170120, 2018.

[111] F. Englert and R. Brout. Broken Symmetry and the Mass of Gauge Vector Mesons. *Phys. Rev. Lett.*, 13:321–323, 1964. [,157(1964)].

[112] G. S. Guralnik, C. R. Hagen, and T. W. B. Kibble. Global Conservation Laws and Massless Particles. *Phys. Rev. Lett.*, 13:585–587, 1964. [,162(1964)].

[113] Peter W. Higgs. Broken symmetries, massless particles and gauge fields. *Phys. Lett.*, 12:132–133, 1964.

[114] Peter W. Higgs. Broken symmetries and the masses of gauge bosons. *Phys. Rev. Lett.*, 13:508–509, Oct 1964.

[115] C. Ford, D. R. T. Jones, P. W. Stephenson, and M. B. Einhorn. The Effective potential and the renormalization group. *Nucl. Phys.*, B395:17–34, 1993.

[116] J. A. Casas, J. R. Espinosa, and M. Quiros. Improved Higgs mass stability bound in the standard model and implications for supersymmetry. *Phys. Lett.*, B342: 171–179, 1995.

[117] J. A. Casas, J. R. Espinosa, and M. Quiros. Standard model stability bounds for new physics within LHC reach. *Phys. Lett.*, B382:374–382, 1996.

[118] Dario Buttazzo, Giuseppe Degrassi, Pier Paolo Giardino, Gian F. Giudice, Filippo Sala, Alberto Salvio, and Alessandro Strumia. Investigating the near-criticality of the Higgs boson. *JHEP*, 12:089, 2013.

[119] Marc Sher. Electroweak higgs potential and vacuum stability. *Physics Reports*, 179 (5):273 – 418, 1989. ISSN 0370-1573.

[120] Gino Isidori, Giovanni Ridolfi, and Alessandro Strumia. On the metastability of the standard model vacuum. *Nucl. Phys.*, B609:387–409, 2001.

[121] Julius Kuti and Yue Shen. Supercomputing the effective action. *Phys. Rev. Lett.*, 60:85–88, Jan 1988.

[122] K. Holland and J. Kuti. How light can the Higgs be? *Nucl. Phys. Proc. Suppl.*, 129:765–767, 2004. [,765(2003)].

[123] P. Gerhold and K. Jansen. Lower Higgs boson mass bounds from a chirally invariant lattice Higgs-Yukawa model with overlap fermions. *JHEP*, 07:025, 2009.

[124] Vincenzo Branchina and Hugo Faivre. Effective potential (in)stability and lower bounds on the scalar (Higgs) mass. *Phys. Rev.*, D72:065017, 2005.

[125] Holger Gies, Clemens Gneiting, and René Sondenheimer. Higgs Mass Bounds from Renormalization Flow for a simple Yukawa model. *Phys. Rev.*, D89(4):045012, 2014.

[126] Holger Gies and René Sondenheimer. Higgs Mass Bounds from Renormalization Flow for a Higgs-top-bottom model. *Eur. Phys. J.*, C75(2):68, 2015.

[127] Matthias Warschinke. *Master Thesis*, 2015.

[128] Holger Gies, René Sondenheimer, and Matthias Warschinke. Impact of generalized Yukawa interactions on the lower Higgs mass bound. *Eur. Phys. J.*, C77(11):743, 2017.

[129] Astrid Eichhorn, Holger Gies, Joerg Jaeckel, Tilman Plehn, Michael M. Scherer, and René Sondenheimer. The Higgs Mass and the Scale of New Physics. *JHEP*, 04:022, 2015.

[130] Jan M. Pawlowski and Fabian Rennecke. Higher order quark-mesonic scattering processes and the phase structure of QCD. *Phys. Rev.*, D90(7):076002, 2014.

[131] A. Jakovac, I. Kaposvari, and A. Patkos. Scalar mass stability bound in a simple Yukawa-theory from renormalization group equations. *Mod. Phys. Lett.*, A32(02): 1750011, 2016.

[132] O. Zanusso, L. Zambelli, G. P. Vacca, and R. Percacci. Gravitational corrections to Yukawa systems. *Phys. Lett.*, B689:90–94, 2010.

[133] Gian Paolo Vacca and Luca Zambelli. Multimeson Yukawa interactions at criticality. *Phys. Rev.*, D91(12):125003, 2015.

[134] Holger Gies, René Sondenheimer, Alessandro Ugolotti, and Luca Zambelli. Asymptotic freedom in Z_2-Yukawa-QCD models. 2018.

[135] Daniel F. Litim. Optimization of the exact renormalization group. *Phys. Lett.*, B486:92–99, 2000.

[136] Daniel F. Litim. Optimized renormalization group flows. *Phys. Rev.*, D64:105007, 2001.

[137] Julia Borchardt, Holger Gies, and René Sondenheimer. Global flow of the Higgs potential in a Yukawa model. *Eur. Phys. J.*, C76(8):472, 2016.

[138] René Sondenheimer. Nonpolynomial Higgs interactions and vacuum stability. *arXiv:1711.00065 [hep-ph].*

[139] L. Rosa, P. Vitale, and C. Wetterich. Critical exponents of the Gross-Neveu model from the effective average action. *Phys. Rev. Lett.*, 86:958–961, 2001.

[140] Holger Gies and Christof Wetterich. Renormalization flow of bound states. *Phys. Rev.*, D65:065001, 2002.

[141] F. Höfling, C. Nowak, and C. Wetterich. Phase transition and critical behavior of the d=3 gross-neveu model. *Phys. Rev. B*, 66:205111, Nov 2002.

[142] Jens Braun, Holger Gies, and Daniel D. Scherer. Asymptotic safety: a simple example. *Phys. Rev.*, D83:085012, 2011.

[143] Kei-Ichi Kondo. Stability of chromomagnetic condensation and mass generation for confinement in SU(2) Yang-Mills theory. *Phys. Rev.*, D89(10):105013, 2014.

[144] T. Papenbrock and C. Wetterich. Two loop results from one loop computations and nonperturbative solutions of exact evolution equations. *Z. Phys.*, C65:519–535, 1995.

[145] Daniel F. Litim and Jan M. Pawlowski. Completeness and consistency of renormalisation group flows. *Phys. Rev.*, D66:025030, 2002.

[146] Markus Q. Huber and Jens Braun. Algorithmic derivation of functional renormalization group equations and Dyson-Schwinger equations. *Comput. Phys. Commun.*, 183:1290–1320, 2012.

[147] Anton K. Cyrol, Mario Mitter, and Nils Strodthoff. FormTracer - A Mathematica Tracing Package Using FORM. *Comput. Phys. Commun.*, 219:346–352, 2017.

[148] Ulrich Ellwanger. Flow equations and BRS invariance for Yang-Mills theories. *Phys. Lett.*, B335:364–370, 1994.

[149] Ulrich Ellwanger, Manfred Hirsch, and Axel Weber. Flow equations for the relevant part of the pure Yang-Mills action. *Z. Phys.*, C69:687–698, 1996.

[150] Marco D'Attanasio and Tim R. Morris. Gauge invariance, the quantum action principle, and the renormalization group. *Phys. Lett.*, B378:213–221, 1996.

[151] Daniel F. Litim and Jan M. Pawlowski. Flow equations for Yang-Mills theories in general axial gauges. *Phys. Lett.*, B435:181–188, 1998.

[152] Yuji Igarashi, Katsumi Itoh, and Hiroto So. BRS symmetry, the quantum master equation, and the Wilsonian renormalization group. *Prog. Theor. Phys.*, 106:149–166, 2001.

[153] Yuji Igarashi, Katsumi Itoh, and Jan M. Pawlowski. Functional flows in QED and the modified Ward–Takahashi identity. *J. Phys.*, A49(40):405401, 2016.

[154] Holger Gies. Running coupling in Yang-Mills theory: A flow equation study. *Phys. Rev.*, D66:025006, 2002.

[155] Holger Gies. Wilsonian effective action for su(2) yang-mills theory with the cho-faddeev-niemi-shabanov decomposition. *Phys. Rev. D*, 63:125023, May 2001.

Acknowledgements

At this point, I would like to take the chance to thank all the people who supported me throughout this long journey and enabled me to write this thesis.
First of all, I express my gratitude to my supervisor Kei-Ichi Kondo. It was a pleasure to work on this interesting topic and I am thankful for the countless discussions that helped me to understand the material. His door was open not only regarding physics, but also for all kind of problems, especially in the first year after my arrival in Japan.
I also thank the elementary particle theory group at Chiba University and in particular Shogo Nishino for his support in daily life, especially in my first months in Japan. Of course, I also acknowledge the many discussions related to our research.
Furthermore, I would like to mention Andreas Schoepe. Thank you very much for the encouragements and motivational words during my PhD, and for carefully reading the manuscript. I thank Oliver Siebert for his Tech-Support.
During the various conferences and workshops, I acknowledge discussions with René Sondenheimer, Anton K. Cyrol, Nicolas Wink, Jan Pawlowski, Holger Gies, John A. Gracey and David Dudal.
Besonderer Dank gebührt weiterhin meinen Eltern und meiner Schwester, die trotz der großen Entfernung immer für mich da waren, in finanzieller Hinsicht aber besonders auch in den emotional schwierigen Zeiten immer die richtigen Worte fanden. Gleiches gilt auch für meine Großeltern.
Am dankbarsten bin ich meiner Frau Xiarui. Ich bin so froh, dass du dieses Wagnis eingegangen und mit mir nach Japan gekommen bist. Du warst der Gegenpol der mich in dieser Zeit in der Spur gehalten hat, wenn mir die Physik mal wieder über den Kopf gewachsen ist. Ich liebe dich über alles und freue mich auf unsere gemeinsame Zukunft.
在此由衷感谢我的妻子夏蕊。你不顾一切陪我来到日本。在我迷失于物理之海时，你始终是我人生轨迹的灯塔。我爱你胜过所有，愿与你白头偕老。

This work was supported by the Chiba University SEEDS Fund (Chiba University Open Recruitment for International Exchange Program) and by the Ministry of Education, Culture, Sports, Science and Technology, Japan (MEXT scholarship).